SIMULATION AND ANALYSIS OF WAVE – STRUCTURE INTERACTIONS

By

PETER TAIWO FASHANU-UDOFE

A Thesis Submitted

In fulfilment of the requirement for degree of

DOCTOR OF PHILOSOPHY

School of Marine Science and Technology,

NEWCASTLE UNIVERSITY,

Newcastle Upon Tyne, U.K.

MAY 2010

ABSTRACT

Today, it is widely recognized that Computational Fluid Dynamics (CFD) methodologies should be used for the analysis of Engineering systems and that design and method of simulation must be practical and realistic to provide cost effective solutions. The recent development in CFD of Engineering Structures has led to the adoption of the Eulerian and Lagrangian concepts of numerical analysis. Although the importance of these concepts cannot be overemphasised in offshore structures hydrodynamics, thus the choice of a concept to define the flow field surrounding a structure is one of the fundamental problems identifiable with marine hydrodynamics, especially where non linear effects become paramount.

A narrow focus and use of a concept not adaptable to the ship hydrodynamic problem cannot guarantee the development of a good CFD code.

Traditional approaches using the Eulerian and Lagrangian concepts have progressed relatively in the last three decades with the continuous rise in computer development.

Smooth Particle Hydrodynamics (SPH), Volume of Fluid Method (VOF), Boundary Integral Method are but a few methods that have been widely used in recent applications. However when a detailed description, evaluation and analysis of the flow field is required in a ship hydrodynamics problem, some of these methods fall short of expectation when they have to strictly adhere to some given assumptions to make the computational analysis stable and provide results.

In the use of Eulerian and Lagrangian concepts in fluid dynamics, mathematical skill is an essential requirement for solving flow problems. Modeling methods require discretization of the flow field equations which can be linear and non linear, depending on the parameters for simulation. The understanding of mathematical principles such as Partial differential equations, Fourier transforms and integrals, Integral calculus, Complex Analysis, Matrices, Vectors, Greens Function, Bessel Function, etc are necessary for solving the various equations of fluid motion when calculating the properties of the flow field associated with the hydrodynamic problem. Solution techniques which have the attributes of providing stability, consistency, convergence and accuracy are part of the mathematical requirements for a valid algorithm.

Moving Particle Semi - Implicit Method is a computational method for incompressible fluid flow problems. MPS is a lagrangian particle method with robust capability for numerical representation. Particle interaction models representing differential operators in the Navier Stokes equation are proposed for divergence, gradient and laplacian. Boundary interfaces are transformed to interactions between particles. Computational difficulties associated with Eulerian methods such as numerical diffusion and regriding due to fragmentation and large deformations can be overcome with MPS method.

This study addresses in detail the MPS method as a computational tool for wave - structure interactions. Investigation of both laboratory and numerical experiments associated with Wave - Structure Interactions were the primary focus of this study with the Development of a 2-dimensional MPS Simulation and Analysis of Wedge Water entries code, and Green Water flow simulation and effects on FPSO deck structure.

Computational codes were developed for the prediction of deck flow and wave loads on the deck structure using the Navier Stokes equations.

An experimental study was carried out at the Newcastle University Marine Laboratory in order to understand the detailed nature of green sea physics. Green Sea effects were measured on a model FPSO.

Empirical relations and data obtained from the experiment were used in the numerical prediction code to obtain the deck flow pattern and validate the wave loads on the deck structure using the MPS method. The experiment on merit was necessary to test the capability of the hydrodynamics facility and provide understanding of the underlying principles surrounding the green water phenomena.

CONTENTS

Chapter 1

INTRODUCTION

Chapter 2

NUMERICAL MODELING IN HYDRODYNAMICS

Chapter 3

MOVING PARTICLE SEMI IMPLICIT METHOD (MPS)

Chapter 4

MODEL TEST AND INVESTIGATION OF GREEN WATER ON FPSO

Chapter 5

EXPERIMENTAL AND NUMERICAL STUDY OF GREEN WATER PHENOMENA

Chapter 6

CONCLUSIONS AND RECOMMENDATIONS FOR FUTURE WORK

APPENDIX

LIST OF FIGURES

LIST OF PLATES

LIST OF TABLES

ACKNOWLEDGEMENTS

People help shape your destiny by your association with them. It gives me great pleasure to thank them all that have in various ways shaped my beliefs, understanding and guided me in my struggles through studentship at Newcastle University. First and foremost is my thesis supervisor Dr Martin J. Downie, I would like to say thank you very much. Dr J. Downie has guided me, provided excellent suggestions and constructive criticism. His endless knowledge of marine hydrodynamics and numerical computation has helped me to build an unparallel level of confidence in my abilities as a scientist. In my years at Newcastle University, he has shown great enthusiasm for teaching, student counselling at the marine school and an inspiration to all his students. I am very proud and honoured to have worked with him.

My gratitude to James , Allen and other staff of the MAST laboratory for their technical support during the period of my experiment. Special thanks go to my brothers Chief Olu Fashanu, Hon. Paul Kehinde Fashanu, Augustine Fashanu, my sisters Auntie Mrs Moni Aideloje, Auntie Ebun, my sisters in law, Mrs Joyce Fashanu, Mrs Flora Fashanu, my secretary Mr Sani Ahmed and my friend Dr Nelson Hsu.

Last but not the least I would like to express my deepest gratitude to my wife Bridget Odufua and my children and nephews for their support and unconditional love.

DEDICATION

To my late Father Chief Gabriel Fashanu Udofe(1915 – 2005), who encouraged me to begin this journey.

To Honourable Paul kehinde Fashanu Udofe. My twin brother, who has been with me throughout the time of my study at Newcastle University

And Finally

TO GOD: YOU ARE THE PLANNER OF ALL THINGS. THANK YOU AND PRAISE BE TO YOUR GLORIOUS NAME.

NOMENCLATURE

a	Local acceleration
a_F	Empirical relation parameter for force
a_P	Empirical relation parameter for pressure
a_U	Empirical relation parameter for velocity
a_H	Empirical relation parameter for water height
B	Width of towing tank
C_e	Compression factor
D_0	Distance between neighbouring particles in the initial configuration.
d	Number of space dimensions
$\vec{F}$	External force vector acting on fluid particles
F_x	Maximum horizontal force
f_b	Freeboard
f_e	Frequency at which amplitude is calculated
f_P	Peak frequency
GM	Metacentric height
g	Acceleration due to gravity or gravitational acceleration vector
H_i	Mean of wave height
H_s	Target Wave height

$H_{\eta\zeta}(\omega)$	Response amplitude Operator (RAO)
h	Smoothing length
$h_{\max}$	Extreme freeboard exceedance.
δH	Class interval of wave records
I	Moment of inertia of wedge body
i, j	Substitute to identify each particle
k	Step of the k_{th} calculation
K_i	Wave number
KG	Centre of gravity
L_m	Model length
LBP	Length between perpendiculars
LCG	Longitudinal centre of gravity from AP
LC1 to LC4	Load cells fixed on model deck structure to measure impact force
m	Total number of particles in computational domain.
m_n	n^{th} spectral moment, (n = 1, 2, 3, 4, etc)
m_0	The area under the spectrum
N	Number of neighbours nearest to particle i
$\overline{N}$	Total number of waves measured at a point
$\vec{n}$	normal direction
n^0	Constant particle number density.
n^*	Temporary particle number density calculated in the first sub process

Δn^{**}	Change in particle number density in the explicit second sub process
P	Pressure
p_0	Pressure at free surface
$P1$	Non dimensional pressure on wedge body surface
PT1 to PT4	pressure transducers to measure water pressure on model deck
q_{wc}	Relative position of a wedge particle to the centre
$\vec{R}$	Rotational velocity of wedge body
r	Position vector of fluid particle
r_e	Threshold of particle interacting area in the kernel function
r_w	Position vector of wedge particle
r_{wc}	Centre of wedge body
r_{WM}	Relative wave motion
$S(f)$	JONSWAP spectrum
$S(\omega)$	Spectral energy
s	Surface area of load cell
$\vec{T}$	Translational velocity of wedge body
T_p	Target wave period
t	Time
Δt	Time step
$\vec{U}^*$	Velocity vector of particles calculated in the explicit first sub process

$\vec{U}^{**}$ Velocity vector of particles calculated in the implicit second sub process

$\vec{U}$ Velocity vector of particles from previous step

$\vec{U}_{GWP}$ Velocity of ghost particle

$\vec{U}_{w}$ Velocity vector of wedge particle in water

$\vec{U}_{WP}$ Velocity of water particle

$\Delta\vec{U}^{*}$ Change in velocity in the explicit first sub process

$\Delta\vec{U}^{**}$ Change in velocity in the implicit second sub process

u Velocity in x direction

$V(t)$ Measured velocity of wedge from Zhao et al (1997)

v Velocity in y direction

$V1$ Non dimensional vertical coordinate on the wedge body surface

W Kernel function

WP1 to WP12 Wave probes to measure wave heights and water elevation on deck.

w Drop velocity or vertical downward velocity of wedge

x Spatial position

$Z1$ Draft coefficient

z Vertical distance travelled by a wedge particle

z_0 Drop height

z_{KEEL} Vertical position of wedge keel.

z_w Vertical position of a wedge particle.

β	Coefficient in the water surface assessment.
γ	Bow flare angle
ε	Band width parameter
ε_i	Phase difference
ζ	Local disturbed wave motion
ζ_{ai}	Wave elevation amplitude
η	Local vertical motion
η_{ai}	Amplitude of ship motion
λ	Coefficient of the laplacian model
ν	Kinematics viscosity
ρ	Density
σ^2	Variance of distribution of scalar quantities.
σ_a, σ_b	sigma factors for the frequencies above and below peak
τ	Conversion factor
ϕ	A scalar quantity
ω	Frequency in radians per second
∇	Differential operator
ϑ	Diffusion Coefficient.
$*$	Explicit first sub process
$**$	Implicit second sub process

CHAPTER 1

INTRODUCTION

The motion of fluids involves natural and complex physical phenomena. The problems associated with these phenomena can be enormous, technically challenging and important since almost everything on this planet is either a fluid or interacts with fluids. To aid in understanding fluid flow problems, researchers and scientists often use either experimental simulations or computational simulations along with a mathematical theory.

Experimental simulation can be prohibitively time consuming and expensive and it may be necessary to turn to computer simulations to provide insights during the engineering process. The components of fluid motion can be very complicated in their structure. It is often random in behaviour, and phenomena like fragmentation and coalescence can occur continuously, especially when the fluid is in an extreme environment such as the sea. In offshore engineering, the challenges of modelling fluid motion become greater because structures have to be placed to work efficiently in wind, wave and current environments that are frequently very harsh. Hydrocarbon exploration and exploitation in deep water fields has made most of these challenges explicit and worthy of thorough scientific research.

Wave-structure interaction in this environment is very dynamic and the flow behaviour uncertain. It continues to be the subject of extensive investigation both from the perspective of experimental and numerical simulation.

1.1 Background

During the last couple of decades, considerable research work has been carried out in the experimental investigation and the development of numerical prediction methods for fluid flow problems associated with wave – structure interactions. The Green Water phenomenon can be classified as a wave – structure interaction activity.

1.1.1 Green Water

Green water is a phenomenon that occurs as a compact mass of water that overtops the bow of a vessel and crashes across the deck with severe impact on deck structures and equipment.

High waves in stormy sea weather and large amplitude ship motions are common occurrences that a ship encounters at sea. These conditions can cause sea water overtopping the deck of the vessel and flowing across the deck to impact on the structures on deck.

In the offshore oil industry, floating production and offloading (FPSO) units are now often installed in areas where the sea environment is very extreme with the consequence that green water problems occur more frequently. As a result the problem of green water is now part of design consideration in FPSO units. Weathervaning is a feature in FPSO units where the vessels respond to the sea conditions by rotating about the turret moored systems. During this activity, the bow of the FPSO unit is constantly exposed to the overtopping green water, with the possibility that sensitive equipment and structures around the bow region could be more susceptible to damage.

Esrdal and Kvitrud(2000) provided a study on the damages experienced by Norwegian FPSOs. Vestbostad (1999) reported a case of green water overtopping from the side of the Norne FPSO resulting in the damage of the piping system.

1.1.2 Literature review on Green water research.

- **Pioneer studies**

A pioneer investigative work was carried out by Newton (1960). The study conducted at the Admiralty Experiment Works used data obtained from a model to develop a method for comparing certain features of a ship with the waves encountered. Three types of wetness were identified; dry, wet and very wet, which corresponds to similar conditions of dry, heavy spray and green water. This classification is used to describe the behaviour of the model when encountering wave conditions in head seas. The results of the investigations were plotted non- dimensionally as a family of curves or "wetness contours" with the Froude number being the main parameter. The effect of increased flare was also investigated and it showed some relationship to wetness. Finally the study concludes that the family of curves developed can be used to assign freeboard to new ship design to avoid undesirable levels of wetness.

Another important early study was carried out by Ochi (1964). An experiment was conducted on a 13ft Mariner model to investigate the extreme behaviour of a ship in rough seas and statistical methods were applied to the results to examine the effects of sea severity, ship speed, course angle and loading conditions on the motions. A comparison of the statistical results between the slamming conditions and pressures associated with slamming and green water was presented.

- **Experimental Studies.**

A number of researchers have carried out different experimental investigations on the problem of green water phenomena. Areas of study have included but are not limited to wave – structure interactions, bow shapes and flare angles. Blok et al. (1984) in a wave structure interaction experiment conducted a comprehensive investigation into the vertical relative motion of the water surface along the bow of a model frigate with forward speed. The experiment and calculations obtained were used to develop a swell up coefficient which was demonstrated to improve the prediction of green water. Lloyd et al. (1985), in an experiment investigated the deck wetness process and its effect on different bow shapes.

The relative bow motion and deck wetness frequency were measured during the experiment. In conclusion the study suggested bow form parameters that would likely minimize deck wetness in irregular seas. Ogawa et al. (2001) in developing a long term prediction method for green water loads on the bow deck structure of ships carried out experiments in regular and irregular waves on a scaled model tanker. Results from the experimental works were used to develop a relationship between the green water loading and relative wave height. They came to the conclusion that green water loading was proportional to the square of the water elevation over the bow top. Cox and Ortega (2002) conducted a small scale laboratory experiment to quantify a transient wave overtopping a horizontal deck and a fixed deck above the free surface. Comprehensive measurements were undertaken of the free surface and velocity profiles with or without the deck structure in the wave tank. Examination of the effects of the deck structures on the wave kinematics revealed that the free surface increased by 20% above the leading edge due to the presence of the deck structure and the velocity profile was uniform.

- **Prediction methods.**

Dillingham (1981) studied the sea keeping characteristics of a fishing vessel numerically. Using an impulse response technique in the time domain, the equations of motion in sway and roll were formulated with the vessel considered to be a two degree of freedom system. A set of non linear hyperbolic equations were also formulated to describe the water flow behaviour on the deck of the fishing vessel. A numerical solution was obtained for the set of equations using the random choice method also known as Glimm's method. The static and dynamic forces exerted on the vessel resulting from the green water was computed and added to the external wave exciting forces to obtain a complete solution in the time domain. As a result the vessel dynamic stability could be examined due to the effect of the green water. A follow up study was done by Pantzopoulous(1988), who proposed a methodology to solve the problem of the three dimensional flow of green water on the deck of a fishing vessel and to calculate the resulting forces and moments at the centre of gravity.

An Eulerian method was adopted for the formulation of the equations of the motion with respect to a system attached to the oscillating vessel. Glimm's method (Random Choice Method) was used to solve the non linear hyperbolic equations of motion. The simulation results revealed complex flow patterns consisting of oblique bores and "swirling" motions of the water on deck for a vessel undergoing pitch and roll motions.

Takagi and Niimi(1990) presented a study on green water and the effects of the flare shape were examined. With the assumption of long wave length and high Froude number it was shown that two dimensional similarity flow techniques can be applied to the analysis of deck wetness. Flare angles were obtained from the calculated result, which indicated that for reduced bow deck wetness, increased flare is considered more effective than a knuckle. In a study by Buchner and Cozijin(1997) , a simplified non linear boundary integral method was applied to a two dimensional flow of green water on deck without ship motions. The method was capable of representing green water simulation on a two dimensional configuration.

Wu et al. (2000) showed that the prediction of bow wave amplification for a ship navigating in head seas can be achieved by means of a non linear slender body theory. The overall capabilities of the method were demonstrated through a systematic study of a frigate and the sequence of probable events that occur in the bow region was studied. Results were summarized in charts that allow for critical evaluation of a selected ship design. Sames (2002), analysed green water loads on a RoRo ferry forward superstructure using the finite volume method as a numerical prediction tool Schonberg and Rainey (2002) developed a design tool for the calculation of water velocities on the deck of a ship as a result of green water. The result of their new design procedure was compared with the results from existing procedures and led to the conclusion that existing procedures are conservative.

Yilmaz et al. (2003) formulated a non linear dam break problem using Fourier series analysis and Fourier transformation techniques. Semi – analytical solutions of the pressure components and displacements were obtained using the above techniques.

The configuration of the water front in the dam problem was similar to a water jet formation in green water. Mori and Cox (2003) used a statistical model to develop wave overtopping volume, horizontal velocity and maximum overtopping rate of extreme waves on a fixed deck. Results from the statistical model compared favourably with the measured exceedance probability seaward of the deck. Greco et al.(2004) introduced a numerical solution using the boundary element method with piecewise linear shape functions for geometry and boundary data to investigate the effects of green water on a deck of a vessel in head sea condition and zero forward speed. The wave structure interaction was analyzed by coupling with the non linear Euler beam. The role of hydro elasticity was also investigated for the impact loading conditions.

Shibata and Koshizuka(2007) simulated green water on deck in three dimensions using the Moving Particle Semi-implicit method. The primary focus of the investigation was to predict the impact pressure on deck and the results of the simulation when compared with an experimental study came in close agreement. However, it was observed that the peak of the calculated pressure was lower than that of the experiment by 50% and the outline of the wave form was close to that of the experiment. The main reasons given for the observed differences in pressure computation were low spatial resolution and the wetness on the deck. It was recommended that using higher spatial resolution could improve the estimate of the impact pressure more accurately.

Shibata et al (2009) carried out further numerical analysis study based on the MPS method to simulate shipping water on a moving ship with a realistic bow. In the numerical study, ship motions obtained from experiment were included in the simulation and a force to move the ship was introduced. The numerical simulation for the shipping water study used the weight function and particle models proposed by Koshizuka and Oka (1996) for the calculations. Results of the study show that, (1) the calculated shipping water behaviour was in agreement with experimental study, (2) The water volume calculated for the shipping water on deck was in close agreement with the experimental study and (3) The impact pressure on deck oscillated in the calculations.

The pressure oscillations were attributed to the full Lagrangian description of the MPS method, inadequate spatial resolution and the experimental noise included from the ship motions.

In a paper presented by LeTouze et al. (2010), Smooth Particle Hydrodynamics (SPH) was applied as a numerical analysis tool to simulate the effects of green water and the flooding effects due to water entering the mid section of a vessel caused by side collision. The results obtained from the SPH model were compared to an experimental study. Lu et al. (2010) also carried out a numerical time domain simulation model using the volume of fluid method (VOF) to study the green water phenomenon. The VOF method was able to capture the violent free surface deformation.

1.1.3 Floating Production and Offloading (FPSO).

Floating Production, Storage and Offloading are major activities in the offshore oil production value chain. With the investments in Exploration, Exploitation and Production of crude oil in the marine environment, the increasing use of FPSOs is expected to feature significantly as a major marine activity in the environment. This is because economic considerations give the FPSO an advantage over other forms of offshore structures in deep water hydrocarbon production and storage.

The Far East and South America oil and gas industry witnessed the early use of FPSOs as a viable economic solution in the exploitation of hydrocarbons in small and marginal oil fields either for the extension of the life of existing fields or allowing for early start up of new fields. Further developments in the North Atlantic and West African oil and gas sector saw a rise in the use of FPSO with deployment covering a wide range of water depths and climatic conditions. Ship Shaped FPSOs are mainly built from converted oil tankers and bulkers with sizes in the VLCC/ULCC range. Conventional new builds are getting attention as the economics sometimes favour a new construction.

The FPSO is a complex facility which comprises a ship shaped structure, process systems, utility systems, turret systems and a flexible riser technology that allows for the conveyance of hydrocarbon fluids from the seabed wells to the process systems. The processed fluids are stored in tanks and exported via pipelines or shuttle tankers. The significant advantage of being a self contained facility gives the FPSO flexibility to relocate at the end of a useful field life to another location. Weathervaning is a major feature in FPSO operations and involves the use of the turret mooring system in harsh environmental conditions which allows the FPSO ability to respond to changing climatic conditions.

FPSO susceptibility to green water is one of the issues under study (Bomel Ltd, 2001) with regards to the critical environmental conditions occurring in the areas of operation. The hostile marine environment is a major concern to the industry, therefore research investigations require accurate prediction methods for the responses to a wide range of environmental conditions experienced in deep water in order to achieve the standards desired for design, safety and operations.

1.1.4 Literature review on FPSO green water studies.

- **Experimental studies.**

Buchner (1999) presented a study on the relative wave motions along the side of a weathervaning FPSO. The study introduced the conditions associated with the green water event in a sea environment and presented a method for the analysis of the non linear relative wave motions along the side of an FPSO.

A new method was also developed that can predict the green water loading on a slender structure. In another experimental work, Stansberg and Karlsen (2001) carried out model tests with an FPSO in irregular waves. The resulting impact loads due to water on deck and bow slamming were investigated. Stansberg and Nielsen (2001) presented model test measurements of waves overtopping an FPSO in steep waves. The study was aimed at supporting the development of simplified engineering design tools, where the most non-linear effects are observed and taken into consideration. Greco (2001) performed a model test to explain the fluid mechanics involved in green water and to validate a numerical method.

The influence of ship parameters, ship motions and hull geometry were investigated. Water impact with a structure in the bow area were studied in details and results compared well with the numerical method.

Soares and Pascoal(2002) carried out detailed experimental work of the probability distributions of the occurrence of water on deck and of the conditional distribution of water height above the deck. In measuring the linearity of the response process, time series of pitch and relative motions were analyzed. The study used a moored FPSO model for the experimental program. Buchner (2002) carried out extensive experimental investigations on green water problems as they affect ship type offshore structures. The tests and measurements from the experiment were used to develop relationships for green water flow onto and on the foredeck, green water impact loading and green water from the side and stern. Han (2003) in his experimental work provided a further understanding of the occurrences of green water on FPSOs and developed a prediction method for the analysis of the forces on the superstructure and the effect of green water on ship motions. In another development, Han et al. (2004) carried out an experimental study of a model FPSO in moderate to extreme regular waves to support and provide validation to numerical work modelling green sea events.

- **Numerical prediction studies.**

Harmoudi and Varyani(1998) investigated the probability of green water occurrence taking into consideration the vertical relative motion exceeding the freeboard.

Probabilistic methods were used to determine the number of green water events of the floating structure. The authors reached the following conclusions (a) there is no direct relationship between velocities in the waves and velocities of the green water on deck. (b) The water velocities around the bow are heavily disturbed by the presence of the bow. Hellan et al. (2001) described the development of a reliable prediction design tool capable of carrying out systematic linear and non linear functions modelling the green water phenomenon.

The tool was developed to handle the environmental load and structural responses beginning from a process of green water occurrence, water propagation on deck, with the computational ability to predict the impact forces on deck structures while taking into consideration the structural responses of the vessel.

Nielsen and Mayer (2004) used the volume of fluid (VOF) as a Navier Stokes solver to model numerically green water effects on a moored FPSO exposed to head sea conditions. Two different scenarios involving a fixed vessel, and a vessel in motion, were investigated and the computations of water height on deck and impact pressure on deck mounted structures were carried out. Gomez-Gesteira et al. (2005) applied the Smooth Particle Hydrodynamics (SPH) method to study the effects of green water on offshore structures. The results from the numerical investigation revealed a jet like formation observed at the rear of the deck during the green water flow process. Zhu et al. (2006) presented a numerical simulation scheme using the volume of fluid (VOF) method to capture the free surface deformation of the green water process on moored FPSO model in the head seas condition. Adoption of a source technique to implement the incident wave generation and vessel oscillatory motions were realized using potential theory. A method using a dynamic mesh was specially introduced in the numerical simulation to generate the green water occurrence on deck and to calculate impact forces. Ryu et al. (2007) using measurements taken from laboratory experiments applied the Ritter's dam break flow solution to predict green water effects on an offshore structure. Bubble Image Velocimetry (BIV) was used to measure the green water velocity on a two dimensional model. The study also examined the influence of the deck length on green water velocity.

1.2 Motivation and Scope of Work

The application of engineering technology to achieve lower capital expenditure and early production in the development of oil and gas fields and production facilities is the main goal of the offshore oil industry. This is because on a worldwide basis several major and marginal oil fields exist in the world's oceans and offshore infrastructure such as fixed jacket platforms, semi submersibles and FPSOs are required for their exploitation. The hydrodynamics of offshore structures becomes an important subject in the design and analysis of these structures when lower capital expenditure (CAPEX) and safety requirements are required. The important areas of concern in the wave - structure interactions are such topics as:

Impact loads on fixed vertical columns;

Green Water on FPSOs in storm conditions;

Slamming loads on semi submersibles with multiple columns.

These problems are encountered due to random non-linear extreme free surface waves interacting with structures.

The goal of the research is to carry out an experimental study to investigate the green water phenomenon on floating production storage and offloading vessel in storm conditions and the establishment of a numerical modelling technique for simulating and analyzing the water flow behaviour on deck and the impact on a deck structure. The literature review reveals that green water is a problem that has been researched extensively but indicates a need for further study in the flow behaviour on deck and the loading process on the structures on deck.

1.2.1 Research Objectives.

The explicit objectives of the research are:

To gain a clear insight into the phenomena of green water events occurring for Floating Production Storage and Offloading systems (FPSOs) located in extreme sea environmental conditions;

To carry out experiments on a model FPSO, and obtain quantitative measurements of green water phenomena;

To use experimental data from this study and empirical relationships from previous research work(Buchner, 2002) to develop a numerical methodology capable of simulating the behaviour of green water flow on deck and predicting the impact loading on the deck structure of a moored FPSO;

To assess the performance of the approach by comparing numerical and experimental results.

1.3 Structure of the Thesis

This work is organized into six chapters, beginning with an introduction to the topic of the Green Water phenomenon and the problems it poses to the offshore oil and gas industry, and leading in to the objectives of this study. In Chapter 2, the numerical modelling methods that are commonly used for predicting and analysing green water incidents are appraised. The methods are highlighted based on Eulerian and Lagrangian approaches to wave structure interaction analysis, with emphasis on their ability to predict some aspects of green water events.

Chapter 3 focuses on the Moving Particle Semi-implicit method (MPS). The chapter describes the method and the algorithm leading to the solution of the Navier Stokes equation in the MPS format and highlights some of its drawbacks. Finally the formulation the MPS method used in the green water calculations has been applied to a wedge entry problem to illustrate its capabilities in a relevant and well documented application.

Chapter 4 describes the experiment carried out at the MAST hydrodynamic laboratory of Newcastle University on green water phenomena. The experimental set up is discussed and statistical analysis of the measured waves is carried out for both regular and irregular waves.

Chapter 5 discusses the Green Water phenomena and presents the associated experimental results, including the profiles of water on deck, and the pressures and forces on the deck and the deck structure of a model FPSO. Experimental data and numerical results obtained from a simulation of green water incident using the MPS method are reviewed in a way to gain further understanding of the green water phenomena

Chapter 6 closes the thesis summarizing the major conclusions of this work, presenting its contribution to hydrodynamic modelling of green water phenomena and giving some indication of which aspects of the model could be improved, and future work to be done in order to implement these ideas.

CHAPTER 2

NUMERICAL MODELLING IN HYDRODYNAMICS

Computer simulations are now a requirement for the analysis of various areas of engineering problems. In the field of offshore engineering, many linear and nonlinear problems in hydrodynamics that were difficult to analyze are now being modelled with numerical schemes. This chapter discusses some of the various computer simulation techniques that have been applied in numerical methods to wave – structure interaction problems with particular emphasis on green water. These techniques have progressively attracted attention and brought about great advances in computational fluid dynamics. The level of success of these computational methods can be attributed to the amount of computer power available and the solutions to complicated free surface flow problems which involve the development of a robust numerical implementation scheme. Wave – structure interaction study focuses on the following aspects (a) the change in the characteristics of the relative wave motion due to the presence of a structure, (b) the wave induced loads on the structure and (c) the dynamic response (motion) of the structure, if it is floating, due to the wave loads and its effect from the further change of relative wave motion. Several researchers have modelled one or all of these aspects of wave – structure interaction and summary reviews are giving below.

2.1 Literature review on modelling of Wave – Structure Interactions

The historical development of the scientific study of wave – structure interactions began in the early 18th century with the famous works of Euler, Bernoulli, Poisson , Froude and Newton. These scientists were able to establish and achieve successes in the development of theories by presenting highly theoretical formulations and experiments to investigate wave structure interactions.
The study of wave structure interactions has since progressed immensely with today's use of modern computers. New methods for simulating and analysing wave - structure interactions have undergone development using numerical computational methods but with the mathematical formulations of the 18th century scientists remaining as the foundations for any computational study.

More recent works investigating the science surrounding floating bodies has been carried out by a number of researchers interested in the interactions between waves and marine structures.

In the mid-20th century, Porter (1960) developed a linearized theory for the pressure distributions, added mass and damping coefficients for horizontal cylinders oscillating vertically with small amplitudes while semi immersed in the free surface of a fluid of uniform depth. Using the theory of infinitesimal waves, he formulated the problem as a linearized boundary value problem. He was able to compute the expansion coefficients for the case of a circular cylinder and the pressure fluctuations at several locations on the surface of a circular cylinder. Two dimensional conditions were simulated.

Two decades later, Chapman (1979) presented a numerical method for solving the transient two dimensional flow induced by the motion of a floating body. The method lineralized the free surface and allowed the computation of large amplitude motion of the body. In this approach, the flow was divided into the wave field and the impulsive flow conditions that satisfy the instantaneous body boundary conditions.

Representation of the wave field was by a finite sum of harmonics and an efficient representation over specified time and space intervals was achieved by non-uniform spacing of the harmonic components.

The source distribution method was used in representing the portion of the body under the free surface water line. Two examples of transient fluid structure interactions were presented, namely water entry of a wedge in a restrained mode of motion, and a rectangular body in a free or unrestrained mode of motion.

Modelling bodies interacting with the free surface involves a number of difficult issues. Lin et al. (1984) addressed the problems associated with singular flow at the intersection of the body and the free surface and secondly the difficulty in imposing a radiation condition at infinity. They investigated the singularity at the intersection of a wave maker and the free surface by constructing a two dimensional model of a non-linear wave maker in a rectangular domain of finite length and depth. An algorithm to analyse the prescribed complex potential at the intersection point was developed. They validated their scheme by demonstrating several computational examples for transient heaving motions and with experimental observations.

Many models of free surface interactions were developed from the mid '80s and into the '90s. Andersen and Wuzhou (1985) developed a numerical method for calculating the two dimensional hydrodynamic coefficients of arbitrarily long cylinders forced to oscillate in or below the free water surface. In the method, the oscillation modes, amplitude and phases of the cylinders could be of different values and special considerations were given to radiation boundary conditions. Their computer program involved a Green's function technique and an eigen function expansion in the far field. They presented numerical results for oscillating cylinders under various boundary conditions. A more practical application of free surface modelling techniques was provided by Elsimillawy and Miller (1986) who carried out investigations on the dynamic stability of a fishing vessel. A time domain numerical simulation of the vessel motions was computed in six degrees of freedom with sinusoidal waves. The method calculated the coefficients of the equation of motion at each time step taking into consideration the exact wave and vessel position using strip theory. The results of the study concluded that the ship's oscillatory motions have the most influence on the righting moment.

A whole series of further time domain solutions to free surface problems was developed over this period.

Wang and Spaulding (1988) formulated a two dimensional potential flow model to predict the wave field and forces generated by a semi submerged body in forced heaving motion. A boundary fitted coordinate system was used to represent the free surface and the heaving body. The coordinate system deformed in response to the motions initiated by the free surface and heaving body. In the investigation of the model computational characteristics, a series of sensitivity studies of grid size and resolution, time step, free surface and body grid redistribution schemes, convergence criteria and free surface body boundary condition specifications were performed. The numerical study confirmed that the model predictions were in good agreement with second order theories, experimental data and showed that third order terms were important when nonlinearities exist. In another study by Spaulding and his co investigators(1990) a two dimensional model to predict the wave and flow fields generated by a wedge, circular and semi-circular cylinders and ship shaped bodies in forced heaving motion was developed. A boundary fitted coordinate system modelling the full nonlinear free surface conditions was used to solve the potential flow equations. The results for the force coefficients and phase angles, together with the hydrodynamic properties of added mass and damping coefficients of the heaving bodies were found to be in good agreement with other research data and analytical theories.

A variety of approaches have been taken for modelling freely floating bodies from the late '90s until present. Sen. (1993) modelled the motions of two dimensional floating bodies subject to an incoming wave train. He used an Eulerian frame of reference, and developed an algorithm based on a boundary integral formulation and time stepping technique for the free surface constraints. In his paper, the simulation of large heave and roll motions as well as drifting of a rectangular body were illustrated and discussed. The numerical model results were validated with a wave tank model test. Another boundary integral approach was taken by Chan and Calisal (1993) who developed a numerical procedure for time domain wave - making problems. A Lagrangian notation was used to define the free surface boundary condition. Small time increment values were obtained from the solutions of linear and nonlinear free surface conditions.

Two and three dimensional surface wave problems were simulated with good results obtained and in agreement with measured values from other research works. Wave - structure interaction problems simulated with the procedure included surface waves in a towing tank, a ship's bow wave calculation and wave diffraction problem for a surface piercing cylinder.

A fully nonlinear fluid - body interaction problem was modelled by Tanizawa (1996) in the time domain. The significance of the procedure he developed lay in the formulation of a hydrodynamic pressure computation introducing the nonlinear acceleration potential in the acceleration field equations. To demonstrate the capabilities of the method, he simulated large amplitude motion of a two dimensional midship section body in a wave basin. A time domain study of nonlinear heave radiation forces on two dimensional single and double hulls was also carried out by Maiti and Sen (2001) using a mixed Eulerian - Lagrangian (MEL) model based on a coupled integral relation formulation and time - integration of the nonlinear free surface boundary conditions. Steady state force histories were computed in a numerical wave tank with wave absorbing beaches at the far ends. Computations for radiation forces and hydrodynamic properties in terms of added mass and damping for a rectangular body were presented and discussed. Triangular single and twin hulls geometries were simulated with results of radiation forces presented.

Wave- structure interaction still remains one of the most complex areas of study in marine science. Despite extensive research in numerical computational models for the study of wave - structure interactions, a requirement for further development still exists. The limitations of the current methods can be attributed to the fundamental complexity of the science of wave – structure interactions studies. This complexity has its origins in the fact that wave -structure interaction presents itself as a single entity with respect to a relationship of two systems. A “hydrodynamic symbiosis" is created when a wave and a floating body interact with each other. The effect of the wave system on the floating body produces its motion and the floating body system in turn induces some influence in the behaviour of the waves surrounding it.

Nonlinear analysis of wave structure interactions continues to be amongst the most popular researched and studied areas of marine hydrodynamics recently. However, linear theory still forms the basis for a rational establishment of the linearized boundary condition on the following assumptions;

a) That the incident wave and resultant body motions are small.

b) Inertia effects resulting from the fluid structure interaction are taken into account in the equations of motion by including the hydrodynamic properties.

Experimental observations have shown that the predictions of wave structure interactions have been fulfilled significantly by linear analysis. Developments in offshore engineering have also shown that linear analysis has successfully predicted good results when applied to variety of fluid loading conditions.

However, some computational problems still exists when non linear effects become dominant in wave - structure interactions, such as wave breaking, slamming, jet impingement and complicated contact problems in fluid flow. The importance of modelling these phenomena where they relate to the survivability of the structure becomes a matter for urgent research and study as methods based on linear analysis are inadequate for such problems. The various numerical modelling methods currently applied in green water modelling will be reviewed in this chapter. These methods are made distinct by the two approaches governing the numerical methods for undertaking wave structure interaction simulation. namely the *Eulerian concept* and the *Lagrangian concept.*

2. 1.1 The Eulerian and Lagrangian Concepts in Fluid Dynamics

The Eulerian concept is to think of the observer as standing on the side lines watching the fluid move past the area of interest. The Eulerian approach is also called a *grid method*. The Lagrangian concept has the observer moving along with the flow. The Lagrangian approach is also called a *Particle Method.* The various numerical computation schemes linked to these two approaches are briefly summarized to acknowledge their importance in providing solutions to wave structure interaction with particular reference to green water problems.

Each of these methods is a topic of research on its own and extensive literature is available on them in the various engineering disciplines in which they are used.

2.1.1.1 The Eulerian Concept

The ability to track behaviour and attributes as fluid flows past objects fixed in space is the Eulerian concept to describing fluid motion. In the Eulerian framework, a fixed reference frame is employed relative to which a fluid is in motion. Time and spatial position in this reference frame $[x,t]$, are used as independent variables. The physical and thermodynamics variables of the fluid such as mass, density, pressure, flow velocity and temperature which describe the properties of the fluid flow in question are dependent variables - as they are functions of the independent variable. Thus their derivatives are partial with respect to $[x,t]$.

For example, the flow velocity at a spatial position x and time t is given by $u(x,t)$, and the local acceleration a at this position and time is then

$$a = \frac{\partial u(x,t)}{\partial t}\Big|_x \qquad (2.1)$$

where the notation signifies that x is kept constant i.e., the time derivative is for the same position.

2.1.1.2 The Lagrangian Concept

Tracking the behaviour and motion of fluid particles as they move with the flow is the Lagrangian Concept. In the Lagrangian framework, the fluid is described in terms of its constituent fluid particles. Different fluid particles have different "labels", for example, their spatial positions at a certain fixed time t, say c. The independent variables are thus $[c,t]$, and the particle position $x(c,t)$ is a dependent variable. One can then ask about the rate of change in time in a reference frame co - moving with the fluid particle, and this then depends on the time and particle label, i.e. which particular fluid particle is being followed.

For example, if a fluid particle has some velocity $u(c,t)$, then the acceleration a will be;

$$a = \frac{\partial u(c,t)}{\partial t}\Big|_c \tag{2.2}$$

where the notation signifies that c is kept constant i.e. the time derivative is for the same fluid particles.

Since the velocity of a point particle is equal to the rate of change of its position x, we may write

$$u(c,t) = \left(\frac{\partial x}{\partial t}\right)\Big|_c \tag{2.3}$$

To this end, we have at our disposal two sets of independent variables that we can use to describe a flow: The Eulerian set (x,t) and the Lagrangian set (c,t). The relationship between the partial derivatives of a function f with respect to these two sets can be established by means of the material derivative $\frac{D}{Dt}$.(Pozerikidis, 1997).

$$\frac{Df}{Dt} == \frac{\partial f}{\partial t} + \vec{U} \bullet \nabla f \tag{2.4}$$

The term $\vec{U}$ is the fluid velocity with components (u,v,w) and ∇ is the vector differential operator.

Equation (2.4) relates the material derivative to the temporal and spatial derivatives with respect to the Eulerian variables. When all point particles, maintain their value of f as they move about the domain of flow, then $\frac{Df}{Dt} = 0$ for all values of c, and we say that the field represented by f is "connected by the flow".

The Equations of motion in fluid dynamics form a complicated coupled system of nonlinear partial differential equations of different orders. As there are no general solutions to these difficult equation systems, computational fluid dynamics (CFD) provides the opportunity to thoroughly study fluid dynamics using computer simulations.

The distinction between the Eulerian concept and the Lagrangian concept leads to different ways to solve the problems of fluid dynamics using computer simulations. In the Eulerian Concept, the fluid is divided into a finite set of cells, each storing numbers for the fluid variables of a given flow. The partial differential equations of fluid dynamics are then solved numerically over this finite set of points. Traditional numerical modelling methods such as the Finite Element Method (FEM), Finite Difference Method (FD), Finite Volume (FV) and Boundary Element Method (BEM) use the Eulerian approach. In the Lagrangian concept, the fluid is divided into a finite set of fluid "elements" (or simulation particles), each of which has a stored position and velocity. The evolution of the fluid is simulated by solving the equations of motion for all of the simulation particles. If the fluid variables are required at any particular point in space, then simulation particles in the vicinity of that point are found and then the corresponding quantities averaged. Particle methods that have been developed for the full Lagrangian approach are Smoothed Particle Hydrodynamics (SPH) and Moving Particle Semi Implicit Method (MPS).

Recent developments tend towards a mixture of these concepts in application to fluid flow problems and this will probably be the way forward in application to complex flow problems in hydrodynamics of offshore structures.

In fluid dynamics, however, both Eulerian and Lagrangian concepts have been used with considerable success. Because each concept presentation has unique advantage and disadvantages, the choice of which one to use depends on the characteristics of the problem to be solved.

2.2 Recently Applied Numerical Methods to Green water problem

2.2.1 Requirements for numerical methods.

Experimental investigations (Buchner, 2002; Han, 2003) have provided the relevant information about extreme free surface motion and the complex nonlinear nature of green water phenomena. These studies have given insight and understanding into the main phases that occur during a green water event and can be summarised below as follows;

1. A wave builds up as a solid wall of water around the bow area.
2. There is a sudden crash of water on deck similar to a dam breaking scenario
3. High velocity shallow water flow on deck ensues
4. The water runs up the front of a deck structure, and impact loading on the structure occurs, with water plunging back on deck after impact.

Prediction methods have advanced progressively in the study of wave structure interactions in the last decade and numerical investigation of green water phenomena continues to be a significant research area for offshore structures. In this chapter some of the numerical methods applied to green water phenomena are discussed and evaluated on the basis of their ability to predict the main phases observed in experimental investigations of green water. The knowledge gained from experimental studies describing the phases in a green water event enables us to determine the relevant requirements that would be needed to develop a suitable prediction method for the simulation and analysis of a wave structure interaction such as a green water event. Specifically, a numerical method should be able to simulate and analyze a green water occurrence with the following features;

1. The build-up of a solid mass of water in the flared bow structure resulting from a wave overtopping the bow area.
2. An extreme free surface motion and violent flow on deck
3. The impact loading on a deck structure for a short period of time.
4. The plunging of water back on deck after impact on deck structure.

On the basis of the above requirements several numerical methods are considered for discussion on their ability to simulate and analyze green water effects on floating structures. It is not the intention of this study to provide numerical details of these methods but to explain the general approach associated to these methods. The literature review sections in the first chapter provide detailed information to relevant research studies that have used these numerical methods.

2.2.2 Appraisal of numerical methods.

The numerical prediction methods and studies relating to complex nonlinear free surface flows are numerous and the present appraisal of some of these methods does not imply that a complete exercise has been carried out in this thesis. The discussion focuses on five methods that are frequently used in marine hydrodynamics and are categorised into two groups by the approach of their modelling concepts, Eulerian and Lagrangian.

- **The Eulerian approach**

The methods following the Eulerian approach evaluated are;

1. Random Choice Method
2. Finite Volume Method
3. Volume of Fluid Method(VOF)

- **The Lagrangian approach**

The methods following the Lagrangian approach evaluated are;

1. Smooth Particle Hydrodynamics (SPH).
2. Moving Particle Semi Implicit method (MPS).

2.2.2.1 The Random Choice Method.

The method was applied to green water loading on FPSO by Han (2003). The method was used to solve the shallow water wave equations of green water occurrence on a moving deck of a moored FPSO. To calculate the water flow on deck in the time domain, the deck area was partitioned into two dimensional grid points and a system of nonlinear hyperbolic equations of motion were solved numerically using the random choice method. By solving the inhomogeneous nonlinear partial differential equations, the water depth and the velocities at each grid point was obtained at each time step. The method is particularly attractive because it can handle flows with multiple shocks, hydraulic jumps and the cases where the deck becomes partially dry. Buchner (2002) compared the results of the method with experimental results of a regular wave and after evaluation came to the conclusions summarised below;

- The random choice method cannot be used on its own when the relative wave motions around the bow and flow onto the bow are to be considered. This is the result of shallow water theory being applied in the formulation, which limits its applicability to water flow onto the deck. The application of the method is however effective in the study of green water on ship motions.
- Another setback is the assumption of constant velocity at the grid points, thus limiting the prediction of green water impact loading on vertical structures.
- The method cannot handle wave overtopping and the plunging phase of a green water event.

The random choice method has some positive attributes such as the ability to handle the effects of green water on ship motions and the global hull girder bending which was investigated in the work of Han (2003). However, to meet the stated requirements that evolve in a green water event, other methods will need to be considered.

2.2.2.2 Finite Volume Method.

Finite Volume Method (FVM) can be regarded as the integral formulation of the conservation equation, with the solution domain established over a finite volume of contiguous control volumes around nodal or grid points. Two main features of the FVM are that the discretization can ensure mass, momentum and energy conservation in each computational cell or small control volume, and unstructured meshes can be used to define complex geometries. The finite volume method is popular with CFD applications in general fluid problems and the formulation is used in commercial software such as FLUENT, FLOW3D, and PHOENICS for 3D Navier Stokes Equation (NSE) solvers. In wave structure interaction problems, the finite volume method can be applied to a problem with irregular physical domain by using boundary conformal meshes. Ai and Jin (2010) used the FVM to simulate non linear waves interacting with a coastal structure. The control domain was established with a 3D grid system made of polyhedrons to solve the unsteady Navier Stokes equation. Test cases which involved modelling of solitary waves interacting with a submerged structure, solitary waves scattering from a cylinder and an array of four cylinders were investigated to verify the capability of the model in the simulation of nonlinear waves interacting with structures.

Sames (2002) introduced the Finite Volume method for the prediction of the loads due to green water impact on the forward bulkhead of the superstructure of a RORO passenger ferry. This is an aspect of the green water event which has been successfully investigated.

However, FVM will have limitations adequately simulating other phases of the green water event which involves wave overtopping, jet impingement and wave plunging back on deck mainly because of its Eulerian characteristics, and will require more detailed studies and further validations.

The free surface is often modelled in the Finite Volume method using the Volume of Fluid approach.

Comment [nmjd1]: Put in VOF section here.

2.2.2.3 The Volume of Fluid Method (VOF)

The volume of fluid method has been applied to the green water phenomena by several researchers amongst which are Buchner (2002), Nielsen and Mayer (2004), Zhu (2006) and Lu (2010) in recent times.

Hirt and Nichols (1981) introduced the volume of fluid (VOF) method. In VOF type methods, the transportation equation of a volume fraction is introduced to describe the evolution of the free surface. Hirt and Nichols (1981) described the VOF technique as a simple, but powerful method that is based on a Euleriaun formulation of a fractional volume of fluid. In VOF in each cell of a mesh it is customary to use one value dependent variable defining the fluid state. The use of several points in a cell to define the region occupied by fluid therefore becomes unnecessarily excessive. Suppose, however, that we define a function F whose value is unity at any point occupied by fluid and zero otherwise. The average value of F in a cell would then represent the fractional volume of the cell occupied by fluid. In particular, a unit value of F would correspond to a cell full of fluid, while a zero value would indicate that the cell contained no fluid. Cells with F values between zero and one must then contain a free surface. Thus the fractional volume of fluid (VOF) method provides the same coarse interface information available to the marker-and-cell particle method.

The VOF method defines which cells contain a boundary and where fluid is located in a boundary cell. The normal direction to the boundary lies in the direction in which the value of F changes most rapidly. Because F is a step function, however, its derivatives must be computed in a special way. When properly computed, the derivatives can then be used to determine the boundary normal. Finally, when both the normal direction and the value of F in a boundary cell are known, a line cutting the cell can be constructed that approximate the interfaces there. This boundary location can then be used in setting of boundary conditions.

Although the VOF technique can locate free boundaries nearly as well as a distribution of marker particles, and with a minimum of stored information, the method is worthless unless an algorithm can be devised for accurately computing the evolution of the F field(Hirt and Nichols,1981). The time dependence of F is governed by the equation.

$$\frac{\partial F}{\partial t} + u\frac{\partial F}{\partial x} + v\frac{\partial F}{\partial y} = 0 \tag{2.5}$$

This equation states that F moves with the fluid, and it is the equivalent partial differential equation analogue of marker particles. Fortunately, the fact that F is a step function with values of zero or one permits the use of a flux approximation that preserves its discontinuous nature. In summary, the VOF method offers a region - following scheme with minimum storage requirements. Furthermore, it follows regions rather than surfaces, all logic problems associated with interesting surfaces are avoided with the VOF technique. The method is also applicable to three dimensional computations, where its conservative use of stored information is highly advantageous. Thus the VOF method provides a simple and economical way to track free boundaries in two-or- three dimensional meshes. In principle, the method could be used to track surfaces of discontinuity in material properties, in tangential velocity, or any other property. The particular case being represented determines the specific boundary condition that must be applied at the location of the boundary. For situations where the surface does not remain fixed in the fluid, but has some additional relative motion, the equation of motion must be modified. Examples of such applications are shock waves, chemical reaction fronts, and boundaries between single phase and two phase fluid regions. The work of Buchner (2002) and Nielsen and Mayer (2004) are reviewed as they are specific to the Volume of Fluid (VOF) method without the coupling of other numerical theories in the application to green water problems.

The application of the VOF method to green water modelling was extensively studied and successfully implemented by Buchner (2002) by simulating the green water problem using empirical and experimental data as initial conditions. The results of the numerical study came in close resemblance to experimental observations and meeting the requirements for green water phenomena.

The relative wave motions obtained from the experiment were used as initial boundary conditions to set up a wall of water around the bow with the VOF method. The flow on deck similar to a dam breaking event and high velocity water jet was simulated successfully and the results were in good agreement with experiment. The impinging water impact of the flow on the structure on the deck with a run up was observed to be similar in nature to experimental observations. The load levels and measured pressure were also in close agreement with measured values from the experiment. However, Buchner (2002) concluded that despite the above good qualities of the VOF method in meeting some of the requirements for green water modelling, the method is sensitive to details of the numerical model close to the free surface and a number of aspects in the numerical model such as the simulation of the moving bodies in the fluid domain require further detailed study.

Nielsen and Mayer (2004) also applied the VOF method to green water modelling. To describe the free surface geometry, an interface capturing scheme similar to the VOF methodology introduced by Hirt and Nichols (1981) was applied, using an implicit representation of the free surface based on volume fractions. Modelling in two and three dimensions was carried out for green water incidents on a fixed (no oscillations) and moving (with oscillations) moored FPSO. The numerical investigation used the VOF method to model the wave generated from a wave maker, wave overtopping the bow of the vessel, flow on deck and computation of the impact load on a deck structure. The numerical results showed good agreement with experimental results in wave heights measurement and water levels on deck, but showed significant discrepancies for the pressure measurements for a fixed vessel in head seas. Satisfactory results could not be obtained for green water on a moving vessel in incident waves.

To date the consensus is that the VOF method can only simulate certain aspects of the green water phenomena when using the results of experimental studies as input information for the initial conditions especially for the water swirl up around the bow region.

Comment [nmjd2]: It is my understanding that the Finite Volume Method uses the Volume of Fluid Method to define the free surface ie, the VOF and the FVM methods can't be thought of as two distinctly different methods.

2.2.2.4 Smoothed Particle Hydrodynamics

Smoothed Particle Hydrodynamics is one of the Lagrangian particle methods in Computational Fluid Dynamics (CFD). Early contributions have been reviewed in several articles - Monaghan (1985); Benz (1990) ; Monaghan (1992,1994), Lucy (1977) and, Gringold and Monaghan (1977) simultaneously developed the Smoothed Particle Hydrodynamics method, which is now called SPH. Further work on SPH was carried out by Petschek and Libersky(1993). The method was initially developed to be used in astrophysical applications where the flows are three dimensional. Astrophysical mechanics involve the formation and evolution of stars or galaxies and their collective movement is similar to the movement of fluid flow in classical hydrodynamics, thus allowing the use of the conservation equation of continuum mechanics. SPH technology has been employed to solve problems of both compressible flow and incompressible flow. Smoothed Particle Hydrodynamics represents a fluid as a collection of particles with local fluid characteristics but instead of calculating flow from one particle to the next, the actual movement of these particles in response to external forces is computed Each one of the these particles has a mass, position and velocity and is influenced by forces such as gravity and characteristics such as density, temperature and pressure forces from the surrounding particles.

The conservation laws of continuum fluid dynamics are transformed into integral equations through the use of an interpolation function that gives the "kernel estimate" of the field variable at a point (Libersky et al. 1993). The term "kernel" refers to a weighting function and defines how much of each field variable contributes to the field variable at some point. Computationally, information is known only at discrete points, so that the integrals are evaluated as sums over neighbouring points. The reason that an underlying grid is not needed is that functions are evaluated using their values at the discrete points (particles) and an interpolation kernel. Schlatter (1999) provides a summary of equations governing the definition of the kernel function $\mathrm{K}(r)$. The idea behind SPH is the determination of the characteristics of a fluid by interpolating from a set of non-ordered points; the particles.

The interpolation is performed using a smoothing kernel W which is a weighted sum over particles within an area defined by a smoothing length h.

The use of smoothed Particles Hydrodynamics as a tool in numerical modelling, as with other traditional particle systems, has been shown to be a successful method for modelling fluid motion. It is a pure Lagrangian particle method with many desirable features such as robustness, conceptual simplicity, ease of adding new physics and the ability to model large scale movements of a fluid due to the use of hydrodynamic equations of motion. Various improvements have been developed on the SPH method through the years. Most of the improvements are aimed at mitigating the following short comings in numerical computation as outlined by Liu and Li(2002):

- Tensile instability. A situation where particles undergo tensile stress resulting in the motion of particles becoming unstable with exponential growth in velocity from small displacements and clumping in a region. Some researchers have suggested methods for tensile stress correction, Randles and Libersky(1996), Monaghan(2000).
- Lack of interpolation consistency or completeness due to smoothing errors. A corrective kernel has to be introduced so that the consistency or completeness of the SPH interpolant can be enforced
- Difficulty in enforcing essential boundary conditions, this due to an inability to accommodate boundary interpolation without special treatment. Ghost particles have to be introduced in most practical computations to overcome this problem.

Besides resolving the above fundamental issues, there has been some progress in the application of SPH to green water phenomena. Gomez – Gesteira et al. (2005) analyzed green water overtopping with the SPH model by modelling an experiment conducted by Cox and Ortega (2002). The study examined the impact of a single wave on a flat deck to study overtopping. In the simulation the SPH model was reasonably capable of reproducing the features of an overtopping sequence, a phase in the green water process and captured a jet like formation in the aft of the deck. Numerical results compared to experimental works of Cox and Ortega (2002) showed very good agreement in wave profile generation and when the wave struck a horizontal platform.

The model met some aspects of the requirements for green water simulation by being able to model the initial water flow, wave overtopping the bow area and further flow restoration on deck.

2.2.2.5 Moving Particle Semi Implicit Method (MPS).

This thesis describes a study investigating the viability of Moving Particle Semi Implicit Method (MPS) as a numerical computational tool for modelling green water phenomena and applications to water flow behaviour on deck. The MPS scheme was chosen for the study because it has the potential for overcoming problems associated with the complexities in the wave - structure interaction boundaries. This is because of the Laplacian operator of the MPS scheme, is modelled as a transient diffusion problem. Part of the physical quantities retained by a MPS particle is distributed to neighbouring particles using a weight function. These physical quantities can be represented as scalars such as pressure, density and viscosity or vectors such as velocity and forces. This characteristic of the method allows it to accommodate constraints that are prohibitive in other more conventional approaches. The typical difficulties encountered in conventional approaches such as the Eulerian methods for wave – structure analysis include: the management of the convective terms and the incompressibility constraint; modelling the free surface; information transfer between fluid and solid; and efficient regridding of the meshes for both structure and fluid. The MPS method has been used extensively by Japanese researchers, and brief reviews of the numerous papers published on various areas of application are presented in the next section.

2.2.2.6 Some Research Work using MPS method.

The application of the MPS method to hydrodynamic problems has been implemented since Koshizuka and Oka (1996) developed and advocated the method for incompressible flows. They successfully implemented the method by applying it to the collapse of a water column. Both experimental development and numerical simulations were carried out and fluid fragmentation was successfully simulated with comparison between experimental and numerical results being in good agreement.

The MPS method was later applied to numerical simulation of breaking waves on slopes by Koshizuka et al. (1998). They considered two types of breaking waves, plunging and spilling breakers together with breaking waves modelled with a passively moving submerged float. A particle gridless method based on MPS method was presented by Yoon et al. (1999) for incompressible flows. The method was applied to the analysis of sloshing problems. The amplitude and period in a sloshing simulation were predicted by the method.

In 1999, Gotoh and Sakai (1999) performed a Lagrangian simulation of breaking waves using the MPS method. In their study, the breaking waves were simulated on several sea bed bottom configurations, namely a uniform bed slope, a permeable bed with uniform slope and a vertical wall with a small foot step. The time series of the water surface profiles and the velocity fields were displayed to show the performance of the MPS method in the wave breaking simulations. An Arbitrary Lagrangian – Eulerian (ALE) scheme was developed by Koshizuka and Oka (2000) combining heat transfer calculations with MPS. The combined method was used to analyze a range of thermal hydraulic problems. Bubble growth and departure in a nucleate boiling environment were calculated and the heat transfer result was shown to be in good agreement with experimental results. Another extension of the basic MPS method was made by Shirakawa et al. (2001) who developed the MPS method to allow application to two fluid systems, introducing a potential type surface tension, and modifying the calculation algorithm to simulate jet flows. The objective of the study was to evaluate the interfacial area (or so called binary contact area) of two immiscible fluid systems with a chemical reaction, where one is injected as a jet pool into the other fluid.

Working at an altogether different scale Gotoh et al. (2001) used the MPS method to simulate the generation process of a tsunami due to a large scale landslide. The inflow sediment induced water wave generation was investigated using a MPS model of solid – liquid two phase flow. The physical process of the wave generation was clarified in detail by tracking the sediment water mixing process and the resultant momentum transfer from sediment to water. The time series of the water surface elevation were compared with some alternative wave generating methods, to estimate the wave making efficiency of inflow sediment.

In another paper on tsunamis, Hayashi et al. (2003) proposed an erosion model combined with the MPS method. The tsunami that overtopped the crown of a sea wall caused a large scale return flow, which induced a dropping jet colliding with the sand beach in the front of the sea wall, and resultant toe scouring of sea wall. The erosion model installed in the MPS method was able to cope with the drastic change of the water surface flexibility, and carry out numerical simulation of the time dependent process of toe scouring of the sea wall due to the dropping jet.

In another simulation of a difficult natural phenomenon in extreme conditions, Gotoh et al. (2002) conducted a simulation using a high level procedure in the MPS method. The approach was extended by using the rigid body tracking routines, to analyze the triple interaction between a fixed structure, a water flow and floats. The computation was carried out to model the submerging process of ice floes beneath the ice cover induced by a wave and uni-directional flow.

In a variant of the basic method Gotoh et al. (2001) proposed the use of a sub particle scale (SPS) turbulence model. The MPS method with the SPS turbulence model was applied to the turbulent mixing layer, or the turbulent free jet, to show its performance on the simulation of a turbulent flow with a simple structure. The mean velocity profile was compared with previous experiments. The unsteady behaviour of the jet and mixing process at the interface of the jet and the still water were displayed and snapshots of the particle motion presented. Another numerical simulation using the MPS method, in which the SPS turbulence model was included, was carried out by Gotoh et al. (2001) to take Sub Particle Scale characteristics of turbulence under the wave breaking and run up process into consideration. Furthermore, the optimization of the particle scale acted to filter out pressure fluctuations, which became a key factor in the evaluation of the SPS turbulence model examined through the wave number spectrum of the velocity fluctuation. The result of the numerical simulation showed that the SPS turbulence model works effectively at least for the phenomenon at laboratory scales.

Gotoh et al. (2002) also used the MPS method to analyze solid-liquid two phase flow. They recognized that a soft bottom mud which is easily entrained sometimes brings a problem of turbidity.

The ordinary layered fluid model for the wave induced sea bed motion, which assumes the existence of the sinusoidal curved interfaces of fluid and mud layers, cannot be applied to a wave breaking.

To overcome this limitation of the layered fluid model, the wave sea bed interaction was simulated using an approach based on the MPS method.

A more complex problem involving a violent free surface flow in marine engineering was presented by Naito and Sueyoshi (2003). They applied MPS method to the problem of sloshing on large car decks, which is an extremely nonlinear and complex free surface flow problem. The investigation carried out looks at the free surface simulation of large amplitude forced roll oscillations on a RORO ship. Time series of force and moment from fluid on the deck and free surface profiles of the water were presented. Zhang et al. (2006) proposed an improvement to the MPS method by introducing additional coefficients to the Laplacian term in the MPS method in its application to convective heat transfer problems. The improvement was proposed to help with calculation stability for flows in an enclosure. The improved method was applied to a Rayleigh – Benard convection phenomena and showed the efficacy of the proposed improved model and method on a numerical simulation of convective heat transfer problem. Lee et al. (2007) demonstrated that the MPS method can be coupled to Eulerian methods such as the finite element method in the analysis of a fluid – shell structure interaction analysis. To demonstrate the coupling scheme, simulation of a sloshing phenomenon was investigated in an elastic thin shell structure. Observation of the investigation showed fluid fragmentation and large structural deformations. Sun et al. (2009), using the MPS method, developed for two viscous fluids a stir mixing process. To understand the flow process and mixing mechanism, the motion of the fluid particles was followed. The results gave useful qualitative suggestions on controlling the mixing rate during chemical reactions.

Khayyer and Gotoh (2009) raised some concerns with regards to the ability of the original MPS method proposed by Koshizuka and Oka (1996) to adequately estimate correctly impact pressure computations.

They introduced a Corrected MPS method (CMPS) for the prediction of wave impact pressure on a coastal structure by proposing new formations to the pressure gradient term and the modification of the Poisson Pressure Equation. Several wave impact studies were examined with the new method and results compared with experimental data showed good agreement.

2.3 Conclusion

The importance of this chapter is to provide the relevant information on the various numerical modelling methods in use for hydrodynamic process simulation. In any Numerical Modelling application, the hydrodynamic concept to follow must first be understood in terms of Eulerian and Langragian approaches. Which theory does the problem fit into much better in terms of approach to solution? The choice of an Eulerian concept introduces the application of a grid method and the choice of a Langragian concept introduces the particle method.

Several of the appraised methods in Section 2.2 have been developed into computer codes for the simulation and analysis of different aspects of engineering applications, but MPS method appears to offer the most benefit with respect to the requirements of the green water problem.

CHAPTER 3

MOVING PARTICLE SEMI- IMPLICIT METHOD.

3.1 Formulation of the MPS Method

Particle methods aim to represent the behaviour of a fluid by modelling it as a collection of particles. Each particle moves accordingly with its own mass and the internal and/or external forces applied to it. External forces are evaluated from the interaction of neighbouring dictated by simple rules.

A particle may be a physical part of the domain or a specific part of the continuous domain. Another characteristic of particle methods is that all the physical and mathematical properties of the domain at the point occupied by the particle are attached to the particle itself and not to the elements. For instance physical properties like viscosity or density, physical variables like velocity, temperature, or pressure and also mathematical variables like gradients or volumetric deformations are assigned to each particle and they represent an average of the property around the particle position.

Governing equations.

An incompressible flow is expressed by the following continuity equation and the Navier Stokes equations;

$$\frac{1}{\rho}\frac{D\rho}{Dt} = -\nabla \bullet \vec{U} \tag{3.1}$$

$$\frac{D\vec{U}}{Dt} = -\frac{1}{\rho}\nabla p + \nu\nabla^2\vec{U} + \vec{F} \tag{3.2}$$

where $\vec{U}$ is the fluid velocity vector with components (u, v, w), t is the time , ρ is the density of the fluid, ν is the kinematic viscosity, p is the pressure, $\vec{F}$ is the acceleration vector due to external force and ∇ is the vector differential operator. The left hand side of the Navier Stokes equations denotes the Lagrangian derivative including convection terms. They are directly, calculated using the motions of the particles. The right hand side consists of pressure gradient, diffusion and external force terms. The differential operators are expressed as particle interaction models.

3.1.1 Particle Interaction Models.

Kernel.

In a physical model consisting of a set of particles, a particle interacts with its neighbouring particles under the influence of a weight function described by means of a kernel function $W(r)$, where r is the distance between two particles. Koshizuka and Oka (1996) described the kernel function as the smoothing function of physical quantities around the particles.

$$W(r) = \begin{cases} \dfrac{r_e}{r} - 1 & \text{for } r \le r_e \\ 0 & \text{for } r > r_e \end{cases} \tag{3.3}$$

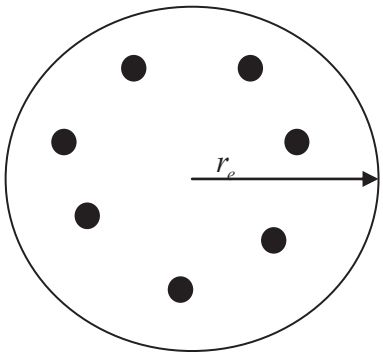

Figure. 3-1 - Interaction area between particles.

The size of the interaction area is restricted by the parameter r_e, see Figure 3.1, which provides the radius of the kernel domain. A particle is expected to interact with a finite number of neighbouring particles bounded within the kernel area due to the restriction imposed by the radius parameter r_e. This characteristic improves the efficiency of computation. This kernel function is infinity at $r = 0$. Koshizuka and Oka (1996) set the value of the kernel size for the gradient model as $r_e = 2.1D_0$ and the size of the Laplacian as $r_e = 4.0D_0$. These values were tuned so that they could obtain from computational results the surface profile of the collapse of a water column to agree with the physical experiment.

A comparison of six different kernel functions were carried out by Ataie-Ashtiani and Farhadi(2006) using the collapse of water column experiment and the MPS method to determine the stability and performance of these kernel functions. They showed that the kernel function in equation (3.3) proposed by Koshizuka and Oka (1996) was successful to simulate the collapse of water column experiment until water impacts on the left vertical wall at about 1s, but after that instability occurred and concluded that by using the equation (3.3), the method used for solving the system of linear equations significantly influences the numerical stability and computation time of the MPS method. They used the Gauss elimination and Gauss – Seidel equation solvers. By introducing an artificial error into the Gauss – Seidel linear equation solver they were able to overcome the instability problem. They suggested a new kernel function proposed by Shao and Lo (2003) for simulating free surface water using SPH to improve stability of the MPS method when used in the collapse of water column experiment. This study used the kernel function in equation (3.3) and the Incomplete Cholesky Conjugate Gradient Method as the equation solver to maintain stability as proposed by Koshizuka and Oka (1996).

Particle number density

In a kernel area consisting of a particle i, with a position vector r_i and interacting with neighbouring particles j, the particle number density of particle i is defined by

$$\langle n \rangle_i = \sum_{j \neq i} W\left(\left| r_j - r_i \right|\right) \tag{3.4}$$

In this equation, the influence of the weight function from particle i itself is not considered. When the number of particles in a unit volume is quantified as $\langle N \rangle_i$, the relation between $\langle n \rangle_i$ and $\langle N_i \rangle$ is written as; (Koshizuka and Oka, 1996)

$$\langle N \rangle_i = \frac{\langle n_i \rangle}{\int_V W(r) dv} \tag{3.5}$$

The denominator of the right hand side of equation (3.5) is the integration of the kernel in the whole domain. Assuming that the particles have the same mass, we can see that the fluid density is proportional to the particle number density.

$$\langle \rho \rangle_i = m \langle N \rangle_i = \frac{m \langle n \rangle_i}{\int_V W(r) dV} \tag{3.6}$$

For an incompressible fluid, the fluid density must remain constant and the continuity equation satisfied. The particle density number plays a significant role in this aspect of the formulation because it needs to be modified at each step to maintain incompressibility. The section on modelling incompressibility further provides an explanation of the role of the particle density number.

3.1.2 Modelling of the Gradient Vector

The Navier Stokes equations (3.2) which are denoted in differential form are expressed with gradient and Laplacian operators.

Within a kernel area in a given physical model, a gradient vector can be evaluated between two particles i and j possessing physical quantities ϕ_i and ϕ_j, at position vectors r_i and r_j. A gradient vector can be evaluated with any combination of particles in a kernel area. The gradient vector of a particle i, with coordinate vector r_i is obtained from the weighted average of the neighbouring particles j with respect to the kernel function. The differential operator is then expressed as a gradient vector at particle i as follows;

$$\langle \nabla \phi \rangle_i = \frac{d}{n^0} \sum_{j \neq i} \left[\frac{\phi_j - \phi_i}{\left| r_j - r_i \right|^2} (r_j - r_i) W\left(\left| r_j - r_i \right| \right) \right] \qquad (3.7)$$

where d is the number of space dimensions and n^0 is the constant particle number density which can be obtained from equation (3.4). For the pressure gradient terms of the Navier Stokes equation, the gradient model of the MPS is applied in the discretization process as follows,

$$-\frac{1}{\rho} \langle \nabla p \rangle_i = -\frac{1}{\rho} \frac{d}{n^0} \sum_{j \neq i} \left[\frac{p_j - p_i}{\left| r_j - r_i \right|^2} (r_j - r_i) W\left(\left| r_j - r_i \right| \right) \right] \qquad (3.8)$$

3.1.3 Modelling the Laplacian

The Laplacian model is defined as a time dependent diffusion problem involving a physical quantity ϕ. The conservation law due to diffusion can be expressed as (Ghoniem and Sherman, 1985).

$$\frac{\partial \phi}{\partial t} = \vartheta \nabla^2 \phi \tag{3.9}$$

where ϑ is the diffusion coefficient and here ∇^2 is the Laplacian.

Each particle is carrying a finite amount of the diffusing physical quantity and the displacement of the particles with time is taken to follow a Gaussian distribution with a growing variance. For a time interval Δt, an increase of the variance of the distribution of ϕ is equal to, (Ghoniem and Sherman, 1979)

$$\Delta \sigma^2 = 2d\vartheta \Delta t \tag{3.10}$$

where d is the number of space dimension. That is if the problem is conceptualized in 2 Dimensions, then d will be equal to 2 or in 3 Dimensions, d will be 3. In this MPS model, the physical quantities ϕ_i, belonging to particle i are distributed to the neighbouring particles using the kernel function so that the variance increase is equal to $2d\vartheta\Delta t$. Thus the disretized representation of the physical quantity transferred from particle i to j is written as (Koshizuka and Oka, 1996)

$$\nabla \phi_{i \to j} = \frac{2d\vartheta \Delta t}{n^0 \lambda} \phi_i W\left(\left| r_j - r_i \right|\right) \tag{3.11}$$

where,

$$\lambda = \frac{\int_v W(r) r^2 dv}{\int_v W(r) dv} \tag{3.12}$$

The coefficient λ is introduced to allow for the increase of variance $\Delta \sigma^2$ in Δt due to the redistribution of physical quantities to equal the increase that could have been obtained from the analytical solution of the diffusion equation.

This will ensure that the iterative redistribution converges to the Gaussian distribution.

λ can be approximated if for the time interval Δt, the variance increase in equation (3.9) is discretized as the sum of the variances of physical properties transferred from particle i to particle j. This is expressed as,

$$\Delta\sigma^2 = \frac{2d\vartheta\Delta t}{n^0\lambda}\sum_{j\neq i}\left[\left|r_j - r_i\right|^2(\phi_j - \phi_i)W\left(\left|r_j - r_i\right|\right)\right] \qquad (3.13)$$

If we consider the case where $\phi_j = 0$ and $\phi_i = 1$, equation (3.13) can be reduced to

$$\Delta\sigma^2 = \frac{2d\vartheta\Delta t}{n^0\lambda}\sum_{j\neq i}\left[\left|r_j - r_i\right|^2 W\left(\left|r_j - r_i\right|\right)\right] \qquad (3.14)$$

Comparing equation (3.10) and equation (3.14), we have

$$2d\vartheta\Delta t = \frac{2d\vartheta\Delta t}{n^0\lambda}\sum_{j\neq i}\left[\left|r_j - r_i\right|^2 W\left(\left|r_j - r_i\right|\right)\right] \qquad (3.15)$$

where by cancelling common terms we get to the next equation

$$\frac{\sum_{j\neq i}\left[\left|r_j - r_j\right|^2 W\left(\left|r_j - r_i\right|\right)\right]}{n^0\lambda} = 1 \qquad (3.16)$$

where n^0 is given by equation (3.4). Thus λ can be represented by

$$\lambda = \frac{\sum_{j\neq i}\left[\left|r_j - r_i\right|^2 W\left(\left|r_j - r_i\right|\right)\right]}{\sum_{j\neq i} W\left(\left|r_j - r_i\right|\right)} \qquad (3.17)$$

If we consider diffusion as a linear process, then distribution of physical quantities from one particle to others within a kernel area can be superimposed. As a result an approximate expression for the Laplacian model is given by Koshizuka and Oka, (1996);

$$\left\langle \nabla^2 \phi \right\rangle_i = \frac{2d}{n^0 \lambda} \sum_{j \neq i} \left(\phi_j - \phi_i \right) W\left(\left| r_j - r_i \right| \right) \tag{3.18}$$

The model of the Laplacian is conservative since the physical quantity lost by particle i is exactly received by particle j. The viscous term of the Navier Stokes equation can be represented by using the discretized formulation of the Laplacian model stated as equation (3.18) and expressed as follows,

$$\nu \left\langle \nabla^2 U \right\rangle_i = \frac{2d\nu}{n^0 \lambda} \sum_{j \neq i} \left(U_j - U_i \right) W\left(\left| r_j - r_i \right| \right) \tag{3.19}$$

3.1.4 Modelling Incompressibility

In an incompressible flow field, the continuity equation requires that the fluid be incompressible at every location in the fluid. Incompressibility is maintained if the fluid density is kept constant, hence in the MPS method, the particle number density being made constant, n^0. When the particle number density n^* (* the first sub process) is the temporary particle number computed in the explicit first sub process deviates from n^0, it is implicitly corrected to n^0 by

$$n^* + \Delta n^{**} = n^0 \tag{3.20}$$

where, Δn^{**} ($**$ indicates second sub process), is the correction in particle number density obtained in the implicit second sub process. This correction is related to the change in velocity $\Delta \vec{U}^{**}$ obtained in the implicit second sub process. Using equation (3.1) in the implicit sub process yields

$$\frac{1}{\Delta t} \frac{\Delta n^{**}}{n^0} = -\nabla \bullet \Delta \vec{U}^{**} \tag{3.21}$$

The change in velocity or velocity correction value is obtained from the implicit pressure gradient term in equation (3.2) as follows;

$$\Delta \vec{U}^{**} = -\frac{\Delta t}{\rho} \nabla p \tag{3.22}$$

With equations (3.20), (3.21) and (3.22) a Poisson equation for the pressure is obtained.

$$\left\langle \nabla^2 p \right\rangle = -\frac{\rho}{\Delta t^2} \frac{\left\langle n^* \right\rangle - n^0}{n^0} \tag{3.23}$$

The right side of equation (3.23) represents the divergence of the particle number density from the initial constant value. The left hand side of equation (3.23) is discretized to simultaneous linear equations with the pressure term as the unknown factor. The discetization is carried out using the Laplacian model in equation (3.18). Finally we have a set of simultaneous algebraic equations that can be expressed as a linear symmetric matrix to allow for the selection of an appropriate solution technique. In this work these equations are solved using the Incomplete Cholesky Conjugate Gradient Method.

3.2 The MPS Method Algorithm

The iterative process of the MPS method is constituted by two sub-processes, (Koshizuka and Oka, 1996). The first process is an explicit computation to obtain the change in velocities $(\Delta U^*)_k$ due to the temporal conditions under the given sets of viscosity and gravity terms. Subscript k indicates the k_{th} time step and $*$ specifies the explicit first sub process. In the first process, the temporal terms for viscosity and gravity terms are considered in the Navier-Stokes equation (3.2), and then the correction of temporary velocities of particle i can be expressed as follows

$$(\Delta \vec{U}_i^*)_k = (\nu \nabla^2 \vec{U}_i + \vec{F}_i)_{k-1} \Delta t \tag{3.24}$$

in which Δt is equal to the time step of the calculation. The viscous and Force terms are now;

$$\nu \left\langle \nabla^2 \vec{U}_i \right\rangle_{\text{k-1}} = \frac{2d\nu}{n^0 \lambda} \sum_{j \neq i} \left((\vec{U}_j - \vec{U}_i) W(r_j - r_i) \right)_{k-1} \tag{3.25}$$

$$\vec{F} = \vec{\mathrm{g}}\,, \tag{3.26}$$

where $\vec{g}$ is the acceleration vector or some external forces.

Consequently, the temporal velocities $\vec{U}_i^*$ and the temporal position vector $\vec{r}_i^*$ are updated in the following expressions;

$$\left(\vec{U}_i^*\right)_k = \left(\vec{U}_i\right)_k + \left(\Delta \vec{U}_i^*\right)_k \tag{3.27}$$

$$\left(r_i^*\right)_k = (r_i)_k + .\left(\vec{U}_i^*\right)_k \Delta t \tag{3.28}$$

After the updating of the coordinates of the particles, the temporal number densities of the particles are computed using equation (3.4). In the temporal field calculated in the first process, there is a deviation of the number densities from the initially defined n^0.

Then in the second process which is indicated with, $**$ in the equations, deviations in the number densities are corrected to satisfy the mass conservation. Also in the second process, the pressure term, which was omitted in the first process, is now considered in the Navier-Stokes equation. Utilising equations (3.23) in the second process, we have the Poisson equation for the pressure.

$$\left\langle \nabla^2 p_i \right\rangle_k = -\frac{\rho}{\Delta t^2} \frac{\left\langle n_i^* \right\rangle_k - n^0}{n^0} \tag{3.29}$$

A combination of equations (3.18) and (3.29) will yield the following expression for each i to generate the simultaneous equations,

$$\frac{2d}{n^0 \lambda} \sum_{j \neq i}^{N} \left\langle \left(p_j - p_i \right) \right\rangle_k W\left(\left| r_j - r_i \right| \right) = -\frac{\rho}{\Delta t^2} \frac{\left\langle n_i^* \right\rangle_k - n^0}{n^0} \tag{3.30}$$

for $i = 1,2,.....m,$ where m is the total number of particles in the computational domain which excludes the wall particles not interacting with the fluid. The wall particles are used only when computing the particle density of the inner wall particles interacting with the fluid. N is the number of neighbours nearest particle to i

We obtain a set of simultaneous equations whose unknown is pressure. The equations can be written in the form $Ax = b$, where x is the pressure matrix components and A is the influence matrix of the particle system. The number of terms in the matrix is limited to a small number due to the cut off radius of the kernel function. This means that the influence matrix of the simultaneous equations is very sparse and symmetric.

The velocity correction $\Delta \vec{U}_i^{**}$ is computed using equation (3.22) and with the values of pressure obtained from equation (3.29)

$$\left(\Delta \vec{U}_i^{**} \right)_k = -\frac{\Delta t}{\rho} \left(\nabla p_i \right)_k \tag{3.31}$$

The pressure term ∇p_i is obtained from equation (3.7) and can be written as follows,

$$\left\langle \nabla p_i \right\rangle_k = \frac{d}{n^0} \sum_{j \neq i} \left[\frac{p_j - p_i}{\left| r_j^* - r_i^* \right|^2} \left(r_j^* - r_i^* \right) W\left(\left| r_j^* - r_i^* \right| \right) \right]_k \tag{3.32}$$

Finally, the velocities and the position vectors of particle i are respectively updated as

$$\left(\vec{U}_i^{**} \right)_{\mathrm{k}} = \left(\vec{\mathrm{U}}_{\mathrm{i}}^{*} \right)_k + \left(\Delta \vec{U}_i^{**} \right)_k \tag{3.33}$$

$$\left(r_i^{**} \right)_k = \left(r_i^* \right)_k + \left(\vec{U}_i^{**} \right)_k \Delta t \tag{3.34}$$

A flow chart of the algorithm for the MPS method is presented in Figure 3.2.

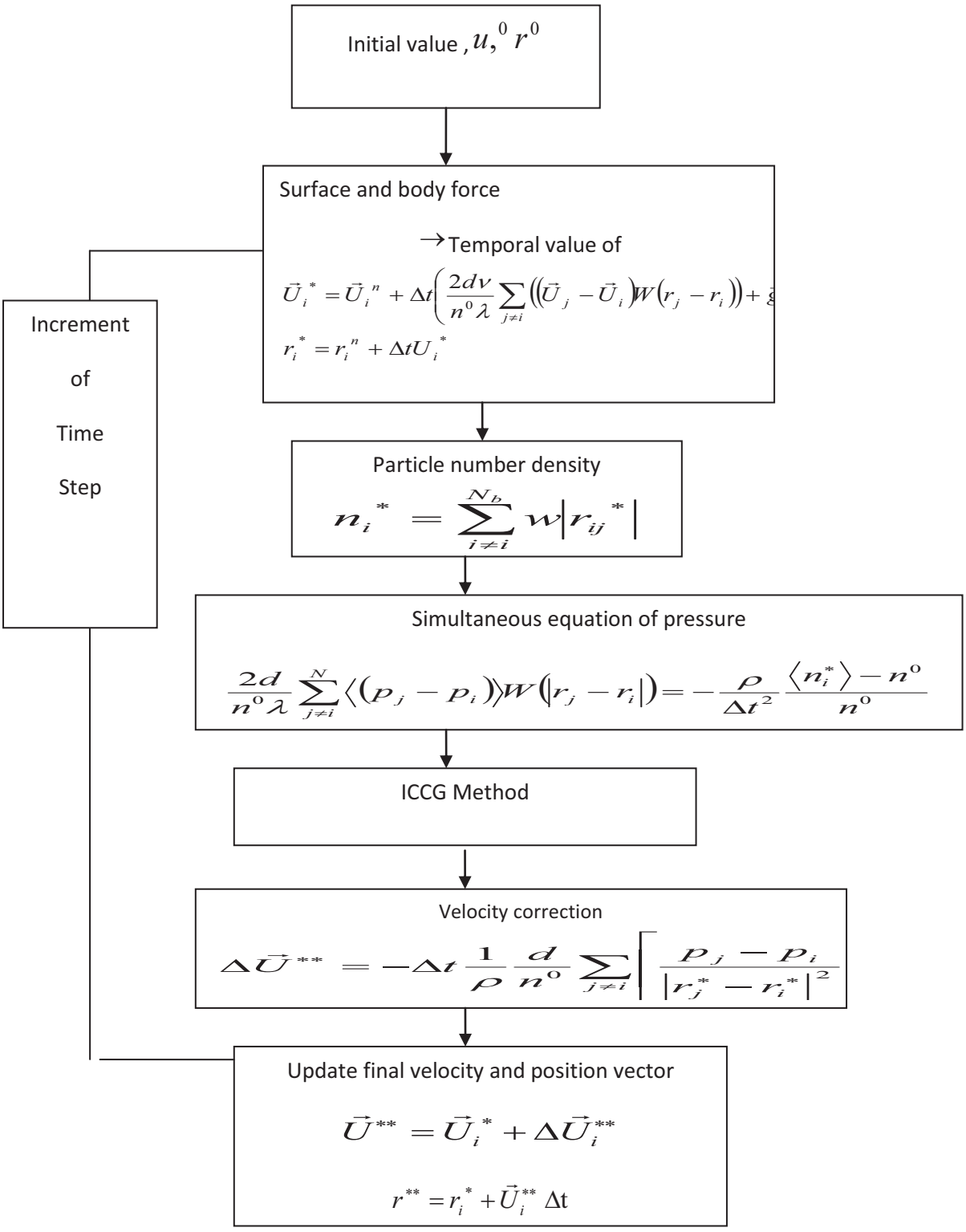

Figure 3-2 Flow chart for MPS computational scheme

3.3 Boundary Conditions

3.3.1 Modelling the Free Surface

Free surfaces are naturally tracked by fully Lagrangian motion particles. Since no fluid particles exist outside the flow domain, the particle number density decreases on the free surfaces. Thus, the particles that satisfy the following condition are considered as on the free surface;

$$n^* < \beta n^0 \tag{3.35}$$

where, β is a parameter below 1.0

Koshizuka and Oka (1996) determined the constant β = 0.97 to be suitable for free surface flows. Pressure $p = 0$ (or atmospheric pressure, if applicable) is applied to these particles on the free surface in the pressure calculation.

3.3.2 Wall Boundaries

The wall boundaries are constituted by the lines of fixed wall particles having zero velocity. Their position remains unchanged during the numerical experiment. Figure 3.3 shows schematics of the wall boundaries and is an example of the typical configuration set up for the MPS simulation scheme. The blue particles represent a fluid column, which in this case is water about to collapse. The particles on the inner first line of the wall (green particles or dummy particles) are the fixed wall particles interfacing with the fluid and are required in the MPS method. They are involved in the pressure and velocity correction calculations. Therefore, the particle number densities must be computed for these particles on the inner first line of the wall. To avoid the inner first line of the wall being recognized as free surface particles, the calculation of the number density at the particles on the inner first line of the wall will require that two other lines of particles should be added outside (black particles) in the particle configuration set up. Without these wall particles, the number density of the particles on the inner first line of the wall is small, and wall particles are identified as the free surface.

The thickness of the wall particles will depend on the kernel size parameter chosen for the computational scheme r_e . In this calculation, the kernel size for the gradient is taken to be $r_e = 2.1D_0$, where D_0 is the distance between neighbouring particles in the initial particle configuration and setup Therefore, the two lines of wall particles fall within the computational domain.

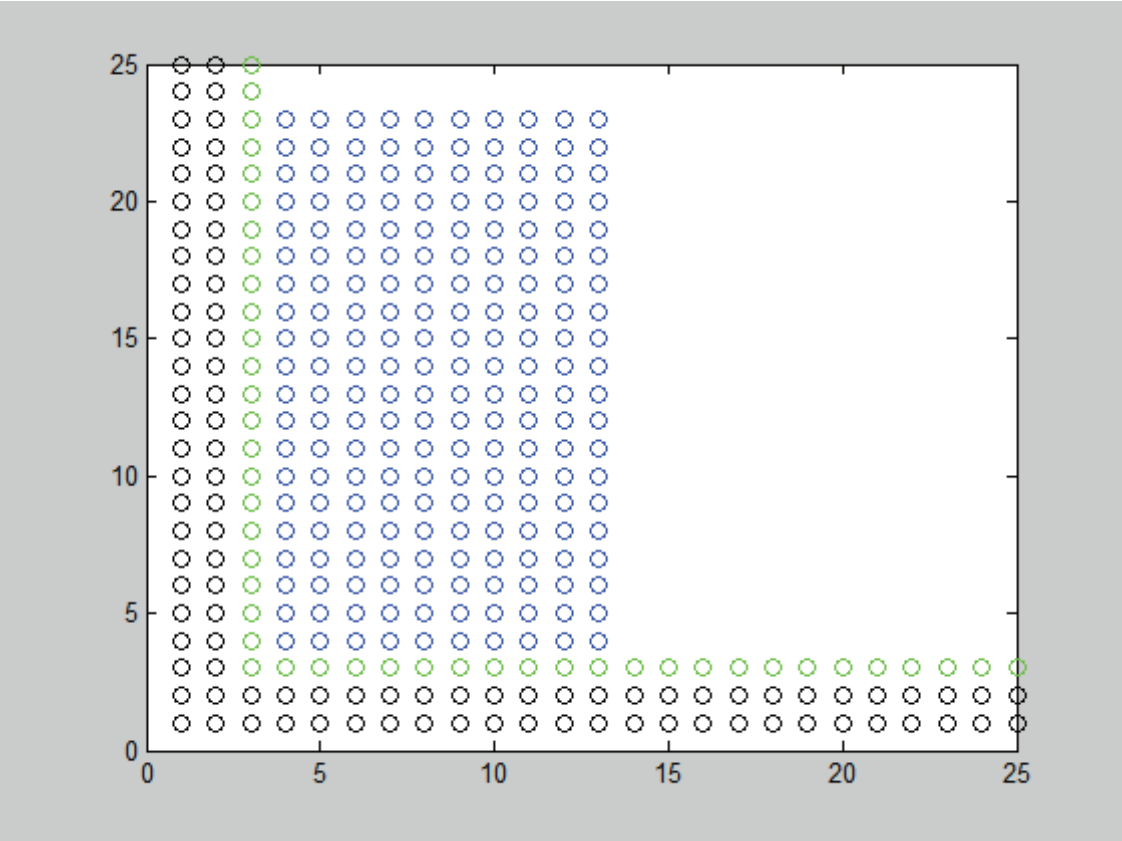

Figure 3-3. - Wall Boundaries.

The velocity of the particles at inner wall boundary can be set to zero when treating boundary conditions in the MPS method. Further, the velocities of the inner wall(dummy) and wall particles are fixed at zero to retain non slip boundary condition..

3.4 Incomplete Cholesky Conjugate Gradient Method.

The discretized Poisson equation for the pressure in equation (3.30) provides a set of linear simultaneous equations with a symmetric influence matrix and the number of unknown pressure p equals the number of particles in the computational domain. An iterative method, the Incomplete Cholesky Conjugate Gradient Method (ICCG) has been used for solving the simultaneous linear equations, (Koshizuka and Oka 1996). Development of the method can be obtained from works of Meijerink and Van der Vorst, (1977) and a detailed study to understand the method is provided in the application by Kershaw (1978). The ICCG method is an efficient technique for solving Elliptic partial Differential Equations.. It becomes optimally efficient when the matrix gets fairly big. To solve the set of equations, $Ax = b$ using the ICCG method, the influence matrix must be symmetric and positive definite. The method is based on the method of steepest descent, in which the quadratic form

$\frac{1}{2} X^T Ax - b^T x$, has a global minimum at the point $x,$ satisfying $Ax = b$

The Steepest Descent method is an iterative approach that searches for the minimum point by starting with an initial guess X_0 and then at each iteration picking a direction and moving from X_n to the minimum point X_{n+1} along that direction. The Conjugate Gradient method is a Steepest Descent method with a particular strategy for choosing its search directions.

Speed up of the conjugate gradient can be achieved by solving $M^{-1}Ax$ instead of $M^{-1}b$. Using $M \approx A$ as M^{-1} is easy to compute.

The Cholesky factorization of A is $A = LL^T$ (L is lower triangular).

Now M can be chosen, such that $M = \hat{L}\hat{L}^T$, where $\hat{L}$ is the incomplete Cholesky factor of A.

$\hat{L}$ is computed similarly to L, but is zero whereever A is zero. So $\hat{L}$ has the same sparsity pattern as A.

An Algorithm for the Conjugate Gradient Method is summarized below in Table 3.1.

Table 3.1 Conjugate Gradient Algorithm

x : Iterated solution.

r : Residual $b - Ax$.

d : Direction.

ε : Tolerance.

Initialization:

$i \Leftarrow 0$, $r = b - Ax$,

$d \Leftarrow M^{-1} r$,

$\delta_{new} \Leftarrow r^T d$,

While $i < i_{\max}$,

And $\delta_{new} > \varepsilon^2 \delta_0$

DO

$\alpha \Leftarrow \dfrac{\delta_{new}}{d^T A d}$ (set α so that $x + \alpha d$ is the minimum along direction d)

$x \Leftarrow x + \alpha d$

$r \Leftarrow b - Ax$ (update the residual, can compute $r - \alpha A d$ instead).

$\delta_{old} \Leftarrow \delta_{new}$

$\delta_{new} \Leftarrow r^T M^{-1} r$

$\beta \Leftarrow \dfrac{\delta_{new}}{\delta_{old}}$

$d \Leftarrow M^{-1} r + \beta d$ (Choose the next orthogonal direction).

$i = i + 1$

3.5 Associated Problems with the MPS Method.

The MPS method discretizes the continuous media using particles. The Particles interact with each other according to a function called the kernel function which expresses how a particle is influenced by another particle in its vicinity. The partial differential equations, such as the Navier-stokes equations are discretized by particle interaction models according to the kernel function. The choice of an appropriate kernel function is vital to approximate the problem satisfactorily. Very often this function depends on the distances between particles and their interaction radii are bounded. Thus a particle interacts with a limited number of particles in its vicinity. This is satisfactory when the storage memory adopted is adequate; otherwise it becomes a critical parameter.

Another problem is to determine how many particles are enough for a good interpolation in a given problem. In a general situation, this problem will depend on the complexity and features required to provide a good representation for initial configuration and the choice of an appropriate kernel size that will satisfy the problem. A difficulty associated with the MPS method, is the necessity to find the neighbouring particles of a given particle, requiring a costly test with all the other particles to determine which of them are inside the interpolation radius. This is called the N – body problem, which requires N^2 computation time. It is worth noticing that in the MPS method, since it is a Lagrangian method, inflow and outflow of fluid is not allowed. However this disadvantage can be mollified by combining MPS with an Eulerian approach to handle the inflow and out flow.

For green water modelling, this is not a significant issue. The green water phenomena can be modelled as isolated or solitary wave overtopping events. Therefore the MPS method can use experimental data and empirical formulation to model the wave or water build up evolution around the bow geometry as inflow boundary conditions. Another problem encountered with MPS is the conservation of energy which is not guaranteed with the current state of development of the method.

3.6 MPS Simulation of water entry of free falling wedge

3.6.1 Background.

Slamming features occur in a marine environment when a body suddenly experiences an impact with sea water, with the process generating an impulsive force and dynamic responses. The loads generated can result in substantial damage in the structures on ship hulls and marine facilities. Barltrop and Adams (1990), state that the hydrodynamics of slamming are highly complex and the precise shape of the water surface at the instant of the slam occurring has a significant effect on the slam force. This wave structure interaction activity has attracted numerous research investigations to different aspects of the wedge water entry problem, owing to its practical and theoretical importance.

Early theoretical research into the subject was presented by Dobrovolskaya (1969), who obtained a complete solution for a class of two dimensional problems of the similarity flow of an incompressible fluid with a free surface. Assuming the fluid is non viscous, no gravity effect and constant entry speed for the wedge, Dobrovolskaya obtained a complete solution by using a complex potential and conformal mapping to transform the problem into an integral equation of a function. A solution of this function results in the pressure and velocity distribution.

Chapman (1979) developed numerical method for solving the transient two dimensional flow problem induced by the motion of a floating body. The linearization of the free surface equations, the spectral representation of the wave field and a source distribution representation of the body were all described in detail. Two modes of body motion, a captive mode and a free mode were discussed. The water entry of a wedge in the captive mode was investigated. The pressure distribution and forces on a wedge were evaluated by Greenhow (1987) using the results of a formulation based on the Cauchy's theorem. Gravity was included in a modified numerical scheme and as a result a jet of fluid which rises up the side of the wedge was experienced. Greenhow suggests that eventually the fluid jet may separate from the wedge surface. In the study test cases presented for the wedge were transient motion, non constant speed entry, oblique entry and full wedge penetration of the free surface.

Zhao and Faltinsen (1993) provided a numerical scheme that uses a non linear boundary element method with jet flow approximation to investigate water entry of a two dimensional body of arbitrary cross-section. Verification of the method was carried out by comparison with other research studies involving similarity solutions for wedges with varying dead rise angles. Lin and Ho (1994) presented numerical results for the entry of a wedge into initially calm water of arbitrary depth. The boundary element method (BEM) was applied for the computation of the flow field with nonlinear free surface conditions. It was observed that the magnitude of impact pressure in shallow water was greater than in deep water on the basis of results obtained in the numerical simulation. Quantitative agreements were obtained when the numerical prediction results were compared with measured experimental data.

Zhao et al (1997) developed two different theoretical methods for two dimensional sections subjected to slamming loads. The first method involved a fully nonlinear numerical simulation of the effect of flow separation from fixed separation points on the body. The problem was solved using a boundary integral equation method. The second method was based on the generalization of the work of Wagner (1932) by applying linearized free surface conditions and without flow separation. Test cases for different wedge angles and a section with flare were presented and the results were compared with detailed experimental work.

Mei et al (1999) considered the analytic solution of the general impact problem of two dimensional bodies entering initially calm water. The areas of their study were the water splash up height, the force history and the pressure distribution over the body. An approach based on the potential flow formulation of Wagner (1932) was followed and extended to an arbitrary body section. The body boundary problem was solved using closed form conformal mapping derived for a range of body sections. Wu et al (2004) analysed the hydrodynamics problem of two dimensional wedge entering water through a free fall motion using potential theory. Assuming the water flow to be similar and with the application of the boundary element method (BEM), solutions were obtained for the body motion and free surface deformation. The water entry problems of a wedge with constant velocity was studied by Hikara (2004) by engaging a boundary element method (BEM) and a mixed Eulerian and Lagrangian method (MEL) for the analysis of the problem.

Hydrodynamic pressure computations on the wedge were shown to be in close agreement with other prediction models in literature.

Oger et al (2006) presented a study based on a particle method, the Smooth Particle Hhydrodynamics method (SPH) to evaluate the pressure distribution on the boundaries of a two dimensional wedge under two distinct test cases. The first was imposed motion for a wedge using experimental data from the works of Zhao et al (1997) and the second was non-imposed motion for a single degree free falling wedge. The pressure prediction results obtained from the SPH simulations were compared with the analytical and experimental studies carried out by Zhao et al (1997) and details of the agreement and differences were discussed.

Wu (2006) investigated twin wedges entering water vertically at constant speed by using potential theory to formulate the problem and developed a solution using the complex potential with the boundary element method (BEM). Implementation was carried out in three stages, firstly by obtaining the similarity solution. Then a stepping technique for each wedge in a stretch system was developed, and finally the interaction between the two wedges was included in the numerical scheme. Results for wave elevation, pressure distribution and force at different dead rise angles were presented. Lee and Rhee (2009) carried out numerical simulations to find out the dominant parameters that are associated with the wedge entry into water. Constant velocity was assumed and the calculated impact loads showed that the effect of viscosity was not of importance in the wedge entry problem. For grid methods, grid size was considered to be the most sensitive parameter.

The hydrodynamic problem of two dimensional wedges entering water was studied by Gong et al (2009). The numerical prediction model was based on the SPH method with an improved boundary treatment to reduce the reflection of sound waves. The improved boundary treatment formulation coupling to the SPH method was used to obtain the boundary pressure, maximum force on the wedge and initial entering velocities of the wedge. Shao (2009) in his research paper discussed the use of an improved SPH model, the Incom – SPH, which stands for incompressible – SPH method. The method is used to simulate the interactions of a wedge entering into water.

Pressure distribution on the wedge, impact forces and free surface deformation were handled adequately by following a two step process using a semi implicit hydrodynamic formulation coupled to a Lagrangian algorithm that provides the ability to track the motion of the free falling wedge in water. The motion tracking scheme was developed by Koshizuka et al (1998).

Lee et al (2010a) also used the MPS method to carry out numerical investigation of the liquid – liquid and liquid – solid collisions and water impact loads caused by falling rigid plates with various incident angles. They concluded that the MPS method as proposed by Koshizuka and Oka (1996) can give accurate results with regards to impact pressure. Lee et al (2010b) in a review, stated that for short duration numerical simulations such as water entry, the original MPS method can adequately predict impact loads.

Further to the detailed experimental work carried out by Zhao et al (1997), other researchers also carried out experimental work on the wedge problem. Tveitnes et al (2008) developed a test rig that drove a wedge section with end plates to enter the water vertically at near constant speed. Entry force and velocity were measured. Analysis of the constant velocity exit tests show that the maximum added mass was utilised in driving the water above the surface level. The low exit forces were also indicated.. Observations indicated that considerable dynamic noise limited the accuracy of the results. Turong et al (2010) presented a report on the experimental work carried out on five degree wedge entering water at constant speed. The wedge was driven by an actuator programmed to generate triangular wave trains. Sensitive pressure transducers were used for measurements and measured results were compared to the results from prediction methods in literature.

Some commercial CFD applications have also been evaluated. Lewis et al (2010) utilised a commercial RANSE Solver (ANSYS CFX, 2007) to calculate wedge impacts with water. The solver by altering the level of the free surface computes the movement of the body using a body fixed mesh. One degree of freedom was investigated for a two dimensional wedge. Marcer et al (2010) carried out validation tests on two CFD codes developed with free surface methods.

These methods are the Volume of Fluid Method (VOF), implemented in URANS 2-phases codes, allowing for large deformations of the free surface up to jet breaks, and the Smooth Particle Hydrodynamics (SPH) method. Benchmarks between the different methods and validations of CFD codes were performed on the wedge impact problem.

The results showed that the VOF and SPH methods give comparable and validated results. They can be used to predict accurate slamming loads on marine structures.

The present thesis is motivated by the experimental work of Zhao et al (1997) and the numerical prediction method using SPH implemented by Oger et al (2006) but is focused on the MPS method as a prediction method for the solution of the general wedge entry into water, and the impact problem. This thesis uses the measured experimental entry velocity of the wedge from Zhao's work but solves the wedge problem using MPS at any instant in time during water entry, computing the pressure distribution along the wedge boundary. The water entry velocity of the wedge and motion in water has been modelled by introducing an additional Lagrangian particle algorithm into the MPS formulation. The results obtained are compared with the experimental results of Zhao et al (1997) and the SPH work from Oger et al (2006), who studied both imposed and non imposed motion, and used for numerical confirmation.

3.6.2 MPS Methodology.

In this section the water entry problem is presented for solution using the MPS framework. For a clear understanding and analysis of the wedge entry phenomena, the problem is divided into three stages. The first stage represents the duration when the wedge is in free fall and before water entry, the second stage represents when the body hits the water and there is impact and deformation of the free surface and the third stage is the wedge motion in water.. The method for solution is presented for each of the stages.

3.6.2.1 Free falling wedge with no air resistance.

At this stage the MPS model formulations are not included in the numerical computational process. When the wedge is dropped into water, the analytical solution for the instantaneous downward vertical velocity and instantaneous vertical distance travelled at each time are equivalent to;

$$w = -g * t \tag{3.36}$$

$$z = \frac{1}{2} * g * t^2 \tag{3.37}$$

where w is the vertical velocity, z is the vertical distance travelled by a wedge particle, g is the acceleration due to gravity and t is the time of travel.

A time marching procedure begins with a small interval Δt and for each time step k,

$$t_k = \mathrm{t}_{\mathrm{k\text{-}1}} + \Delta t \tag{3.38}$$

The wedge body configuration is composed of particles. For the numerical simulation of a wedge in free fall, the free fall downward vertical velocity of each wedge particle and the position of the wedge particles at any given time during free fall are obtained as follows;

$$(w_i)_k = -g * (t)_k . \tag{3.39}$$

$$(z_i)_k = z_0 - \frac{1}{2} \mathrm{g} * (t^2)_k \tag{3.40}$$

for a given drop height z_0.

These equations will become no longer applicable as soon as the wedge reaches the free surface and enters the water.

3.6.2.2 Wedge entry into water.

At this stage the MPS model equations are applied to all particles represented in the computational domain. These are the wedge particles, the inner wall particles of the NWT and the water. However, the wall particles are involved in the computation of the inner wall particle density number. All particles are treated equally and without distinction at this stage.

The first sub process of the MPS method is considered and equations (3.24) and (3.27) are applied to obtain the temporal velocities. Equation (3.28) is applied only to the water particles to update their positions. The wall particles remain fixed so there is no need to update the positions.

The wedge particle positions are not updated yet. Poisson equation of pressure, equation (3.29) is used to obtain the pressure for the wedge particles, water particles and inner wall particles. For the second sub process of the MPS method, equation (3.31) and (3.33) are employed to obtain the velocities of all the particles in the computational domain. Again, only the position of the water particles is updated with equation (3.34).

3.6.2.3 Wedge motion in water.

The third stage involves the position update of the wedge particles in water. Water entry of a wedge in free fall requires that the motion in water needs to be resolved in stage 2 as the acceleration and position in water will depend on the hydrodynamic force on the body. A procedure to accommodate this mechanism was developed by Koshizuka et al (1998) as a rigid body tracking routine in a flow field. Gotoh et al (2002) successfully applied it to a float flow interaction simulation. Shao(2009) in his numerical simulation of the free falling wedge combined the ISPH method to the tracking scheme to obtain the motion of the wedge in water. Lee et al (2010) used the tracking scheme for the motion free falling rigid plates in water. The routine is introduced in this study as an additional procedure for the computation of the wedge particle's position in water. The rigid body tracking routine algorithm is based on Newton's second law and can be easily coupled to the MPS method. At water entry the falling wedge is composed of particles with fixed relative configuration and a known entry velocity for all particles. During the implementation of the MPS two sub processes, the same computational procedure is applicable to both the water and wedge particles for the calculation of particle velocities. That means there is no differentiation between the water particles and the wedge particles as they are treated equally in the MPS formulation.

Thereafter, an additional measure is applied to the wedge particles to only to update their relative positions to the initial configuration.

Assuming the free falling wedge is represented by a number of particles N_w and each with position vector r_w, the centre of the solid wedge r_{wc}, the relative position of a wedge particle to the centre q_w and the moment of inertia I of the wedge body can be obtained as follows (Koshizuka et al, 1998);

$r_{wc} = \frac{1}{N_w}\sum_{i=1}^{N_w} r_{wi}$	for $i = 1,2,3.....N_w$	(3.41)

$$q_{wi} = r_{wi} - r_{wc} \tag{3.42}$$

$$I = \sum_{i=1}^{N_w} \left| q_{wi} \right|^2 \tag{3.43}$$

The velocities of the wedge particles obtained from the MPS model equations are now used in the following routine to obtain the average translational $\left(\vec{T}\right)$ and rotational velocity $\left(\vec{R}\right)$ of the wedge body,

$$\vec{T} = \frac{1}{N_w}\sum_{i=1}^{N_w} \vec{U}_i^{**} \tag{3.44}$$

$$\vec{R} = \frac{1}{I}\sum_{i=1}^{N_w} \vec{U}_i^{**} \times q_{wi} \tag{3.45}$$

Note that $\vec{U}_i^{**}$ is the velocity of a wedge body particle obtained from the MPS equation (3.33). Finally each of the wedge body particle velocity is updated to $\vec{U}_{wi}$ and the initial wedge body structure is retained by

$$\vec{U}_{wi} = \vec{T} + q_{wi} \times \vec{R} \tag{3.46}$$

At this stage the wedge particles now have the same velocity and their position can be updated.

$$\left(r_{wi}\right)_{\mathrm{k}} = \left(r_{wi}\right)_{\mathrm{k\text{-}1}} + \left(\vec{U}_{wi}\right)_k \Delta t \tag{3.47}$$

The application of this rigid body tracking scheme to correct the velocity of the solid wedge due to the presence of the hydrodynamic forces recognised during the implementation of the MPS formulation for particle interaction allows for the complete solid wedge body motion to be traced. A program flow chart is shown in Figure 3.4 which provides a summary of the numerical implementation.

3.6.3 Free surface and Boundary conditions.

The numerical handling procedure of the free surface and boundary conditions for the simulation of the water entry of a wedge and treatment of the wall conditions have been treated as follows:.

3.6.3.1 Free Surface

For the MPS method, free surfaces are assessed based on the equation (3.35) proposed by Koshizuka and Oka (1996). To simplify the dynamic free surface boundary condition, each water particle that satisfies equation (3.35) is given a zero pressure in the pressure calculation.

3.6.3.2 Fixed wall Boundaries.

The velocities of the wall and the inner wall particles (dummy) of the numerical wave tank (NWT) are set to zero to represent non slip boundary condition.

3.6.3.3 Free falling wedge boundary.

Zhao et al (1997) clearly stated in their work that the viscous boundary layer effects are negligible and not important. Lee and Rhee (2009) in their investigation of dominant parameters that are associated with wedge water entry problem reiterated this observation that viscous boundary effects are not significant in the wedge entry problem. In this study, viscous effects were also assumed to be negligible at the boundaries. However, the wedge body being a solid structure, a non-penetration condition is applied to the water particles coming in contact with the wedge boundary. A mirrored approach is adopted by following Oger et al (2006).

$$U_{nGWP} = \left(2\vec{U}_{Wi} - \vec{U}_{WP}\right) \cdot \vec{n}, \ . \tag{3.48}$$

where U_{nGWP} is the velocity of the ghost particle mirroring the water particle, $\vec{U}_{Wi}$ is the velocity of the wedge particle at the wedge surface, $\vec{U}_{WP}$ is the velocity of the water particle and $\vec{n}$ correspond to the normal direction.

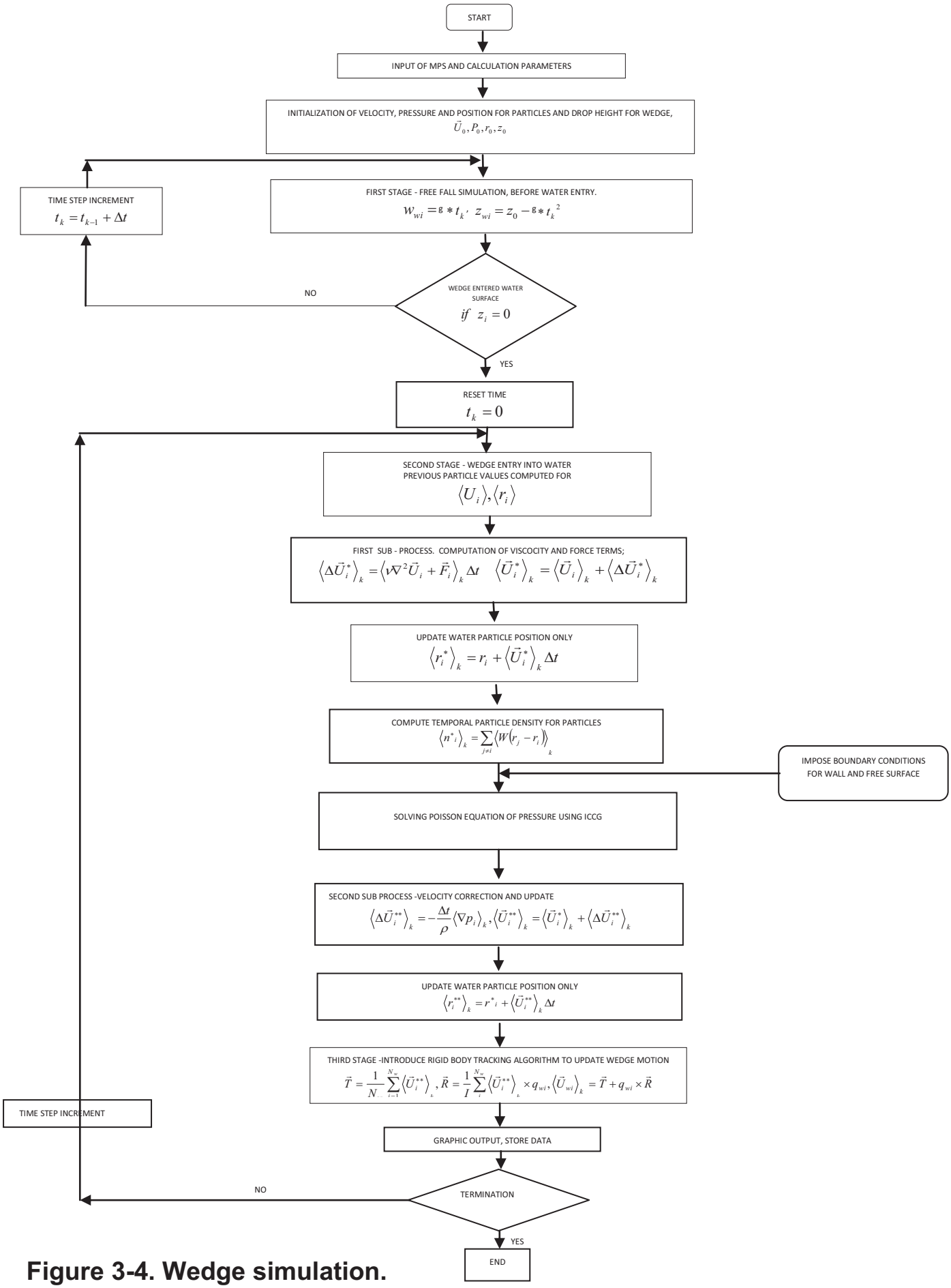

Figure 3-4. Wedge simulation.

3.6.4 Experimental Test description.

The water entry of a wedge experiment was carried out by Zhao et al (1997) at the Norwegian University of Science and Technology, MARINTEK. The objective of the test was to validate theoretical methods. A full description of the drop test and drawings are provided in Appendix A of this thesis. In the experiment the vertical acceleration of the drop rig was measured using an accelerometer and the vertical drop velocity was measured using an optical sensor. The vertical motion of the wedge is the only degree of freedom allowed in the experiment. The wedge sections were dropped against calm water. The measured velocity at the instant of water entry in this experiment is used as part of the initial conditions for the numerical simulation.

3.6.5 Numerical Test description and Simulation of Wedge entry.

The numerical simulation for the wedge entry problem in this thesis is based on the experiment of Zhao et al (1997) and the numerical work of Oger et al (2006) is used for further comparison. The sketch and the dimensions of the wedge are given in Figure (3.5) and Figure (3.6) shows the schematic representation of the wedge falling into a numerical wave tank. The conditions used for simulating the water entry of a wedge to reproduce the experiment is presented below

- Width of the wedge : 0.5m
- Dead rise angle : 30^0
- Drop inclination with vertical : 0^0
- Vertical drop velocity of wedge -6.15m/s (measured at the instant of contact with water from experiment).
- Drop height z_0 : 2m
- Time step Δt : 1 x 10^{-5}s.

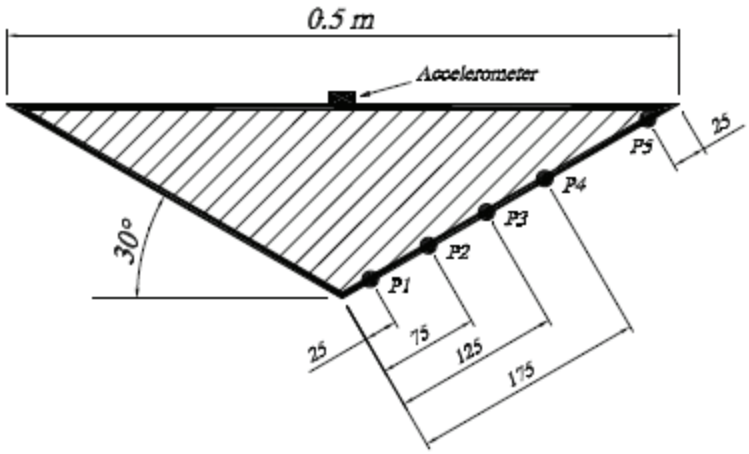

Figure 3-5. Sketch of the wedge geometry (Oger et al, 2006)

Flow conditions for simulation are:

- Nominal density used for water is ρ = 1000 kg/m^3
- Viscosity ν is taken as 1 x 10^{-6} m^2/sec
- Atmospheric pressure is taken as p_0 = 0.

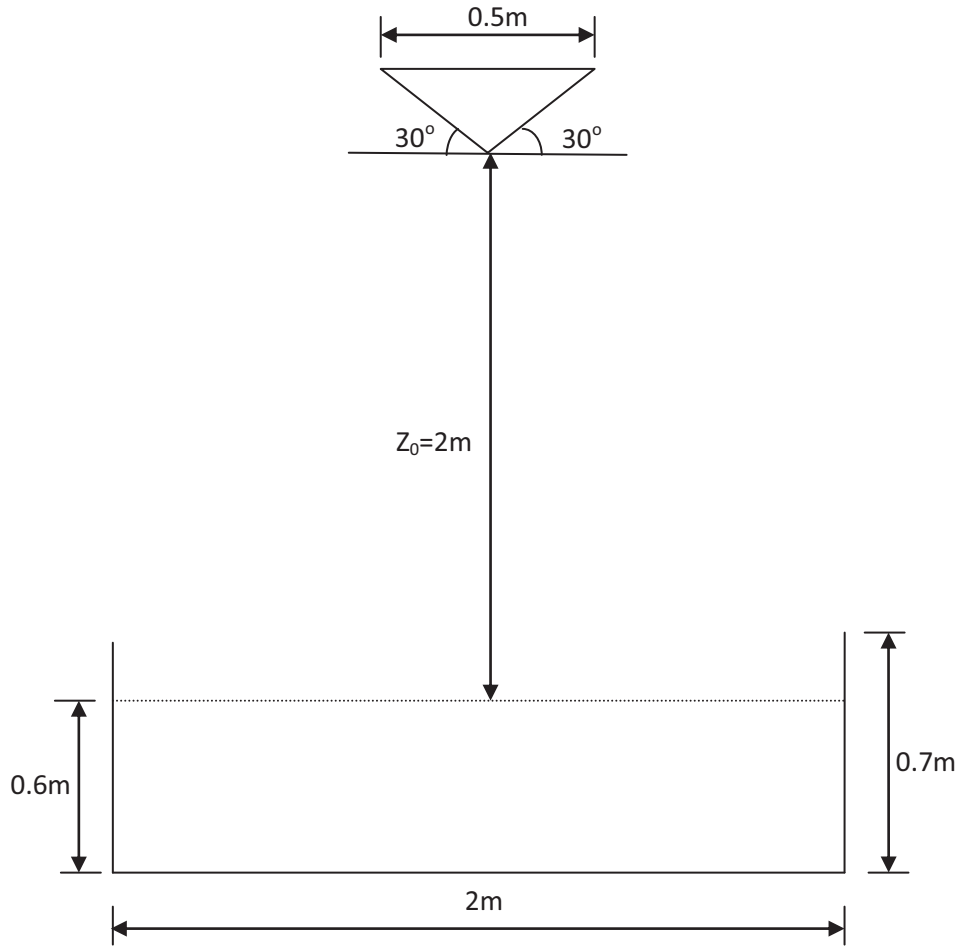

Figure 3-6 Sketch of wedge falling into NWT (internal dimensions).

The wedge body representation is composed of particles, also the water particles and wall particles of the numerical wave tank. The particle configuration comprise of the following.

- Number of wedge particles : 7939
- Number of water particles: 313,100.
- Number of tank wall particles: 54,900.
- Distance between particles : 0.002m

For visualisation presentation, the particles are packed into circles, with each circle containing ten particles. For example in the graphical output, the particles are represented as follows;

- Water - X – axis = 1010 particles, Z – axis = 310 particles..
- NWT – X –axis, Bottom wall three layers of particles consists of 1070particles 1050 particles and 1030 particles and Z – axis consists of three rows, each with a thickness of 10 particles. Therefore the number of particles for the bottom wall is (10700) + (10500) + (10300). Same can be done for the side walls which have three layers of wall particles consisting of 400, 390, and 380 particles in the Z – axis and three layers with a thickness of 10 particles each in the X -axis. The number of particles is (4000+3900+3800) x 2 side walls. The combination of bottom and side walls particles is 54,900 particles.
- Wedge - The wedge is 0.5m wide, 0.144m deep and has a sloping side of 0.289m. If the horizontal spacing between the particles is 0.002m there are 250 particles across the width of the wedge at its widest point. If the vertical spacing is 0.00231m, the number of particles per row decreases by 4 on each succeeding layer and 62 rows are required to represent the wedge, giving a total of 7939 particles. In the figures, the particles are represented by circles, each of which contains 10 particles so that there are around 75 circles representing the first three rows of particles.

The visualisation presentation for the initial particle configuration setup for the simulation to mimic the experiment is shown in Figure 3.7

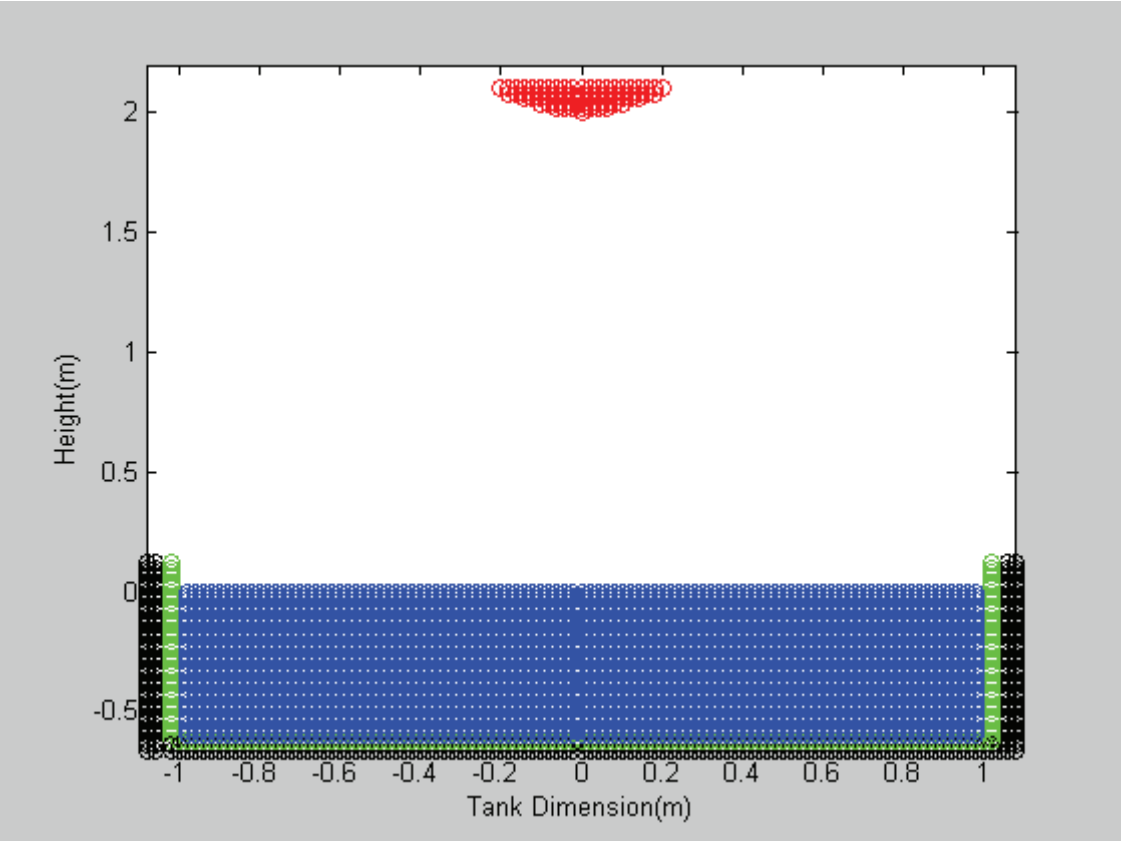

Figure 3-7 Initial particle configurations for wedge body entry.

3.6.6 Summary of Results and Validation.

The present work in this section of the thesis is to demonstrate the capability of the MPS method to simulate a slamming effect in a 2D numerical wave tank by a free falling wedge body. To reduce the computational effort of the demonstration only the single degree of freedom, excluding the other parameters such as wind and current was evaluated.

The free fall velocity of the wedge, water elevations and pressure distributions in the NWT and on the wedge were computed. It is shown from Figure 3.8 that the velocity of the wedge drops considerably during immersion in water, due to the effect of hydrodynamic forces that result in a deceleration in the downward vertical motion of the wedge. The computation of the downward velocity using the MPS method with the motion tracking scheme agrees with the experimental data of Zhao et al (1997).

The maximum deviation in the values of falling velocity between the numerical and experimental measurements was 2.7%.

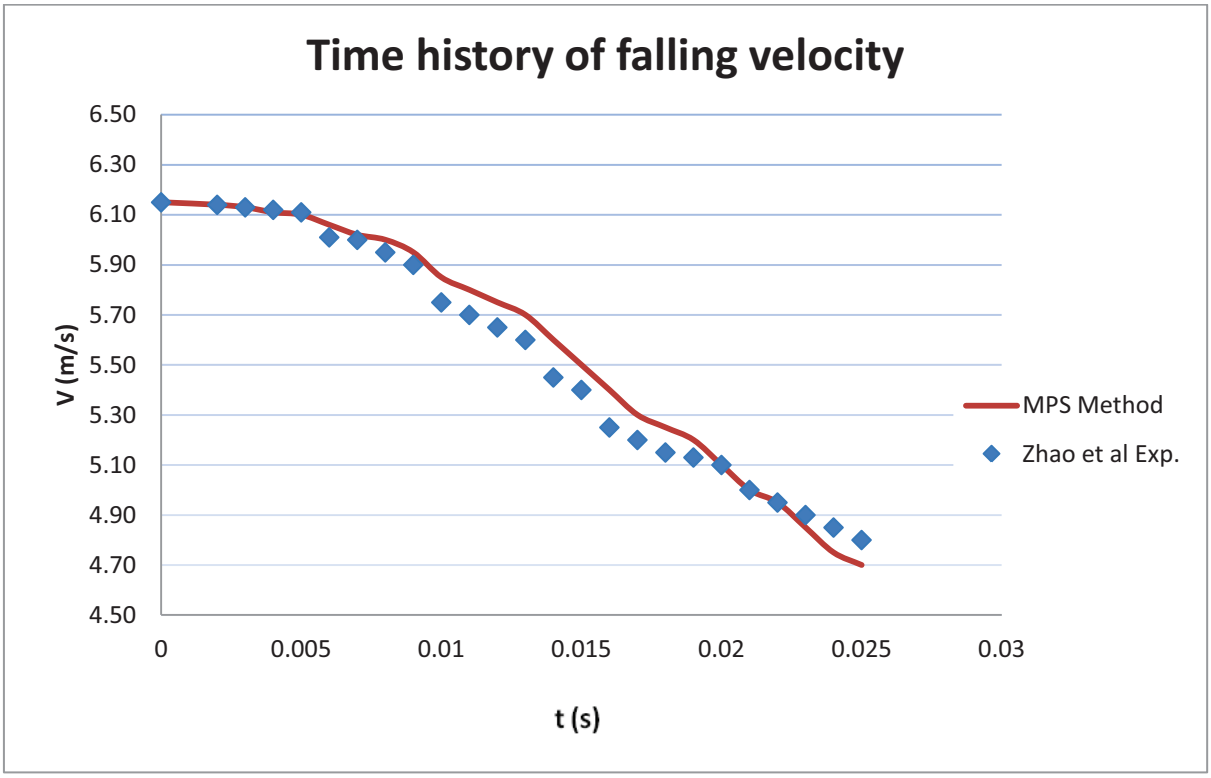

Figure 3-8 Time history of experiment and simulated falling velocity

Flow features during the wedge entry from the MPS simulations are shown in Figures 3.9(a) to (c).The figures also show the evolution in time of the free surface deformations during the wedge entry and impact. They illustrate the successive deformations of the free surface as the wedge body enters the water and the subsequent jets generated during impact. The presence of fragmentation at the tip of the water jet created at the free surface can be observed in the figures. Fragmentation is a natural physical phenomenon that generally occurs when there is a violent motion at the free surface of fluids and its occurrence in fluid dynamics problems is unavoidable. Surface tension effects were not considered in the numerical simulation. The simulation is limited in capacity due to computational resources, as it would have been ideally continued for larger submergence.

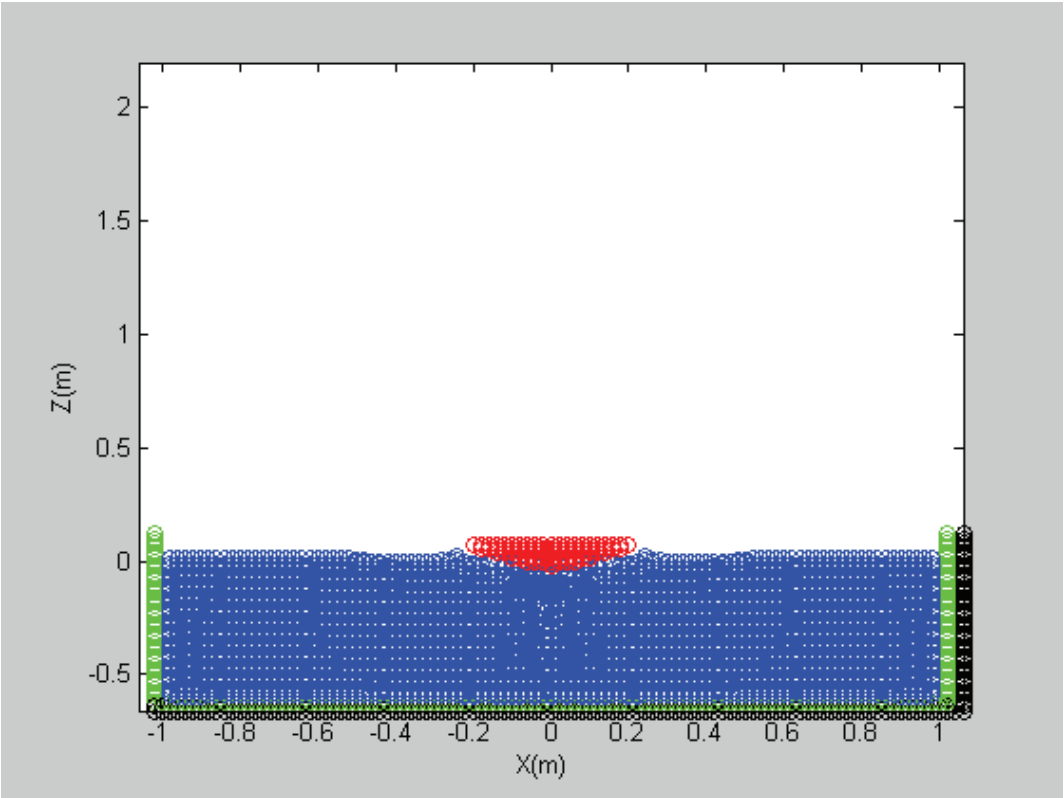

Fig 3-9a Wedge body slamming effect and water surface deformation at t= 0.004s

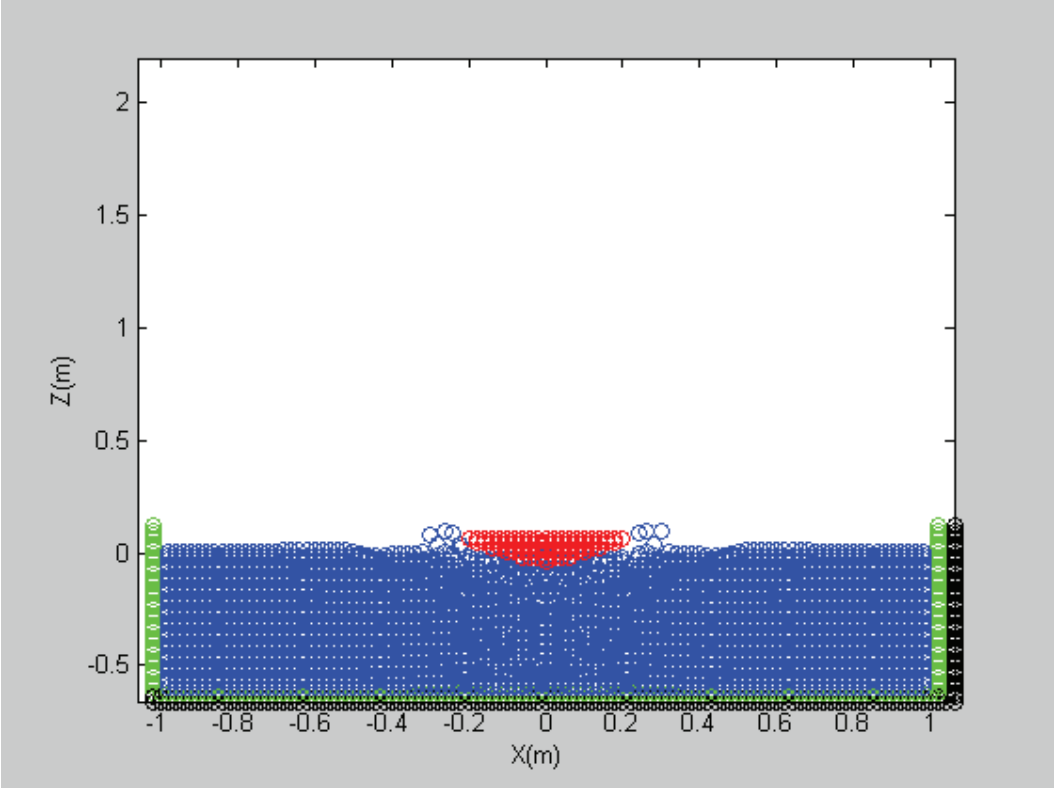

Fig 3-9b Wedge body impact and free surface deformation at t= 0.016s

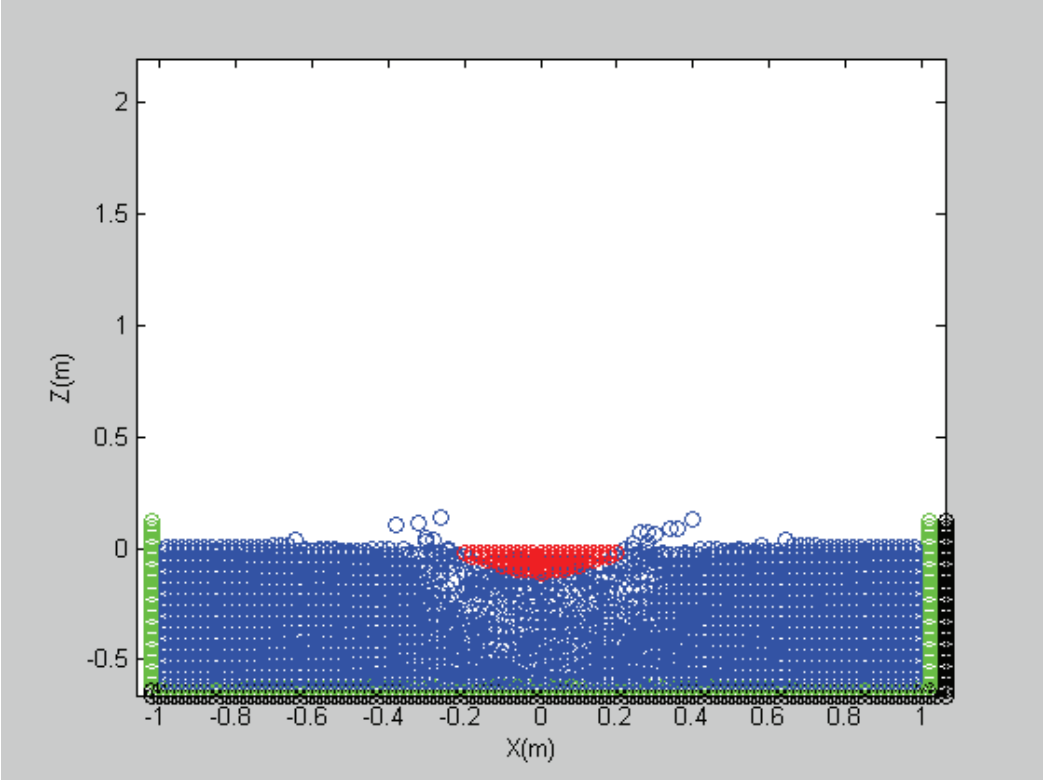

Fig 3-9c Wedge body submergence in NWT at t= 0.0202s

The MPS method numerically predicted pressures are compared with the results from Zhao et al (1997) numerical model and experiment, and also the numerical work by Oger et al (2006) using the SPH model. Following the format of presentation by Zhao at three instances t = 0.00453s, being the instant the wedge has entered the water, t = 0.0158s when the wedge is partially submerged and at t = 0.0202s when the wedge is submerged, the results are presented in Tables 3.1, 3.2 and 3.3. Figures 3.10 to 3.12 show the pressure distribution comparison. For t = 0.00453s, the MPS method gives a pressure distribution profile that is in good agreement with the experiment work and numerical model of Zhao et al (1997). However comparison with SPH imposed and non-imposed motion, the SPH model provides a lower pressure profile. Oger et al (1997) attributed the lower pressures to lack of stability in the SPH model caused by compressible effects that could have been generated by changes in fluid flow characteristics at the beginning of the impact. At the instances when t = 0.0158s and t = 0.0202s the MPS method also shows pressure profiles that are in good agreement with the experiment results of Zhao et al (1997). There is a difference when compared to the numerical work of Zhao et al (1997) and the SPH model of Oger et al (2006).

A reason for the difference could be the pressure solution methods in the various simulation methods. In the MPS method, the pressure was implicitly calculated by a Poisson pressure equation, whereas Oger et al (2006) in the SPH model used an equation of state to compute the fluid pressure. Another reason can be attributed to the handling of the numerical deceleration using the MPS motion tracking scheme implemented in the simulation. No relevant effects associated with pressure fluctuations were found in the results presented in this study. This can be attributed to the short duration of 0.02s for the wedge entry simulation. Ataie- Ashtiani and Farhadi(2006) confirmed in their study that the kernel function as proposed by Koshizuka and Oka (1996) used in this study was numerically stable in the collapse of water experiment for upwards of 1s, despite using a different equation solver. Lee et al (2010b) also indicated in a discussion that for short duration simulations the particle models and equations in the original MPS method by Koshizuka and Oka (1996) can provide qualitative results.

The following parameters are used for the numerical computations in Tables 3.1, 3.2 and 3.3

- z_w is the vertical position of a wedge body particle
- z_{KEEL} is the vertical position of a wedge keel particle
- Z_D is the draft of the wedge which is depth of the keel below the water line
- Pressure distribution along wedge boundary:

$$P1 = \frac{p - p_0}{0.5\rho\left\langle V^2(t)\right\rangle}\ , \tag{3.49}$$

where $P1$, is the non dimensional pressure on the wedge surface , p is the calculated pressure on the wedge surface and $V(t)$ is the vertical drop speed of the wedge measured by Zhao et al 1997 and given in Figure 3.8

- Elevation of free surface along the wedge boundary:

$$V1 = \frac{z_w}{\int_0^t V(t)dt} \tag{3.50}$$

where $V1$ is the non dimensional vertical co-ordinate on the wedge surface

- Draft coefficient, $$Z1 = \frac{z_w - z_{KEEL}}{Z_D} \tag{3.51}$$

Table 3-2 Pressure distribution along the wedge boundary t = 0.00453s

V1	Zhao Numerical	Zhao Experiment	Oger-SPH Imposed	Oger-SPH Non-Imposed	MPS Method
-1.00	4.80		4.00	4.60	4.70
-0.90	4.80		4.00	4.40	4.60
-0.80	4.60		4.00	4.00	4.50
-0.70	4.80		4.20	3.80	4.50
-0.60	4.90		4.40	3.80	4.40
-0.50	4.90	4.20	4.30	4.00	4.20
-0.40	5.00		4.20	4.50	5.00
-0.30	5.10		4.10	4.80	5.20
-0.20	5.20		4.20	4.60	5.30
-0.10	5.30		4.30	4.40	5.40
0.00	5.40		4.40	4.20	5.50
0.10	5.60		4.50	4.40	5.60
0.20	5.80		4.60	4.80	5.80
0.30	6.50		5.00	5.40	6.60
0.35	7.10	7.30	5.00	5.20	7.20
0.40	7.00		3.00	5.20	7.20
0.50	4.00		2.00	3.40	3.80
0.60	0.00		0.00	0.00	0.00

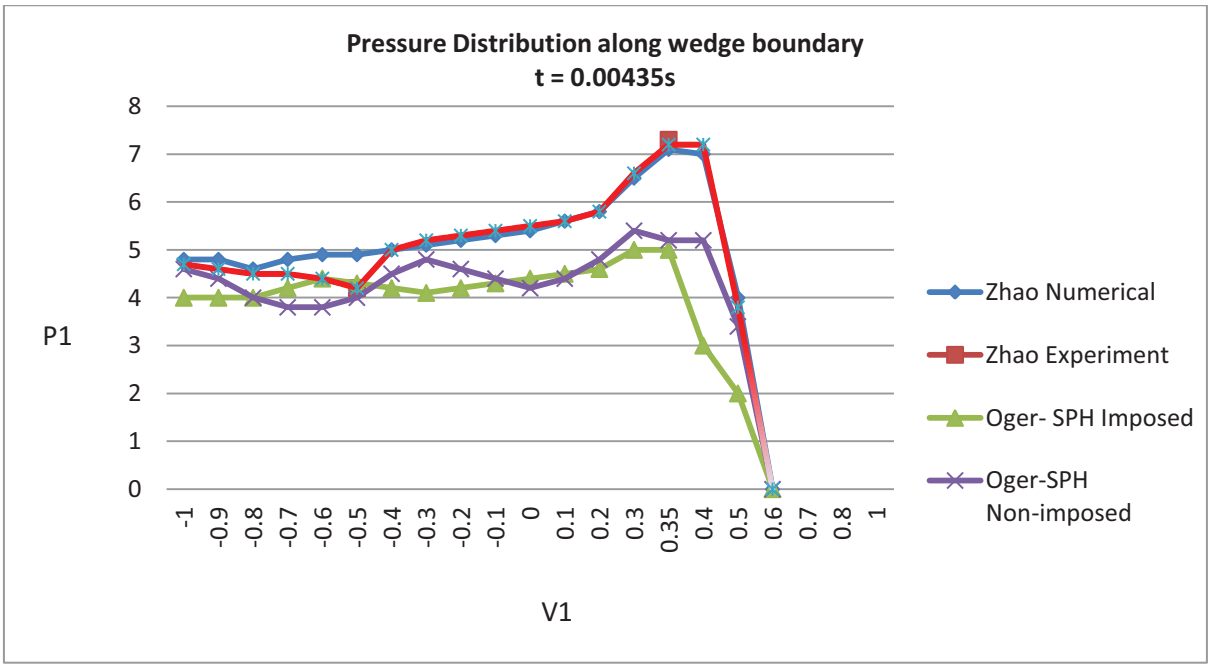

Figure 3-10 Pressure distribution comparison at t = 0.00435s

Table 3-3 Pressure distribution along wedge boundary t = 0.0158

V1	Zhao Numerical	Zhao Experiment	Oger – SPH Imposed	Oger-SPH Non Imposed	MPS Method
-1.00	3.50		3.80	3.60	3.80
- 0.90	3.60		3.80	3.70	3.70
- 0.80	3.70		3.80	3.60	2.80
-0.75	3.70	3.20	3.80	3.60	2.80
-0.70	3.80		3.90	3.70	2.60
- 0.60	3.90	3.00	3.90	3.60	2.80
-0.50	3.95	2.80	3.95	3.70	3.00
-0.40	4.00		4.00	3.80	3.20
-0.30	4.20		4.10	3.90	3.30
- 0.20	4.30		4.20	3.95	3.40
-0.10	4.60		4.60	3.95	3.60
0.00	4.80	3.20	4.80	4.00	3.80
0.10	5.00		5.00	4.20	5.00
0.20	5.80		5.20	4.40	5.40
0.30	6.80		5.40	5.00	5.60
0.35	7.00		5.60	5.20	5.80
0.40	6.00	6.00	5.70	6.00	6.20
0.50	3.00		2.80	2.80	4.00
0.60	0.00		0.00	0.00	0.00

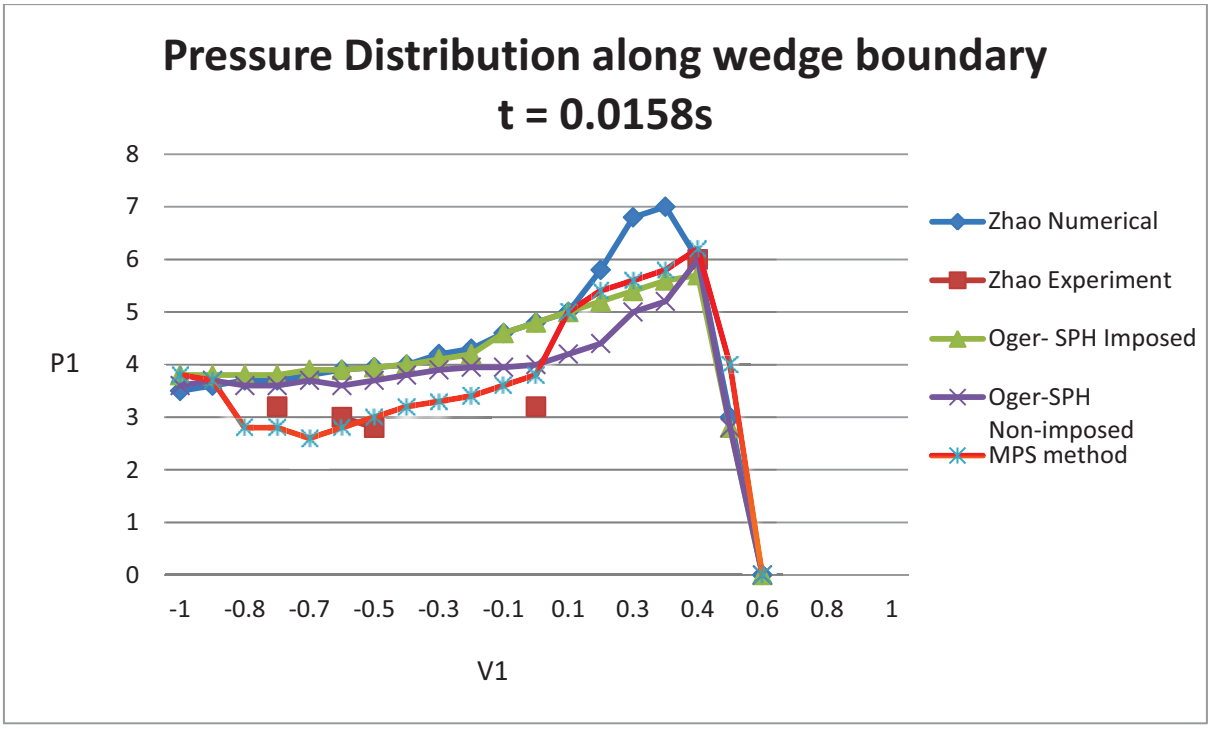

Figure 3-11 Pressure distribution comparison at t = 0.0158s

Table 3-4 Pressure distribution along wedge boundary t = 0.0202s

Z1	Zhao Numerical	Zhao Experiment	Oger - SPH Imposed	Oger- SPH Non Imposed	MPS Method
0.00	2.65		3.60	3.40	2.20
0.05	2.60		3.65	3.30	2.00
0.10	2.60	2.40	3.70	3.00	2.00
0.15	2.55		3.40	3.00	2.00
0.20	2.50		3.50	3.00	1.90
0.25	2.50	1.80	3.55	2.95	1.90
0.30	2.50		3.50	2.85	1.90
0.35	2.50		3.45	2.80	1.95
0.40	2.50	1.60	3.40	2.80	2.00
0.45	2.55		3.45	2.80	2.00
0.50	2.60		3.35	2.80	2.00
0.55	2.65		3.30	2.80	2.00
0.60	2.70	1.70	3.32	2.85	1.95
0.65	2.75		3.10	2.85	1.90
0.70	2.80		3.00	2.90	1.85
0.75	2.90		3.10	2.85	1.85
0.80	3.00		3.20	2.90	1.80
0.85	2.80		3.10	2.85	1.80
0.90	2.50	2.30	3.00	2.80	1.75
0.95	1.40		2.80	2.65	1.70
1.00	0.00		1.60	1.60	1.65

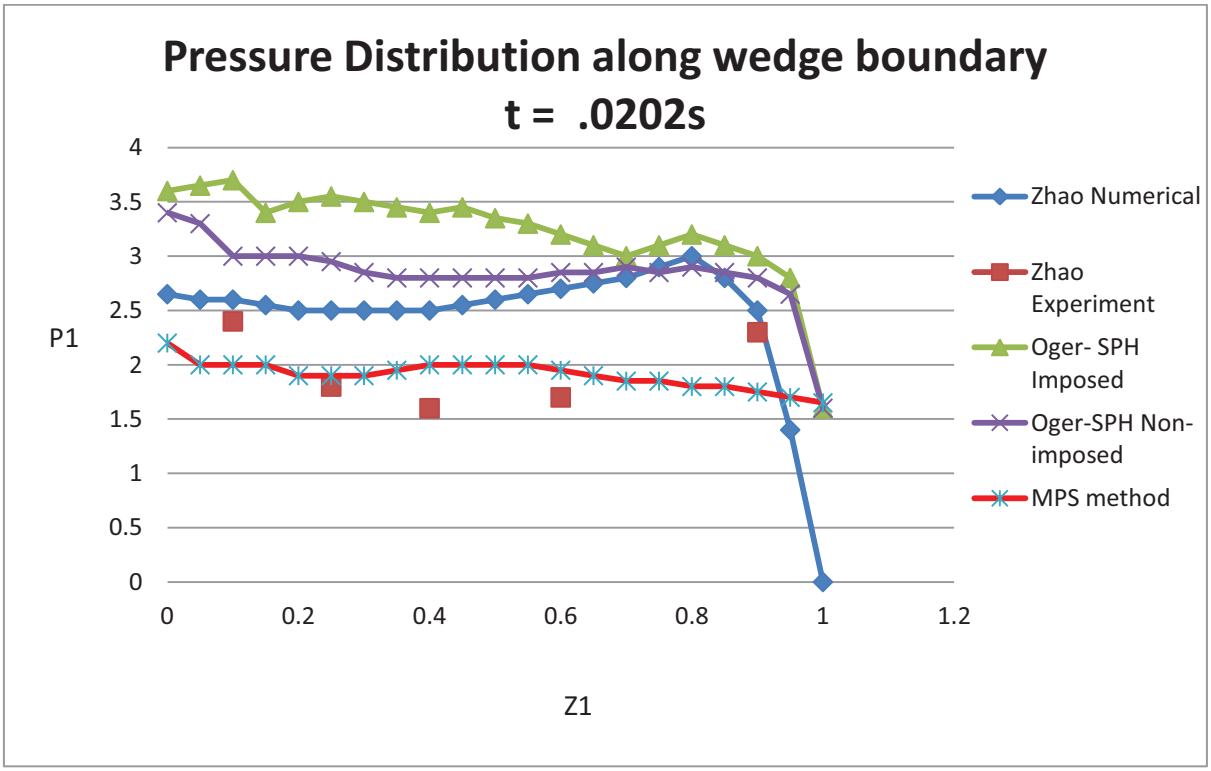

Figure 3-12 Pressure distribution comparison at t = 0.0202s

3.7 Conclusion.

A numerical simulation method was presented to show a typical fluid structure interaction application. The results from the simulation showed that the presented modelling technique could be applied to a marine hydrodynamic problem involving large free surface deformation and fluid fragmentation.

This study presents the MPS method as a prediction tool to extract solid boundary pressures in simulations involving slamming effects and able to provide visualisation results showing the free surface deformation. The pressure distribution profiles on the wedge boundary have been compared with experimental and numerical studies involving a case of a wedge impacting on the free surface by Zhao et al (1997) and an SPH scheme introduced by Oger et al (2006) to test a free falling wedge whose vertical linear motion was the only degree of freedom. The MPS method showed closer agreement with the experiments for free falling wedge than for both numerical simulations of Zhao et al (1997) and Oger et al (2006).

On the basis of these results, it may be concluded that the numerical method MPS proposed in this study represents a reasonable approximation for the prediction of violent free surface problems such as slamming effects.

The main advantages of the MPS method in terms of implementation are that is not necessary to use a computational grid (mesh less property) and it offers the possibility of handling fragmentation and non-deformable solid boundaries. The method is further developed to simulate water flow behaviour on deck of a FPSO having a green water problem, offering a higher simplicity for solving a complex hydrodynamic problem.

CHAPTER 4

MODEL TEST AND INVESTIGATION OF GREEN WATER ON FPSO

4.1 Introduction

A brief study of the FPSOs in the North Sea was undertaken following the information presented in the HSE report by HR Wallingford (2002). A summary of the data giving the principal particulars in full scale are found in Table 4.1. The experimental setup has been designed by using the prototype FPSO from the experiments on green water by Han (2003) as reference for the model parameters. Han (2003) used a scale model of 1.55 in the green water experiments conducted at MARINTEK. In this study a scale of 1.127 was used due to the size limitation of the MAST wave tank. The prototype FPSO from Han (2003) is found to be representative of the FPSOs currently in operation when we compare the database parameters and that of the FPSO in the research.

Table 4.1. Average of the principal particulars of the FPSOs in the Central North Sea area in full scale.

	HSE DATA	**FPSO IN THIS RESEARCH**
Length between perpendiculars (m)	216.6	200.31
Beam (m)	41.5	38
Depth (m)	21.3	28.8
Mean draught (m)	15	16
Loaded displacement (tonnes)	112,567	105,648

An experimental study was conducted on a moored FPSO model in the Newcastle University MAST Hydrodynamic Facility. The aim was to provide information and data to increase the understanding of the physics and processes that a floating vessel undergoes when it encounters green water loading caused by both regular and irregular waves.

4.1.1 Objectives

The tests were carried out to investigate green water phenomena on a moored FPSO model encountering regular and irregular waves generated in the MAST Wave tank. In the investigation of green water effects on the FPSO, the following were evaluated in the experiment;

- Flow pattern observation of green water on deck taking into consideration vessel motions.
- Pressure conditions on deck
- Impact loading on deck structure

Measured data collected from the experiment were used for comparison with numerical simulations. The water heights measured at the deck boundary were directly used in the numerical simulations.

4.2 – Methodology and Experimental Setup

4.2.1 – The Facility

Newcastle University – Marine Science and Technology (MAST) hydrodynamic laboratory is located on the ground floor of the Armstrong Building. The test facility consists of a Towing tank, Mechanical Workshop, Electrical Workshop, Flumes, Preliminary Test Tank, Model Building Workshop, Electronic assembly office and Computer Work Stations.

The main facility for the green water experiment was the Towing Tank. Details of the tank comprise as follows;

TANK SIZE – 40m Length, 3.65m width, and 1.2m depth.

WAVES – Regular and Irregular waves generated via control signals from the computer station installed with the wave generation software 'OCEAN' and 'WAVE' - Edinburg Design Ltd.

WAVE MAKER - 8 hinged paddles with servo controlled by an electro – mechanical actuator. Control signals for the wave maker are inputted from the computer using the software 'OCEAN'.

BEACH-: Sponge material encased in vertical 'saw tooth' meshed cages located at the opposite end of the tank from the wave makers, to absorb the incident waves.

The water depth required for the green sea experiment is 150m prototype. The Towing tank depth of 1.2m was able to meet these criteria, without modification at a scale of 1:127.

LIMITED TANK WIDTH: - Due to wall interactions, the occurrence of experimental errors and measurement uncertainty is very possible in wave tank model tests. The situation can be avoided by using a model such that the ratio of tank width to model transverse dimension is at least 5: 1. (Chakrabarthi, 1994). The ITTC 17 Procedure (1984) also recommends the following relationship between the model length L_m and the tank width B for narrow tanks, which the MAST laboratory falls into the category;

$$L_m \cong 1 + B/4 \qquad (4.1)$$

Since the tank width and model breath are 3.65m and 0.3m respectively, the tank width to model breath ratio is 12:1 which is greater than the recommended ratio of 5:1. From Equation 4.1, L_m is recommended not to be more than 1.91. Actual value of L_m is 1.65 is within recommended limits.

PLATE 4.1 - A section of the towing tank showing the paddles.

4.2.2 Coordinate System Convention

The coordinate system convention adopted in this experimental investigation is illustrated in Figure 4.1 and defines the motion directions as follows;

SURGE - ((X) - Positive towards the bow (forward)

SWAY - (Y) - Positive to port

HEAVE - (Z) - Positive upwards

ROLL - (Q_x) - Positive star board side down

PITCH - (Q_y) - Positive bow down

YAW - (Q_z) - Positive bow to port

The Qualysys Tracking system captures the motion and the output data configuration follows this format.

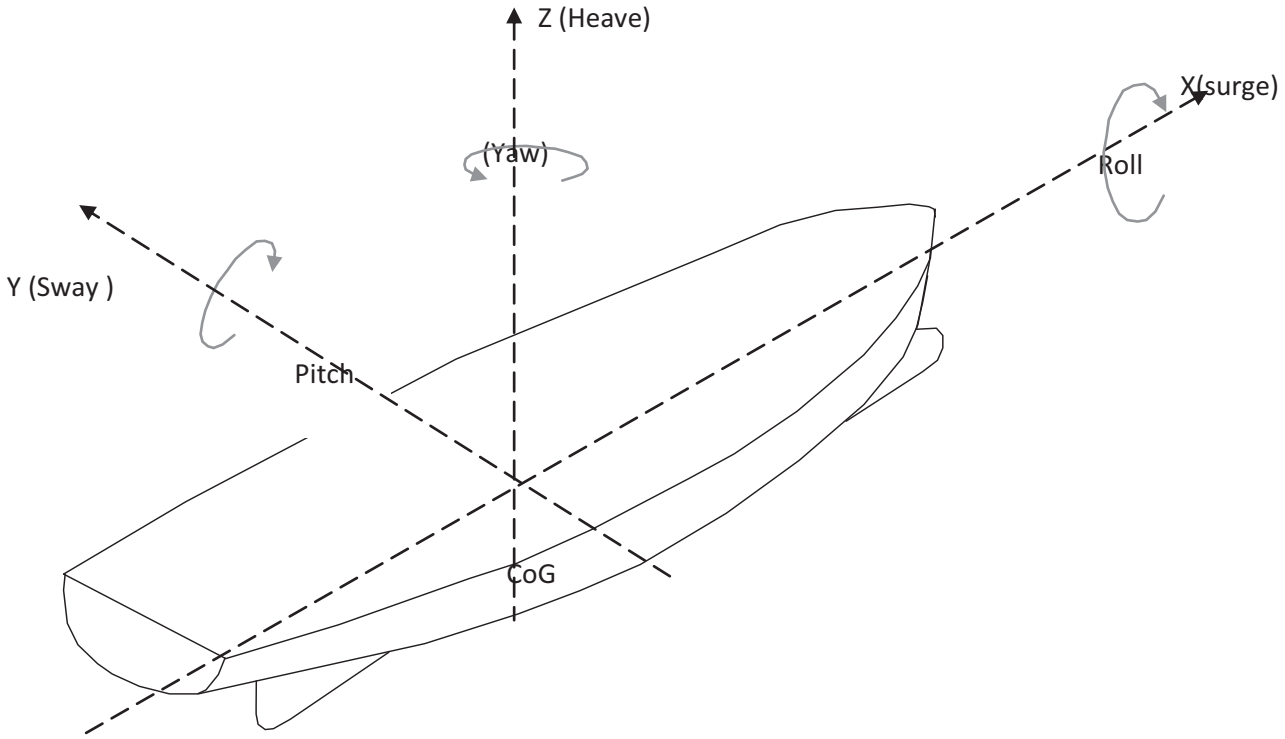

Figure 4-1 Reference system for directions of motion

4.2.3 Model Properties and Environmental Consideration.

4.2.3.1 Model Scaling.

The experiments were carried out using a scale of 1: 127 because of wave tank size limitations and Froude scaling was applied to the model tests. In this experimental investigation, all figures are expressed in model scale unless stated. Table 4.2 shows the Froude scaling of the physical quantities (λ is the scaling factor applied to the lengths, which in this case is 127). The ratio between the salt water density and fresh water density is taken as 1.025 and it is represented using ρ_R

TABLE 4.2 – Scale factors

QUANTITY	SCALING FACTOR	UNIT
Length	λ	m
Time	$\lambda^{1/2}$	sec
Frequency	$\lambda^{1/2}$	Hz
Velocity	$\lambda^{1/2}$	m/s
Acceleration	1	m/s^2
Volume	λ^3	m^3
Angle	-	degree
Angular Velocity	$\lambda^{1/2}$	degree/s
Water Density	ρ_R	$Tonnes/m^3$
Mass	$\rho_R \lambda^3$	Tonnes
Force	$\rho_R \lambda^3$	KN
Moments	$\rho_R \lambda^4$	KN. m
Extension Stiffness	$\rho_R \lambda^2$	KN/m

4.2.3.2 Construction of Model

The model construction was undertaken by the Thompson Model Shop in Southampton, U.K. On its completion, the following 'approval' checks on the model were made by physical observation in compliance with conditions set up by the Marine technical team of the MAST Laboratory, Newcastle.

1 Symmetry
2 Twist (Looking Forward to Aft.)
3 Smoothness of the curves.
4 Painting (if required). The white colour was maintained.
5 Coating of fiberglass inside the model
6 Deck watertightness to prevent flooding.

These checks were necessary because of the instrumentation and measuring devices needed to be attached to the model. The model was required to be water proof; and was required to possess a surface finish that is attractive to the photographic requirements. Also the painting was required to allow visibility of the model underwater. The model was also required to be strong enough to represent a rigid body.

The FPSO was built using polymer resins for the hull construction and wooden ply board for the bulkheads to support the deck – see Plates 4.2 to 4.4 for pictures taken during the construction process.

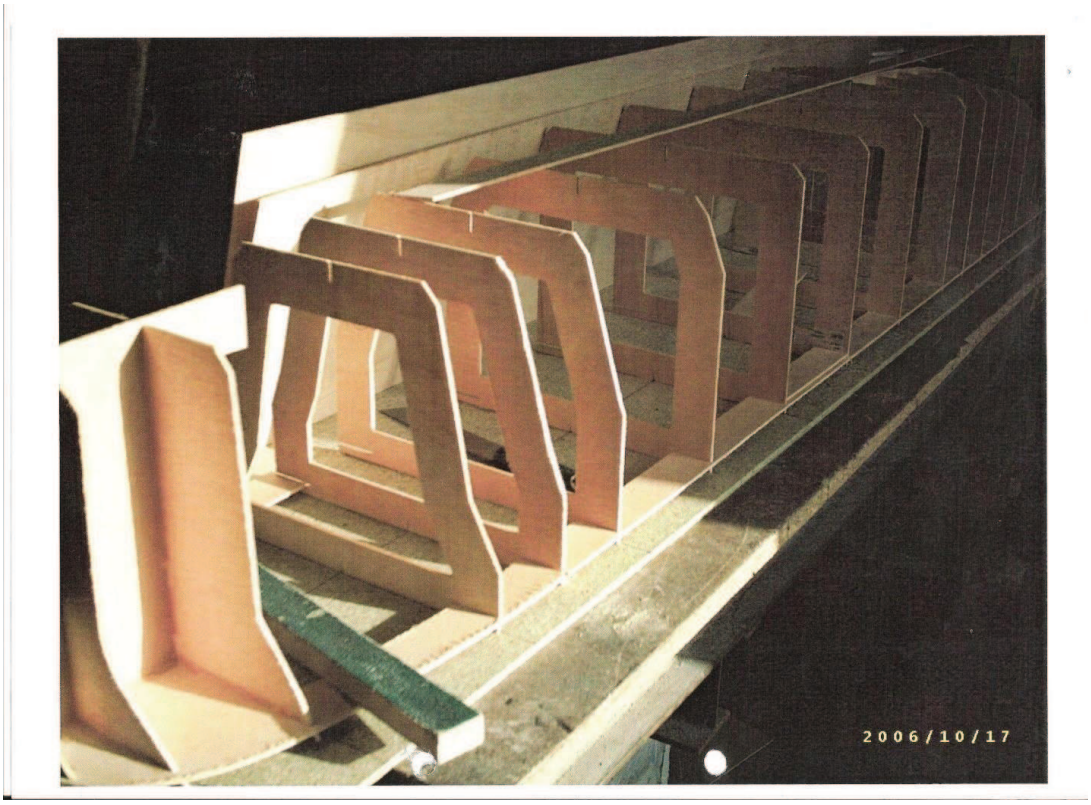

PLATE 4.2 FPSO hull constructions.

PLATE 4.3 FPSO transverse members

PLATE 4.4 FPSO hull prepared from fiber glass epoxy resin

Lines plan, body plan and table of offsets were prepared and made available to the model shop for the construction of the of the FPSO model. Plates 4.5, shows the lines plan and body plan of the prototype FPSO.

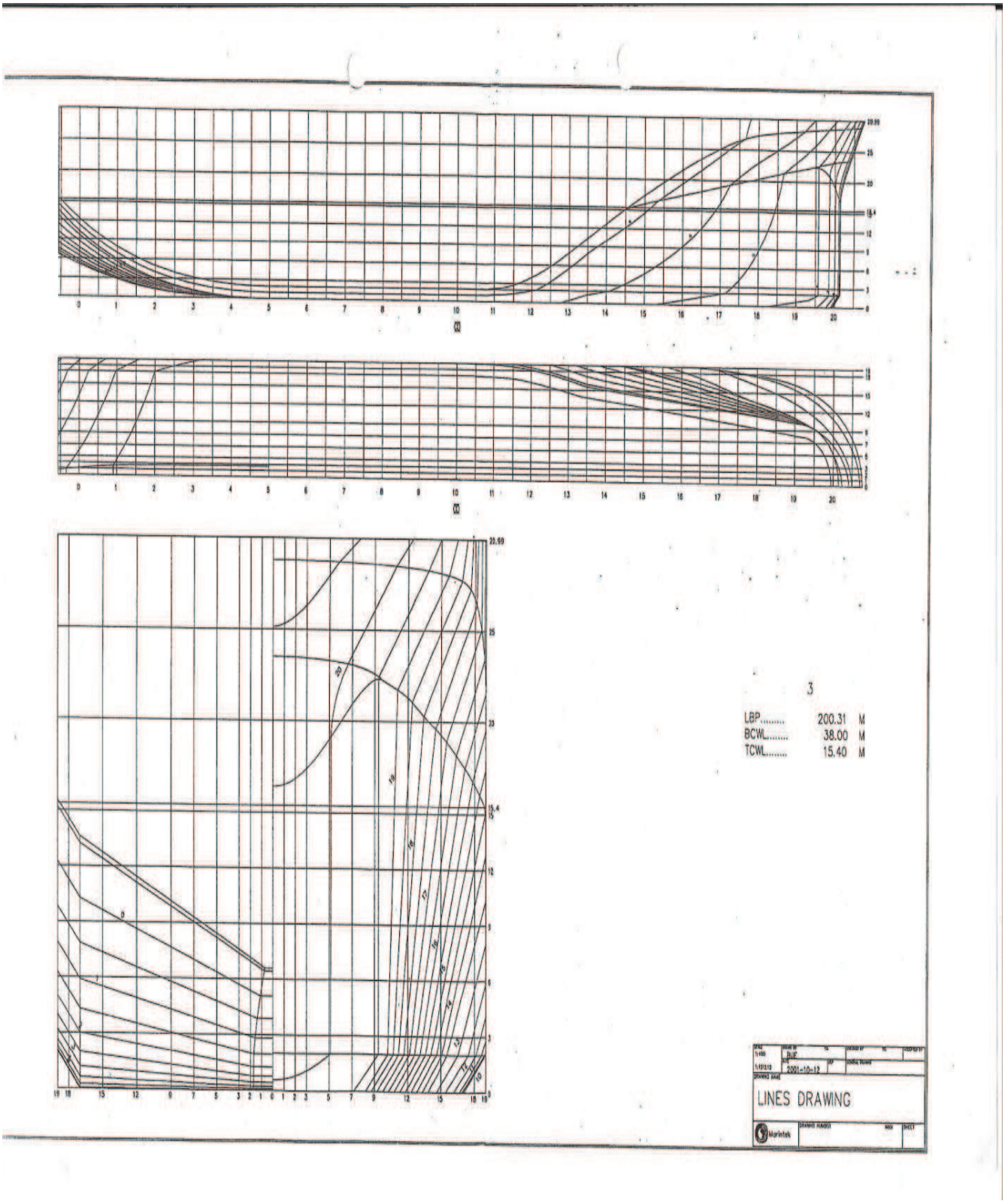

PLATE 4.5 FPSO lines drawings

A forward deck structure as seen in Plate 4.6, made of flat aluminium plating was installed at some distance from the bow. This could represent major processing equipment on the main FPSO vessel deck

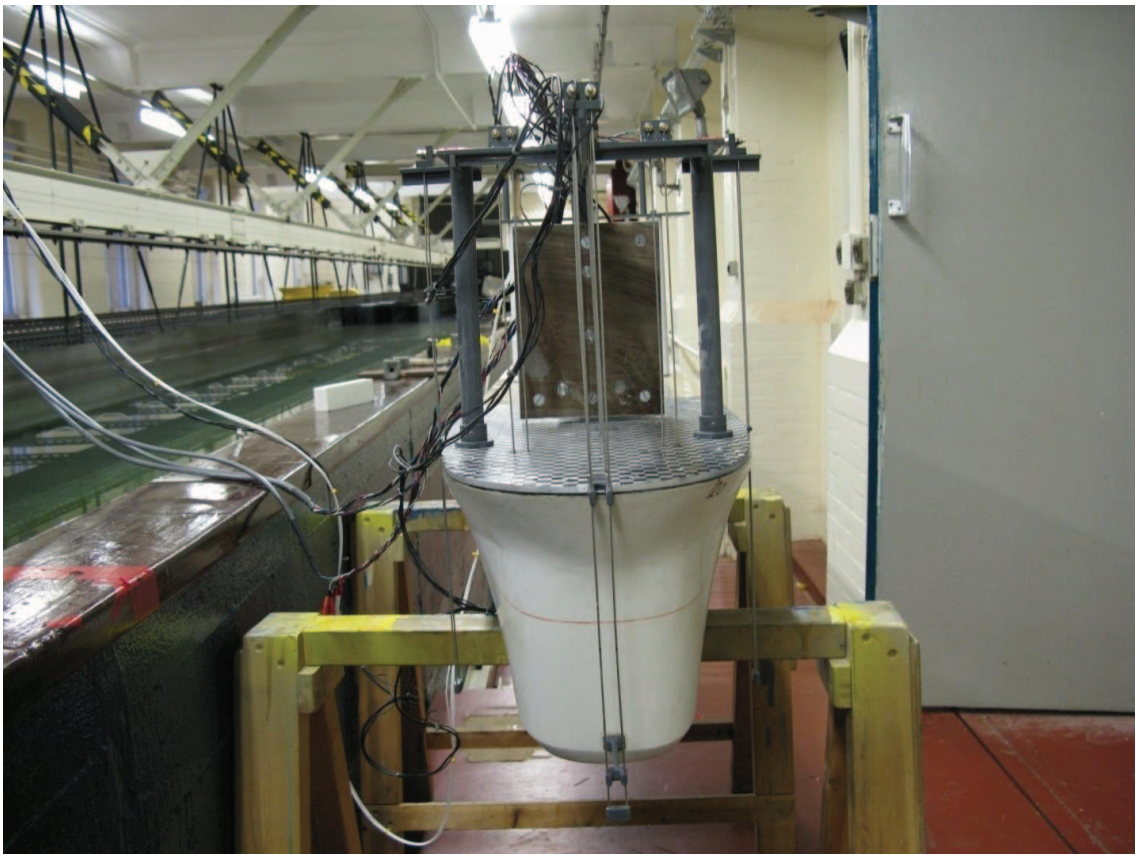

PLATE 4 .6: Section showing forward deck structure

For the mooring system, three mooring lines were adopted and modelled to achieve the overall stationary requirements for the FPSO model during the green water experiment. The Mooring lines were represented with polymer coated steel wires. The configuration parameters of the mooring system are set in Table 4.3.

TABLE 4.3 – Mooring system parameters.

MATERIAL	**Coated Steel Wire**
Number of mooring lines	3
Angle between forward mooring lines	60 Degrees
Length of mooring lines	7 Metres
Number of anchors	3
Weight of two forward anchors	11.5kg each
Weight of aft anchor	10.5kg

The parameters and layout of the mooring system are presented in Table 4.3 and shown in Figure 4.2 respectively. The mooring system is intended only to hold the FPSO in place during the green water experiment and not represent the scaled dynamics of the real mooring system in open sea conditions.

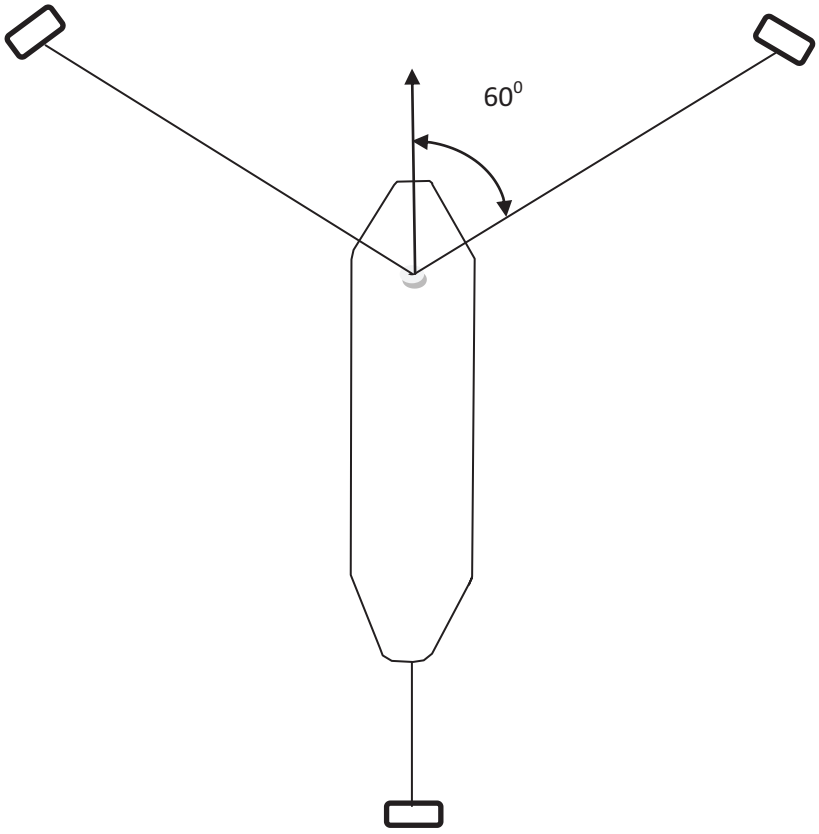

Figure 4- 2 Mooring layout

4.2.3.3 Principal particulars of Model.

The principal particulars of the model are outlined in Table 4.4.

TABLE 4.4 – Model particulars.

Length - LBP(m)	1.572
Breadth moulded –B(m)	0.300
Depth moulded – D(m)	0.226
Draft – T(m)	0.1256
Displacement - Δ(Kg)	54.300
Centre Of Gravity –KG(m)	0.118
Metacentric Height – GM(m)	0.013
Longitudinal Centre Of Gravity – LCG(m) from AP	0.748
Radius Of Gyration - Kyy(m)	0.400

The principal particulars of the model were obtained from the prototype FPSO used by Han (2003) using a model scale of 1.127. In order to confirm some of the target values presented in the table, an inclining experiment and knife edge test were conducted to obtain the KG, GM and LCG. A difference of 0.13% was obtained between the knife-edge test value and the target value. The other results obtained were in close agreement with the target values in Table 4.4

The model was ballasted to represent the full draught operating condition using steel weights placed and fixed at three different locations in the model to achieve the loading draft and trim. Figure 4.3 shows the ballasting arrangement in the FPSO with steel weights positioned at locations A, B and C. The ballast weights and location dimensions are provided in Table 4.5 to provide information on the required weights and location that allows the model achieve the target draft in Table 4.4 and keep an even keel in the wave tank.

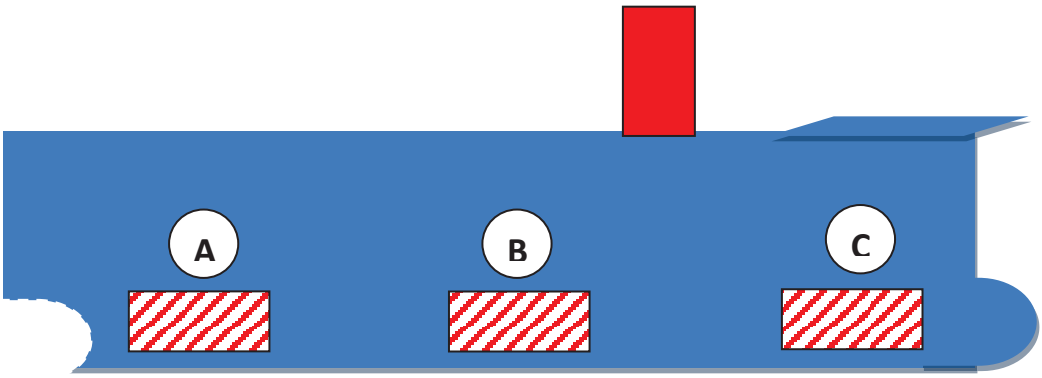

Figure 4-3 Ballast weight arrangements for model (A, B, C – show weight position)

TABLE 4.5 – Ballast weights location in Figure 4.3

Position	Weight	Dist from AP(m)
A	11kg.	0.3925
B	9.4kg	0.7850
C	16.2kg	1.1775

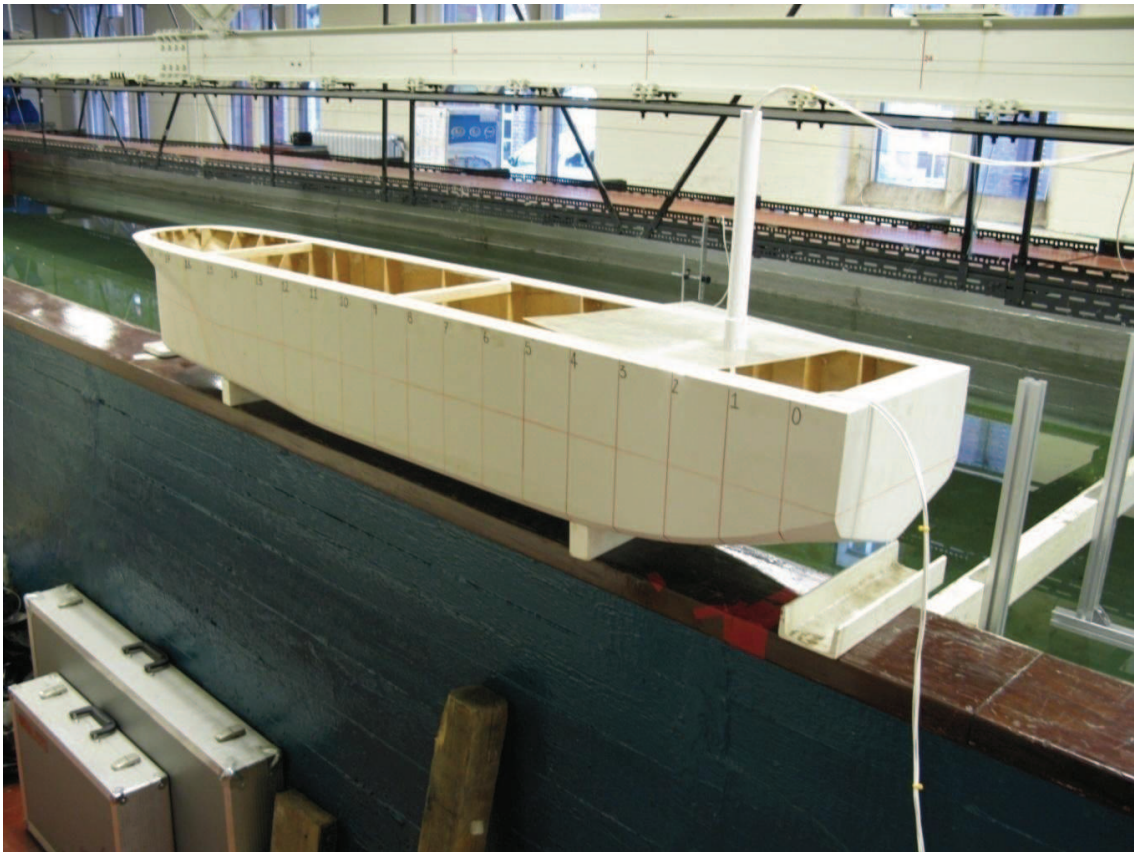

PLATE 4.7 – Station marks on FPSO model

4.2.4. Experimental Conditions – Tests in Regular and Irregular Waves

Wave conditions were calibrated in the MAST towing tank at the beginning of the research investigation in the absence of the model in the tank. Each test condition for regular and irregular waves was run without the model in the tank and the measurements were analyzed and compared with target conditions. This was necessary to ensure that the computer software and measuring probes were working adequately and that the correct target conditions were produced at the location where the model was to be tested. Measurement uncertainty can be caused by possible errors in the experimental setup and when the results from the tests are analyzed. A detail of possible errors that can occur during experiments are given in the work of Greco (2001) where such errors are attributed to sources from wave tank, wave probes, pressure gauges and human errors. In the case of this

experiment, the error sources from the wave tank such as wave reflections are mitigated by the tank width ratio of 1:12. Also measurements uncertainties due to initial conditions in the tank are also reduced by allowing a time interval of eight minutes between each run. Greco (2001) suggests a mean value of five minutes between each run.

A series of experiments were thereafter carried out in regular and irregular waves with the model moored in the tank. Each test was run for sixteen minutes model scale which is equivalent to prototype three hour storm conditions in open sea. The regular waves tested were used for measuring the RAO for the model while the irregular wave represented sea state conditions in the North Sea conditions that could generate green water phenomenon.

Table 4.6 lists the tank wave conditions targeted for the series of regular waves run with the model present in the wave tank. Some of the tests could not be carried out due to the limitations of the wave making software. √ -Signifies the wave conditions carried out successfully in the MAST Wave Tank.

TABLE 4.6 Regular waves tests in model scale

TEST NUMBER	WAVE HEIGHT (m) in model scale	WAVE FREQUENCY (Hz) in model scale	REMARKS
1	0.086	0.75	√
2	0.095	0.75	√
3	0.110	0.75	√
4	0.130	0.75	√
5	0.086	0.80	√
6	0.095	0.80	√
7	0.110	0.80	√
8	0.130	0.80	√
9	0.086	0.85	√
10	0.095	0.85	√
11	0.110	0.85	√
12	0.130	0.86	√
13	0.086	0.90	√
14	0.095	0.90	√
15	0.110	0.90	√
16	0.130	0.90	√
17	0.086	0.95	√
18	0.095	0.95	√
19	0.110	0.95	√
20	0.130	0.95	√
21	0.086	1.00	√
22	0.095	1.00	√
23	0.110	1.00	√
24	0.130	1.00	√
25	0.086	1.05	√
26	0.095	1.05	√
27	0.11	1.05	√
28	0.086	1.15	√
29	0.086	1.15	√
30	0.095	1.15	√
31	0.086	1.20	√
32	0.095	1.20	√

The model was also tested in irregular seas generated using a JONSWAP spectrum. The sea states were achieved using the software package named OCEAN developed by Rogers and King, Edinburg Designs Ltd (1997). In this software the JONSWAP spectrum $S(f)$ as stated in the manual is repeated below; (Rogers and King, Edinburg Design Ltd, 1997)

$$S(f) = \frac{\alpha g^2}{(2\pi)^4 f'^5} \exp\left[-\frac{5}{4}\left(\frac{f_p}{f'}\right)^4\right] \gamma^{\exp\left(-\frac{1}{2}\left(\frac{f/f_p - 1}{\sigma}\right)^2\right)} \qquad (4.2a)$$

where $$\sigma = \begin{cases} \sigma_a & f > f_p \\ \text{if} & \\ \sigma_b & f < f_p \end{cases}$$

and $$f' = \frac{f_e}{\frac{f_p / f - \tau}{C_e} + \tau} \qquad (4.2b)$$

f_p is the frequency of the peak Spectral density and f_e is frequency at which amplitude is being calculated. C_e is the compression factor.

γ is the value of peak enhancement.

σ_a and σ_b are the sigma factors for the frequencies above and below the peak

$\alpha = 8.1E-3$
$\gamma = 1.0$
$\sigma_a = 0.07$
$\sigma_b = 0.09$

τ is set to 0.857222, a conversion factor

The data above are the default settings provided in the 'OCEAN' software prior to the user specified settings. Selected settings and program values can be specified in the 'OCEAN' software for generating waves in the desired sea states in the wave tank.

Table 4.7 shows a listing of the settings and parameters for the sea states used in the experiments.

The experimental programme covered a similar range of sea states to those used in a series of 'green seas' experiments carried out on a similar model at larger scale (1:55) in the ocean wave basin at MARINTEK. Han (2003).

The wave conditions of significant wave heights and wave peak periods (H_s, T_P) used at MARINTEK were set at (10, 14) and (12, 12) prototype scale. The waves were successfully generated at the MAST wave tank using the 'OCEAN' program with JONSWAP sea spectrum. To achieve some of the desired wave conditions, the gamma in equation (4.2) can be calculated from Torsethangen equation in Baltrop and Adams (1991) as follows;

$$\gamma = \exp\left[3.4843\left(1 - 0.1975\left(0.036 - 0.0055\frac{T_P}{\sqrt{H_S}}\right)\frac{T_p^4}{H_S}\right)\right] \qquad (4.3)$$

TABLE 4.7 – Irregular wave tests in model scale.

TEST NUMBER	Peak Frequency (Hz) in model scale	Significant Wave Height(m) in model scale	Wave Height(m) in prototype scale(H_s)	Wave Period(s) in Prototype scale(T_p)	γ	α	REMARK
1	0.80	0.110	14.0	14	3.3	8.1E-3	
2	0.80	0.110	14.0	14	3.3	8.1E-2	
3	0.93	0.110	14.0	12	3.3	8.1E-3	
4	0.93	0.110	14.0	12	3.3	8.1E-2	
5	0.93	0.110	14.0	12	1.0	8.1E-3	
6	0.93	0.086	11.0	12	1.0	8.1E-2	
7	0.93	0.095	12.0	12	1.0	8.1E-3	
8	0.93	0.095	12.0	12	5.0	8.1E-3	
9	0.93	0.110	14.0	12	5.0	8.1E-3	
10	0.93	0.130	16.5	12	3.3	8.1E-2	
11	0.93	0.095	12.0	12	3.3	8.1E-2	
12	0.93	0.078	10.0	12	3.99	8.1E-2	
13	0.93	0.110	14.0	12	4.74	8.1E-2	
14	0.94	0.078	10.0	12	3.99	8.1E-2	
15	1.24	0.110	14.0	9	4.74	8.1E-3	
16	0.93	0.095	12.0	12	4.3	8.1E-3	MARINTEK
17	0.93	0.095	12.0	12	4.3	8.1E-2	MARINTEK
18	0.80	0.078	10.0	14	3.3	8.1E-2	MARINTEK
19	0.80	0.078	10.0	14	4.74	8.1E-3	MARINTEK

4.3 Instrumentation and Measurement Systems.

4.3.1 General Description.

The instrumentation and measurement systems for obtaining the required data collection, data analysis and data characterisation consists of a number of different groups of systems.

- A system of probes to measure the incoming waves
- A system for tracking and measuring the FPSO motion displacements in 6 DOF
- A system of probes to measure wave run up and green water level on deck
- A system of pressure transducers to measure green water pressure on deck.
- A system of load cells to measure force due to water jet impact on the deck structure of FPSO

In house computer programs for wave measurement recordings, wave data analysis, graphical presentation and FPSO motion recording and analysis were used in the experiments.

Visual recording was carried out at each stage of the experiment.

Table 4.7 provides a summary of the instrumentation used in the research study. The fore deck instrumentation of the FPSO model is shown in Figure 4.4 and Figure 4.5. Plates 4 .8 to 4 .11, show the instrumentation arrangements and deck structure configuration of the model.

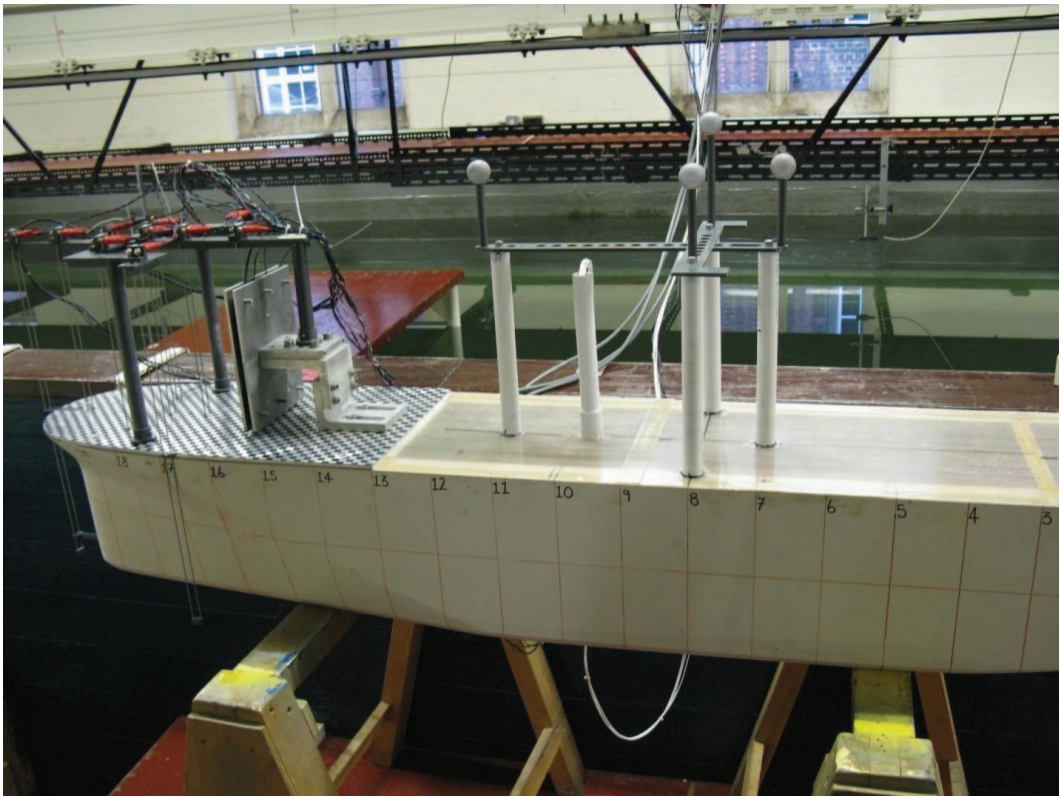

PLATE 4.8: Section showing FPSO instrument configuration

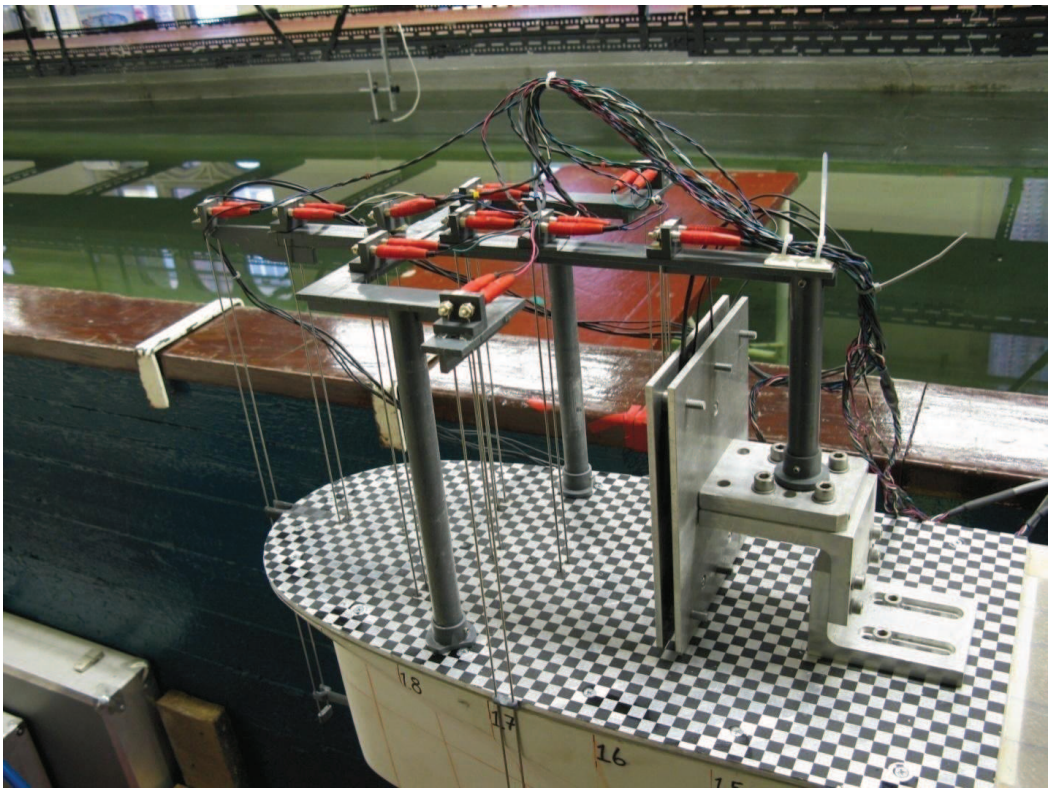

PLATE 4.9: Section showing wave probes for deck Green Water measurement and decktructure configuration.

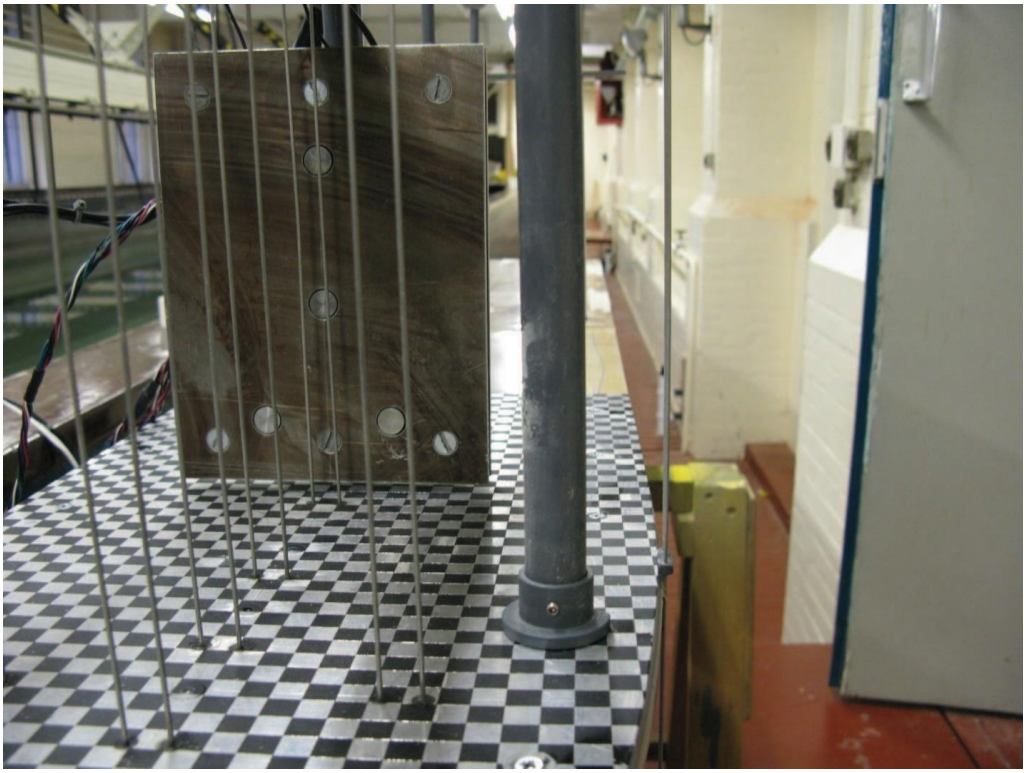

PLATE 4.10: Section showing load cells on deck structure

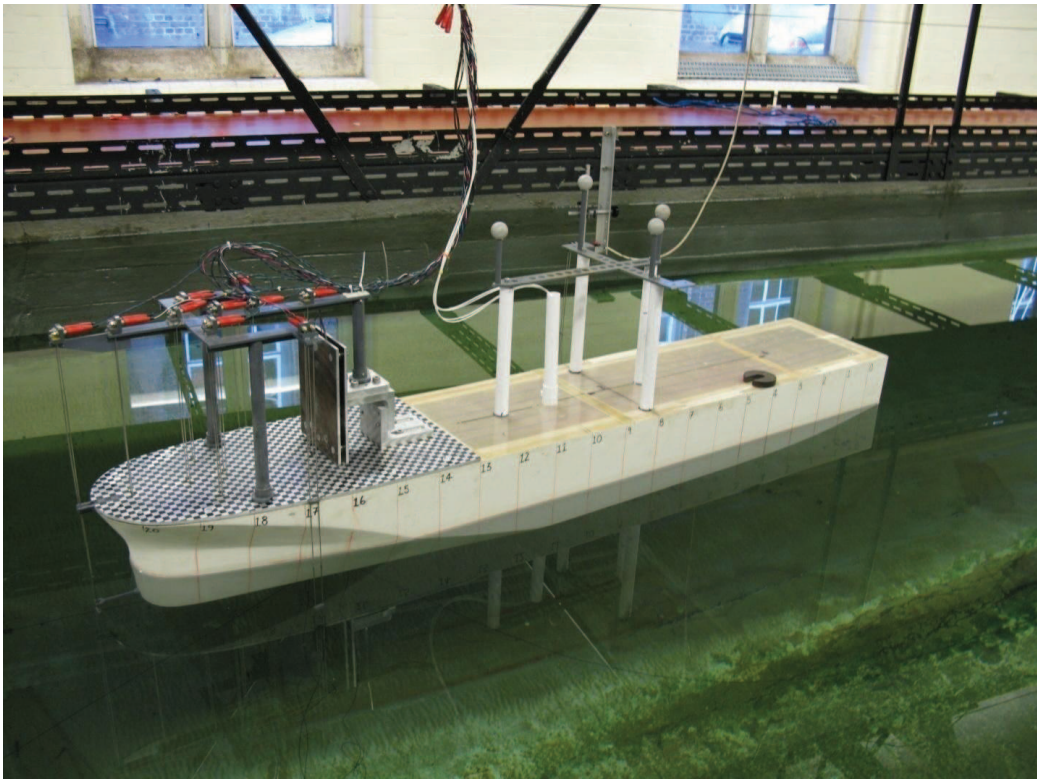

PLATE 4 -11: FPSO moored and stationed In Mast Towing Tank

TABLE 4.8 – Instrumentation and Measurement systems used

CHANNEL NUMBER	PARAMETERS TO BE MEASURED	INSTRUMENT	ACCURACY	UNIT
WP 1	WAVE RUN UP BOW	WAVE PROBE	1mm	mm
WP 2	WAVE RUN UP STARBOARD	WAVE PROBE	1mm	mm
WP 3	WAVE RUN UP PORT	WAVE PROBE	1mm	mm
WP 4	GREEN WATER LEVEL MID DECK FWD	WAVE PROBE	1mm	mm
WP 5	GREEN WATER LEVEL MID DECK FWD	WAVE PROBE	1mm	mm
WP 6	GREEN WATER LEVEL DECK PORT	WAVE PROBE	1mm	mm
WP 7	GREEN WATER LEVEL DECK STBD	WAVE PROBE	1mm	mm
WP 8	GREEN WATER LEVEL FWD OF S'STRUCTURE	WAVE PROBE	1mm	mm
WP 9	GREEN WATER LEVEL FWD OF S'STRUCTURE	WAVE PROBE	1mm	mm
WP 10	GREEN WATER AT S'STRUCTURE	WAVE PROBE	1mm	mm
WP 11	INCOMING WAVE ELEVATION	WAVE PROBE	1mm	mm
WP 12	OUTGOING WAVE ELEVATION	WAVE PROBE	1mm	mm
LC1	FORCE TOP SIDE OF S'STRUCTURE	LOAD CELL	1%	NEWTONS
LC2	FORCE MID POINT OF S'STRUCTURE	LOAD CELL	1%	NEWTONS
LC3	FORCE BOTTOM OF S'STRUCTURE PORT SIDE	LOAD CELL	1%	NEWTONS
LC4	FORCE BOTTOM OF S'STRUCTURE STBD SIDE	LOAD CELL	1%	NEWTONS
PT 1	WATER PRESSURE ON DECK	PRESSURE TRANSDUCER	0.05%	mbar
PT 2	WATER PRESSURE ON DECK	PRESSURE TRANSDUCER	0.05%	mbar
PT 3	WATER PRESSURE ON DECK	PRESSURE TRANSDUCER	0.05%	mbar
PT 4	WATER PRESSURE ON DECK	PRESSURE TRANSDUCER	0.05%	mbar
	X – SURGE	QUALYSIS	1mm	mm
	Y – SWAY	QUALYSIS	1mm	mm
	Z – HEAVE	QUALYSIS	1mm	mm
	ROLL	QUALYSIS		degree
	PITCH	QUALYSIS		degree
	YAW	QUALYSIS		degree

4.3.2 Wave Measurements

Water surface elevations at selected locations were measured with wave probes. Twelve probes in all were selected overall and arranged at different locations both in the wave tank and on board the FPSO model shown in Figures 4.4 and 4.5, and Plates 4.9 and 4.10. Of the twelve wave probes, two wave probes were installed at 240 mm from the forward perpendicular at the starboard and port side of the model (WP2 and WP3). A wave probe (WP1) was installed at the bow to measure the incoming green water. On the deck of the model are five wave probes in a row (WP4, WP5, WP8, WP9, and WP10) to measure the water level on deck and forward of the deck structure to measure the elevation of the impinging green water jet. Two additional wave probes (WP6 and WP7) are fixed at 60mm from both port and starboard sides of the deck at 150mm from the FP to also measure the water level on deck and adequately capture the water levels after green water impact with the deck structure. In the wave tank, a wave probe (WP 11) was installed to measure the incoming wave elevation of the waves generated at the wave maker just before impacting on the model and another wave probe (WP 12) to measure the elevation of the outgoing waves after impacting with the model. The sampling rate for all wave measurements is 100Hz.

All the wave probes on the model are characterized by two metal strips, placed parallel to each other with a 5mm separation. When the green water jet impacts on the deck structure, there is a likely formation of bubbles which can result in measurement uncertainty in wave probe WP10. This is mitigated by wave probe WP9 which still captures the flow aftermath of the bubble collapse.

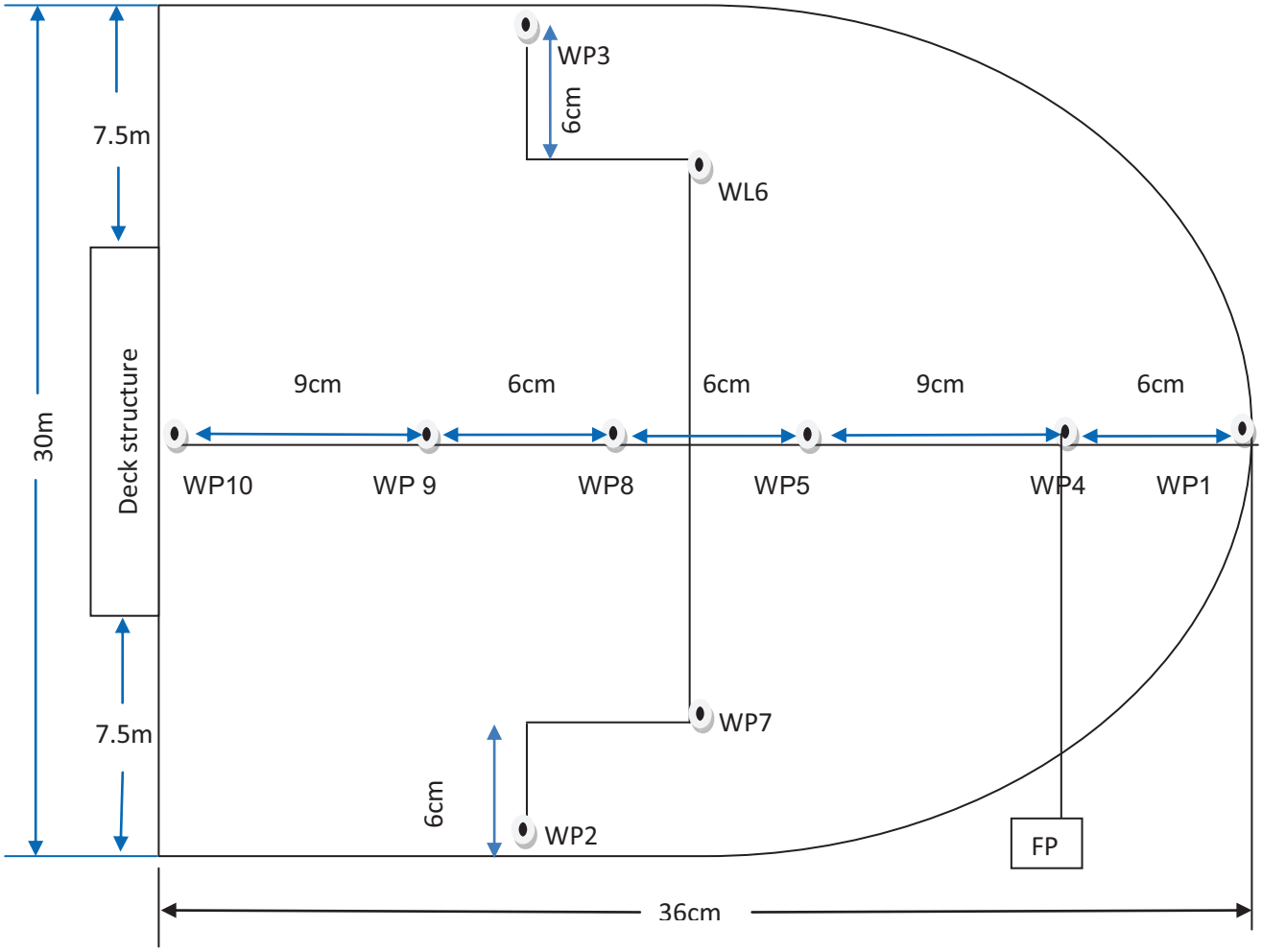

Figure 4-4 Deck instrumentation - wave elevation probes position on FPSO.

4.3.3 Force and Pressure Measurements.

To measure the green water loading impact force on the deck structure mounted on the model, four load cells as shown if Figure 4.5 were fixed at the various points on the aluminium plating representing equipment on a prototype FPSO. A load cell (LC1) was fixed at the top section of the plating, one in the mid section (LC2) and two load cells at the bottom of the plating, fixed at each end (LC3 and LC4). The load cells are about 9mm in diameter.

On the forward deck of the model, aluminium plating was used to represent the deck up to the deck structure mounted, and pressure transducers were fixed to measure the green water pressure on the deck plating. A total of four pressure transducers (PT1, PT2, PT3 and PT4) shown in Figure 4.6 are spread out on the deck in a straight line running fore to aft on the deck plate. The pressure transducers have a diameter of 8mm. A significant shift in the zero values after each test given by a pressure transducer can occur due to changes in the temperature resulting from the dry wet cycles encountered during tests. To control this error source, the pressure cells are constantly kept wet to ensure the same conditions and thus the same zero levels before and after each test.

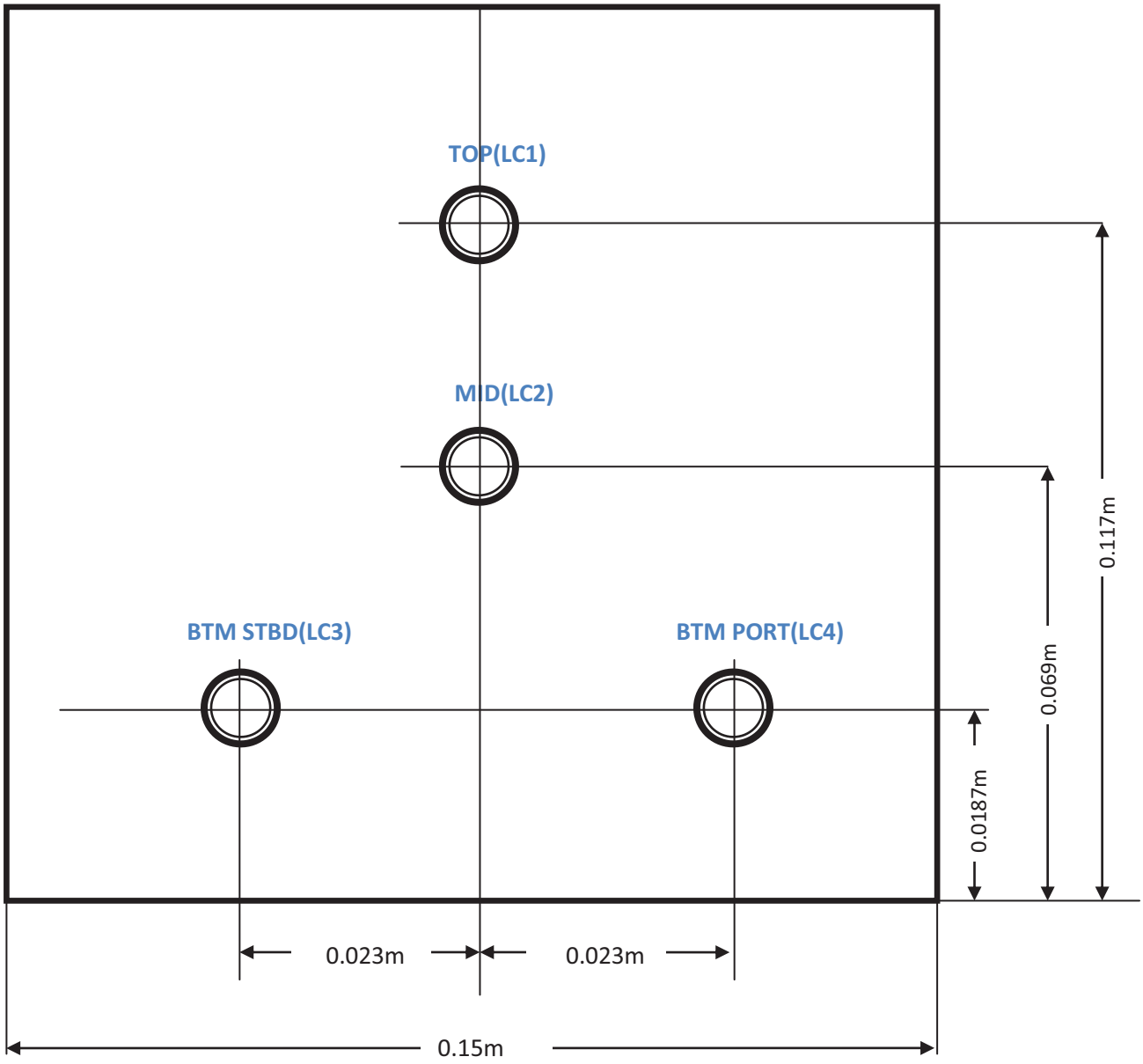

Figure 4-5 Deck instrumentation - load cells on deck structure

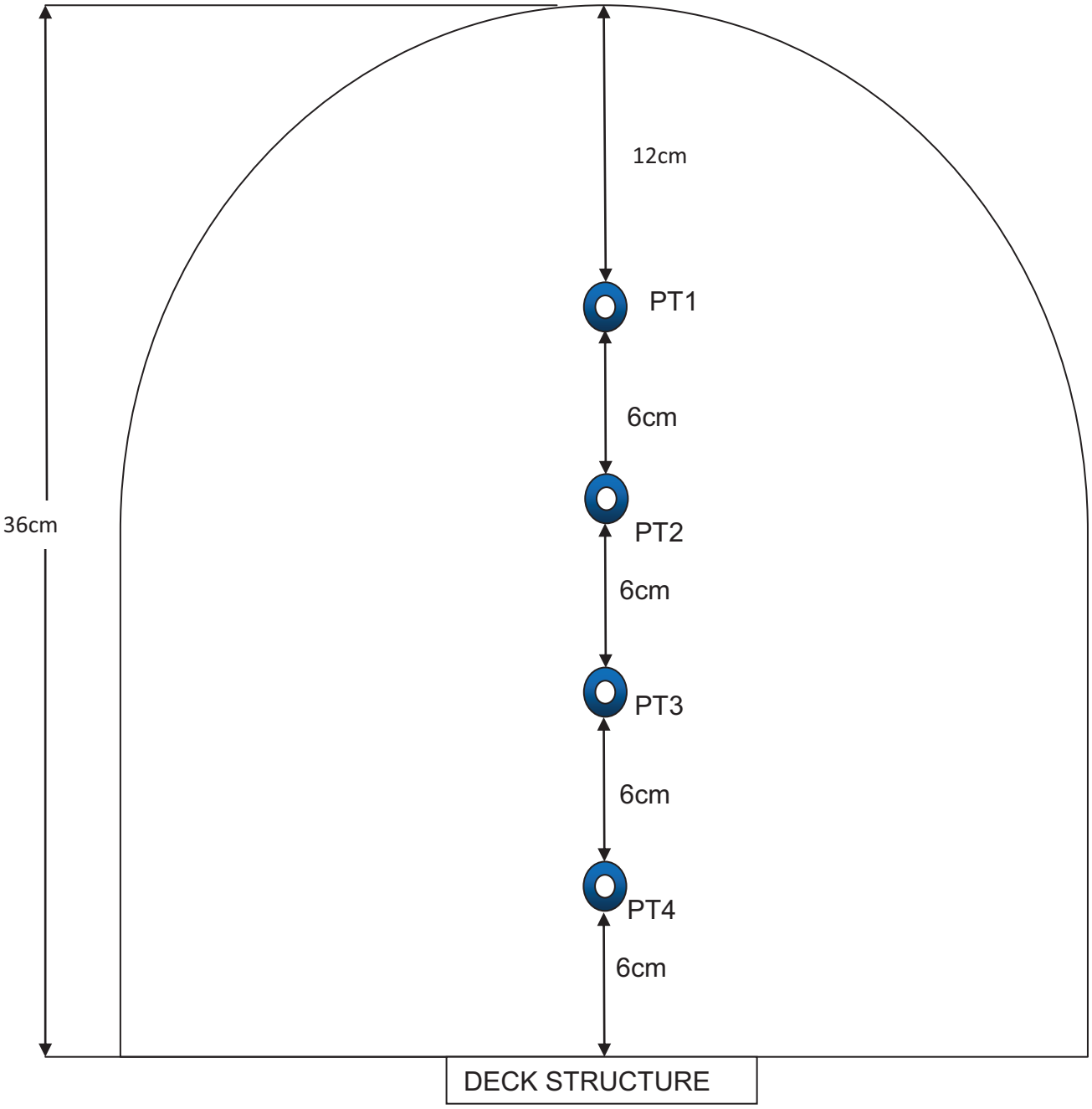

Figure 4-6 Deck Instrumentation-Pressure transducers

4.3.4 Model Motions

The motion displacements of the model FPSO in six degrees are measured using an infra red tracking system, controlled form a computer software package 'QUALYSIS'.

Four reflectors are mounted on the model deck section above the Centre of Gravity (see Plate 4.8). The targets are recorded by two cameras positioned to capture the complete motion sequences of the model in the wave tank. The mooring systems and camera locations are designed to ensure that the model does not drift out of the tracking area when the experiment is in progress. The motion with six degrees of freedom can be deduced from the relative motion of the four targets.

4.3.5 Visual Recording

A SONY video recording handy cam was used to record each stage of the experiment. Each test took a total of 16 minutes of recording, representing a 3hour sea state.

4.4 Measured Data Recording and Presentation

Measured data acquired by the instrumentation system are forwarded to the computer work station installed with the proprietary software programs 'LABVIEW' and 'QUALYSIS'. The computer programs provide a comprehensive graphical and analytical representation of the measured data. Data recording time was 16 minutes in model scale which is equivalent to a three hour extreme condition at sea.

Labview records the acquired data from the wave probes, pressure transducers and load cells. At the completion of each test a spectral analysis was carried out using LABVIEW to determine whether the target wave height from the wave maker is achieved with the input wave conditions sent to the wave maker. Close agreements in measured values to target values indicate a successful run. Also graphical representation of the wave is displayed to illustrate the profile. The pressure and load measurements are graphically displayed to show the intensity of the loading and the impact of a test condition.

The acquired six degrees of freedom are recorded and can be displayed graphically using QUALYSIS. At each test completion, the captured motion of the model is replayed to make sure that the movements of the model are within the bounds of the cameras throughout test proceedings.

4.5 Wave Statistical Analysis

4.5.1 Wave Data Analysis

An important aspect of experimental study is the statistical analysis of the measured records. The analysis allows for a comprehensive evaluation of design parameters and or a successful demonstration of a marine offshore operation.

The statistical analysis of wave measurements enables the prediction of the behaviour of a wave surface for a particular sea state.

Rayleigh Distribution

In design considerations, the distribution of wave heights in a record is an essential part of the environmental analysis. Therefore for engineering purposes, it is desirable to have a model for the distribution of wave heights measured from the experiment. Wave heights in the ocean are often modelled using a statistical distribution named the Rayleigh Distribution. The use of this distribution is appropriate when the wave energy spectrum reflects a narrow band width,

The probability density function $p(H)$ of a wave height H following the Rayleigh distribution can be written as;

$$p(H) = \frac{2H}{(H_{rms})^2} e^{-\left(H/H_{rms}\right)^2} \tag{4.4}$$

The root mean square wave height for a group of waves, H_{rms} is defined as

$$H_{rms} = \sqrt{\frac{1}{\overline{N}} \sum_{i=1}^{m} n_i H_i^2} \tag{4.5}$$

where $\overline{N}$ is the total number of wave heights measured at a point , n_i is the number of wave height in wave record i , H_i is the mean wave height of wave record i and m is the total number of wave records.

A statistical comparison, of the measured data with the theoretical distribution can be made by deriving the appropriate histogram for the wave heights. The wave height histogram is obtained from the measured wave records at the start of the experiment without the model in the tank. The wave heights were measured at wave probe WP11, which is located in the tank. . A plot of the wave height histogram along with the theoretical Rayleigh distribution for each generated wave condition was developed.

The ordinate of the plot in Figure 4.6 is the measured $p(H)$ and can be obtained from the statistical data presented in Table 4.9,

$$\text{Measured } p(H) = {}^{n_i}\!\!\diagup\!\!_{\overline{N}_\cdot \cdot \delta H} \tag{4.6}$$

$n_i =$ Number of occurrences of wave heights in wave record i.

$\delta H =$ Class interval of wave records is chosen to be 10mm

TABLE 4.9 Histogram data and Rayleigh ordinates for Test 18, H_s=0.078m, T_p =1.176s

WAVE RECORD	**MEAN HEIGHT(mm) H_i**	**Occurrence n_i**	**Measured $p(H)$**	**RayleighProbability density $p(H)$**
0 - 10	5	3071	0.012789	0.003204
10 - 20	15	3073	0.012798	0.009010
20 - 30	25	3417	0.014230	0.0013196
30 - 40	35	2998	0.012485	0.015220
40 - 50	45	2461	0.010249	0.015113
50 - 60	55	2342	0.009753	0.013374
60 - 70	65	1918	0.007988	0.010727
70 – 80	75	1198	0.004989	0.007876
80 - 90	85	834	0.003473	0.005324
90 - 100	95	680	0.002832	0.003327
100 - 110	105	652	0.002715	0.001928
110 - 120	115	576	0.002399	0.001037
120 - 130	125	384	0.001599	0.000519
130 - 140	135	244	0.001016	0.000242
140 - 150	145	164	0.000683	0.000105

Table 4.9 and Figure 4.7 show the histogram data and plot for one of the JONSWAP Sea conditions (Irregular wave test) used in the experiment. The figure indicates a fit between the experimental data and the theoretical Rayleigh distribution curve, which indicates a narrow band and the significance of the histogram is that instead of showing all individual wave elevations, it provides the number of waves in various wave height intervals.

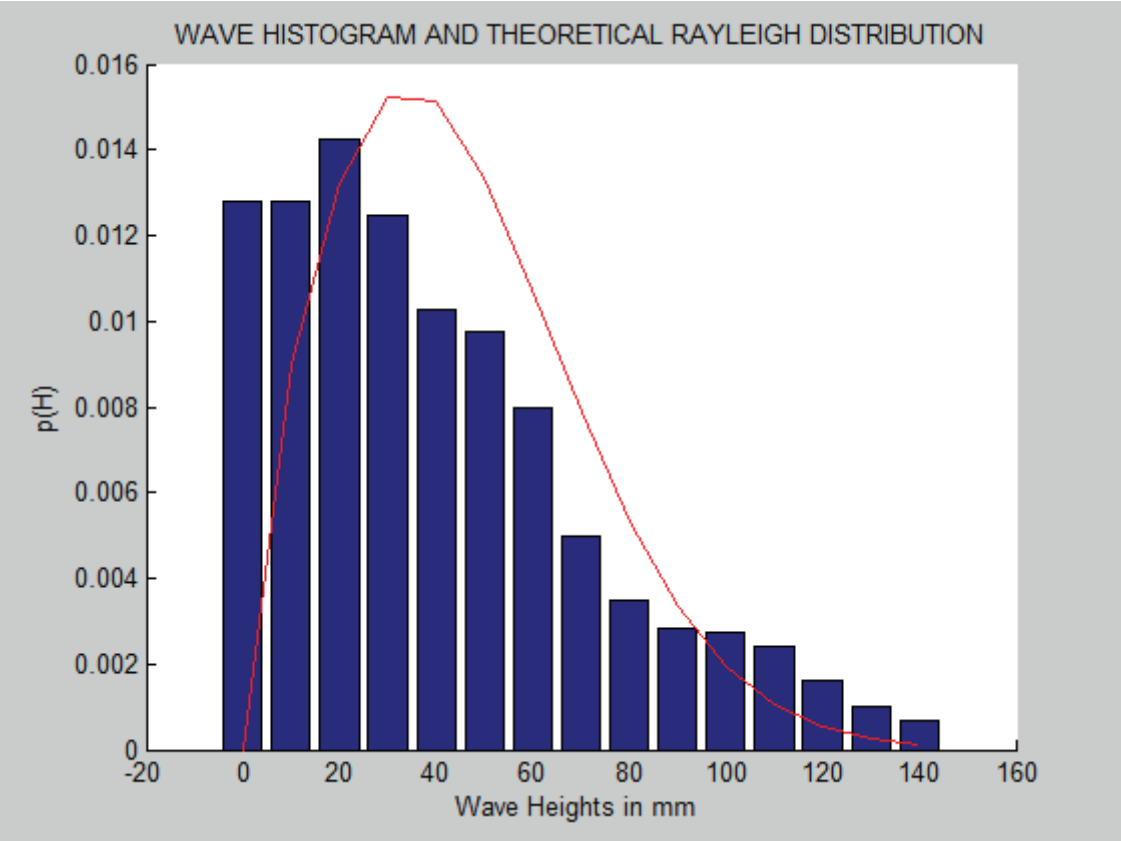

Figure 4-7 Histogram for wave condition test 18 H_s = 0.078m,T_p = 1.176s

4.5.2 The Wave Spectrum

The wave measurements in the experiment are composed of components of many waves. To take account of the distribution of the energy in these wavelets is to determine the wave spectrum for a measured wave condition. The measured wave heights time series are transformed to the wave spectrum using the Fourier Transform technique. In this study, the Fourier Transforms are carried out by the Fast Fourier Transform FFT code $\left[fft(x)\right]$ in MATLAB. The estimate of the energy spectrum from the wave records $S(f)$ for several wave conditions measured during the experiment is computed using the simple averaging method or direct method. A detailed description of this method is presented by Goda (2000) and Kim (2008).

A computer program incorporating the MATLAB $fft(x)$ and the moving average method is used to compute the energy density spectrum of some measured wave conditions and the results compared with their target wave spectrum based on the theoretical JONSWAP spectrum also incorporated into the computer program. Figures 4.8a to 4.8d show the correlation of the theoretical JONSWAP spectrum of the target wave condition with the wave spectrum of the measured wave records (Irregular wave tests).

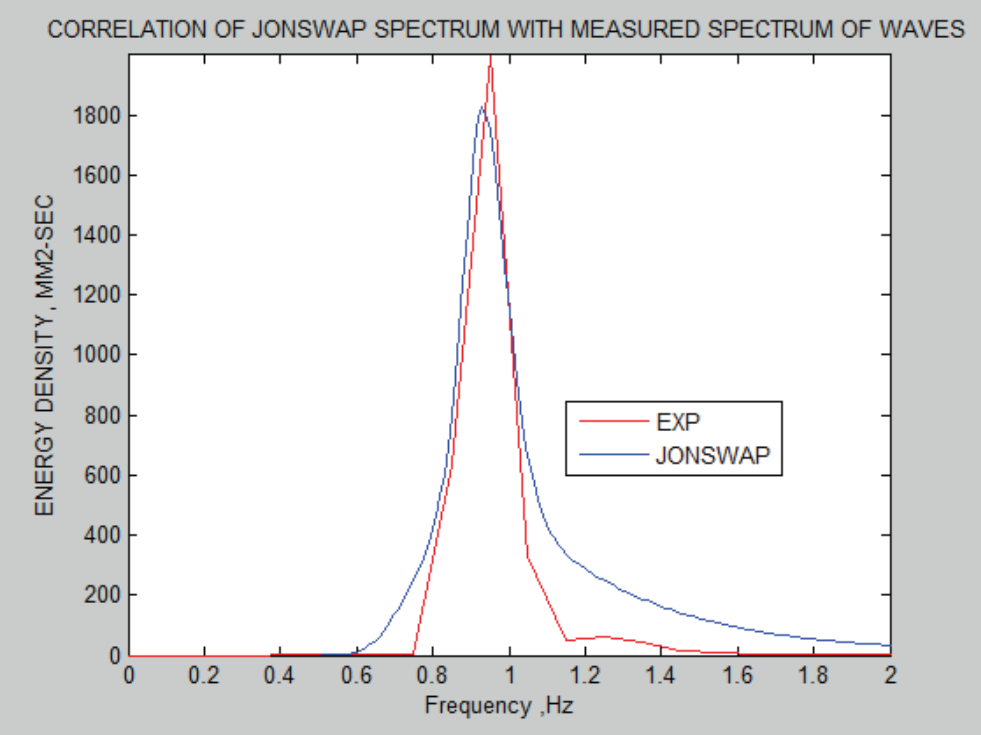

Figure 4-8a Spectral energy density for Test 12, Hs = 0.078m, T_p = 1.075s

The wave spectrum in Figure 4.8a indicates that the wave energy is spread in the frequency range of about 0.81Hz to 1.6Hz or equivalently of wave period with range from 0.625s to 1.25s even though the target wave period is 1.075s. The figure also indicates that the wave energy is concentrated around the frequency range of 0.95 Hz which is close to the frequency of 0.93Hz corresponding to the target wave frequency.

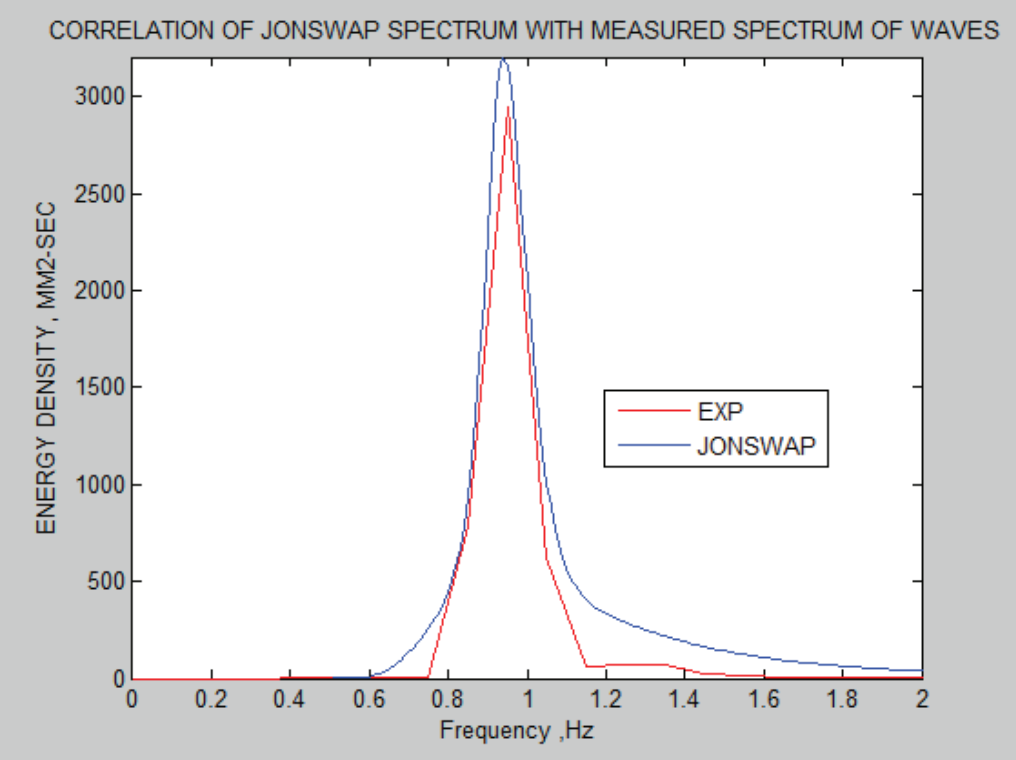

Figure 4-8b Spectral energy density for Test 17, Hs = 0.095m, T_p = 1.075s

For Figure 4.8b, the wave energy is spread between 0.78Hz and 1.5 Hz with concentration around the target wave frequency of 0.93Hz. In Figure 4.8c, the spread is in the full range up to 2Hz, however with concentration around the target frequency of 0.8Hz and Figure 4.8d show the wave energy is spread between 0.78Hz and 1.6 Hz with energy concentration around the target frequency value of 0.93 Hz.

Some differences are observed in all the plots (Figures 4.8a to 4.8d) between the measured spectra and the standard JONSWAP spectra which can be attributed to the MAST wave tank configuration and possible uncertainties during measurements as outlined in Section 4.2.4.

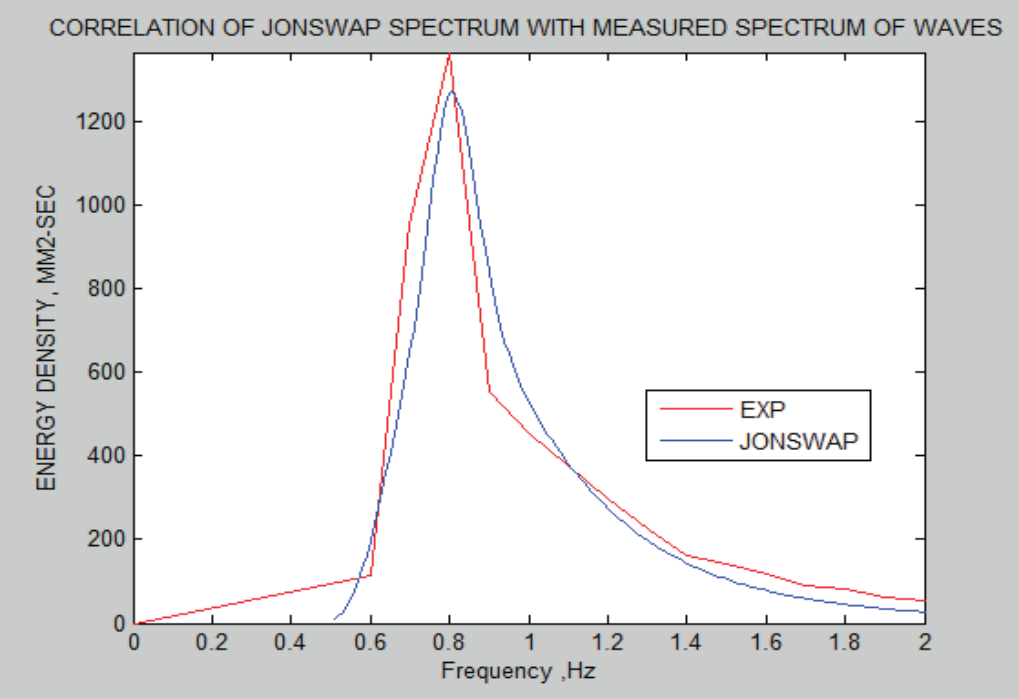

Figure 4-8c Spectral energy density for Test 18, Hs = 0.078m, T_p = 1.176s

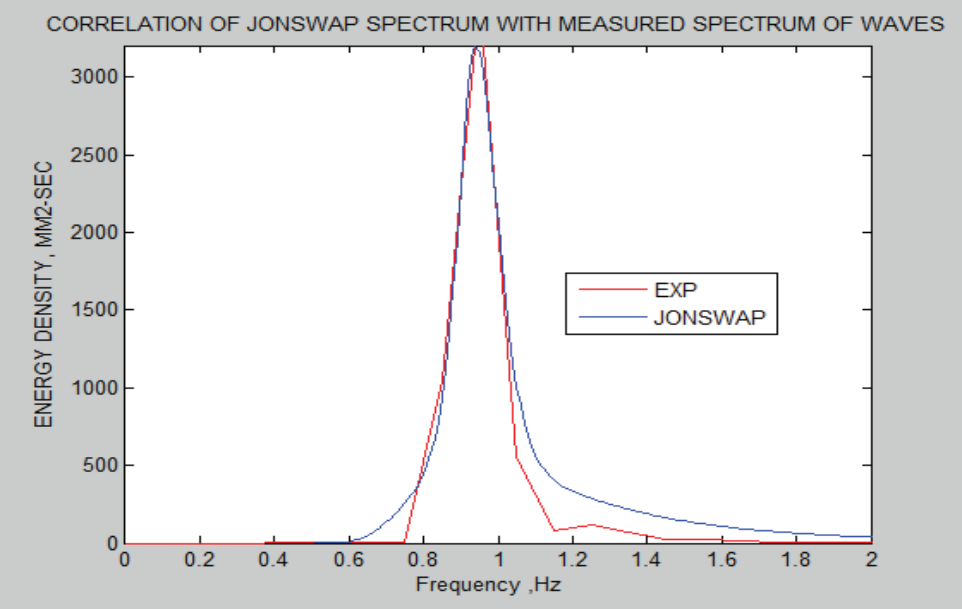

Figure 4-8d Spectral energy density for Test 13, Hs = 0.11m, T_p = 1.075s

In experimental studies, useful information can be derived from a wave spectrum analysis of the measurements or records.

For example spectral analysis allows for the evaluation of equipment efficiency especially such as the wave makers and input signal systems configurations. A comparison of the wave input signal frequency and the spectra record can determine if the wave making system is generating significantly the input data. Spectra can also provide useful information regarding the range of frequencies that is useful and significant in the wave records, the frequency at which the maximum energy of the spectrum is obtained.

A useful characteristic of the wave spectrum is the spectra moments. This is moment of the area under the curve of the wave spectrum taken about the line of zero frequency as shown in Figure 4.9.

The n^{th} spectra moment is defined as;

$$m_n = \int_0^\infty S(\omega)\omega^n d\omega \qquad (4.7)$$

where m_n is defined as the n^{th} moment of the spectrum calculated, $S(\omega)$ is the spectral energy and ω is the frequency in radians per second.

The values of the significant wave height H_s and the peak period T_p can be calculated from the measured spectra using the following relationships.

$$H_s = 4\sqrt{m_0} \qquad (4.8)$$

The peak period is obtained from the peak frequency f_p at which the energy spectra value is at the maximum.

$$T_p = 1/f_p \qquad (4.9)$$

And the bandwidth parameter of the spectrum $\varepsilon = \left(1 - \frac{m_2^2}{m_0 m_4}\right)^{\frac{1}{2}}$ (4.10)

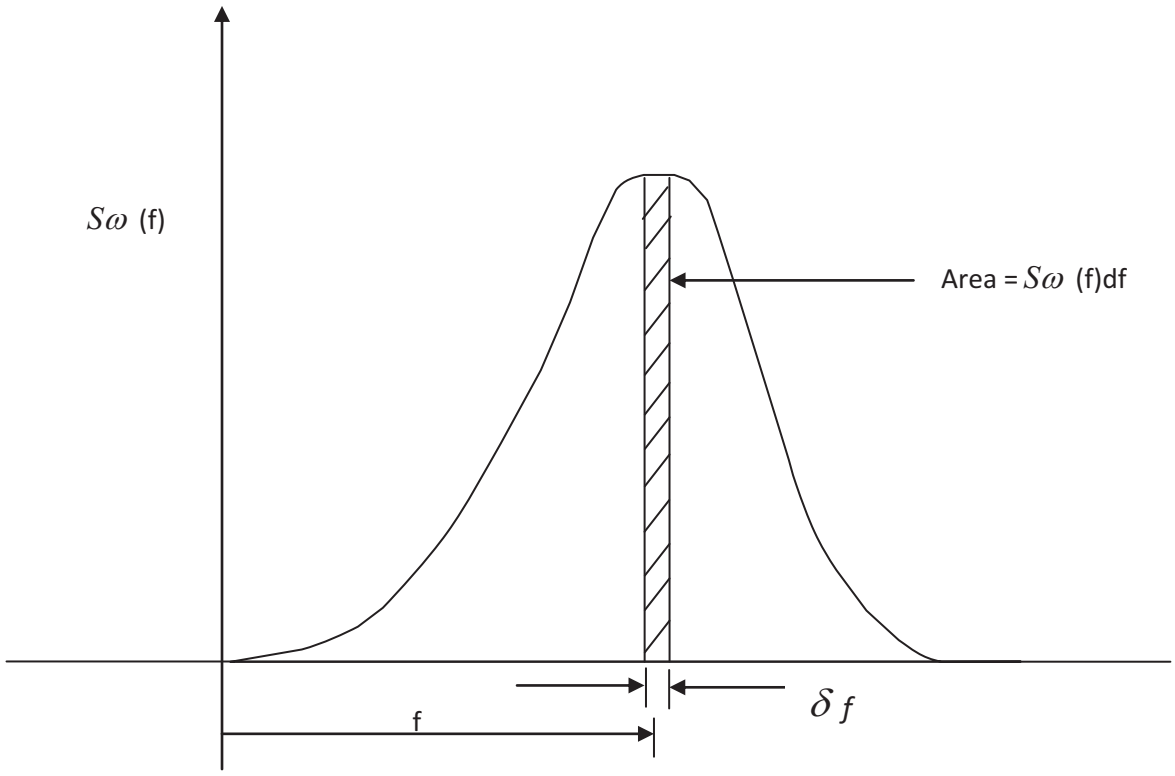

Figure 4-9 Spectral Moments (Barltrop and Adams, 1991)

Table 4.10 Calculated spectral moments, wave height and period.

WAVE CONDITION (Target values)	m_o $\left(m^2\right)$	f_p Peak frequency(Hz)	H_s (m)	T_p (s)	ε
JONSWAP Hs=0.078m, T_p=1.075s (H_s=10m,T_p=12s)	5.87 x 10^{-4}	0.950	0.096	1.052	0.690
JONSWAP H_s=0.11m T_p = 1.075s (Hs=14m, T_p=12s)	1.12 x 10^{-3}	0.950	0.133	1.052	0.690
JONSWAP H_s = 0.095m, T_p = 1.075s (Hs= 12m, T_p=12s)	5.52 x 10^{-4}	0.950	0.094	1.052	0.688
JONSWAP H_s= 0.078m T_p = 1.176s (Hs= 10m, T_p=14s)	5.59 x 10^{-4}	0.820	0.095	1.122	0.70

A review of the results presented in Table 4.10 show measured H_s values greater than the target value of wave heights. The factors listed below could be responsible for this variation.

1. The position of the model in the wave tank.
2. Transfer functions of the wave maker
3. Possible reflections from side walls, beach and wave maker.

4.6 FPSO Motion

In the calculation of ship responses in irregular wave using the technique of linear superposition, Bhattacharyya (1978) defines two fundamental assumptions on which the technique is based;

- The response of a vessel to any individual regular wave component is a linear function of the amplitude of this component , and is assumed to be the response that would be experienced had the vessel been subjected to a train of the same regular waves for a long period of time previously.
- The response of the vessel to any individual wave component is independent of the response to any other wave component. This shows that in any given sea condition the response of the vessel comprises of the sum of its responses to the individual wave components that make up the sea condition

The output responses of the vessel can relate to the input responses of the waves when their power spectral densities functions relate through a transfer function relation called the response amplitude operator (RAO). Thus the output spectral energy density of the ship response is the product of the spectral energy density of the encountering waves and the response amplitude operator (RAO). This relationship can be used to evaluate the statistical properties associated with the vessel motions in a sea state. When the assumption is made that a vessel in a marine environment is a linear system which converts the energy from the sea waves into energy of vessel motions, the response spectrum of the vessel can be obtained from the wave spectrum.

The behaviour of a ship in a seaway is induced by the ocean wave's characteristics, if we take the fluid structure interaction as a linear system, the sea wave's act as the input of the system and the output response of the system is the motion of the ship. If we follow the assumptions proposed above, the principles of superposition holds and the induced irregular ship motions are now considered as a linear superposition of an infinite number of small, regular motions each of which is caused by a simple regular wave component.

A relationship can now be developed for the spectral energy densities of the wave elevation ζ_i and output response η_i.

INPUT: $$\zeta_i = \zeta_{ai}\cos(k_i x - \omega_i t) \quad (4.11a)$$

OUTPUT: $$\eta_i = \eta_{ai}\cos(k_i x - \omega_i t + \varepsilon_i) \quad (4.11b)$$

where ζ_{ai}, is the wave elevation amplitude, η_{ai} is the amplitude of the ship motion, which can be any of the six degrees of motion or a combination (Surge, Sway, Heave, Roll, Pitch and Yaw), and ε_i is the phase difference.

The ratio between the output signal amplitude and the input wave amplitude for regular wave tests can be denoted as follows;

$$H_{\eta\zeta}(\omega) = \left[\frac{\eta_{ai}}{\zeta_{ai}}\right] \quad (4.11c)$$

This ratio is defined as the Response Amplitude Operator.

The regular wave tests conducted in the laboratory are a general source of data for determining the RAOs experimentally.

The heave and pitch RAOs obtained for the model in regular head waves are shown in Figures 4.10a to 4.10b. For the Pitch motions, the RAOs are made dimensionless in the MATLAB program by dividing the pitch measurements with the amplitude of the wave slope, which is the product of the wave amplitude and the wave number.

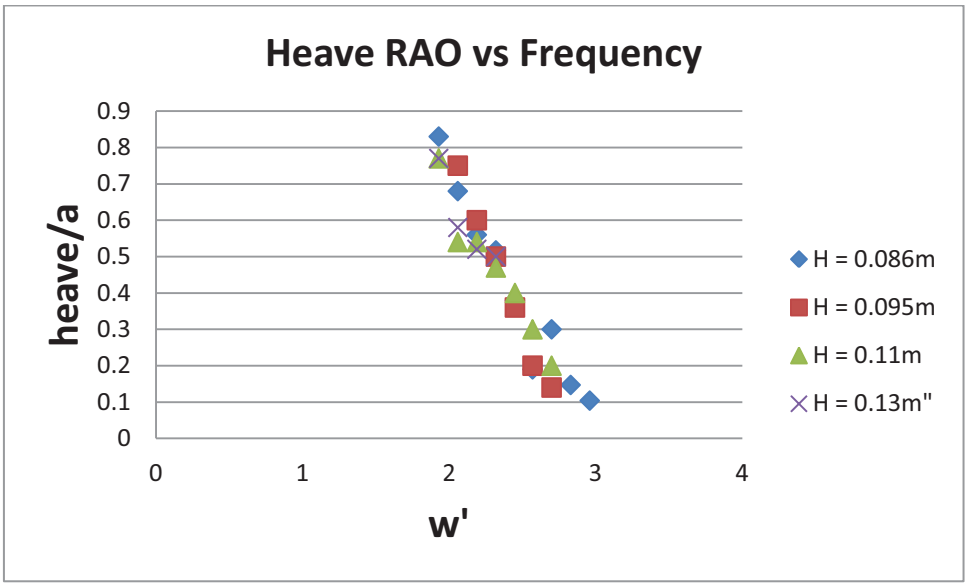

Figure 4-10a – Heave RAO from regular waves

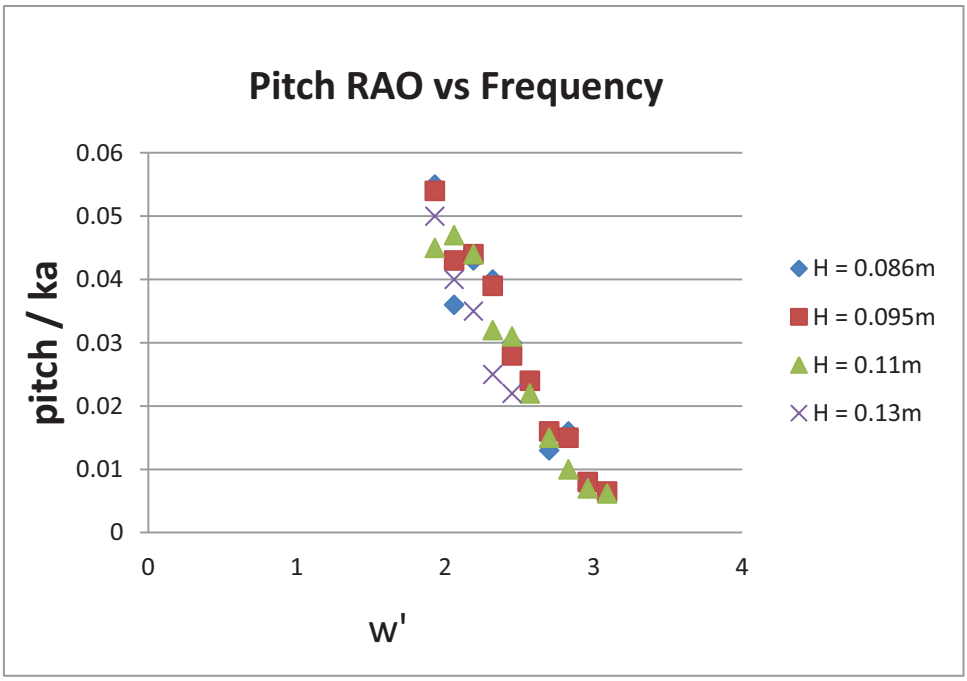

Fig. 4.10b – Pitch RAO from regular waves

In Figures 10a and 10b, w' is the dimensionless wave frequency defined as;

$$w' = \omega\sqrt{L/g} \tag{4.12}$$

The heave RAO results from an experimental study by Han et al (2004) of a larger model FPSO (model scale 1:55) in moderate to extreme regular waves was compared to the results obtained in this study. The experimental results are presented together in Figure 4.11 and it showed good agreement for the FPSO motions. The significance of this observation is that in ship model testing, scale effects may not necessarily affect the performance to a large extent of small models and the test results when using models of different sizes.

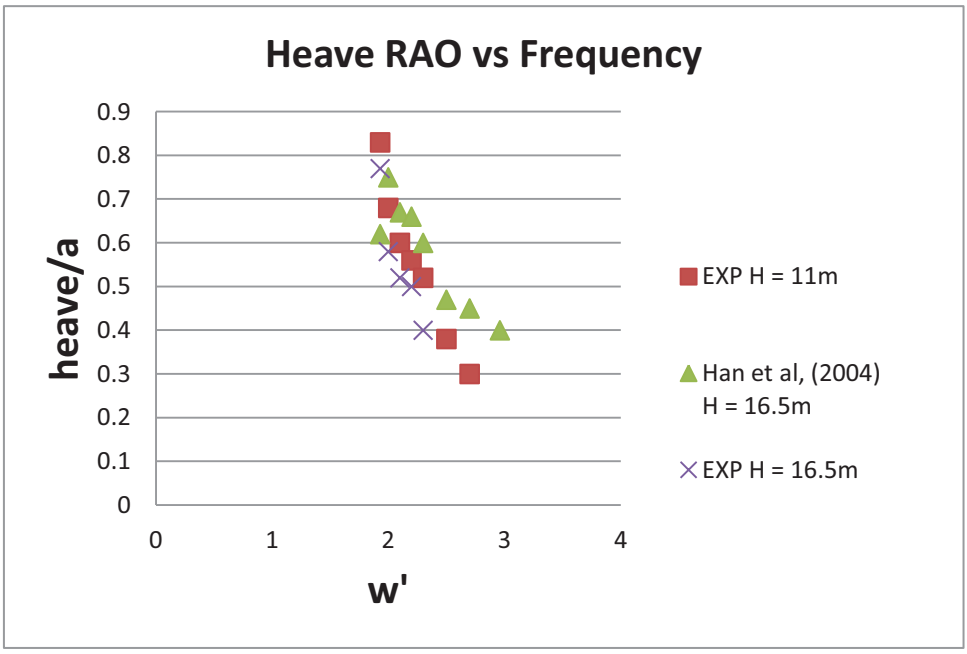

Figure 4-11a - comparison of heave RAOs between the model in this experiment and the model in Han's experiment at prototype scale.

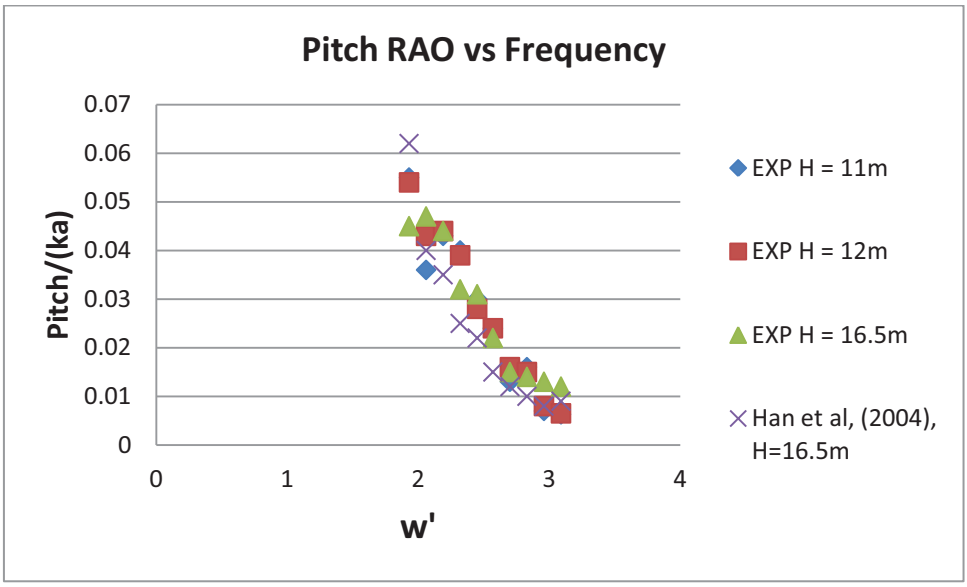

Figure 4-11b - Comparison of Pitch RAOs between the model in this experiment and the model in Han's experiment at prototype scale.

The motions data shown in Figures 4.10 and 4.11 include results from experiments on two models that are virtually geosyms, at scales of 1:55 (MARINTEK) and 1:127 (Newcastle). There is an indication that the smaller scale model is giving slightly smaller responses, but the discrepancy between the two sets of results is about 7%. The implication of these results is, at least for the experiments undertaken, there are no significant scale effects. Where this is a problem, it is usually Reynolds number scale effects that are significant. The dominant green water phenomena are gravity driven and therefore more associated with Froude scaling, although viscous effects (Reynolds number related) are evident to some extent in phenomena such as the formation of foam on the breaking waves. However, on the limited evidence of the data available, it could be concluded that scale effects do not play an important role in green water scale model experiments.

CHAPTER 5

EXPERIMENTAL AND NUMERICAL STUDY OF GREEN WATER PHENOMENA

5.1 Green Seas

Green water phenomena generally follow a characteristic pattern when they occur as a systematic outcome of the wave environmental conditions. A series of photographs were taken under laboratory conditions to capture the sequence of events derived from visual observation of green water effects (See Plates 5.1 to 5.4). The sequence can be described as follows:

- The encounter wave interacts with the bow and deck creating relative wave motion.
- The wave around the bow creates a solid jet of water which flows over the bulwarks and onto the deck.
- The solid mass of water on the deck, called green water, flows in longitudinal and transverse directions in the form of a water wave.
- The green water impacts on the deck, and the deck structure and/or equipment, resulting in impact loads that could cause structural damage and equipment failure due to the impact.

The sequence of events is analysed in more detail in the following and subsequent sections of this chapter. In addition model tests carried out during the experiment to measure water heights on deck at different locations, water flow behaviour on deck and impact loading will be described.

An observation made by Buchner (1995) was that the water falls on deck as a breaking wave. This scenario has been observed in the model tests carried out in the MAST laboratory. The water flows along the deck resembling the flow generated due to the breaking of a dam. The green water sequences of events found in the experiment are illustrated with sketches similar to the work of Greco (2001), which describes a green water event in the context of a breaking dam.

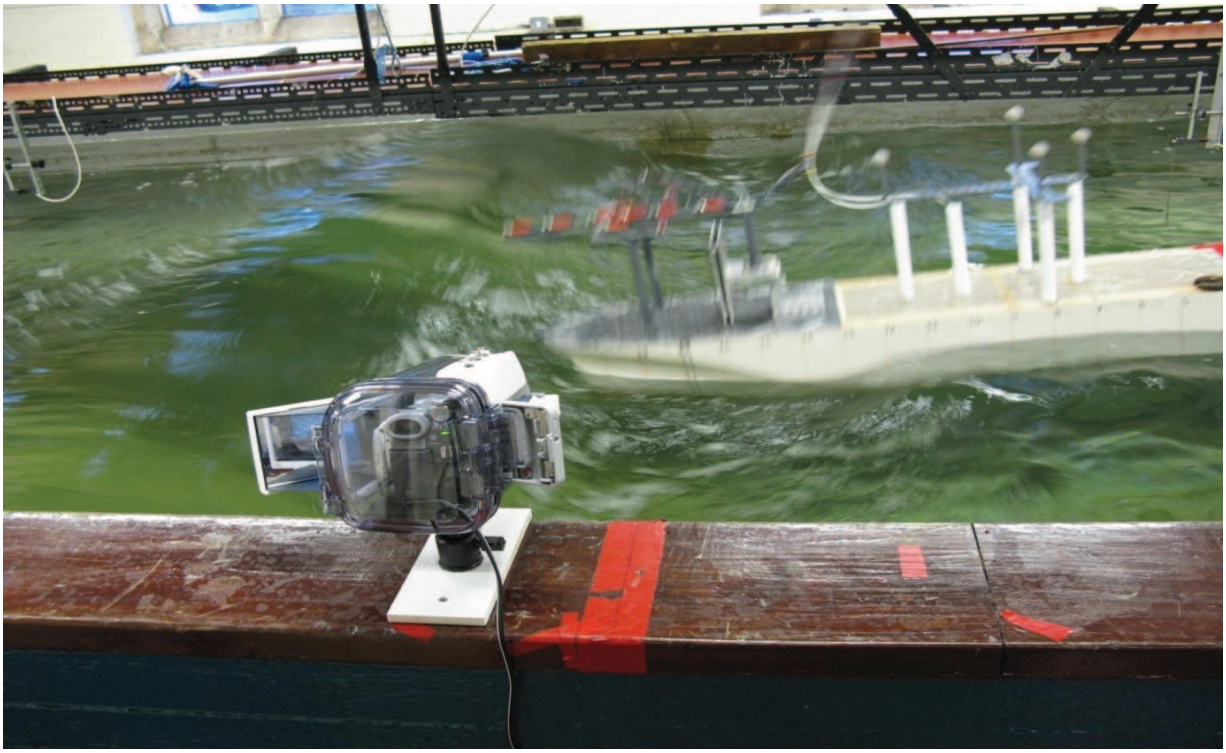

Plate 5-1. Green water event – wave build up at bow

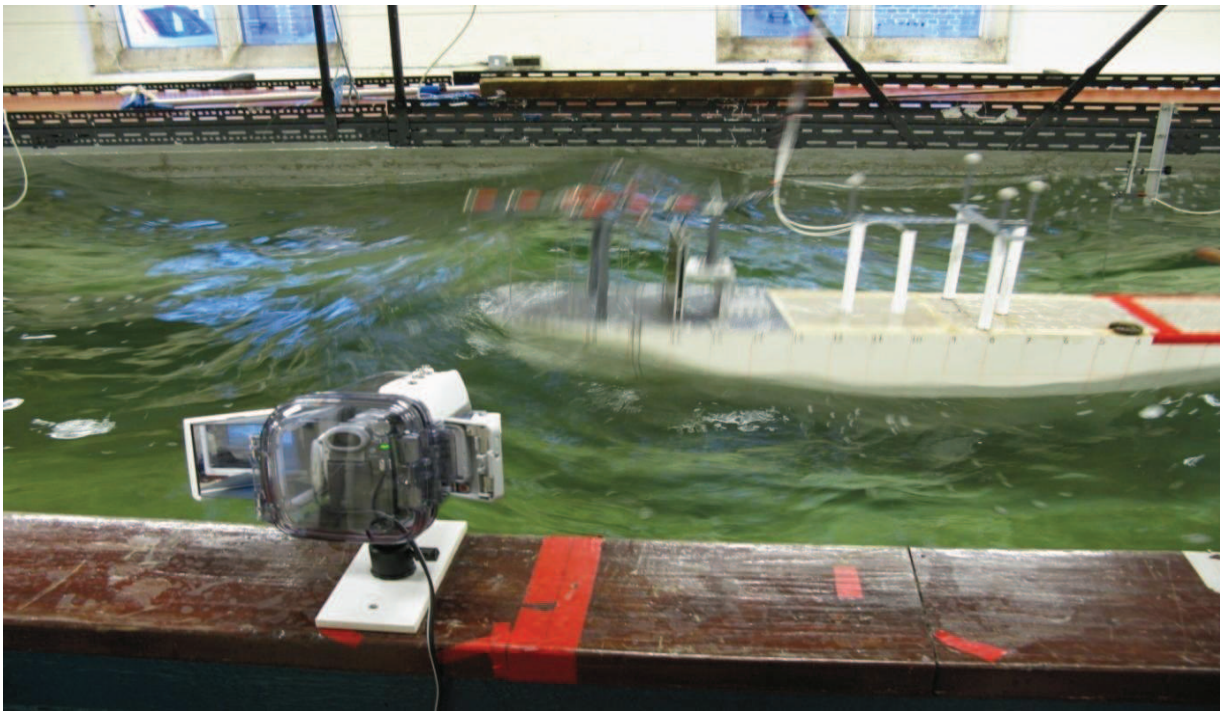

Plate 5-2 Green water event – wave overtopping, green water on deck

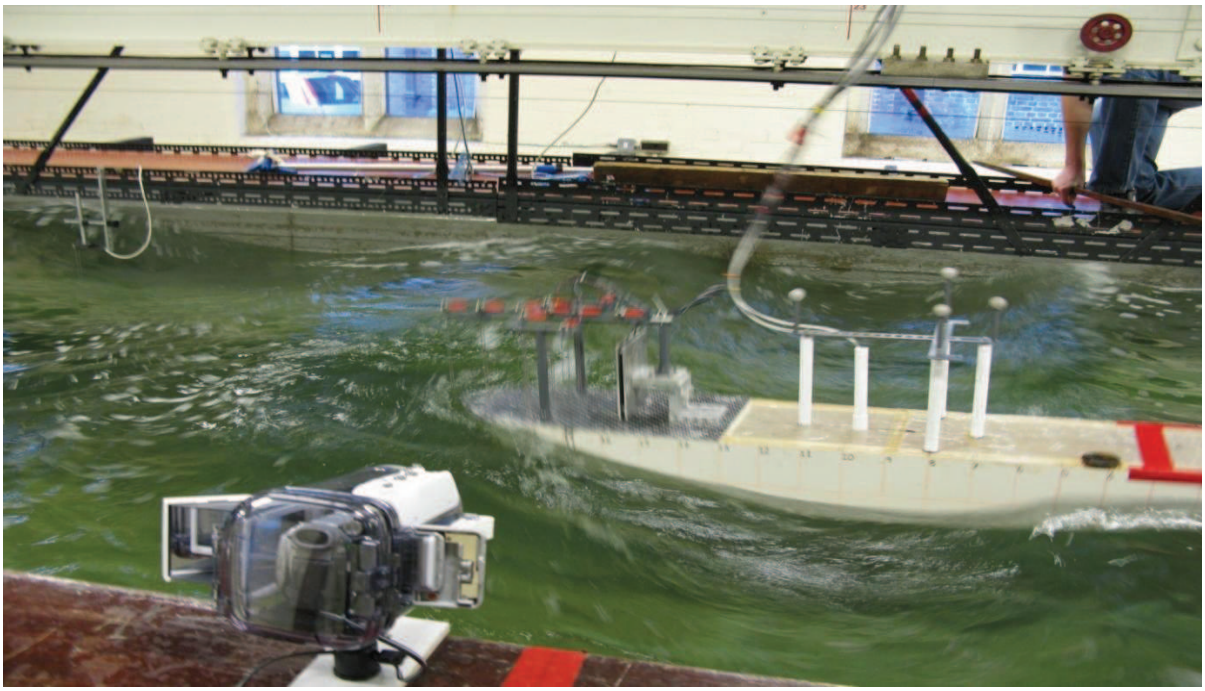

Plate 5-3 Green water event – water jet impact on deck structure

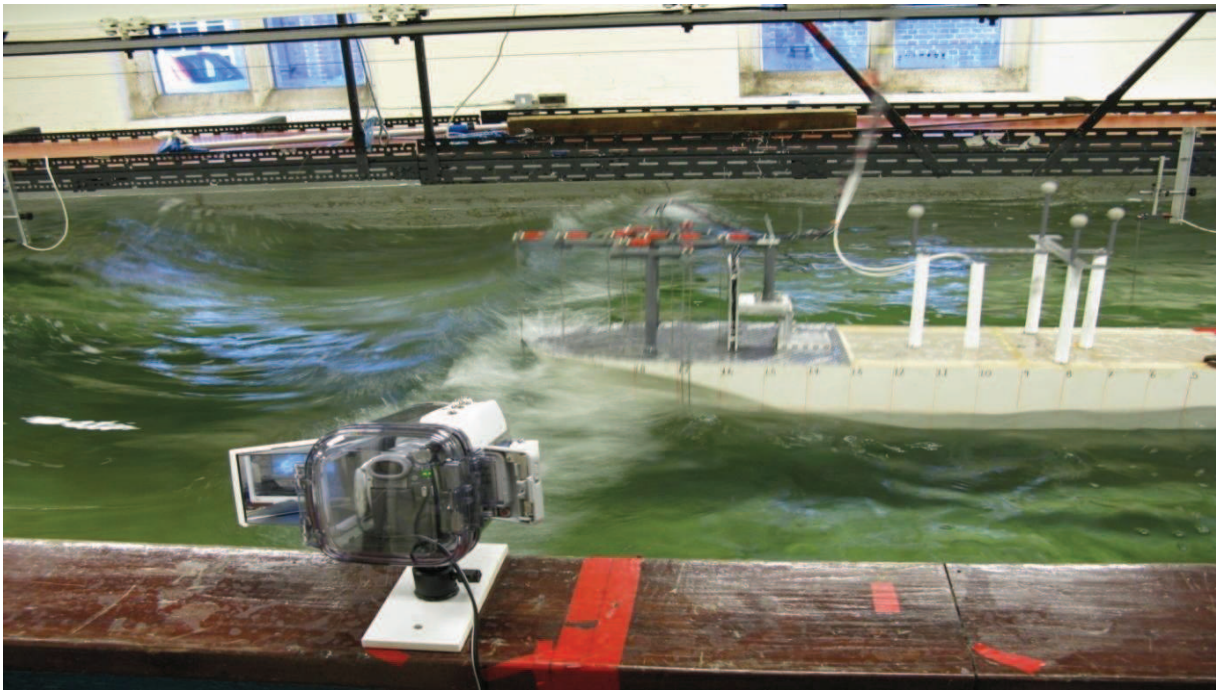

Plate 5-4 Green water event – water reflection from deck and deck structure

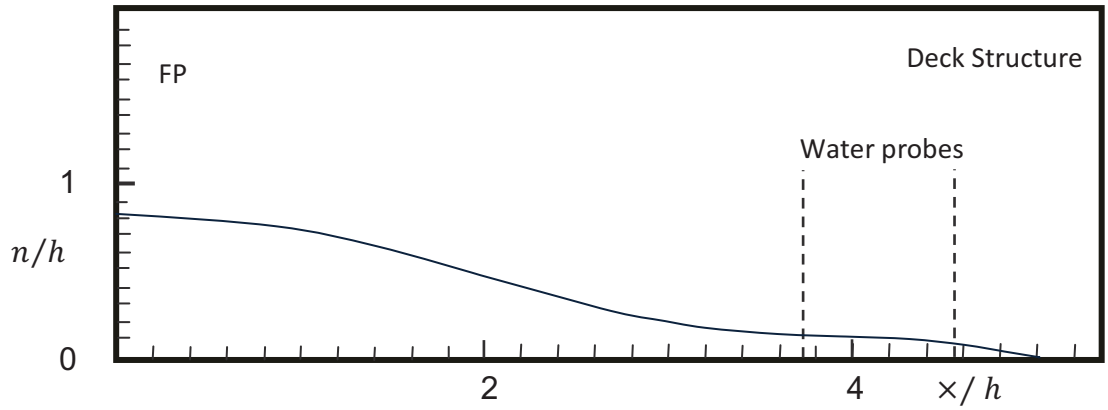

Figure 5.1a Sketch showing water flowing on deck. (Greco, 2001)

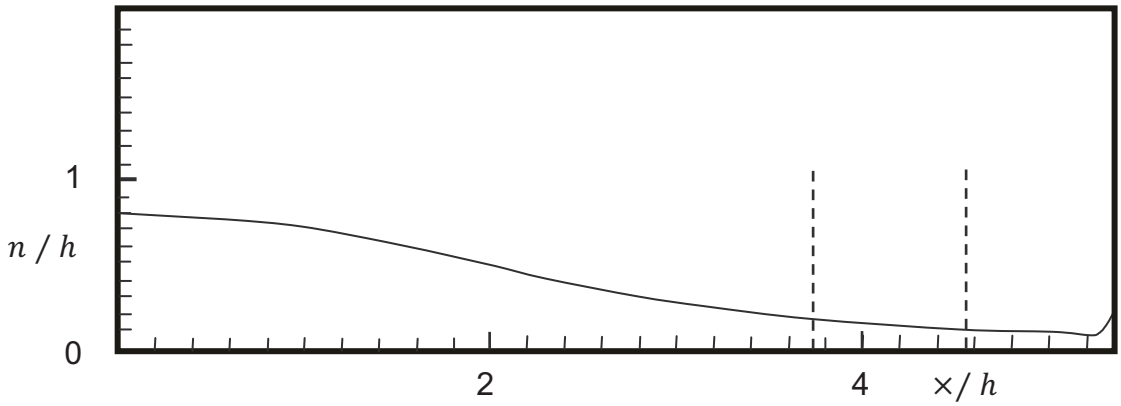

Figure 5.1b Sketch showing water flow reaching the deck structure (Greco,2001).

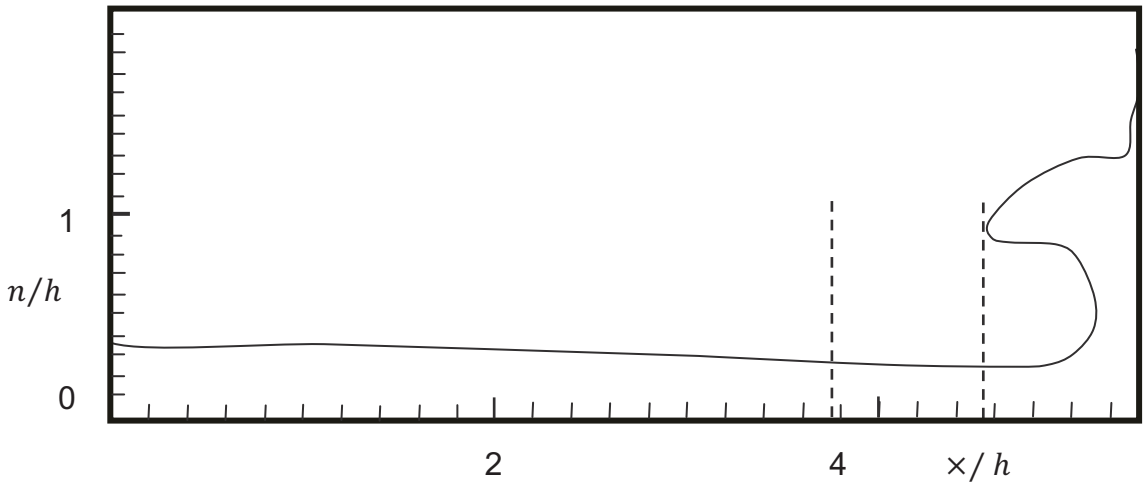

Figure 5.1c Sketch of wave impacting with deck structure and motion of water reversed. (Greco,2001).

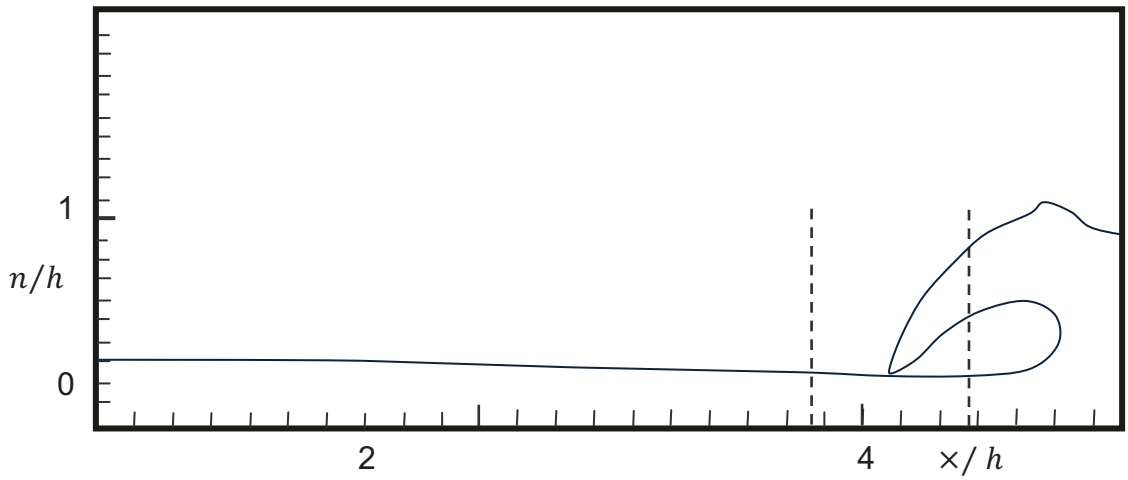

Figure 5.1d Sketch of wave overturning and plunging on deck. (Greco, 2001).

Figure 5.1a shows that the flow along the deck resembles a similar event in the breaking of a dam. Figure 5.1b illustrates the green water event further, showing the water reaching the deck structure with the occurrence of impact on it. At impact in Figure 5.1c, the motion of the water is reversed. Figure 5.1d presents the water overturning and resulting in the form of a wave plunging on the deck. n/h is a ratio of the free surface elevation to water depth, where n is the free surface elevation and h is the water depth. x/h is a dimensionless location along the x - axis

A similar series of events have been captured from the experiment in a time series showing simultaneously the flow behaviour and the pressure distribution on the deck. An impact study was carried out to present the flow behaviour, pressure distribution and load distribution on the deck structure as the water impacts on it.

5.2 Water Flow Behaviour on Deck due to Green Water.

The measurements taken from the test conditions carried out in the experiment have been analysed to understand the flow behaviour on deck. From the list of tests conducted in the experiment, six tests which gave the most extreme green water occurrences have been selected for analysis. Two of these six tests are regular wave conditions and the remaining four tests are irregular wave conditions. Figures 5.2 to 5.7 show the flow behaviour pattern at different locations on the deck. At each specific position along the deck water height measurements taken from the test conditions have been used to represent the water flow along the centreline of the deck. The wave probes WP4, WP5, WP9 and WP10 represent the positions along the centreline at which the water heights have been measured during a green water event. The wave probe WP4 measures the water height at the fore perpendicular. The beginning of a green water event can be assumed to be when water touches the wave probe WP4 and there is a significant level of water at an instant of time at this probe. The flow pattern of the water can be observed over some time interval over the wave probes WP5 and WP9 until the water reaches the deck structure at WP10. At the time the water reaches WP10, it is assumed as the impact stage and the close of the green water occurrence for the time period. This information taken from the measurements, and illustrated with a time series to describe the flow pattern, indicates that the green water phenomena occur in the vicinity of the bow and fore perpendicular. The water then hits the deck, flows along it to hit the deck structure, and piles up in front of it. As time progresses, dissipation of the water occurs due to the vessel motion and reversal of the motion of water from the deck structure after impact. The figures clearly demonstrate and support the typical sequence during a green water event as described by Buchner (2002).

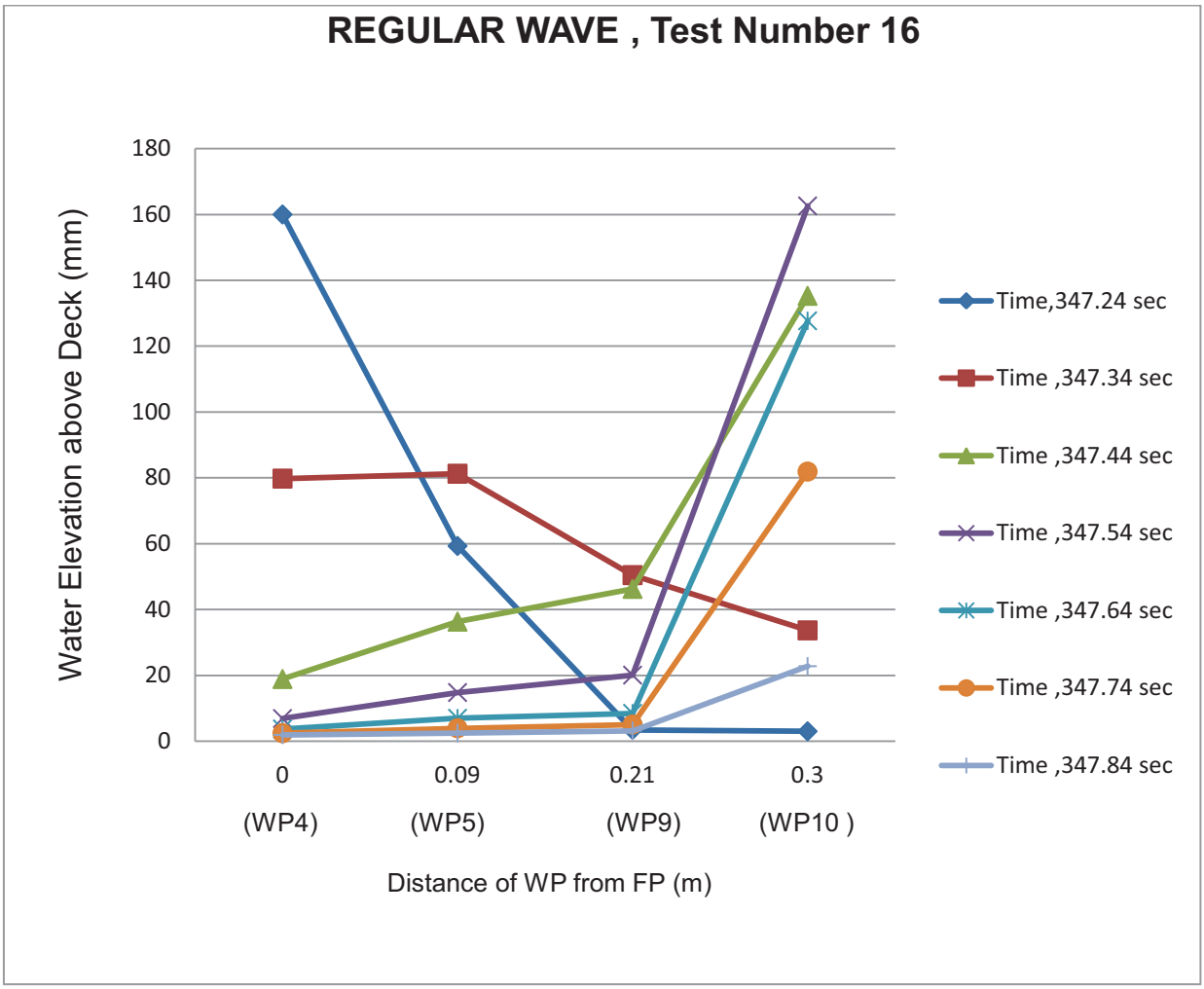

Figure 5.2 – Water flow on deck, H = 0.13m, T = 1.11s

Figure 5.2 shows a flow pattern for the model test condition 16, with H = 0.13m, T = 1.11s and water height measurements at wave probes WP4, WP5, WP9 and WP10 on the deck at the time step of 0.1sec to represent the water flow along the centreline of the deck. From the recorded measurements, it can be observed that the water touched the wave probe WP4 at time of 347.24sec. shown in Figure 5.2 during the test and recorded a water height measurement of 160mm, which can be regarded as a substantial water build up for a green water event in the vicinity of the bow and fore perpendicular. At 347.34sec, most of the water was flowing on deck as can be observed at WP5 and WP9. The water front hit the deck structure at 347.44sec. Observation of the water height at WP10 and at time 347.54sec shows that the water piled up in front of the deck structure.

Following the build up at the deck structure, at the times 347.64s, 347.74s and 347.84s the accumulated water was reflected onto the deck. A similar phenomenon can be observed in Figures 5.3 to 5.7 for the other test conditions selected for a time instance when there is an occurrence of green water.

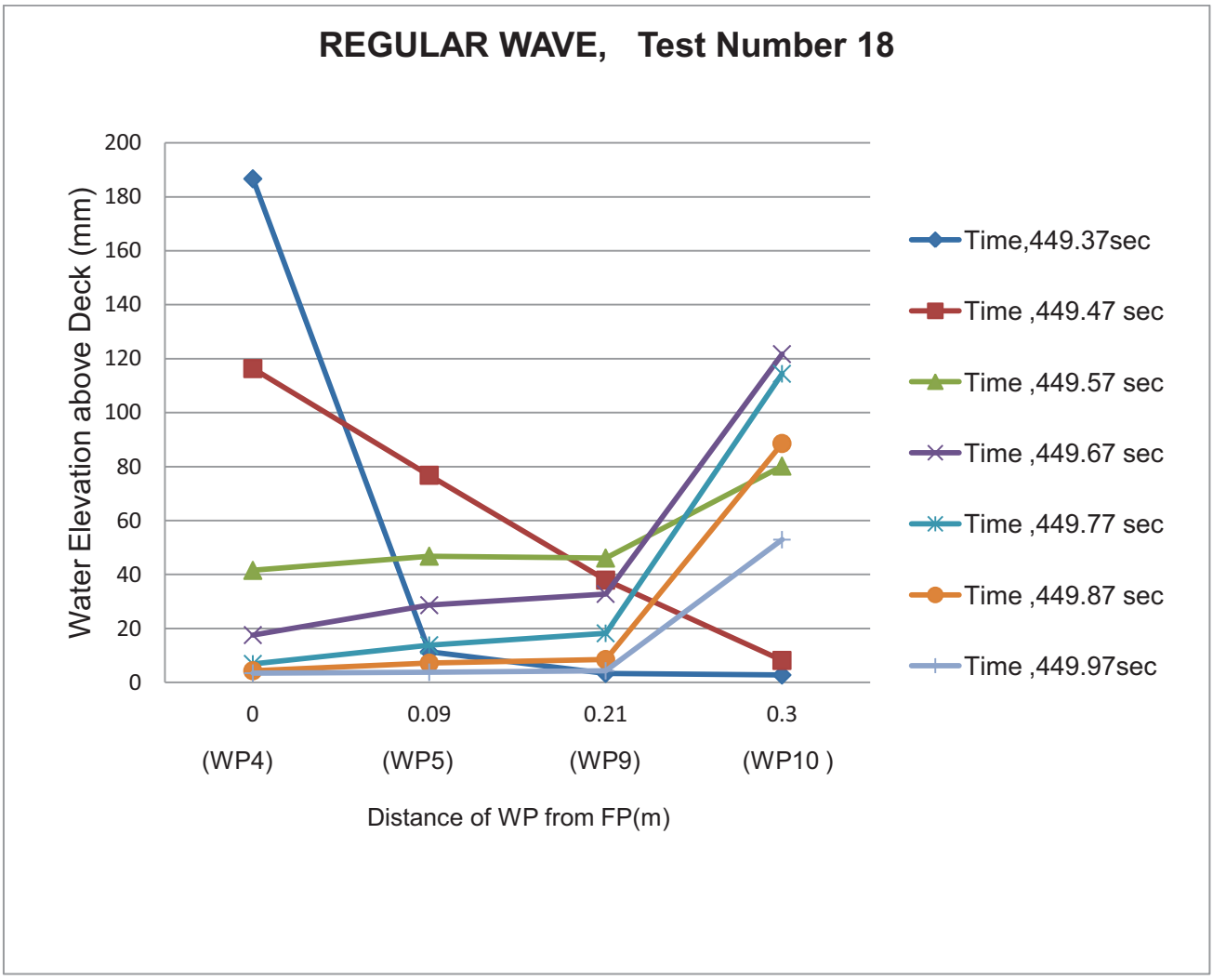

Figure 5.3 – Water flow on deck, H = 0.095m, T = 1.05s

The flow pattern observed in Figure 5.3 shows that the water reached the wave probe WP4 at 449.37s. There was flow of water on deck at 449.47s. A mass of water hit the deck structure at 449.57s and water pile up can be observed at this location at 449.67s. At the times 449.77s, 449.87s and 449.97s, the water began a process of reflection onto the deck.

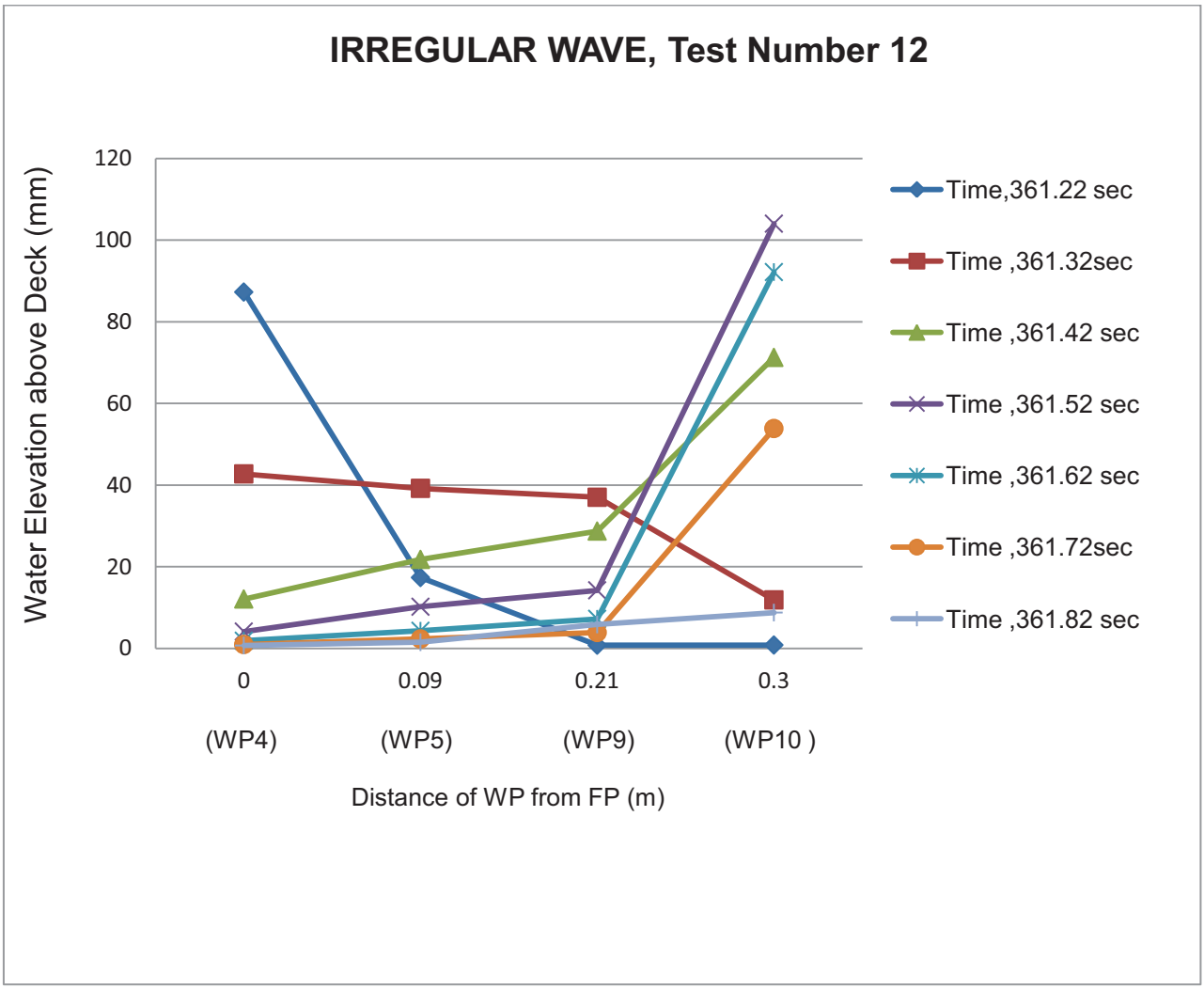

Figure 5.4 – Water flow on deck, H_s = 0.078m, T_p = 1.07s

At 361.22s, in Figure 5.4, the wave probe WP4 recorded a water height of 90mm, which can be considered to be the beginning of a green water event in the vicinity of the bow and fore perpendicular. At WP5 and WP9, a flow process on deck could be observed at 361.32s and the water reached the deck structure at 361.42s. There was an accumulation of water there at 361.52s and at the times 361.62s, 361.72s and 361.82s, the piled up water was reflected onto the deck.

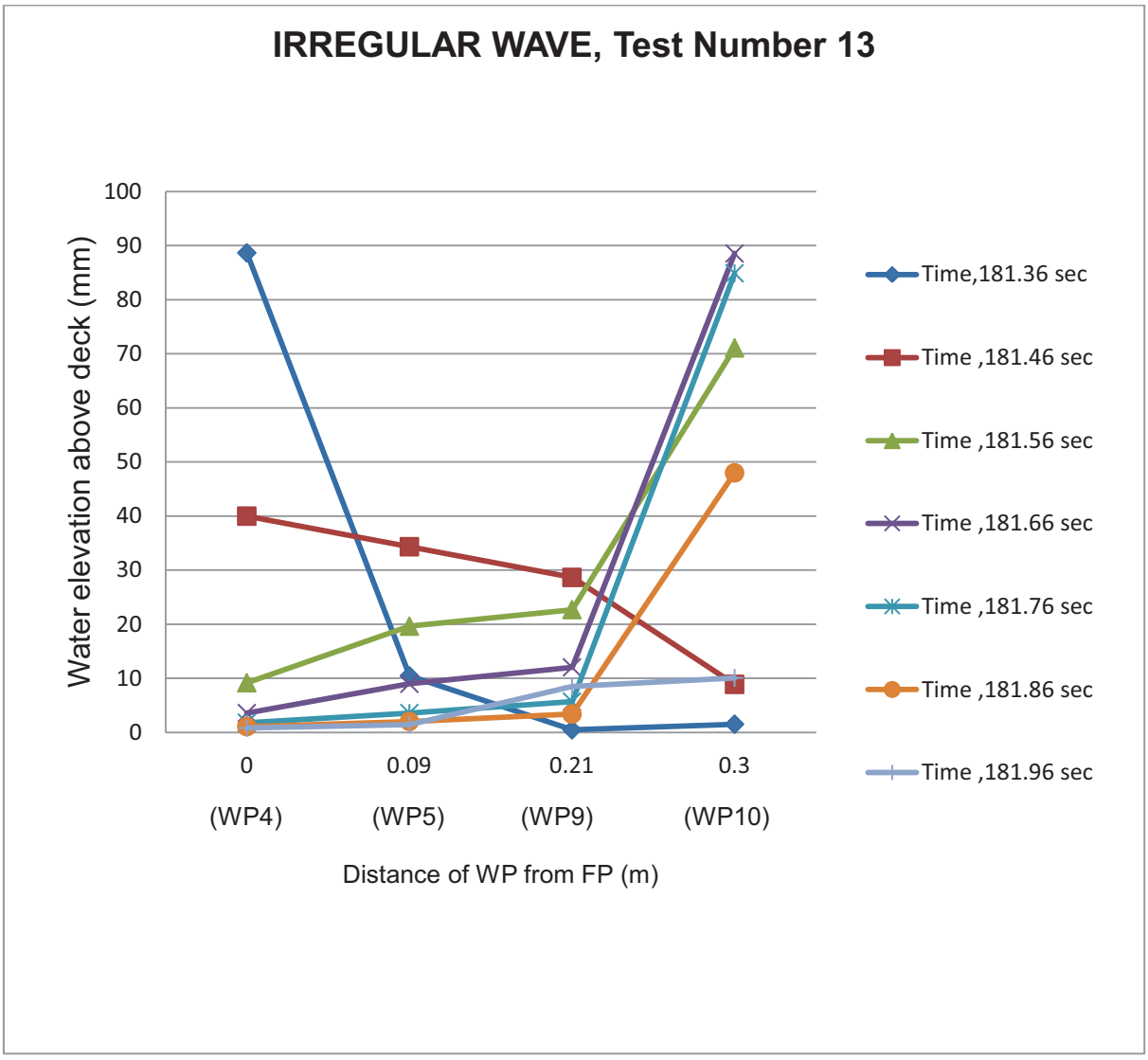

Figure 5.5 – Water flow on deck, H_s = 0.11m, T_p = 1.07s

A similar trend can be observed in Figure 5.5 for the flow behaviour on deck. At 181.36s, the water reached the wave probe WP4. At 181.46s, there was flow of water on deck. The water hit the deck structure at 181.56s and a build up of water there occurred at 181.66s. Water was reflected back on deck at times 181.76s, 181.86s and 181.96s

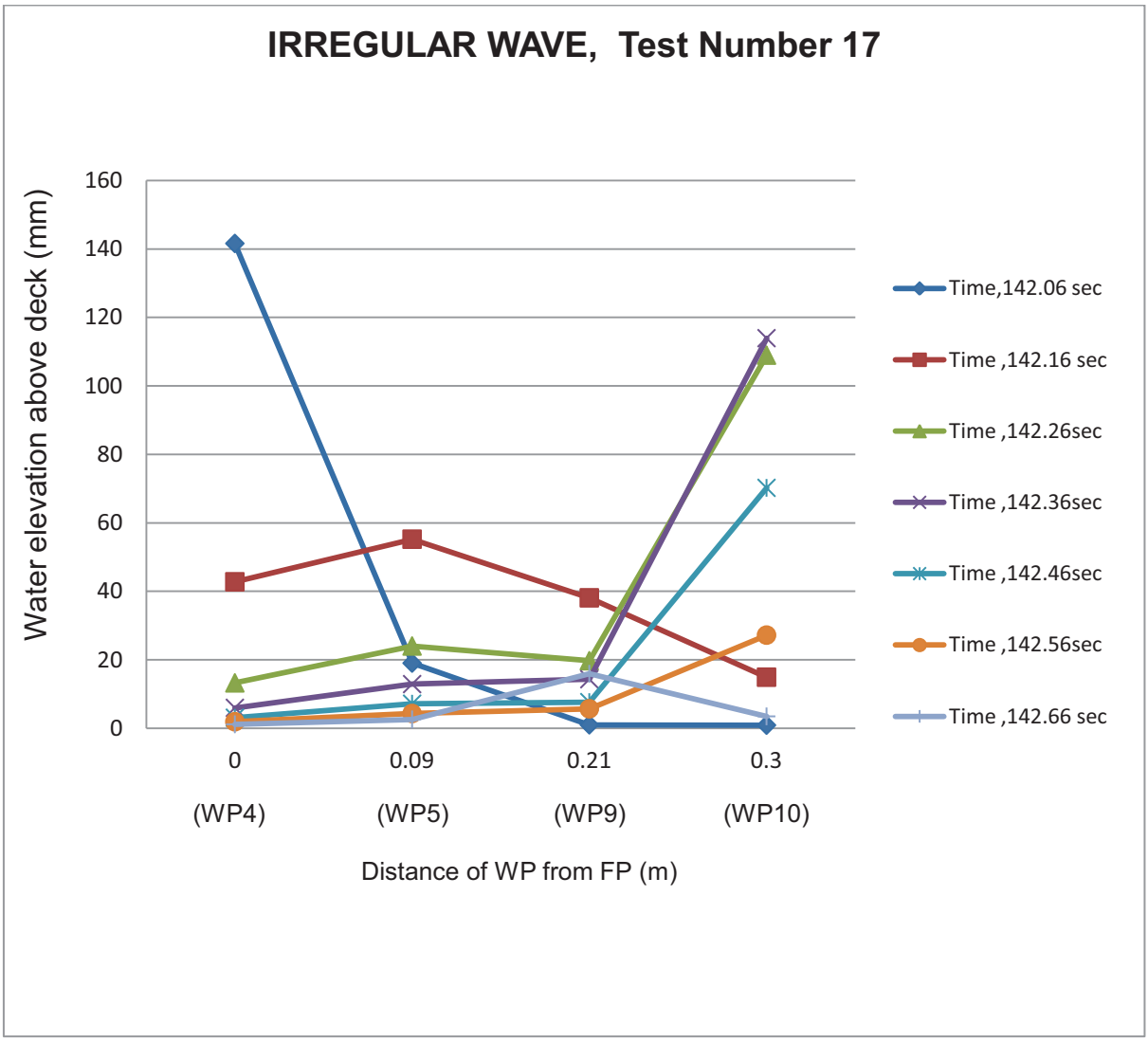

Figure 5.6 – Water flow on deck, H_s = 0.095m, T_p = 1.07s

Figure 5.6 shows the water touching the probe WP4 at 142.06s. Flow of water on deck took place at 142.16s as can be observed at WP5 and WP9. The water hit the deck structure at 142.26s from the observed water height measurement at WP10. The water piled up in front of the deck structure at 142.36s and was reflected back on deck at the times 142.46s, 142.56s and 142.66s.

At the time instance selected for the test condition in Figure 5.7 to show a green water event, a slight deviation was observed in the flow pattern. The deviation is a change in the time of the process flow though the sequence remained the same. The water touched wave probe WP4 at 308.01s and at 308.11s, water flow on deck can be observed.

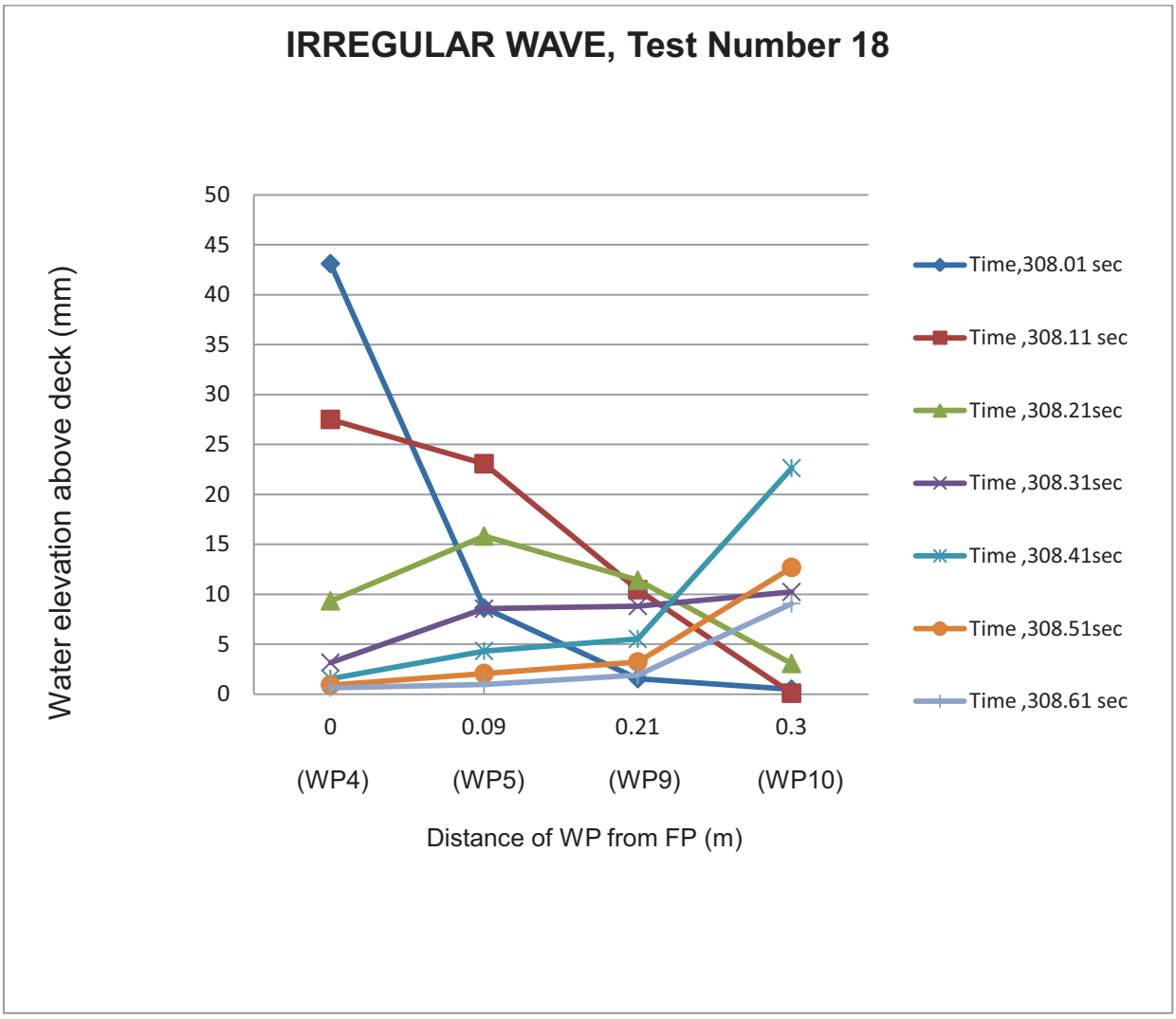

Figure 5.7 – Water flow on deck, H_s = 0.078m, T_p =1.25s

The process continued at 308.21s and water finally reached the deck structure at 308.31s. The build up process of water at the deck structure can be observed at 308.41s. Water was reflected back on deck at the times 308.51s and 308.61s. The change can be attributed to the selection of the water heights measurement from the records at a time when the green water process was already taking place. The significance of this observation is that the sequence of events in the green water phenomena remains consistent no matter the time at which it occurs and at what stage the process is captured.

5.3 Pressure Distribution on Deck due to Green Water

In a green water event, the pressure distribution on deck should take into account the vertical accelerations of the deck and some additional combinations of deck velocity and water height. A study of the regular wave test 16 condition shown in Figure 5.8 indicates a jet like impingement of water coming across the deck and hitting the deck with some impact around pressure transducer PT3. It can be observed that high pressure readings at PT3 indicate that most of the activity making up the green water event such as water impingement, rapid flow on deck and impacting on the deck structure, reflection and plunging of water back on deck all occur as time progresses at the position of the pressure transducer PT3. At the beginning of the green water event in this time series, Figure 5.2 shows the water reaching the wave probe WP4 at a maximum water height of 160mm at time 347.24s. At the pressure transducers PT1 and PT2, which are nearest to the water probe WP4, low pressure readings can be noticed. This is an indication that the water front coming on deck is in the form of an impinging jet formation and not the solid water wall as in the dam type build up at the fore perpendicular.

At the same time instant, an impact of water on deck can be observed from the pressure reading at PT3, which reads approximately 50mbars. PT2 records a small pressure reading, which can be attributed to some water traversing the bow not in a massive jet formation, but flowing like a shallow wave across the fore perpendicular. A later increase in the pressure reading at PT2 could mean that the water reflecting from the impact with the deck structure flows back on deck and reaching PT2 causes a secondary pressure reading.

As the time progresses in the time series of events, the full impact of the impinging jet formation is recorded at PT3, resulting in progressively higher pressure readings due to the full impact on deck, flow of water reaching the deck structure, and water reflection from the deck structure. High pressure readings at PT3 before and during impact with the deck structure from the times 347.34s to 347.54s can be regarded as a period of primary pressure distribution on the deck around PT3.

The period spanning times 347.64s to 347.84s is when the water has attained maximum impact, reflection and plunging back on deck, resulting in further higher pressure readings at PT3. This period can be considered as a secondary pressure distribution stage on the deck and is mainly caused by reflected and plunging water going back onto the deck. The pressure readings at PT4 indicate initial lower pressure readings at the early stage of the green water event and then increases with time but not as much as the pressure readings observed at PT3. The reason for this observation can be due to the bubble effects at the position of this pressure transducer. During water impact with the deck structure, foaming occurs which can lead to lower pressure readings. As the water solidifies again and returns back on deck, it already reaches PT3, which accounts for the higher pressure reading at this pressure transducer. Similar phenomena can be observed at the other selected test conditions as shown in Figures 5.9 to 5.13.

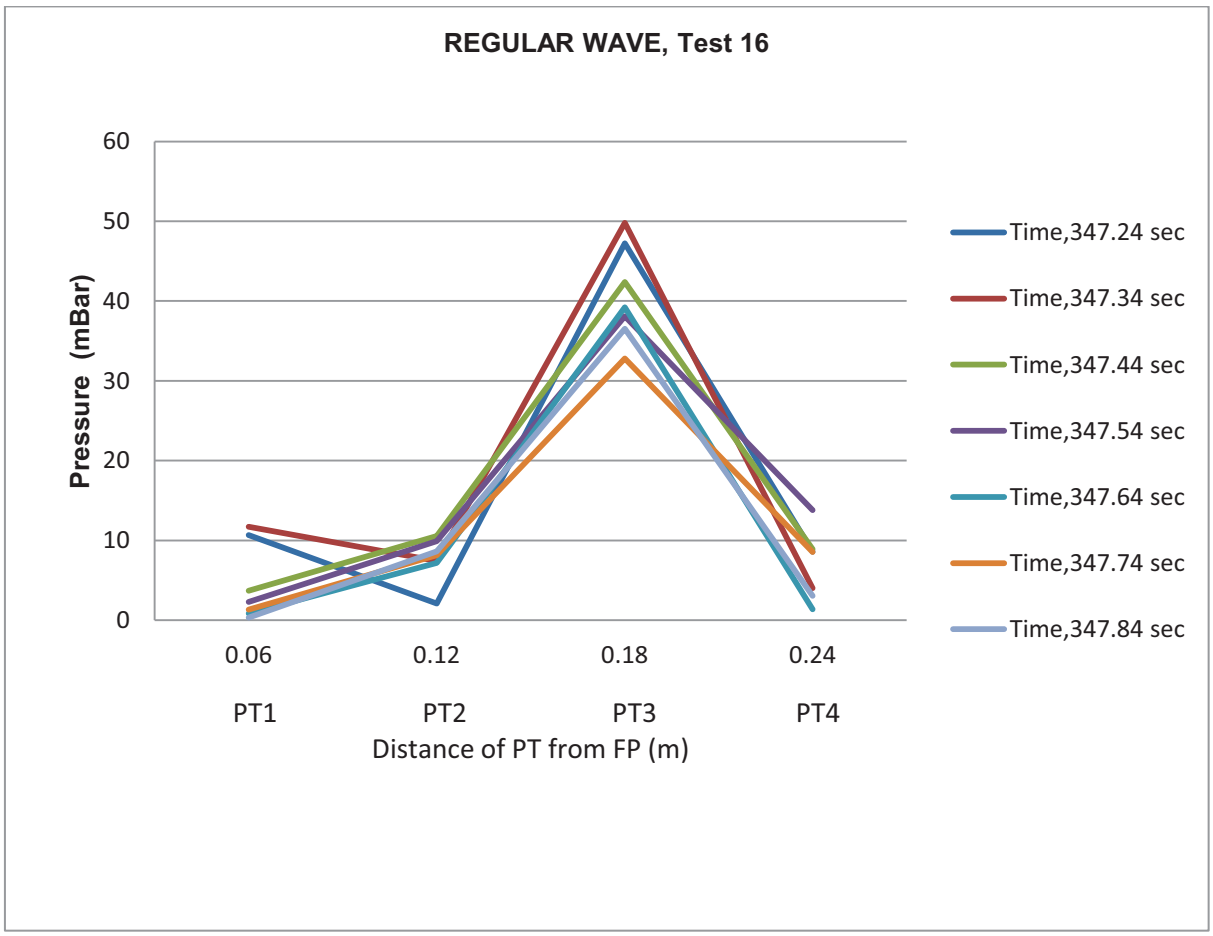

Figure 5.8 – Pressure distribution on deck, H = 0.13m, T =1.11s

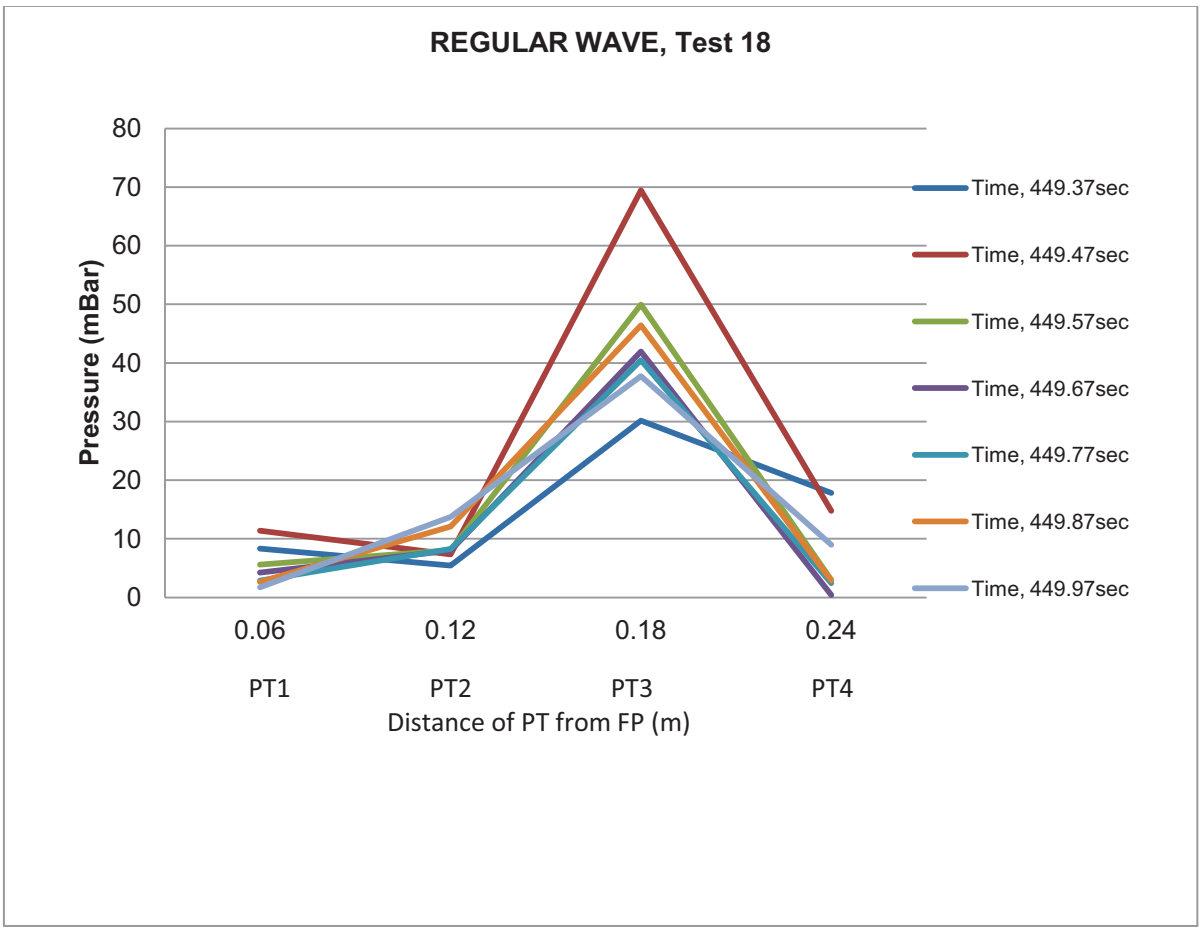

Figure 5.9 – Pressure distribution on deck, H = 0.095m, T =1.05s

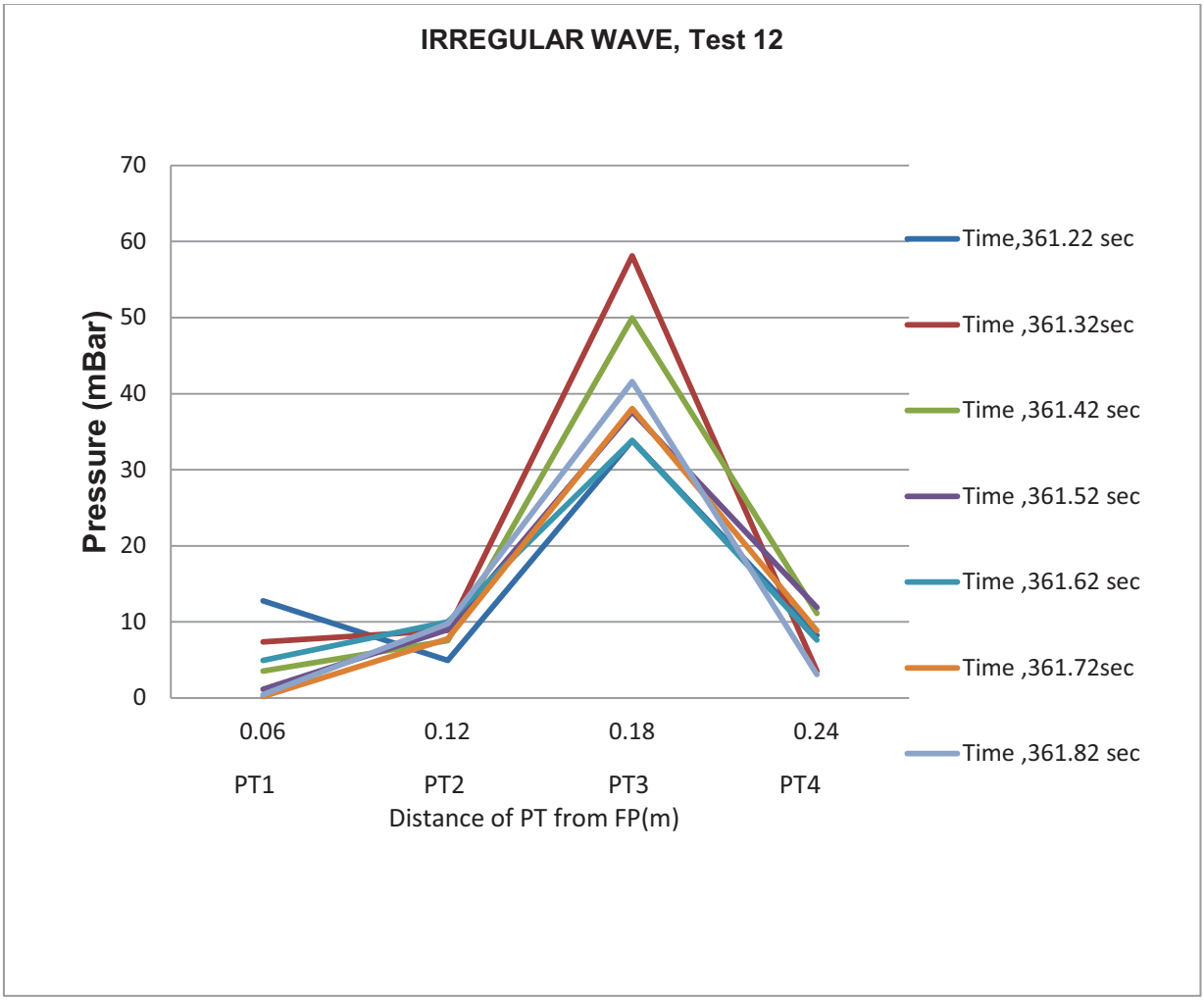

Figure 5.10 - Pressure distribution on deck , H_s = 0.078m, T_p =1.07s

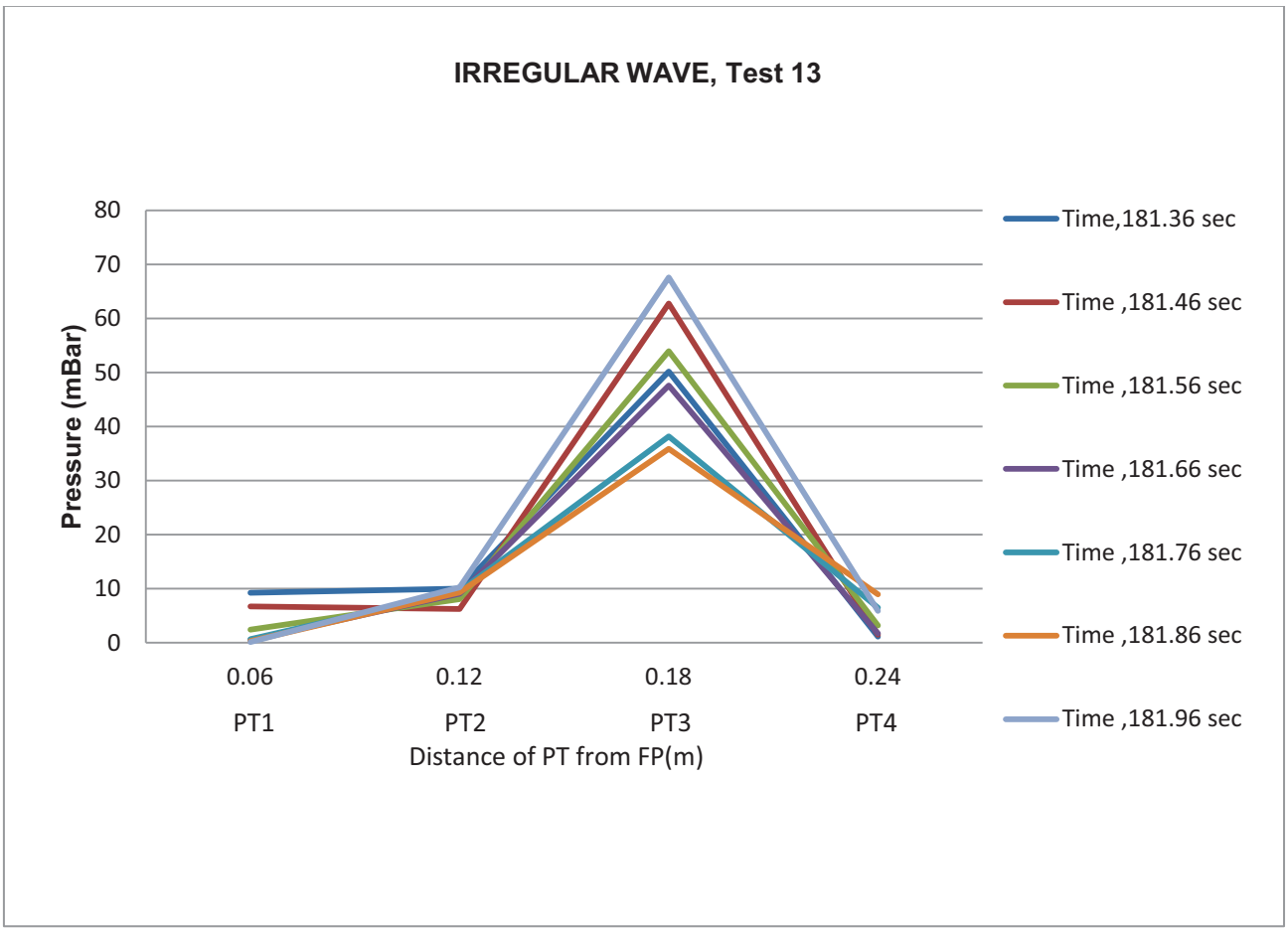

Figure 5.11 - Pressure distribution on deck , H_s = 0.11m, T_p =1.07s

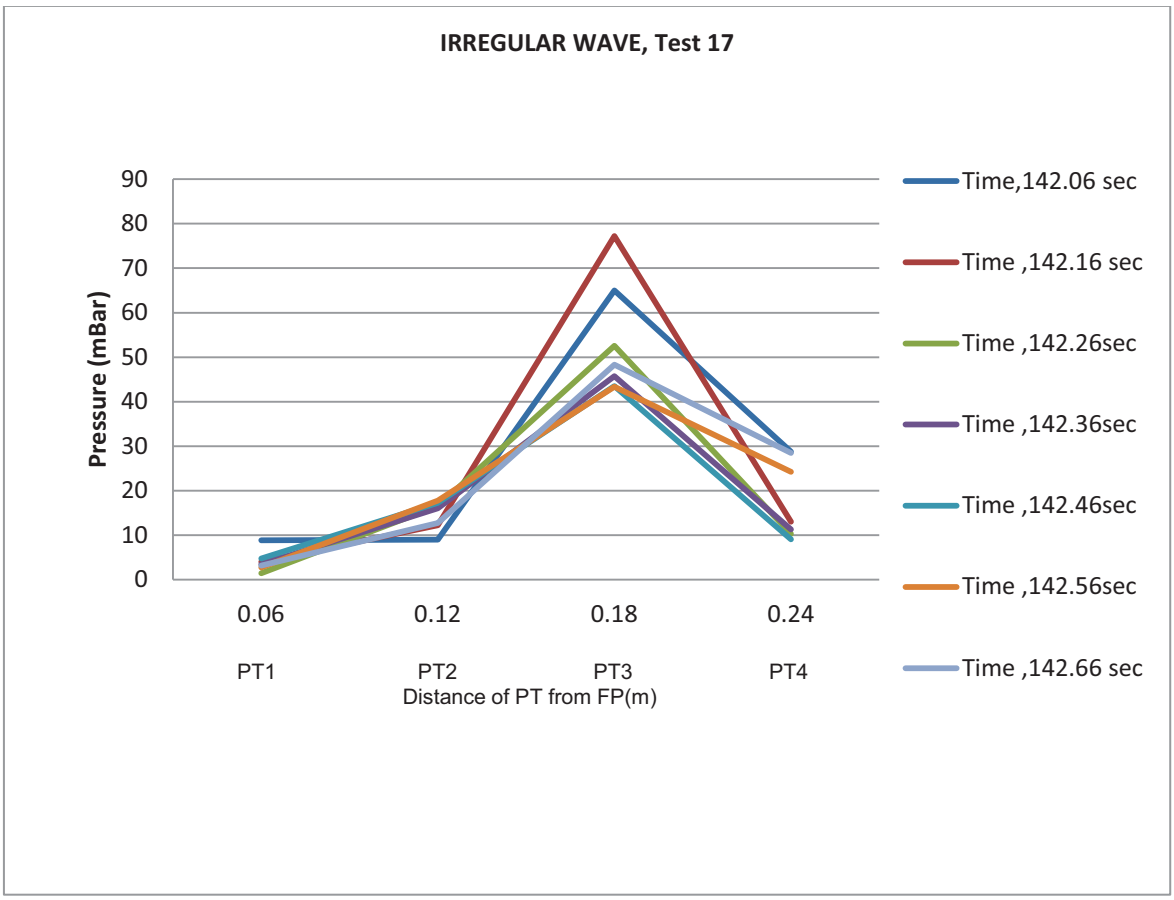

Figure 5.12 – Pressure distribution on deck, H_s = 0.095m, T_p =1.07s

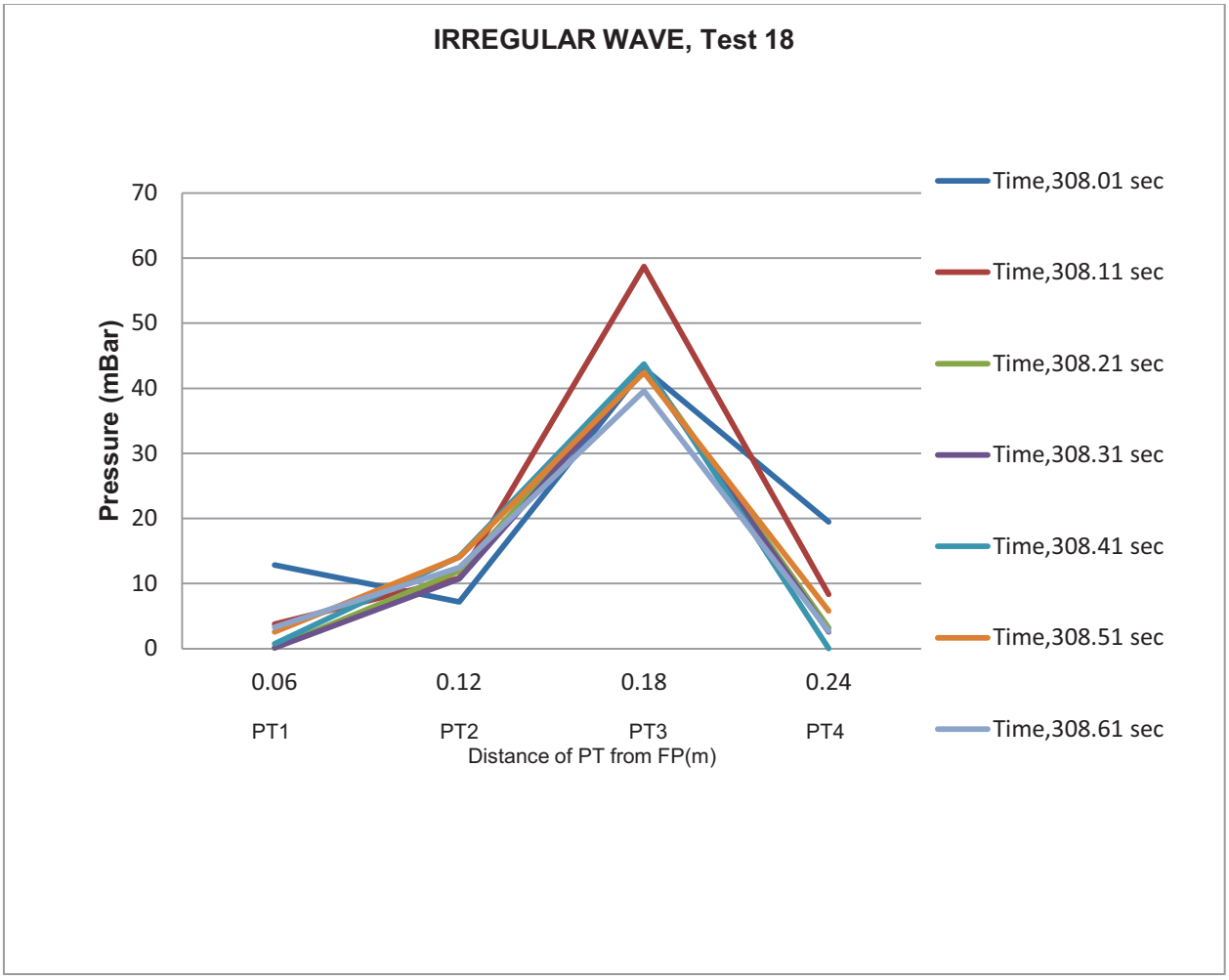

Figure 5.13 – Pressure distribution on deck , H_s = 0.078m, T_p =1.25s

5.4 Green Water Impact Study

This section focuses on the resulting green water loading on the deck structure. The model tests and measurements have been used to evaluate and study green water impact loading on a structure on the deck. If a green water event sequence is followed as previously described, a high velocity water front is created which hits the deck structure. A significant impact loading on the structure results from this event. Three stages have been identified by Buchner (2002) when the loading of water on a structure occurs during a green water event. The first is the *impact stage,* which has the character of an impinging jet or wedge entry, creating a first and highest peak load in a short period.

The second is the *quasi-static load* stage during which most of the kinetic energy is dissipated out of the fluid and a large amount of water builds up in front of the structure. The third is the *plunging water stage* when the accumulated water in front of the deck structure falls back onto the deck. A secondary maximum in the pressure arises from this occurrence when the water falls back.

These phases are very evident in the results obtained in the experiments carried out in the MAST tank.

5.4.1 Impact loads.

In the study of the impact loads, the time traces of measured loads on the deck structure are presented in Figures 5.14 to 5.18. The first impact stage attributes are clearly depicted in the graphs showing a rise and fall in maximum force over a short period of time which can be characterised as loading resulting from water jet impingent on the deck. Figure 5.14a to 5.14c are for the regular wave test condition 16 and show the time series of events during an impact load caused by green water loading. At the time 358.86s to 358.96s in Figure 5.14a, the force measurements at load cells LC3 and LC4 show a rapid rise and fall of the force on the structure.

A corresponding time in Figure 5.14b shows that the water reaches the water probe WP10 at the same time period, coming as an impinging jet formation and building up to the highest level at 394.04s. This period at which the highest load recording is observed is called the impact stage. During the period from 358.9s to 359s, pile up of water can be observed at WP10, Figure 5.14b and a secondary force measurement showing a rise in force at LC2, Figure 5.14a can be noticed. This is the quasi static load stage in a green water event. The water reached a maximum level at WP10 in the time 359.04s, Figure 5.14b and began to fall back on the deck. This is the plunging stage and the force recordings at the load cells reduce considerably.

Figure 5.14c shows the pressure distribution on deck during the impact loading stage during the same time instances. The pressure transducer PT3 records the pressure distribution most effectively due to the position along the deck. The water impingement, water run up to deck structure and plunging of water back on deck are activities which occur around the position of the pressure transducer (PT3). The initial flow of water impinging on the deck and reaching the deck structure recorded at PT3 can be considered as a primary pressure distribution on deck. After impact, the water plunges back on deck and the pressure measurements at PT3 can be described as secondary pressure distribution. The flow process on deck can be described as a shallow water wave and as a result the pressure measurements at PT1 and PT2 have shown lower pressure readings. At pressure transducer PT4, lower readings of pressure can be observed due to the fact that the water build up at the deck structure is not in the form of a solid wall but a plunging type activity and during impact, water foaming occurs which can result in low pressure readings. However during the time of water build up at the deck structure, there is a corresponding rise in pressure at PT4 but not as significant as the readings at PT3. A study of the other wave conditions shows a similar trend in profile.

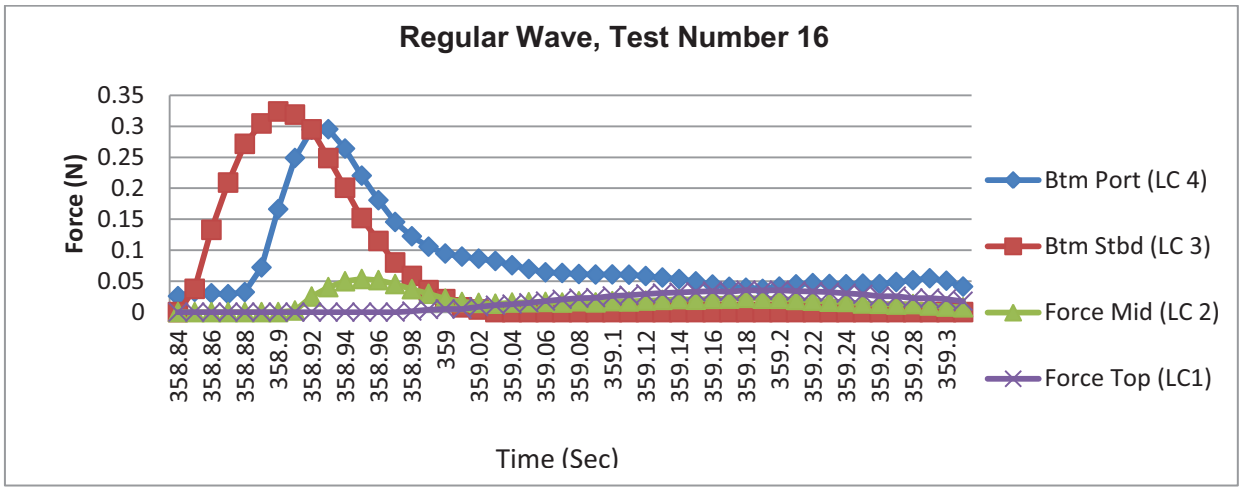

Figure 5.14a Force due to water impact on deck structure, H=0.13m, T=1.11s

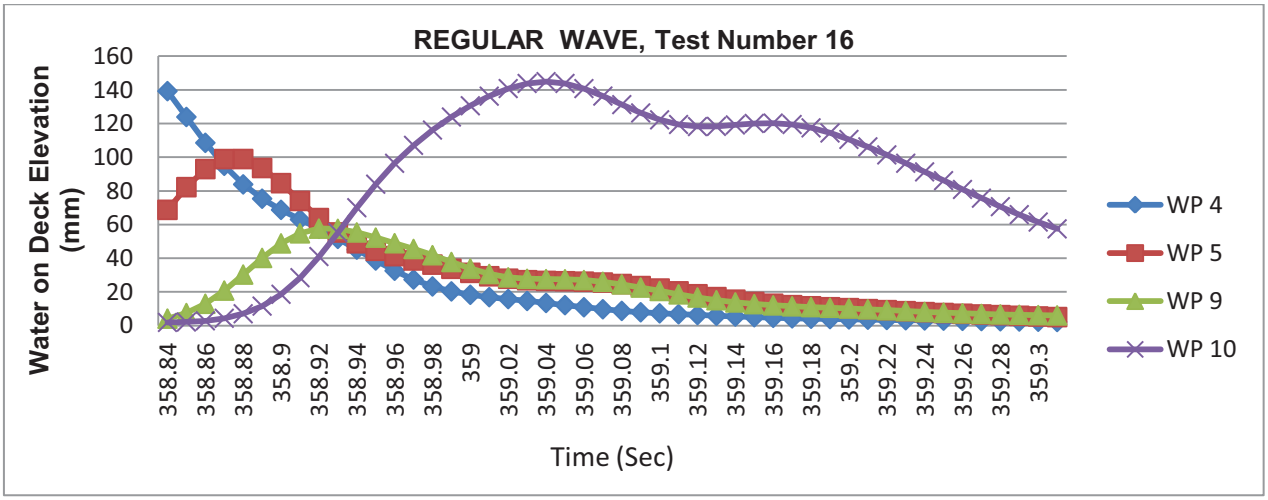

Figure 5.14b Water height on deck at impact with deck structure, H=0.13m,T=1.11s

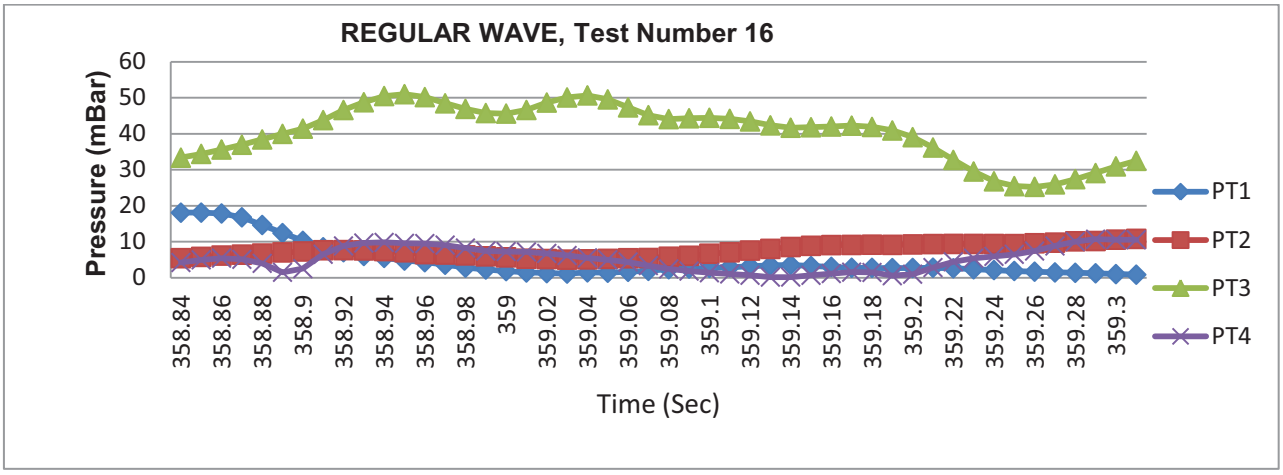

Figure 5.14c Pressure distribution on deck at water impact on deck structure, H=0.13m, T=1.11s

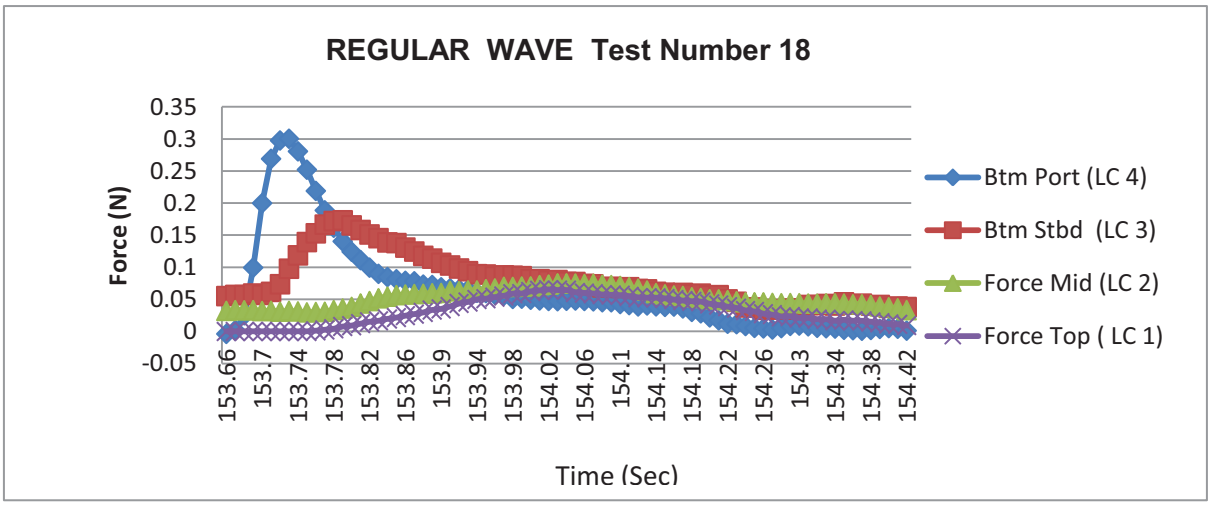

Figure 5.15a Force due to water impact on deck structure, H=0.095m, T=1.05s

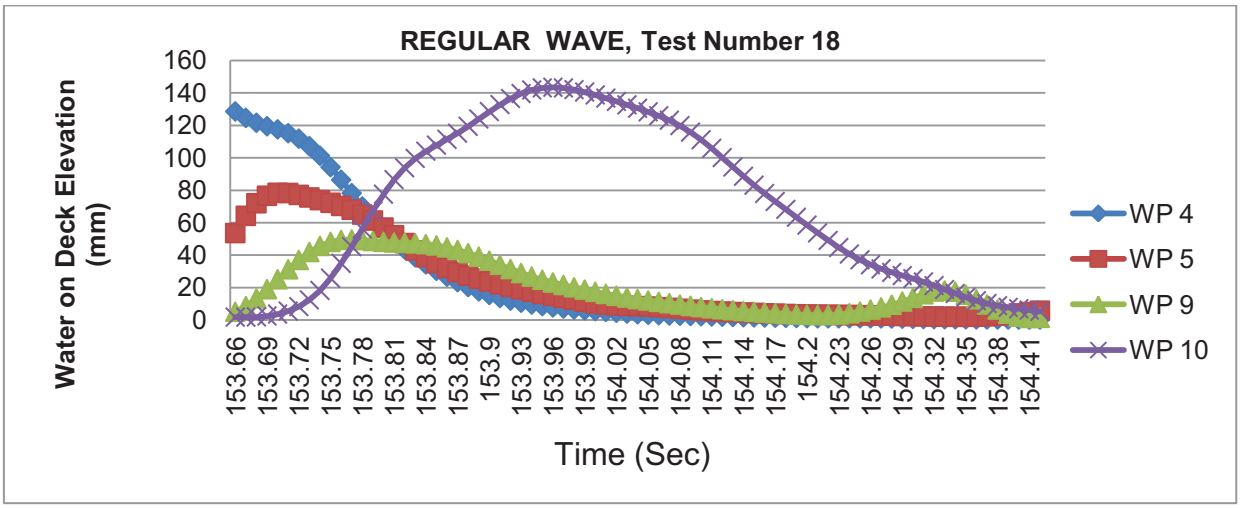

Figure 5.15b Water height on deck at impact with deck structure, H=0.095m, T=1.05s

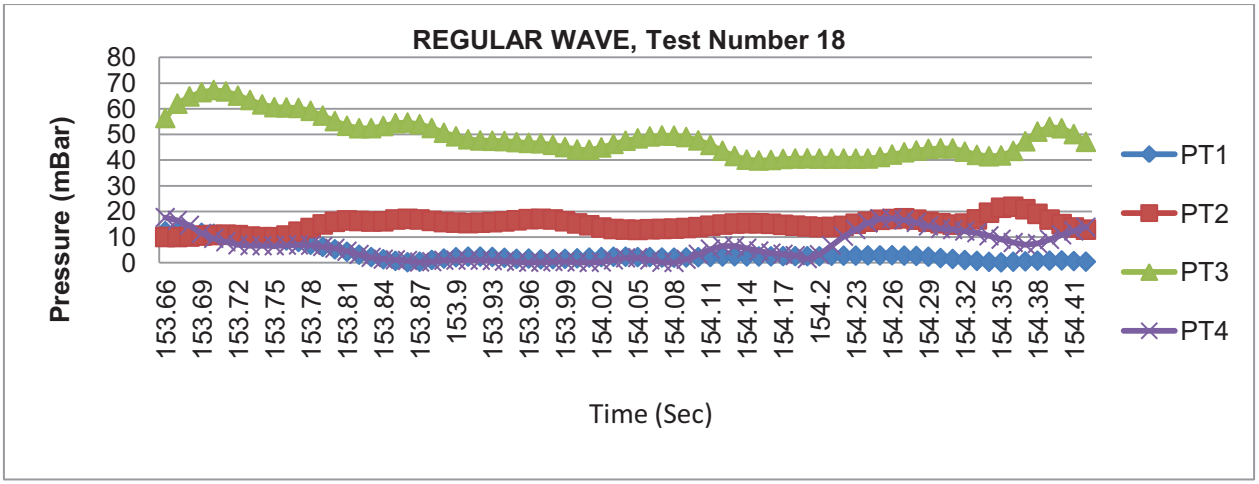

Figure 5.15c Pressure distribution on deck at water impact on deck structure, H=0.095m, T=1.05s

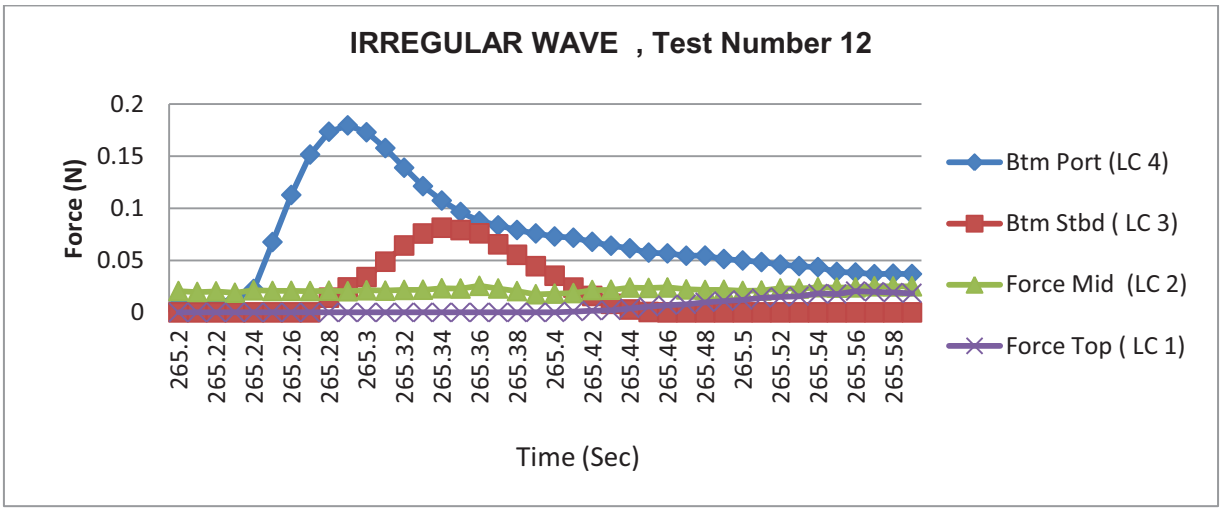

Figure 5.16a Force due to water impact on deck structure, H_s=0.078m, T_p=1.07s

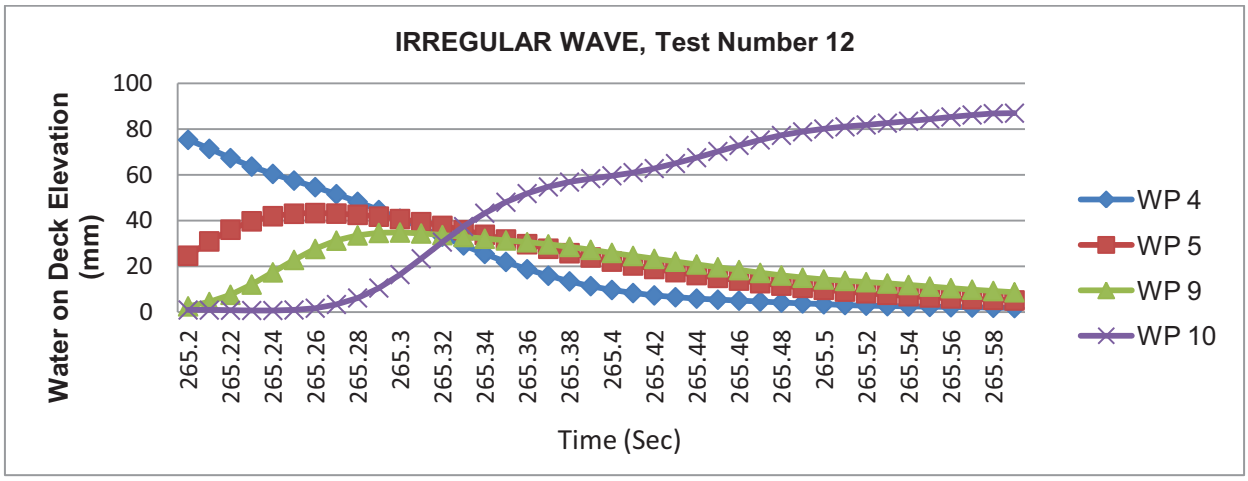

Figure 5.16b Water height on deck at impact with deck structure, H_s=0.078m, Tp=1.07s

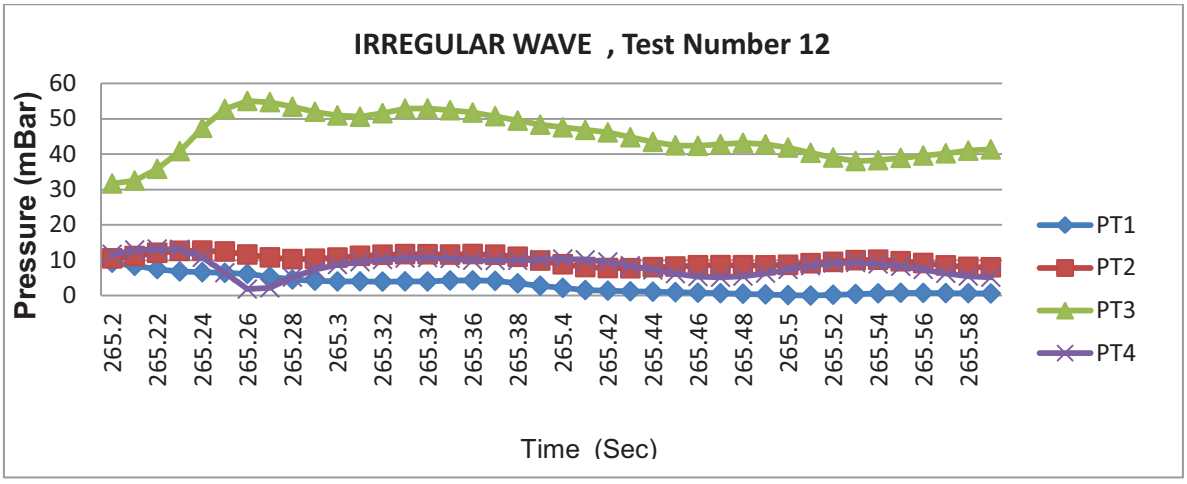

Figure 5.16c Pressure distribution on deck at water impact on deck structure, H_s=0.078m, T_p=1.07s

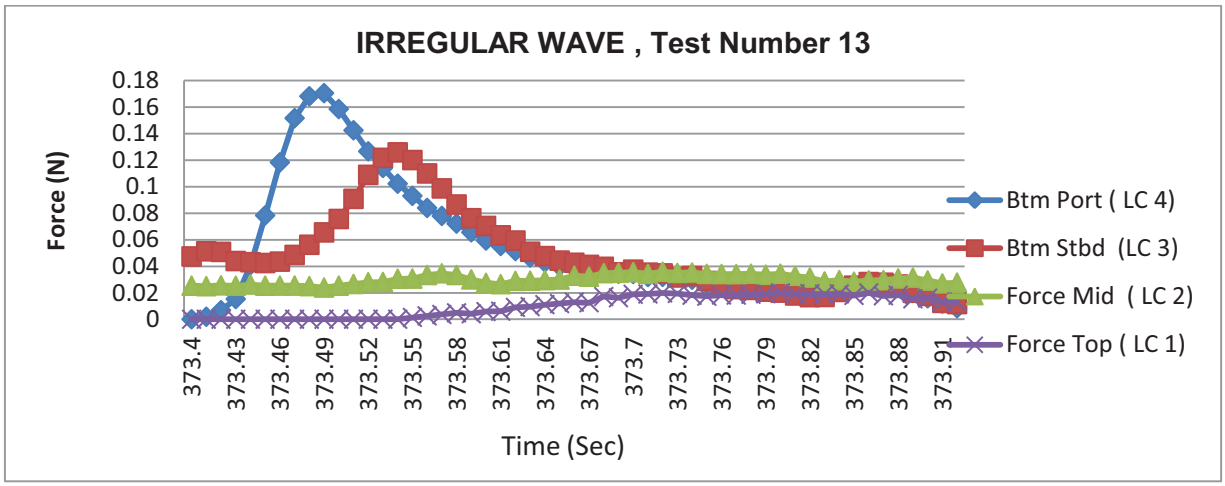

Figure 5.17a Force due to water impact on deck structure, H_s=0.11m, T_p=1.07s

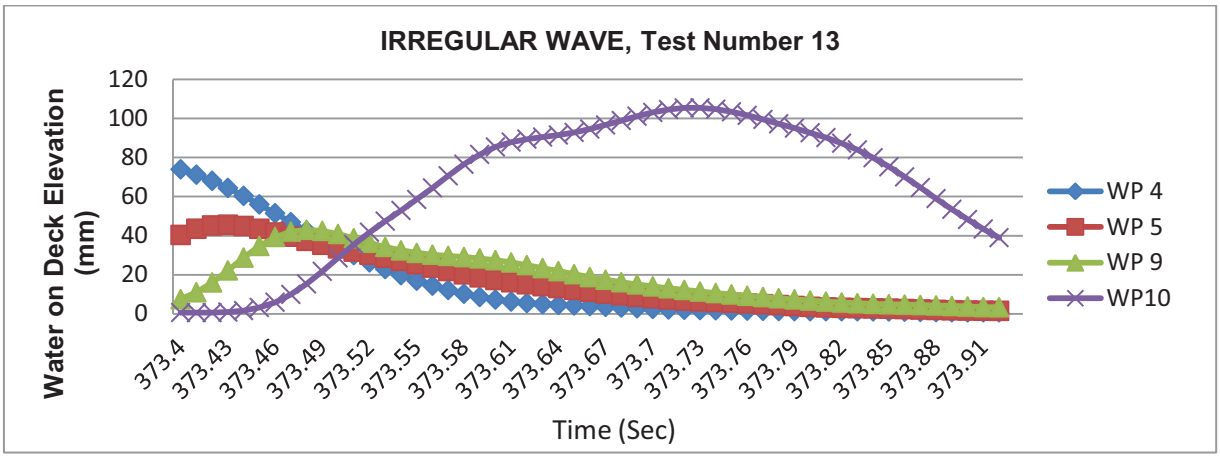

Figure 5.17b Water height on deck at impact with deck structure, H_s=0.11m, T_p=1.07s

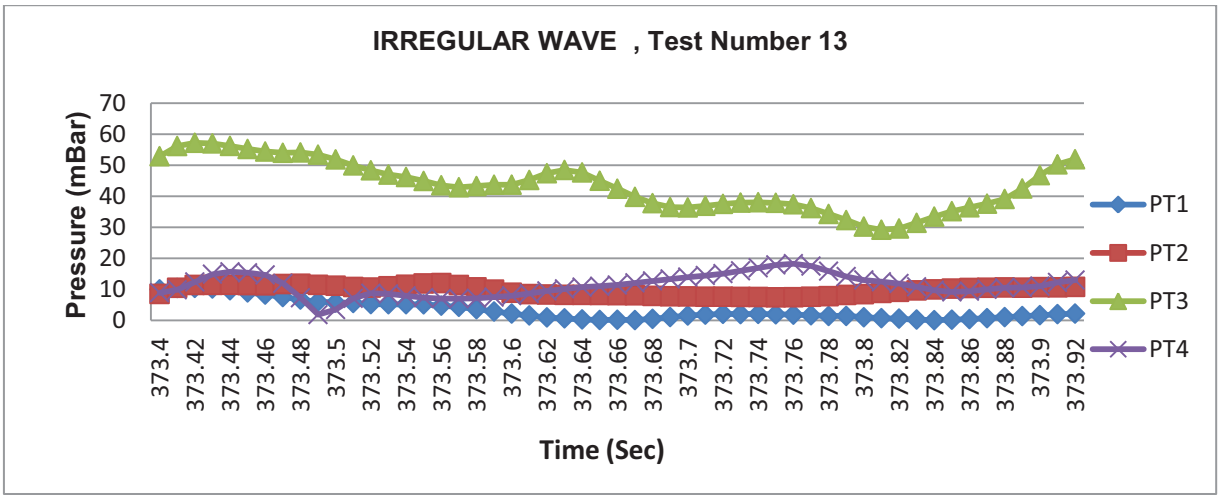

Figure 5.17c Pressure distribution on deck at water impact on deck structure, H_s=0.11m, T_p=1.07s

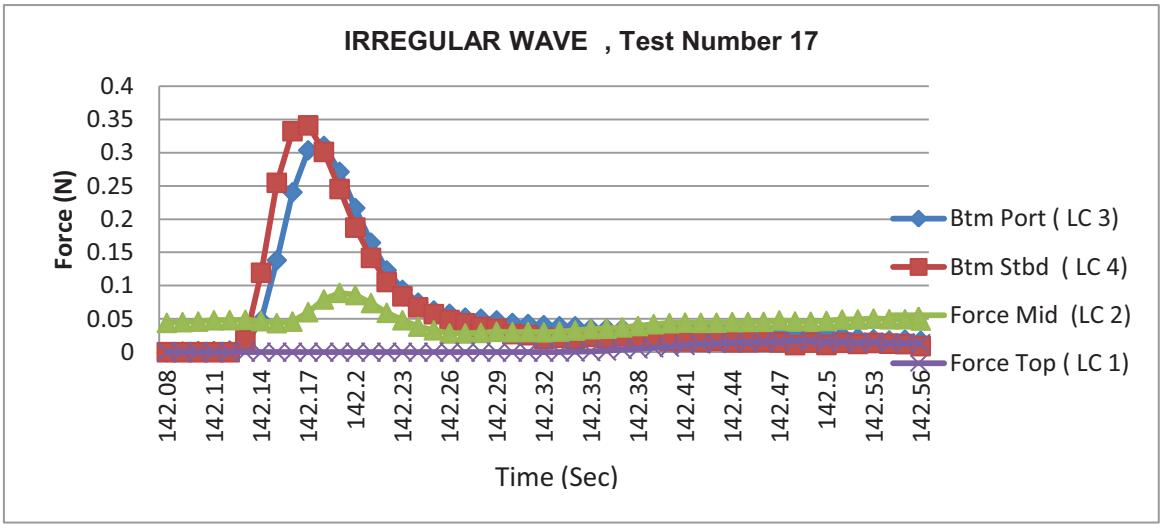

Figure 5.18a Force due to water impact on deck structure, H_s=0.095m, T_p=1.07s

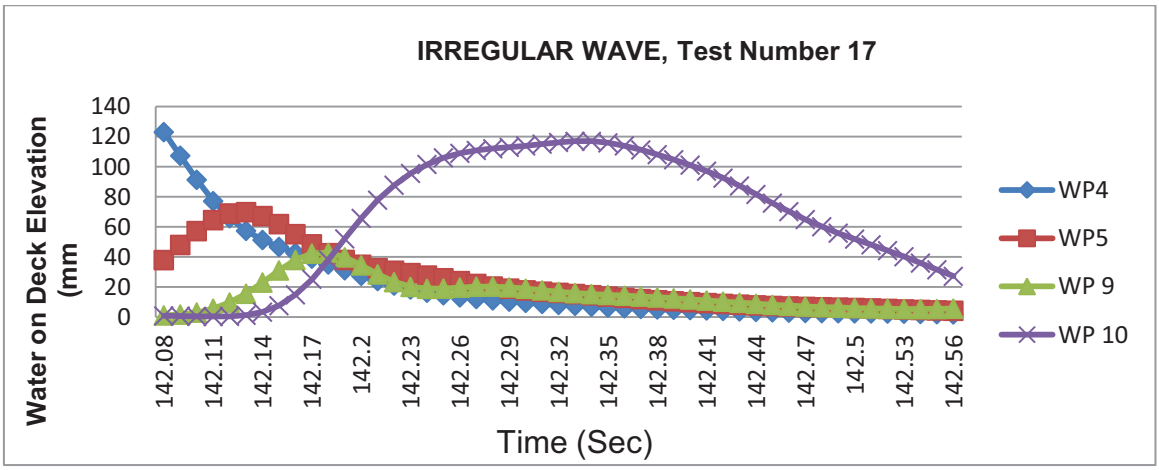

Figure 5.18b Water height on deck at impact with deck structure, H_s=0.095m, T_p=1.07s

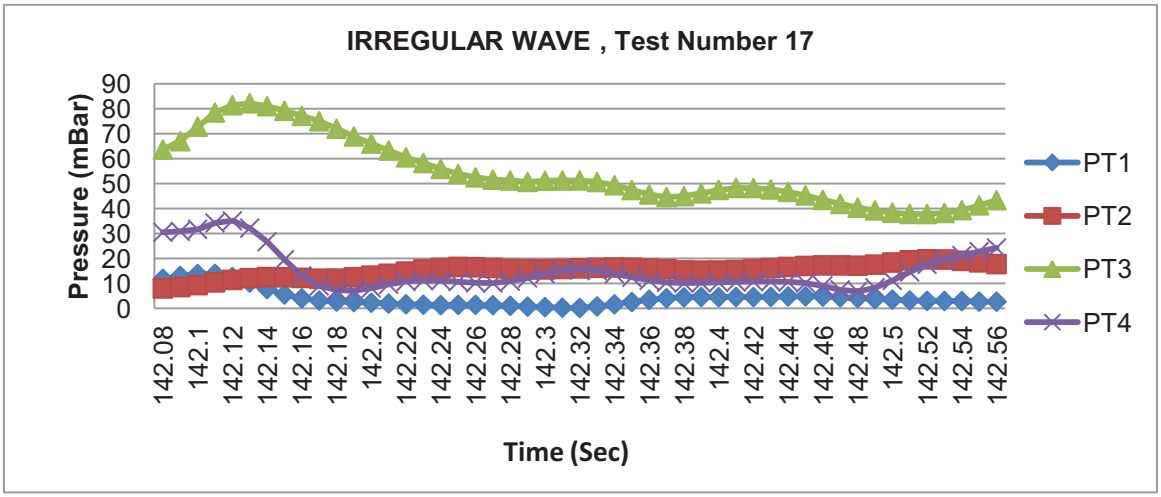

Figure 5.18c Pressure distribution on deck at water impact on deck structure, H_s=0.095m, T_p=1.07s

5.4.2 Relation between freeboard exceedance, velocity, pressure and force.

The principal parameter that determines the occurrence of Green Water in a weather condition around the bow of a vessel such as the FPSO is the relative wave motion at the bow region. This vertical motion can be assumed to be linear when the wave and vessel motions are taken to be small, and can be defined as follows;

$$r_{WM} = \zeta - \eta \tag{5.1}$$

where r_{WM} is the difference between the local disturbed wave motion ζ and the local vertical motion, η

Green Water occurs when the relative wave motion r_{WM} exceeds the freeboard f_b as illustrated in Figure 5.19. The extreme freeboard exceedance $h_{\max}$ is defined as;

$$h_{\max} = r_{WM} - f_b \tag{5.2}$$

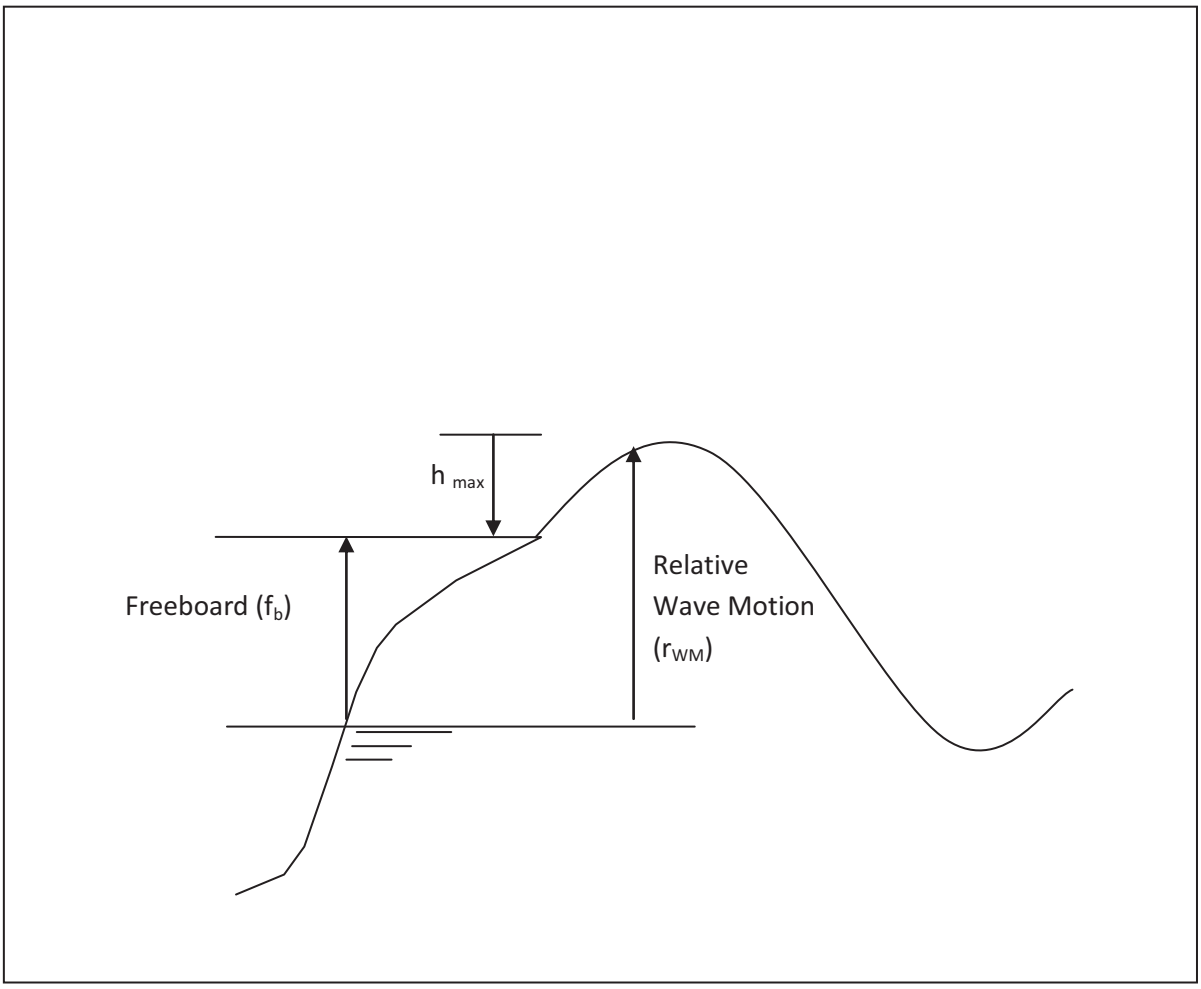

Figure 5.19 - Definition of relative wave motion (r_{WM}) and freeboard with respect to the waterline in calm water (Buchner 2000)

Buchner (2002) presented tables and figures to describe relationships between freeboard exceedance at the bow centreline and water heights at various distances from the fore perpendicular of FPSOs with full elliptical bow and different bow flare angles. To describe this relationship, he suggested that the nearly linear relationship between the water height on deck (H) at distances from the fore perpendicular and the extreme freeboard exceedance $h_{\max}$ can be taken as a starting point for developing other relationships for water velocity on deck, pressure and force on deck structures.

$$H = a_H h_{\max} \tag{5.3}$$

Consequently, Buchner (2002) developed the following relationship for the horizontal velocity of water at H_0, the water height at fore perpendicular.

$$u = a_U \sqrt{H_0} \tag{5.4}$$

A relationship between maximum pressure $p_{\max}$ and maximum freeboard exceedance $h_{\max}$ on deck was also developed.

$$p_{\max} = a_P h^2{}_{\max} \tag{5.5}$$

A similar expression was also given for the maximum horizontal impact force F_x on a graduated deck structure.

$$F_x = a_F h^3_{\max} \tag{5.6}$$

Where the parameters a_H, a_U, a_P and a_F are factors that are dependent on the distance from fore perpendicular, bow shape and bow flare angle.

The parameter tables have been taken from Buchner (2002). Table 5.1 presents the values for a_H and Table 5.2 the values for the velocity parameter a_U. The parameters a_P and a_F of regular and irregular waves for full elliptical bows are provided in Tables 5.3 and 5.4. The relationships in equations (5.5) and (5.6) were determined based on a least square fit, through the measurements taken at the impact load cells of the structure.

The relation between freeboard exceedance and water height on deck has been investigated in this study. The investigation was performed to assess the performance of the Buchner (2002) relation for water heights to establish how well it can be applied to a sea condition when the freeboard exceedance is known for a given bow shape.

To check the relation between extreme freeboard exceedance and the water height on deck at the fore perpendicular H_0, the measured water heights at WP4 of all the regular wave tests results for all tested wave heights and wave frequencies have been presented in Figure 5.20a. The results as shown in the figure 5.20a are compared with Figure 5.20b for the values obtained from the calculation using equation (5.3) for the water height H. The measured extreme freeboard exceedance $h_{\max}$ was obtained at WP1 for all tests. The value of a_H taken from Table 5.1 was 0.83387.

The comparison of the values of the water heights on deck for the test results, as presented in Figures 5.20a and 5.20b, in general show that there is reasonable correlation and agreement to justify the use of the Buchner (2002) relation for specific bow shapes.

The pressure and velocity relationships were not investigated, as no measurements were taken for water velocity on deck and pressure on the deck structure. Investigation of the horizontal impact force F_x has been treated in Appendix B.

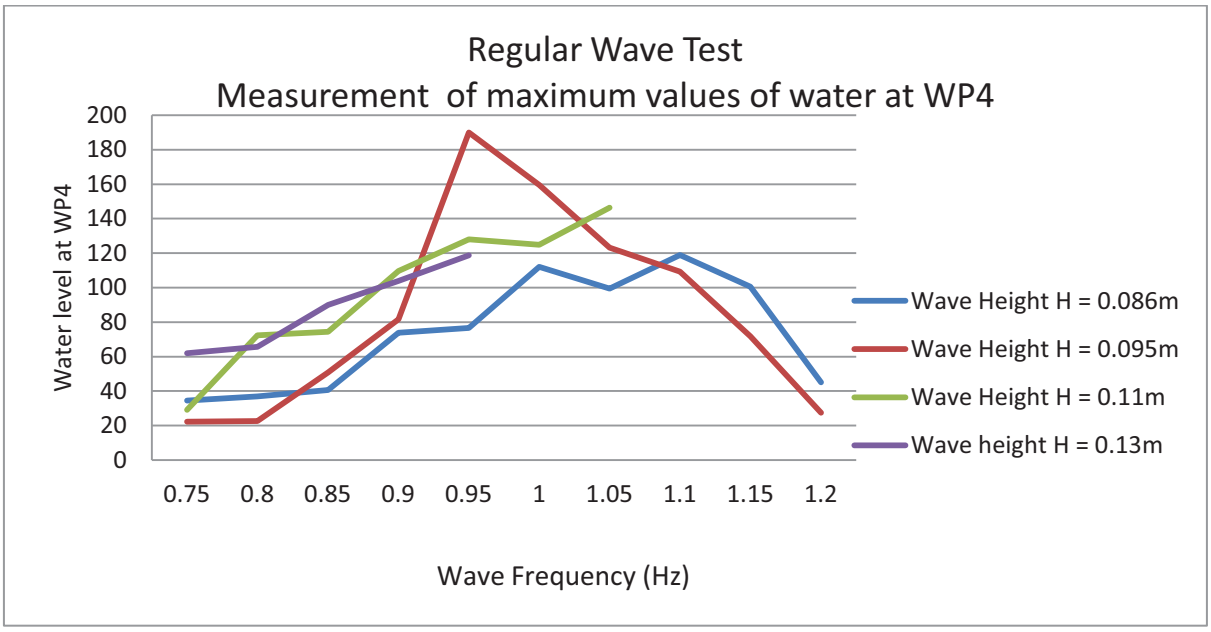

Figure 5.20a Water height on deck at FP (H_0) obtain from WP4 in regular waves for all test conditions.

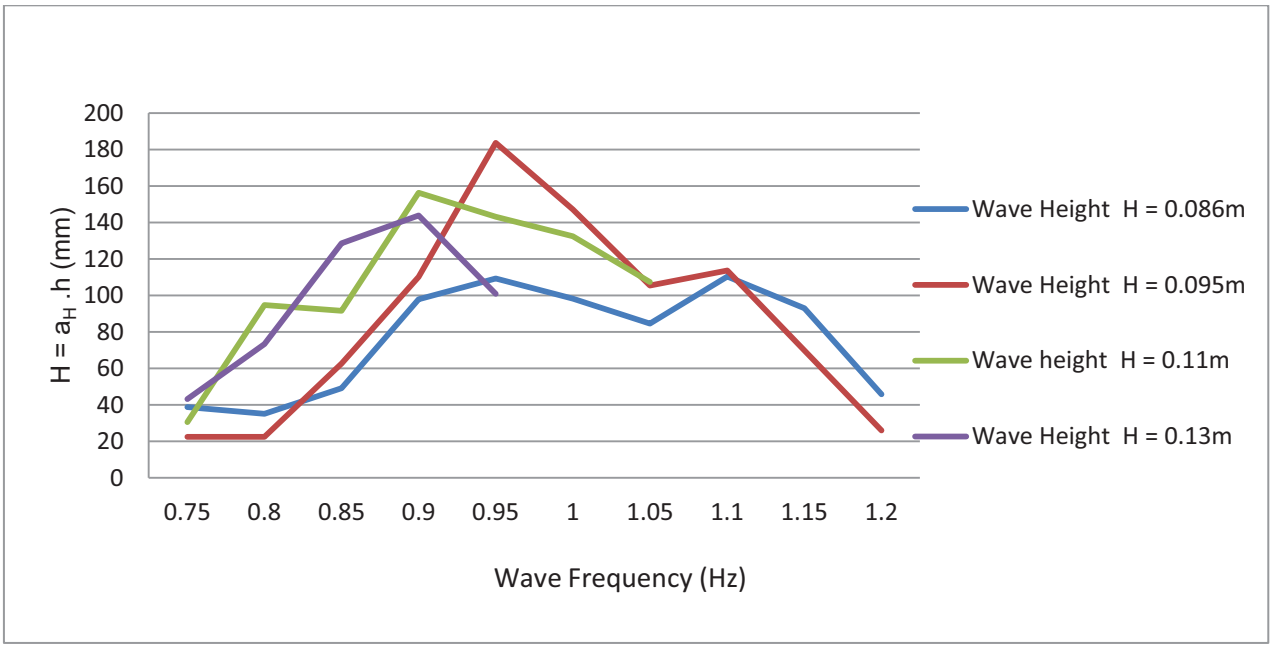

Figure 5.20b Water height at FP (H_0) obtain from relation $H= a_H.h_{max}$ in regular waves for all tests conditions.

A standard error check was made for the cubic relation between the freeboard exceedance and the loads on the structures on deck where the standard error is defined as (Buchner,2002)

$$\text{Standard error} = \sqrt{\frac{1}{n-2}\sum_{i}^{n}(F_{i,\text{measured}} - F_{i,\text{least square}})^2} \qquad (5.7)$$

and n = number of measurement points.

The FPSO model used in this study has a full elliptical bow with a 10 degree bow flare angle. Therefore the standard error computation and chosen parameters from Tables 5.3 and 5.4 were based on these characteristics. Table 5.5 shows the standard error results for the regular wave condition test 18. The results indicate and support the previous assumptions by Buchner and justify the chosen cubic relation. The cubic relation gave the lowest standard error for the regular wave tests. For the irregular wave test 17, the factor a_F of 76.4 was taken from Table 5.4 and used for the computations. The standard error was also found to be lowest for the cubic expression as defined in Table 5.6.

The results are in agreement with the recommendations of Buchner (2002) for the computation of the maximum horizontal F_x forces on the deck structure.

The expression in equation 5.4 for the determination of the horizontal water velocity at the fore perpendicular was used in the numerical simulation of green water event as it relates to the initial condition for velocity of the green water occurrence at the fore perpendicular of the FPSO.

In the numerical prediction approach carried out in this study a_U was taken from Table 5.2 as 4.94793 corresponding to an FPSO with a bow flare angle of 10 degrees.

Table 5.1 Parameter a_H as function of bow flare angle and position from the fore perpendicular from Buchner (2002)

Bow flare angle	**0 m from FP**	**10 m from FP**	**20 m from FP**
γ = 0 degrees	0.88499	0.60117	0.62701
γ = 10 degrees	0.83387	0.58068	0.58776
γ = 30 degrees	0.74172	0.58961	0.55541
γ = 50 degrees	0.62279	0.50507	0.34959

Table 5.2 Parameters a_u for the fully elliptical and thin triangular bow as function of flare angle Buchner (2002)

Bow flare angle	Full elliptical	Thin triangular
γ = 0 degrees	4.63376	-
γ = 10 degrees	4.94793	7.39312
γ = 30 degrees	6.34439	8.16391
γ = 50 degrees	8.52956	9.97322

Table 5.3 Parameters a_P and a_F for the regular wave test results of the full elliptical bow Buchner (2002)

Full elliptical bow (flare angle)	Factor a_P (least square fit)	Factor a_F (least square fit)
γ = 0 degrees	2.37	85.4
γ = 10 degrees	2.27	81.7
γ = 30 degrees	2.20	93.4
γ = 50 degrees	1.39	45.3

Table 5.4-Parameters a_P and a_F for the least square fit for the irregular wave test results of the full elliptical bow Buchner (2002)

Full elliptical bow (flare angle)	Factor a_P (least square fit)	Factor a_F (least square fit)
γ = 0 degrees	2.12	82.6
γ = 10 degrees	1.86	76.4
γ = 30 degrees	1.99	70.9
γ = 50 degrees	1.49	51.0

Table 5.5- Standard error for the different least square fit curves for the full elliptical bow with bow flare of 10 degree. (Regular wave, test 18)

Assumed relation	Standard error
$F = a_F \cdot h_{\max}$	8.23
$F = a_F \cdot h_{\max}^2$	2.58
$F = a_F \cdot h_{\max}^3$	1.27

Table 5.6- Standard error for the different least square fit curves for the full elliptical bow with bow flare of 10 degree. (Irregular wave, test 17)

Assumed relation	Standard error
$F = a_F \cdot h_{\max}$	2.72
$F = a_F \cdot h_{\max}^2$	0.817
$F = a_F \cdot h_{\max}^3$	0.27

In conclusion, the green water events generated in this research experiment were found to follow broadly the trends identified by Buchner (2002). That is green water coming across the bow in a jet formation, hitting the deck and flow rapidly reaching the deck structure. A reflection takes place with water plunging back on deck. At the deck structure, three phases of the events have been identified – Impact loading stage, quasi–static load stage and the plunging load stage were evident in the experiments carried out in this study. The relation between the water heights on deck H and the freeboard exceedance was investigated and found to be valid and can be justified for specific conditions. The relation between the horizontal force on the deck structure F_x and the freeboard exceedance $h_{\max}$ was also investigated and found to be valid. The experimental data obtained in this part of the work together with the empirical formulations for the water velocity on deck discussed will be used to define the initial conditions in the numerical modelling.

It should be noted that Buchner's experiments were carried out with a scale factor of 1:60, whereas the experiments in the present study were carried out at a scale of 1:127 The good agreement obtained between the two studies indicates that the relationships studied are relatively insensitive to scaling issues. This reflects that viscous effects (associated with Reynolds number scaling) are not significant for these phenomena which one in any case expects to be dominated by gravity effects (associated with Froude number scaling that has been observed).

5.5 Numerical Method and Simulation of Green Water

Wave structure interaction problems are marine hydrodynamic problems that involve the response of ships or marine structures to wave excitation forces. The green water phenomenon is an extreme example of such an event and there is an increasing interest in developing a robust and efficient numerical modelling approach for the analysis of problems associated with green water in marine design.

As described earlier, the green water problem occurs when water amasses on the deck of a floating structure due to waves overtopping the bow or side of the structure. The experimental studies presented in this thesis have given a considerable insight into nature of the green water phenomenon. The material in Chapters 4 and 5 combined with the MPS method in Chapter 3 are now used to model the water flow pattern on deck, pressure distribution on deck and the prediction of the force on the deck structure.

Buchner, (2002) suggested the following requirements for adequate modelling of the green water phenomena in order to deal with the nonlinear complex flow;

1 Wave entry around the flared bow structure
2 Complex nonlinear flow onto the deck
3 Water flows on the deck
4 Water impact on deck structure

This study aims at evaluating requirements (3) and (4) and modelling the process using the MPS method.

The MPS method as advocated by Koshizuka and Oka (1996) is used as a basis for solving the governing Navier Stokes equations. This equation which describes the motions of a fluid in general terms is applied to the green water physics as observed in the model tests. The method as described in Chapter 3 solves the incompressible Navier Stokes equations for flows with free surfaces. The method has been chosen because it effectively handles the treatment of convective terms in the flow equation.

The Laplacian and Gradient models of the MPS method are applied to the partial differential operators in the mathematical formulations as described in Chapter 3. The Navier Stokes equations are discretised in accordance to the Laplacian and Gradient formulation of the MPS method. The Poisson pressure equation as described by the MPS method is used to determine the pressure on the deck and on the deck structure. The final outcome of the simulation is to determine the flow pattern, water height on deck, pressure on deck and the force on the deck structure at each step.

In this study, the ship motions are not integrated with the green water event by provision of the motions of the vessel from the model tests. This study did not incorporate the motion of the vessel in the simulation process as it was not in the scope of work. The fundamental requirement was aimed at providing an efficient prediction method that is able to overcome the difficulties encountered by earlier conventional approaches. These difficulties in wave-structure interactions include the treatment of the convective terms in the flow equation, incompressibility constraints, large free surface deformation, and grid and mesh updating. The MPS method is able to overcome these constraints because of its Lagrangian description of the behaviour of fluid particles.

A green water incident is a complicated flow process which involves the motion of the ship as well as complicated flow effects such as turbulence and wave plunging. The experience from the model test experiment and numerical simulation suggest a mixed Lagrangian-Eulerian concept for deeper analysis of the green water phenomenon. In this way, the various effects associated with this phenomenon can be studied. A possible way forward is to undertake a fluid structure interaction analysis using a coupled MPS method and a ship motion analysis in a mixed Lagrangian–Eulerian format for future work. The MPS method will be used to analyse the fluid flow and the ship motion analysis for the structure in a coupled scheme. In the coupling scheme, the MPS method will resolve the issue of the convective terms and incompressibility constraint in the fluid equations, modelling and tracking of the free surface in the fluid and the transfer of information between the fluid and solid domain via the contact interfaces.

The solid deck can be represented as particles but the interface between the fluid and solid deck would be modelled as a rigid body whose motion is computed from the sea keeping analysis. The deck particle conditions can be updated with the motion effects such as heave, roll, or pitch motions. The coupling scheme is utilized on the basis that fluid particles on the deck move with the introduced motions from the sea keeping computation and the pressure on the deck is computed using the MPS method under a time integration scheme. A preliminary work along these lines using the random choice method was undertaken by Han (2003) but the coupling between the two analyses was not rigorous.

5.5.1 Computational domain

As the basis for the simulation in this study, the deck section configuration was approximated by a strip of rectangular section, following the line of arrangement of the deck wave probes and pressure transducers in the experiment along the centreline of the foredeck. Also the deck structure has been positioned at the far end of the rectangle.

Taking into account the resemblance of the phenomenon with the jet like formation, the wave height above the deck measured at the fore perpendicular in the experiment was translated into an initial condition of horizontal velocity of water particles around the bow. At the start of the simulation, the water height measurement was used as a basis to determine the number of particles of water used for the simulation. The sketch of the computational domain is presented in Figures 5.21a to 5.21c for the irregular wave condition test 17 showing the dimensions of the deck and position of the instrumentation. The dimensions of the pressure transducers and load cells from chapter 4 are taken to be about 8mm and 9mm respectively in diameter. About 20 particles make up a pressure transducer or load cell. The deck is reduced in width to 200mm from 300mm for convenience of computation and to reduce the number of particles due to computer resources limitation. The pressure transducers and load cells in the experiment were located well within this boundary and so the numerical model will reflect the dominant effects, although some minor effects due to the curved nature of the deck plan will be neglected.

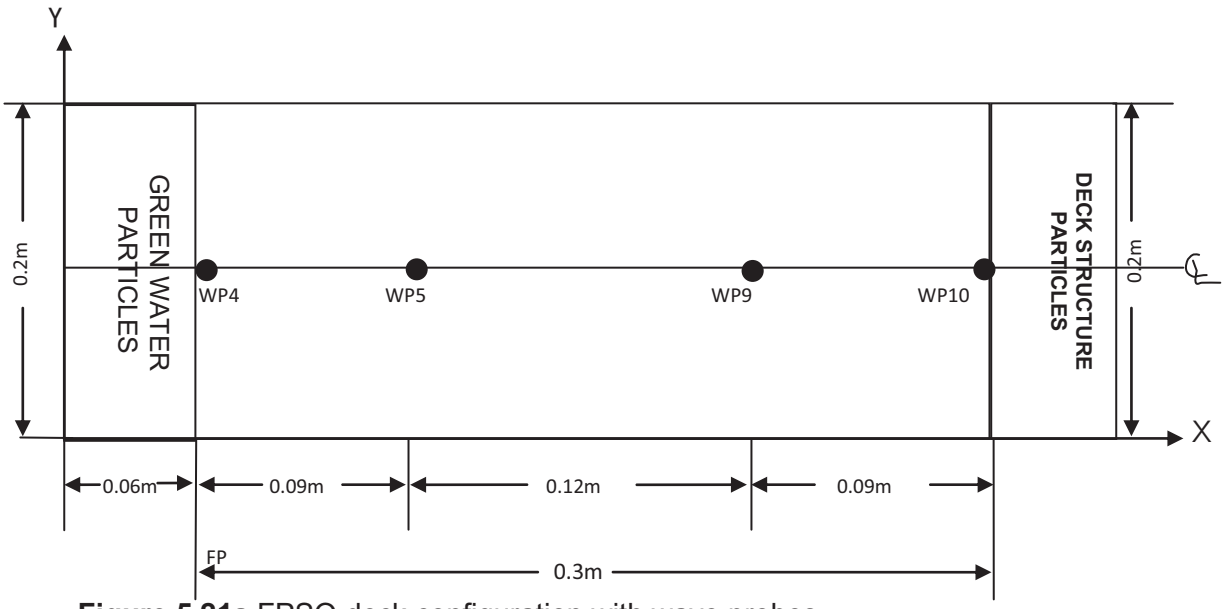

Figure 5.21a FPSO deck configuration with wave probes**.**

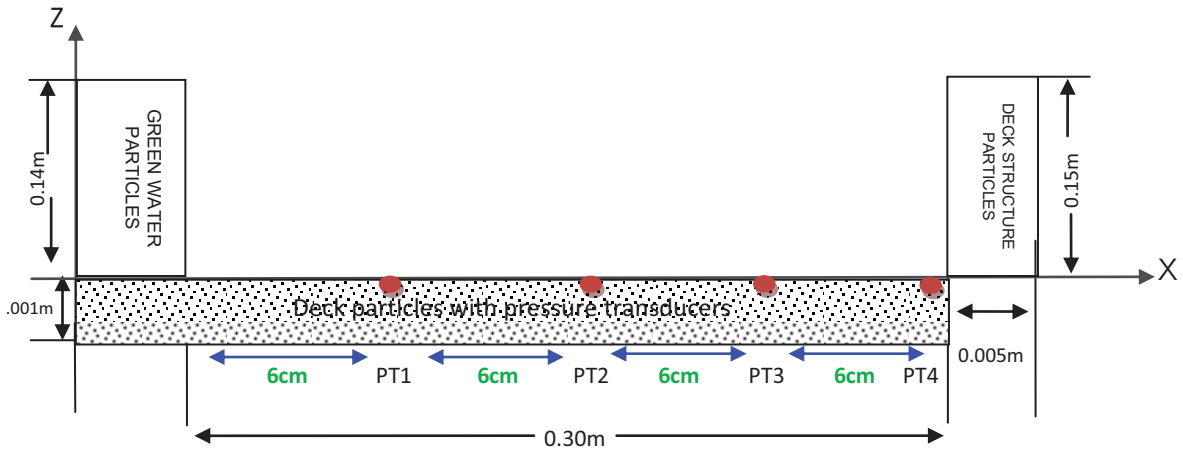

Figure 5.21b Detailed deck configuration with pressure transducers on deck and force load cell on deck structure, H_0 = 0.14m

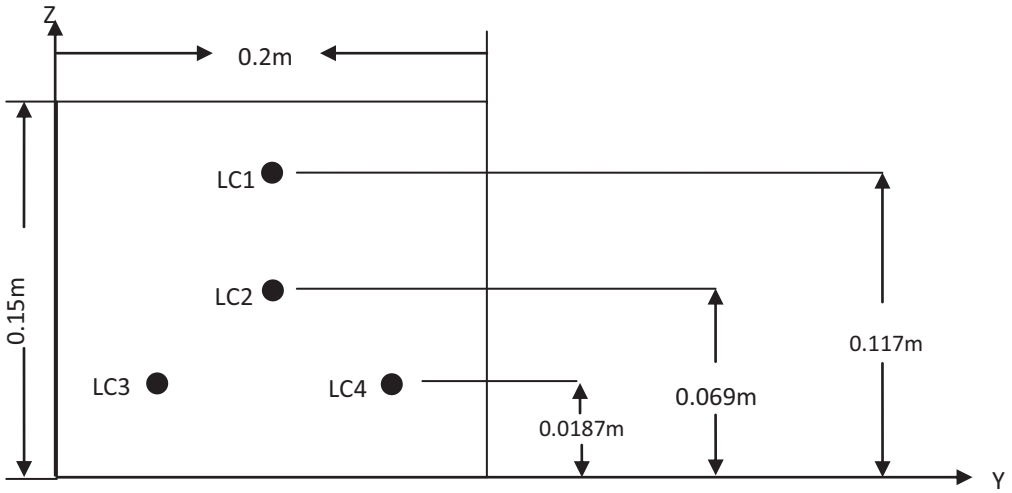

Figure 5.21c Location of Load cells on deck structure YZ plane. H_0 = 0.14m

5.6 Structure of Numerical Simulation

A computer program was written to simulate green water flow on the deck and compute the force on the deck structure due to the green water impact. The source code was written in MATLAB and was run on an Ultra 40 Sun Micro System Work Station. A flow chart which provides a summary of the simulation is shown on Figure 5.22.. The incoming body of water representing a green water wave was modeled with particles. The water front position in the simulation was set up to be the same as that measured with the vertical wave probe WP4 positioned at fore perpendicular in the experiment. The FPSO deck and deck structure were modelled with particles. For the computational domain, only particles making up the deck before the deck structure and the deck structure itself interact with the water particles making up the green water.

5.6.1 Boundary Conditions

The deck structure and the deck are treated as wall boundaries, with wall boundary conditions in the flow control domain. The sides of the rectangular deck are treated as closed wall boundaries. Water particles reaching the boundary are given a negative velocity to avoid out flow from the deck. This will allow the number of particles to remain constant within the MPS computation. The velocities of deck and dummy particles used in the computation are defined as zero to retain the no–slip boundary condition, as is normally adopted in the MPS method (Koshizuka et al, 1998), (Gotoh et al,1999) and (Shao, 2009)

The initial conditions of the Green Water event were taken from the model test results together with the semi empirical equation of Buchner (2002) which express the relationship given by equation 5.4 that the horizontal velocity of the water front over the deck was found to be proportional to the square root of the freeboard exceedance or the resulting water height at the fore perpendicular. To compute the initial velocities of the water particles, the discretized form of equation 5.4 is presented below;

$$u_i = a_U \sqrt{H_{0i}} \tag{5.8}$$

where H_{0i} = measured water particle height on deck at the fore perpendicular WP4

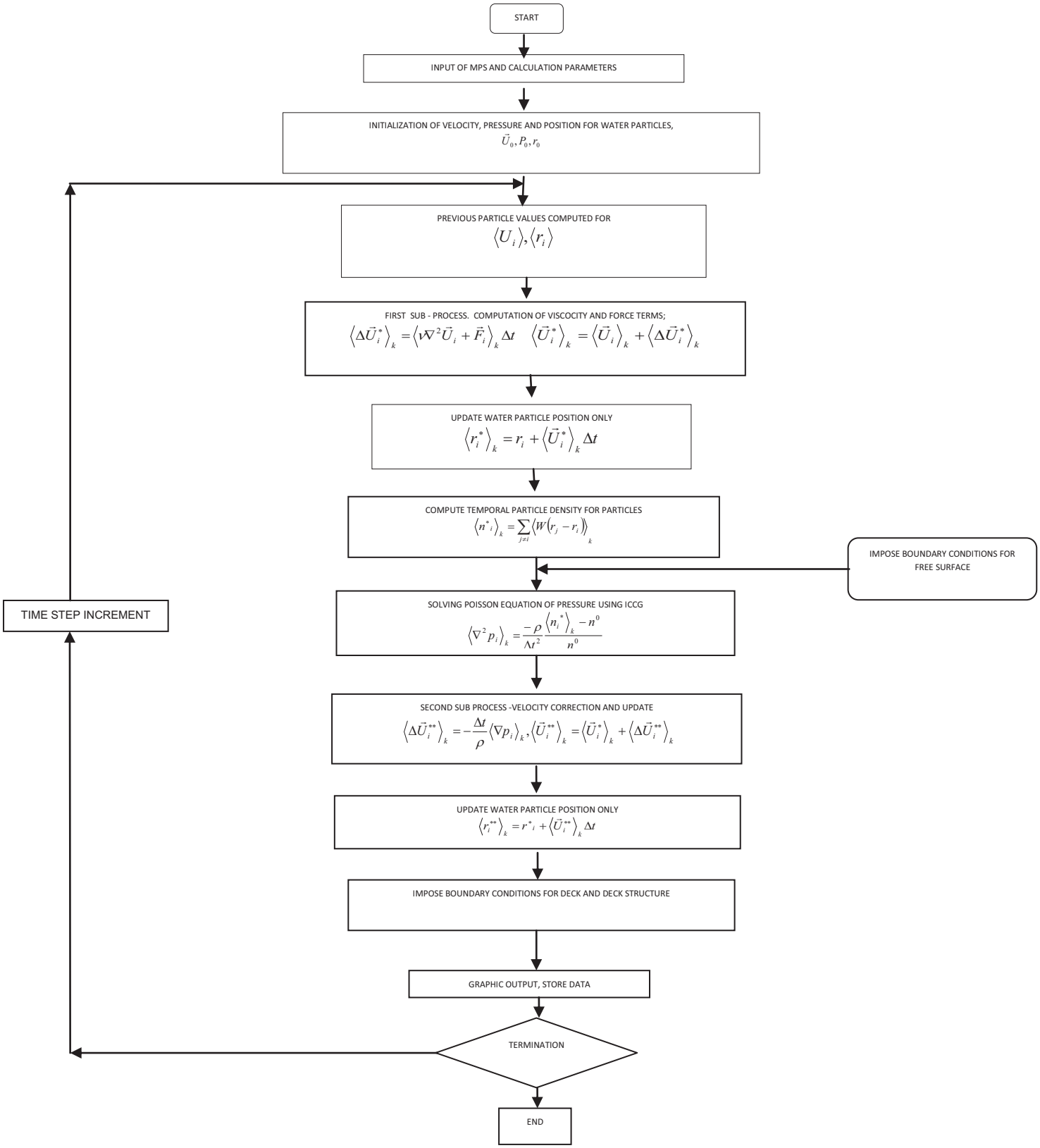

Figure 5.22 Flow chart for green water simulation

Having set the initial and boundary conditions, the water flow pattern was then simulated from the initial position until the water jet impinged on the deck structure. During the process, the deck pressure due to the interaction of the water particles with the deck were computed from the Poisson pressure equation. The water impacts on the deck structure and the pressure on the deck structure were computed and the horizontal force at each load cell was calculated by integrating the pressure over the surface area of the load cell on the deck structure. A non penetration condition was applied at the deck structure similar to the procedure taken in Section 3.6.3.3. Equation (5.9) describes the non penetration condition.

$$U_{nGWPi} = -\vec{U}_{WPi} \cdot \vec{n}_i \tag{5.9}$$

where U_{nGWPi} is the velocity of the ghost particle mirroring the water particle i, $\vec{U}_{WPi}$ is the velocity of the water particle and $\vec{n}$ correspond to the normal direction.

This approach only models the behaviour of the fluid in the vicinity of the leading front of the green water ingress. A more complete model would include the following inflow, but this is not possible with the standard MPS model and requires a mixed Eularian-Lagrangian approach.

5.6.2 Test Conditions.

The simulation statistics and the particles configuration comprises of the following.

Pressure p_0 is taken to be 0 mbar at the free surface

Nominal density used for water ρ = 1000 kg/m^3

Acceleration due to gravity g = 9.8m/s^2

Kinematic viscosity ν = 1.004 x 10^{-6}m^2/s

Threshold of particles interacting area in the kernal are as

r_e for the particle number density 2.1 D_0

r_e for the gradient model 2.1 D_0

r_e for the Laplacian model 4.1 D_0

D_0 : The distance between adjacent particles in the initial configuration.

The distance between neighbouring particles D_0 is chosen to be 0.002m.

To be always within the Courant–Friedrichs–Lewy (CFL) stability condition, the time step, Δt, was chosen as 0.0001s. The CFL condition states that for a given space discretization, a time step should not be taken bigger than some computable quantity (Courant–Friedrichs–Lewy, 1928). A computable quantity in this case is the particle velocity. For the avoidance of numerical instabilities during the evaluation of the convective term, Koshizuka et al (1998) explained that the restriction would need to be put on the time increment Δt and the term that determines the stability is C_i, the Courant number. As convective terms are responsible for the movement of particles in the MPS method, maintenance of numerical stability can be achieved by using the Courant number to restrict the time step.

To determine the Courant number, the maximum velocity $u_{\max}$ is used in order to achieve computational efficiency with equation (5.10) from Koshizuka et al (1998);

$$C_i = \frac{\Delta t.u_{\max}}{D_0} \tag{5.10}$$

The rearrangement of equation (5.10) leads to the equation for the time step Δt used in the MPS method.

$$\Delta t = \frac{D_0 C_i}{u_{\max}} \tag{5.11}$$

In this study, the numerical simulations were carried out with a Courant number of 0.2. The number was used based on the experience gained from the literature review on the MPS method.

The time step for the experiment is 0.01s and a green water event in the experiment occurs within a period of 0.6 seconds. The time step for the numerical simulation is 0.0001s for a simulation period of 0.20 seconds to capture a full Green Water occurrence. A total of 42 hours and 38 minutes was required to complete a Green Water event simulation on the work station.

The number of particles in the computation domain was set as follows:

1 For a given test, select the maximum water height recorded at the wave probe WP4. This forms the basis of the maximum number of particles to compute for the water particles
2 Deck particles are fixed, based on the dimensions Length X Breadth X Depth
3 Deck structure particles are fixed based on the deck structure dimensions.

The total number of particles computed was based on the on the incoming wave height measured in model scale and the dimensions of the rectangular deck strip and the deck structure element attached to the deck. This number is proportional to the measured wave height record at the fore perpendicular. The breakdown of the domain particles for both the regular wave test 16 and the irregular wave test 17 are presented in Table 5.7.

Ideally a higher density of particles over a larger computational domain would have been processed, but calculations were limited by computer hardware resources. However, the calculations were sufficient to address the primary objective of the study to assess the viability of the method for simulating green water events.

Table 5.7 Initial particle configuration of a Green Water event

TEST CONDITIONS	REGULAR WAVE TEST 16	IRREGULAR WAVE TEST 17
Time series	347.24s – 347.44s(0.20s)	142.06s – 142.26s(0.20s)
H_0 (max)	160mm	140mm
No. of water particles	240,000	210,000
No. of FPSO deck particles	180,000	180,000
Deck structure particles	187,500	187,500

5.7 Results of Numerical Investigation

A graph for the variation of velocity u_i with the water height on deck H_{0i} at the fore perpendicular is provided in Figure 5.23. At the start of simulation Figure 5.23 gives an insight into the initial velocities of the water front particles at the fore perpendicular. Particles at the same water height have the same velocity.

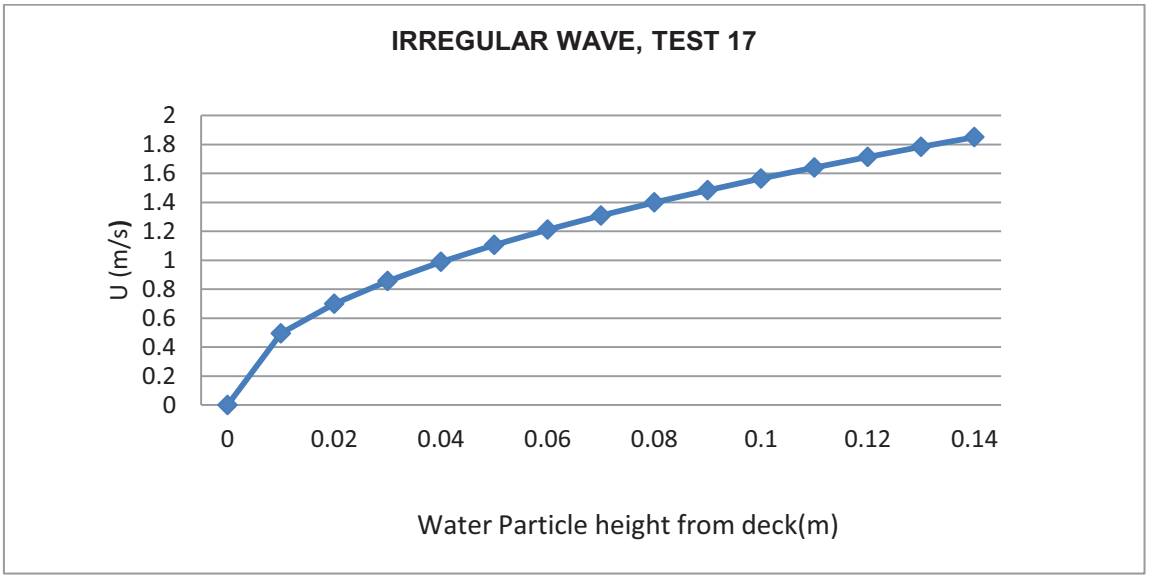

Figure 5.23 Variation of horizontal velocity u_i with water height H_{0i}

The visual observation at some time steps of the water flow on deck for the irregular wave test 17 conditions simulated with the MPS method is presented below in Figure 5.24. This type of green water event involves the following phenomena: a solid wall of water front with horizontal velocity initiates a flow process on deck resulting in an impact load on a deck structure. At impact on the structure the green water flow direction is changed with considerable water falling back on deck after hitting the structure.

The flow visualization of Green Water simulation shown in Figure 5.24a at t = 0.0s and H_0=14cm shows a wall of water with initial horizontal velocity variations as presented in Figure 5.23. Due to gravitational forces, internal pressure and the initial horizontal velocity input, the wall of water translates across the deck and evolves into an impinging water jet as shown in Figures 5.24g and 5.24h. In Figure 5.24j, the water jet impacts the deck structure at the lower end. There is some water build up

and run up at the front of the deck structure in Figures 5.24k and 5.24l. The water plunges back on deck after impact in Figure 5.24m. Flow back occurs in Figures 5.24m to 5.24n. Further observation of the figures, indicate the following

I. There is no significant transverse movement of particles. This is because the input flow is uniform across the computational domain, which itself is not wide enough to encompass the 3D nature of the deck geometry in the transverse direction.

II. The motion of the water particles are governed by the sum of the effects of gravity, internal pressure or energy which varies with depth and viscosity. These effects allow the solid wall of water to freely flow similar to a dam break problem. The introduction of the initial horizontal velocities of water particles from equation (5.8) did not allow a collapse of the solid wall of water profile as in the dam break problem but help create a jet like formation, allowing the top of the water profile to trail the leading edge of water flow created by the total forces consisting of the gravitational force and internal pressure.

III. The MPS method cannot model an outflow condition due to the fact that the total particle number has to remain constant. Therefore the boundary condition imposed at the deck boundary constrains the particles to keep inside the deck area and the water will flow back only within the deck area made represented by the rectangular strip in the computation.

IV. As mentioned earlier, the model represents the leading front of the Green Water flow, and does not include the inflow of water that would follow it.

V. The impact flow on the structure did not result in a build up and run up in front of the deck structure to the extent shown by the Green Water events in the experiments. This can be attributed to the constraints discussed above and to the fact that the ship motion is not included in the model.

Despite the above observations the sequence of events predicted by the model follow a very similar sequence to those discussed earlier and the simulation demonstrates that the MPS method can model water flow on deck, water impact on a deck structure within a short period of time and overturning or plunging flow of the water after impact with the deck structure. Results for numerical simulation of regular wave test condition 16 are presented in Appendix C.

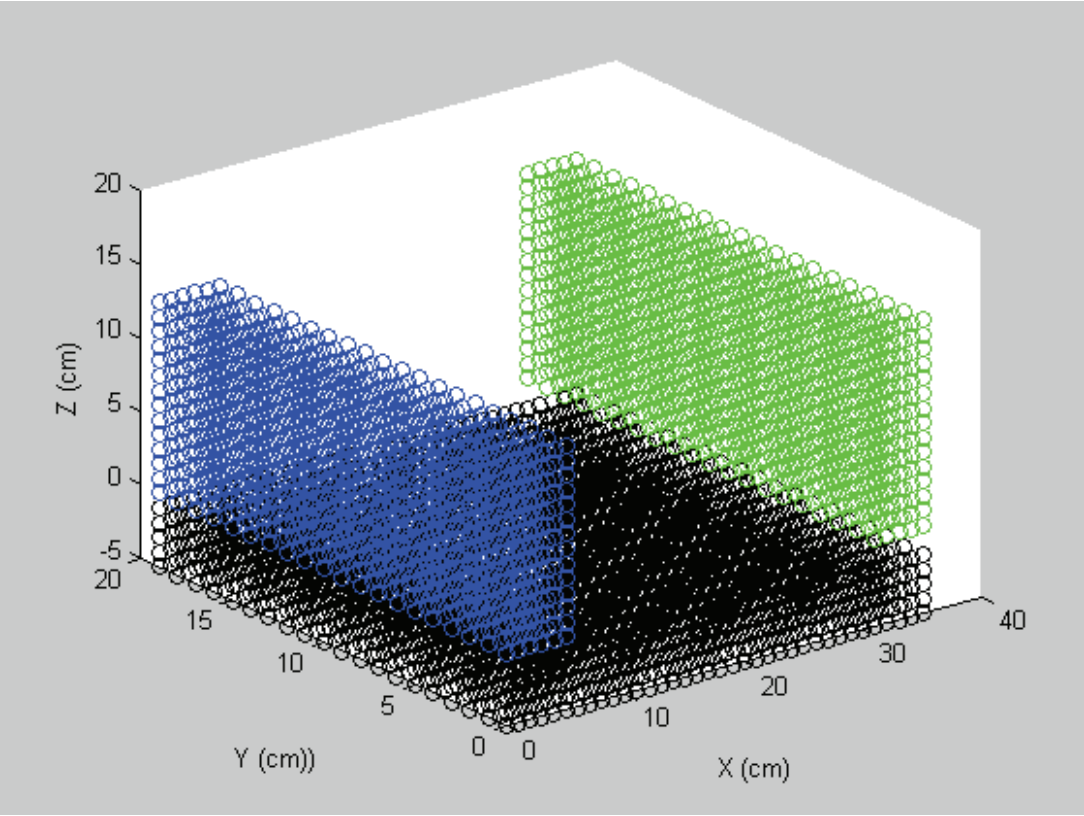

Figure 5.24a Flow visualisation of Green Water simulation at t = 0.0s, H_0 = 14cm

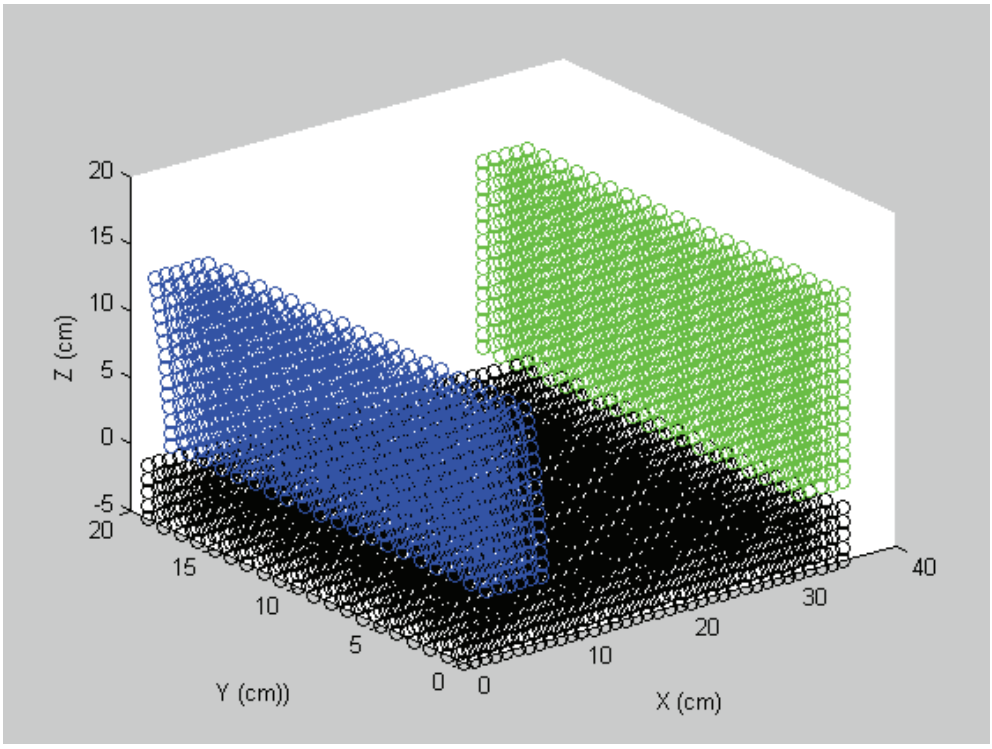

Figure 5.24b Flow visualization of Green Water simulation at t=0.015s, H_0= 14cm

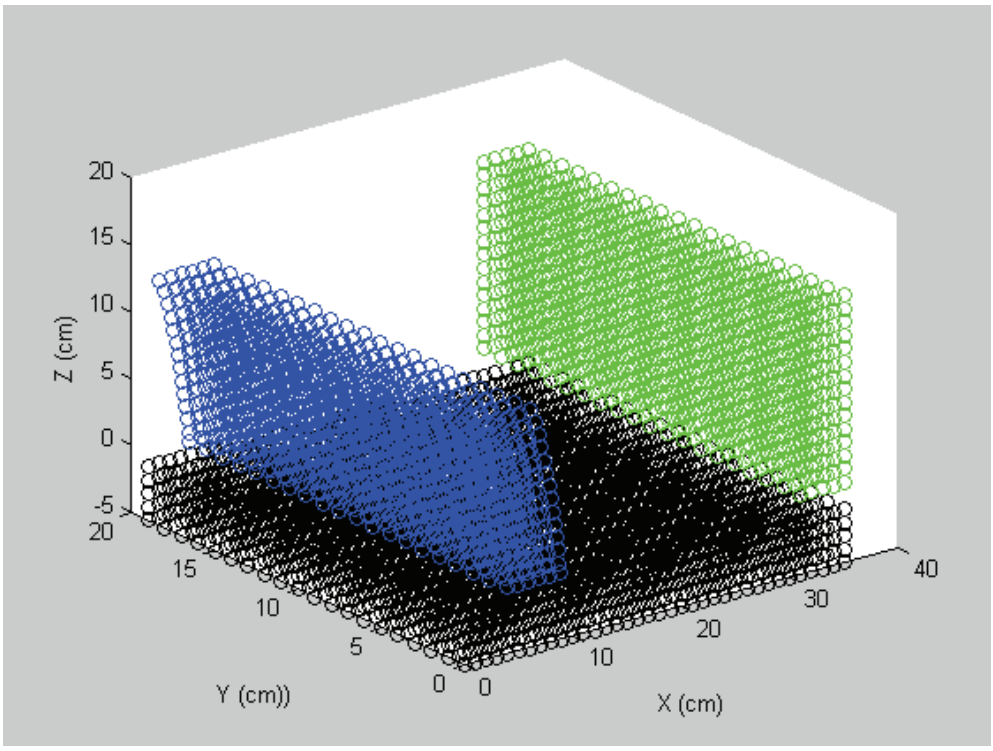

Figure 5.24c Flow visualisation of Green Water simulation at t = 0.020s, H_0 =14cm

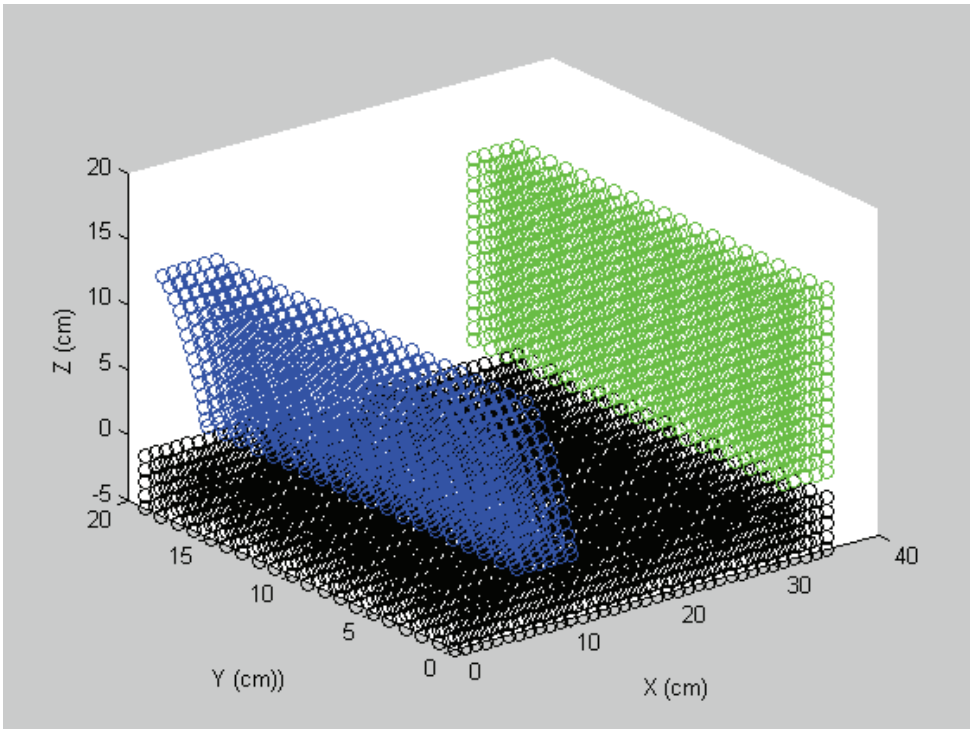

Figure 5.24d Flow visualisation of Green Water simulation at t = 0.025s, H_0 = 14cm

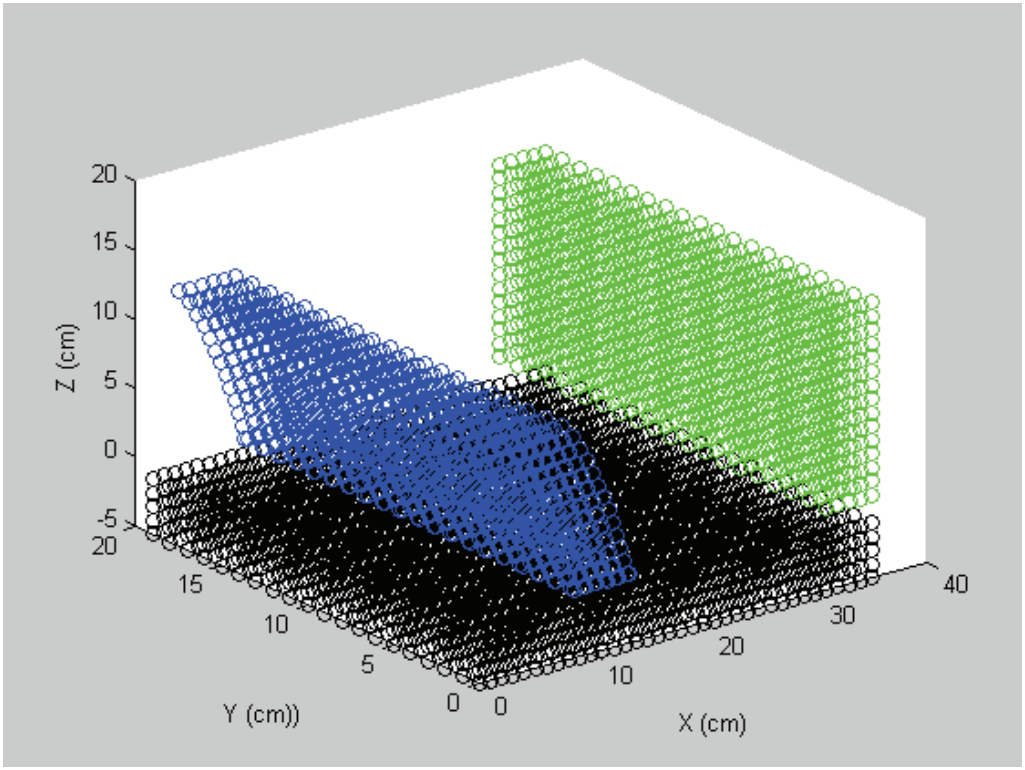

Figure 5.24e Flow visualisation of Green Water simulation at t = 0.030s, H_0 = 14cm

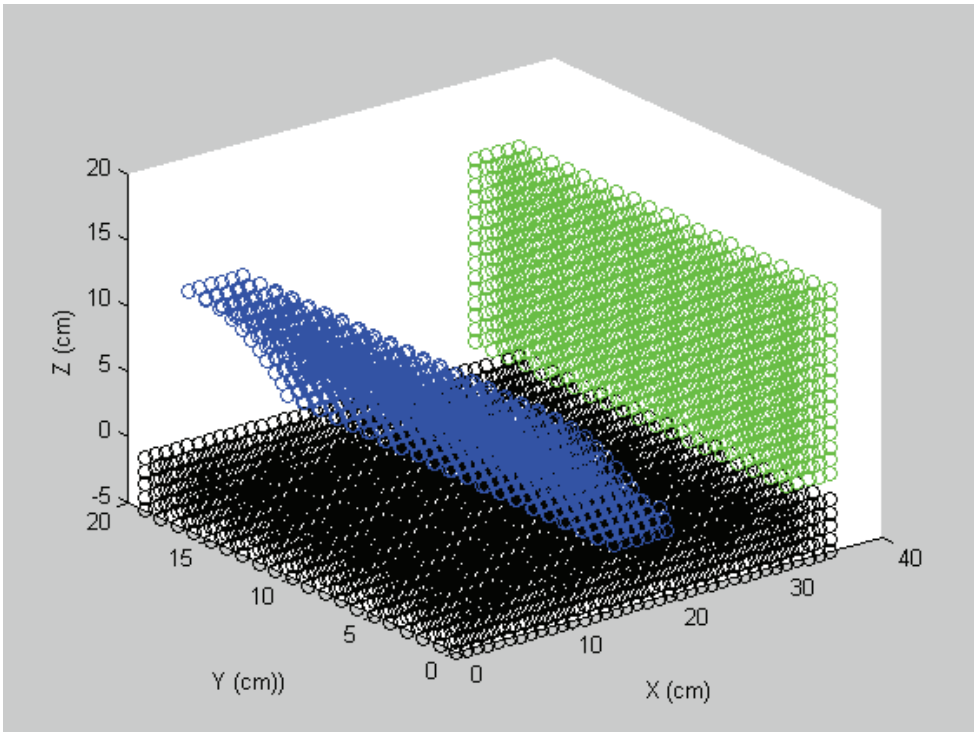

Figure 5.24f Flow visualisation of Green Water simulation at t = 0.040s, H_0 = 14cm

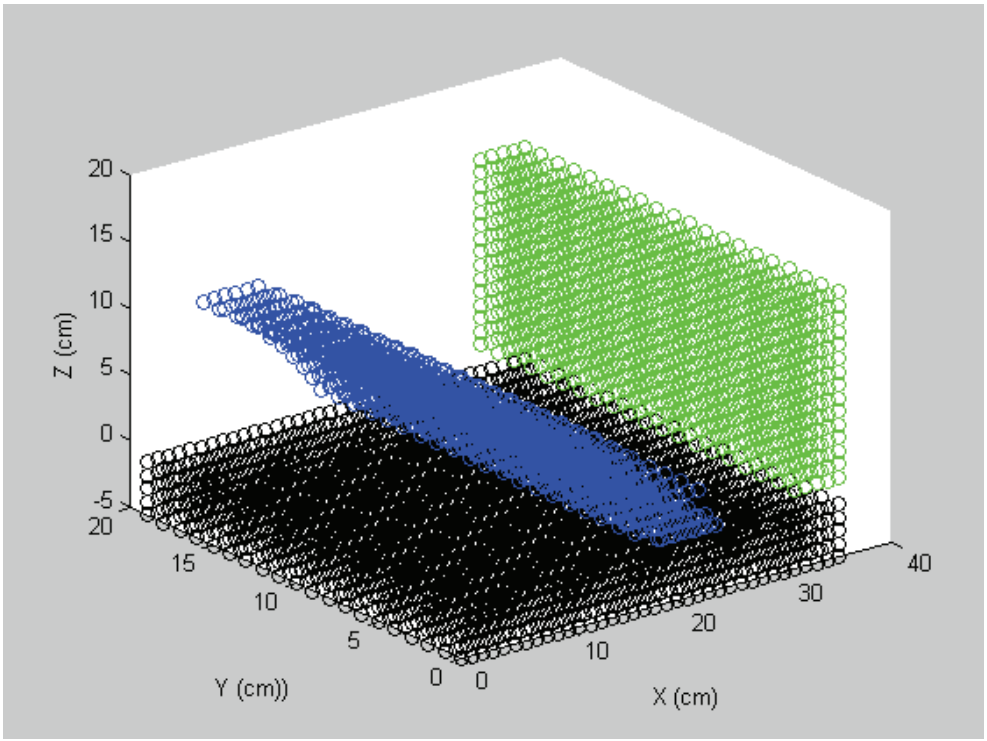

Figure 5.24g Flow visualisation of Green Water simulation at t = 0.045s, H_0 = 14cm

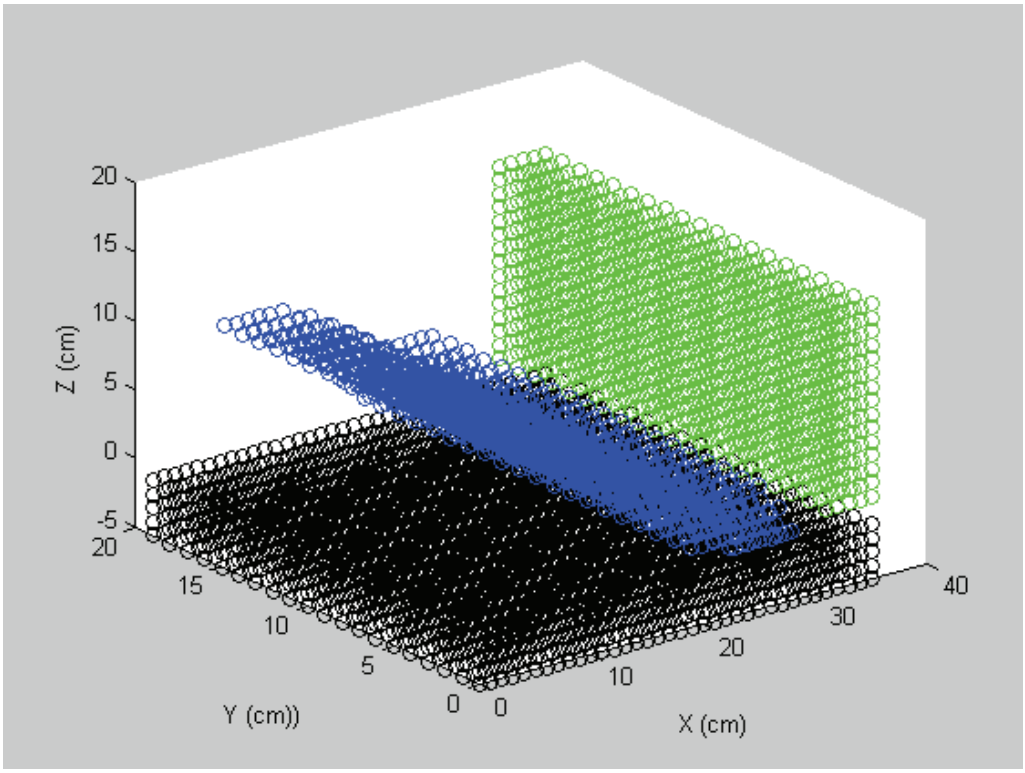

Figure 5.24h Flow visualisation of Green Water simulation at t = 0.050s, H_0 = 14cm

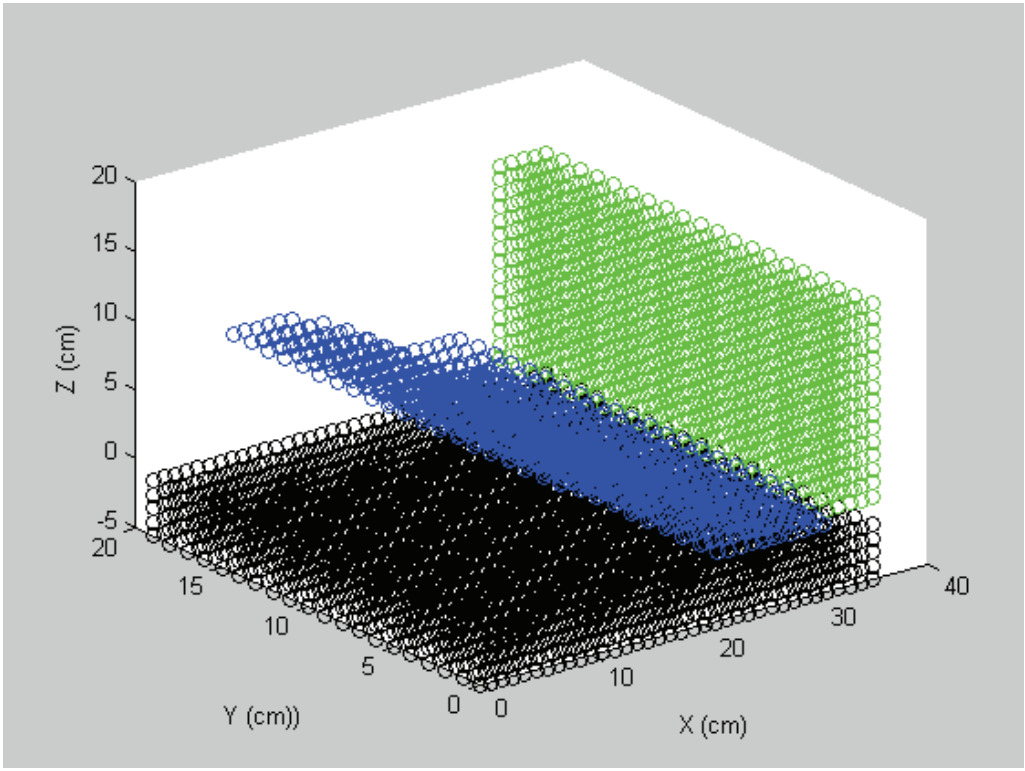

Figure 5.24i Flow visualisation of Green Water simulation at t = 0.060s, H_0 = 14cm

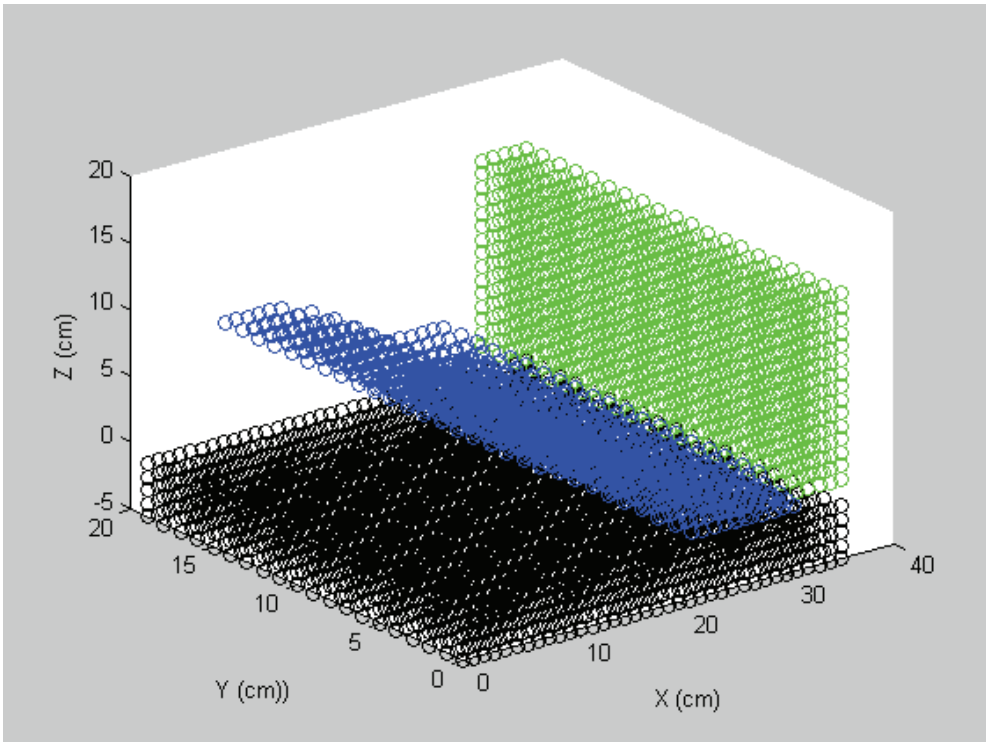

Figure 5.24j Flow visualisation of Green Water simulation at t = 0.07s, H_0 = 14cm

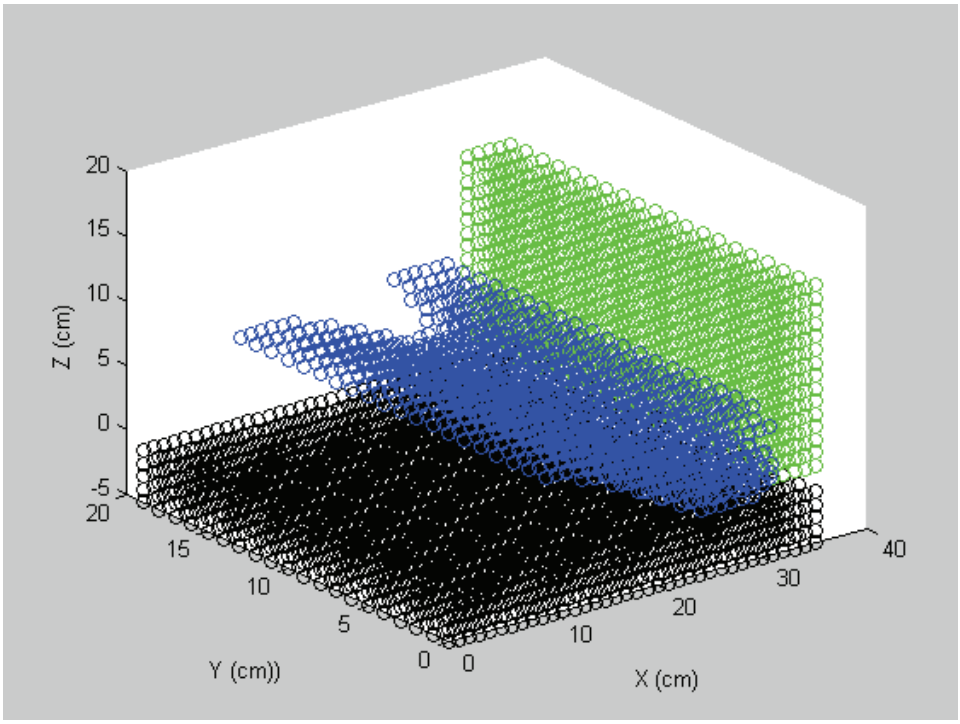

Figure 5.24k Flow visualisation of Green Water simulation at t = 0.10s, H_0 = 14cm

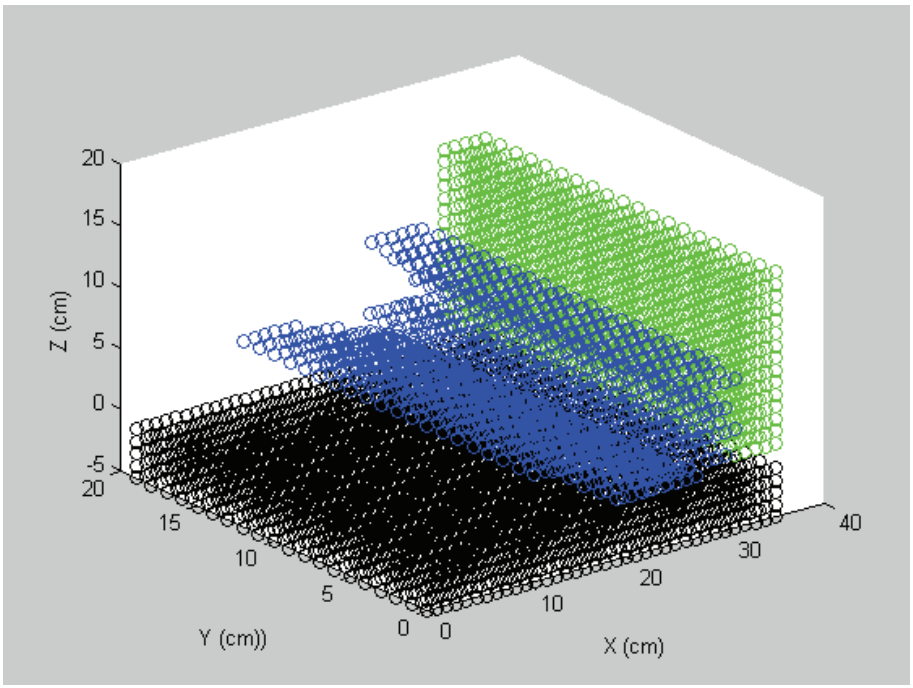

Figure 5.24l Flow visualisation of Green Water simulation at t = 0.12s, H_0 = 14cm

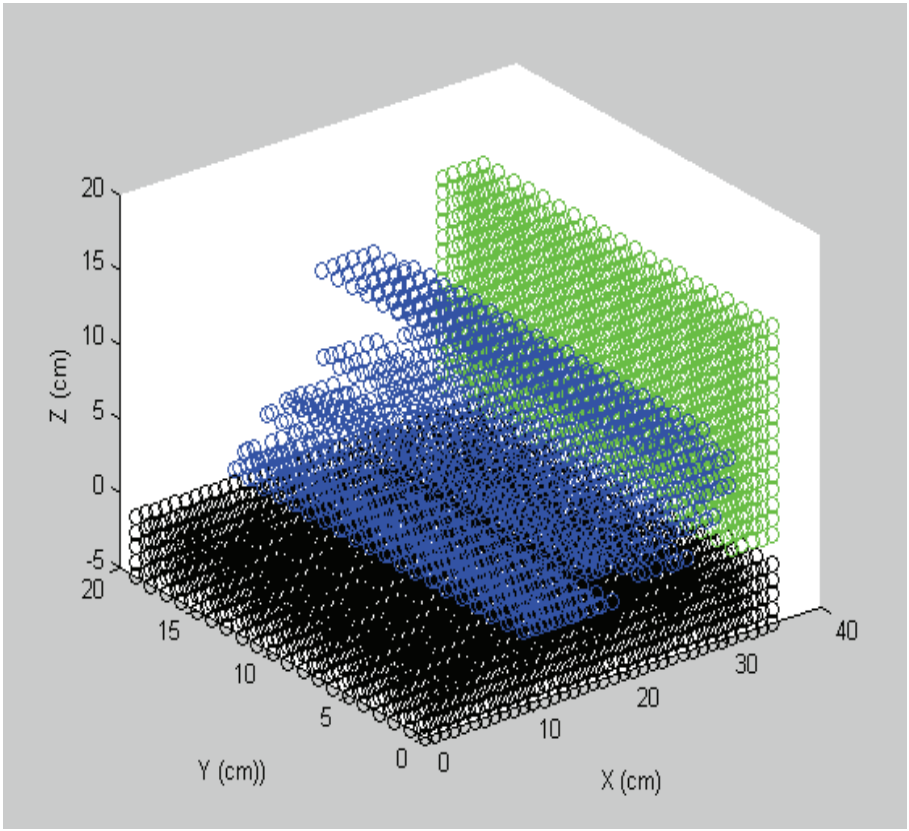

Figure 5.24m Flow visualisation of Green Water simulation at t = 0.15s, H_0 = 14cm

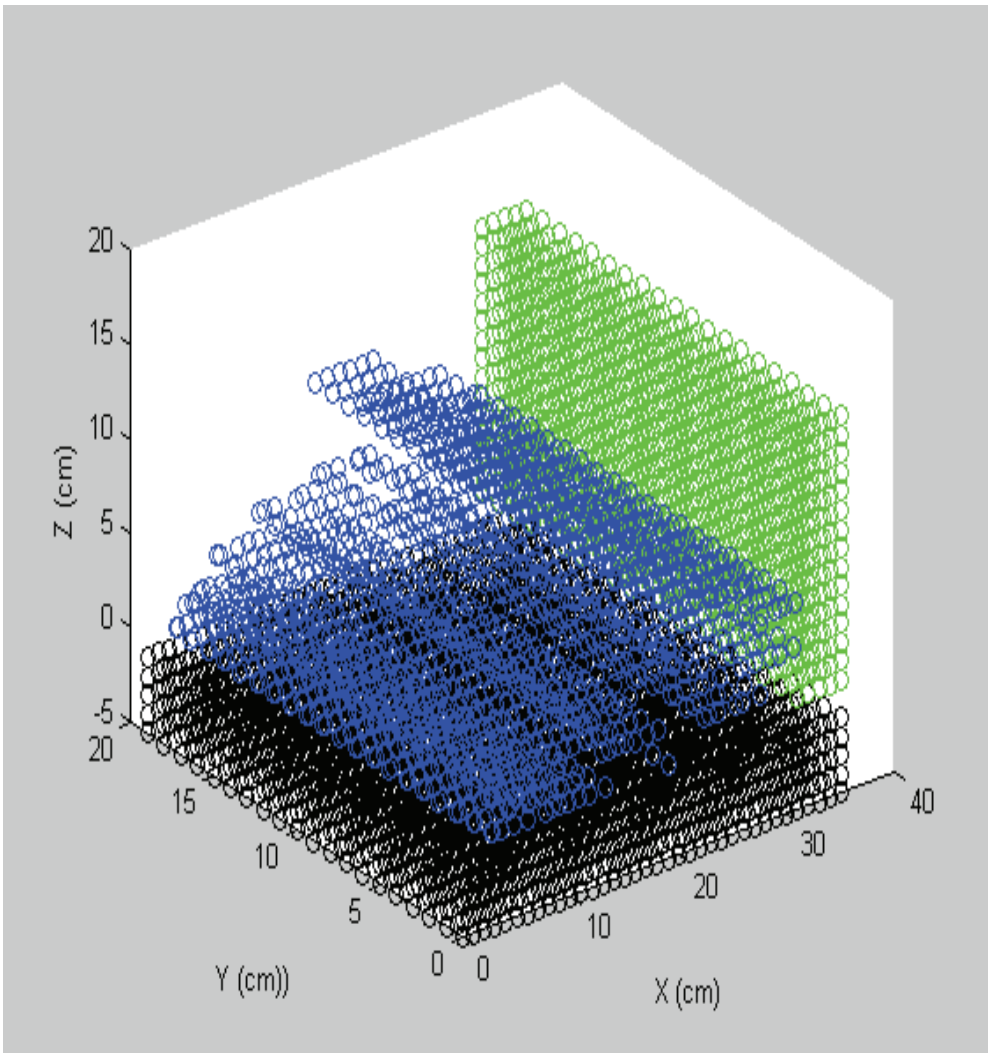

Figure 5.24n Flow visualisation of Green Water simulation at t = 0.20s, H_0 = 14cm

5.7.1 Water Height on Deck.

The numerical computation and experimental measurements are compared for the water levels at the wave probes WP4, WP5, WP9 and WP10 for the given time series in Figure 5.6, Section 5.2 of this chapter.

Figure 5.25 shows the measured and computed water levels at WP4. The water particles travel away from the wave probe WP4 in full form when compared to the gradual variation in height measurements of the experimental records. This is due to the particle configuration which may be different from the profile of the water build up in the experiment. However, the time traces are similar in character which shows a drop in height as the water travels away from the probe. At the later stages, the numerical computations indicate that there is a secondary measurement in water height, which can be attributed to the reflected water flowing back from the deck structure.

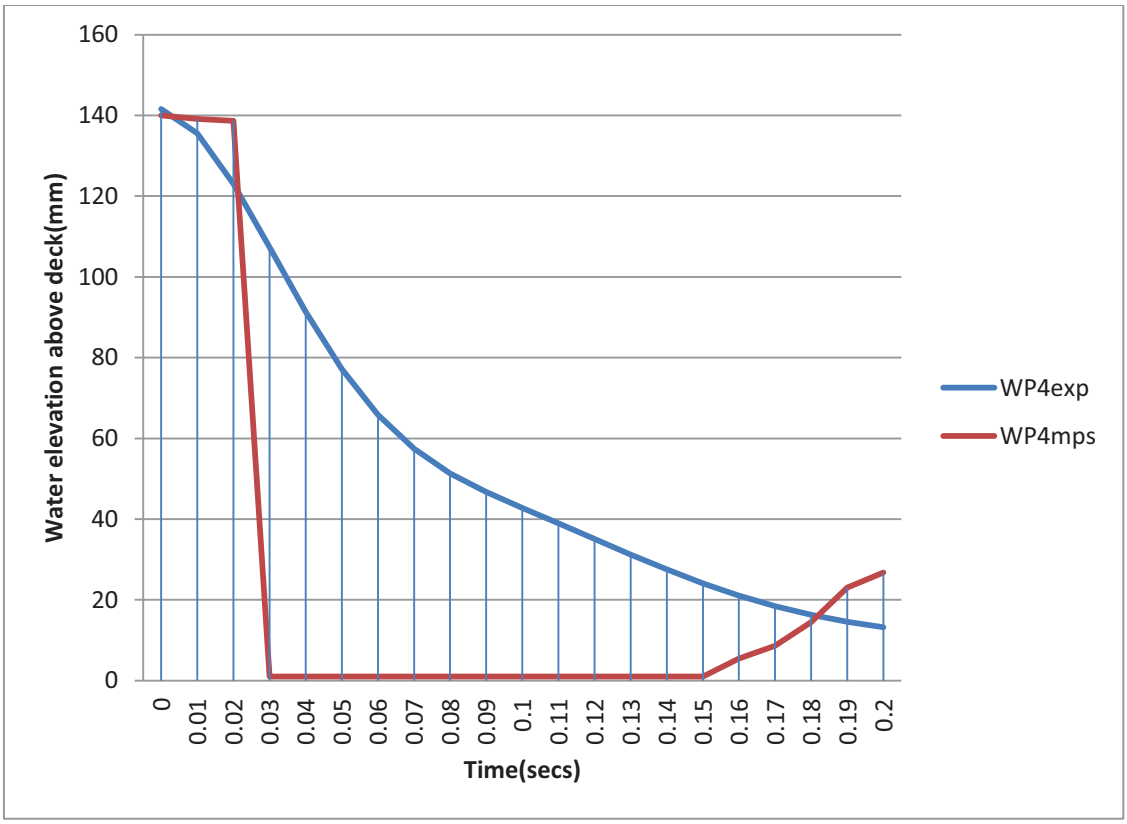

Figure 5.25 Measured and Computed water height on deck at WP4, H_0=140mm

The time traces and water levels are shown in Figure 5.26 for the wave probe WP5. Behavioural trends of the time traces of the numerical and experimental measurements are in good agreement, which shows an initial water level increase as the water front passes over the probe and then gradually decreases. It is also an indication that the water particle configuration is becoming more in the form of the experimental water profile. Secondary measurements can be observed for both the numerical and experimental results as the water level does not drop off to zero as in Figure 5.25 but remains due to flow back from the deck structure.

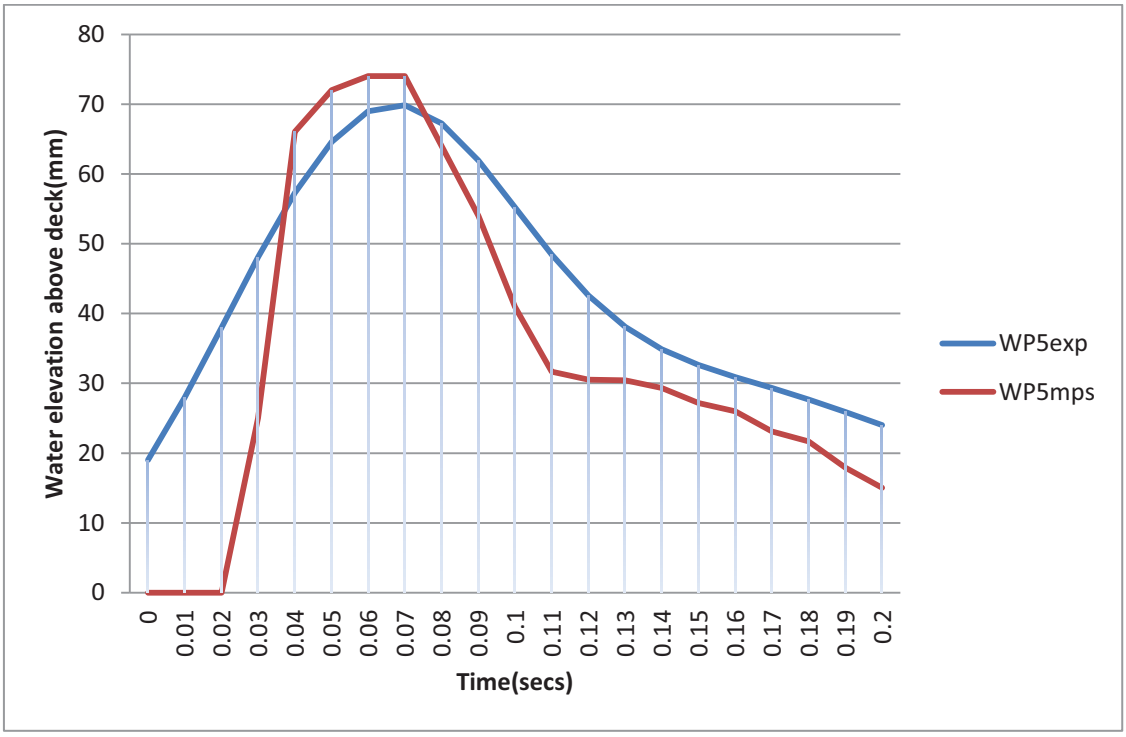

Figure 5.26 Measured and Computed water height on deck at WP5, H_0=140mm

A considerable difference in water levels can be observed in Figure 5.27 at the wave probe WP9. The drop in water height for the experimental results at the wave probe WP9 can be attributed to some water already leaving the deck due to the FPSO motion. In the numerical simulation, water outflow was not allowed due to the MPS method limitations. However, the results show close similarities in their time trace characteristics and the recording of secondary measurements due to flow back

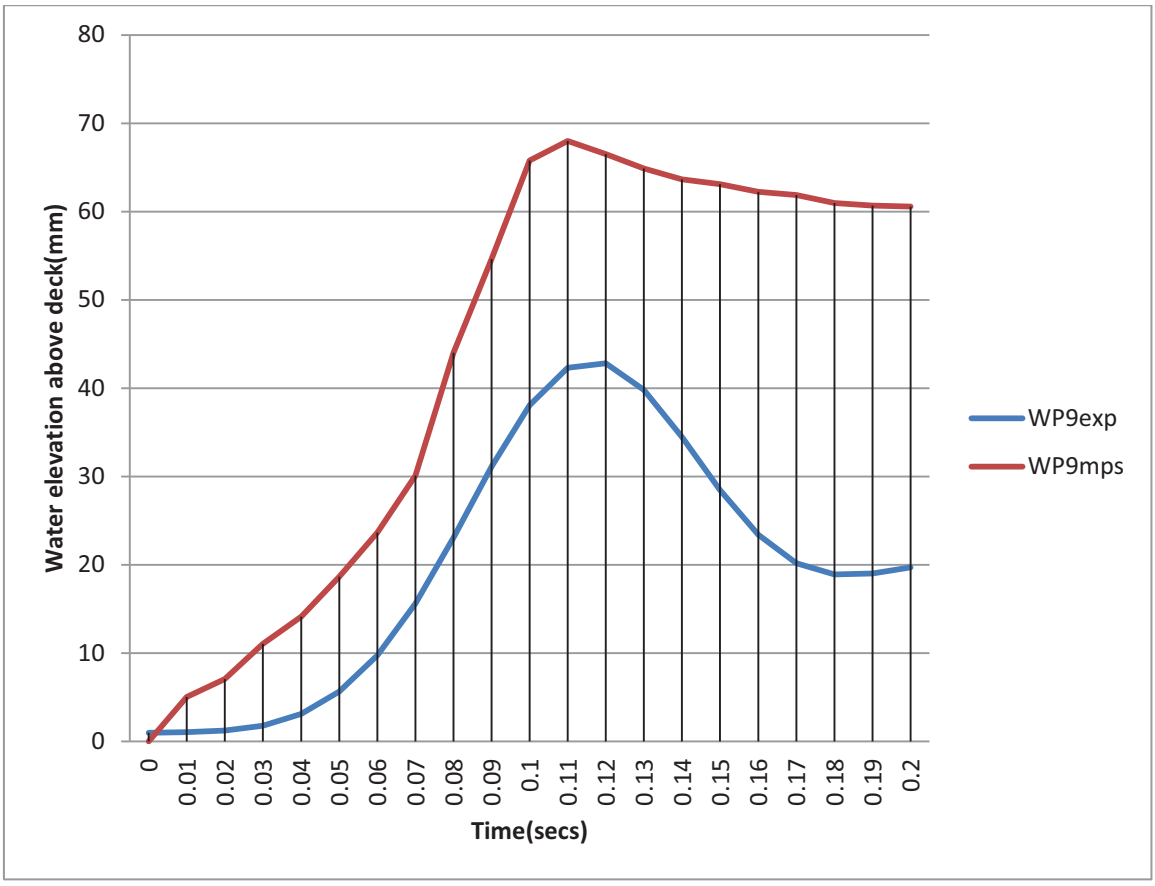

Figure 5.27 Measured and Computed water height on deck at WP9, H_0=140mm

In Figure 5.28, the comparison of the water height measurements for both experiment and numerical computation is presented. At the later stage in the green water event, the experimental water levels show higher measurements. This is due to a large run up of water in front of the deck structure caused by the FPSO motion. In the numerical simulation deck motion was not included in the computational process.

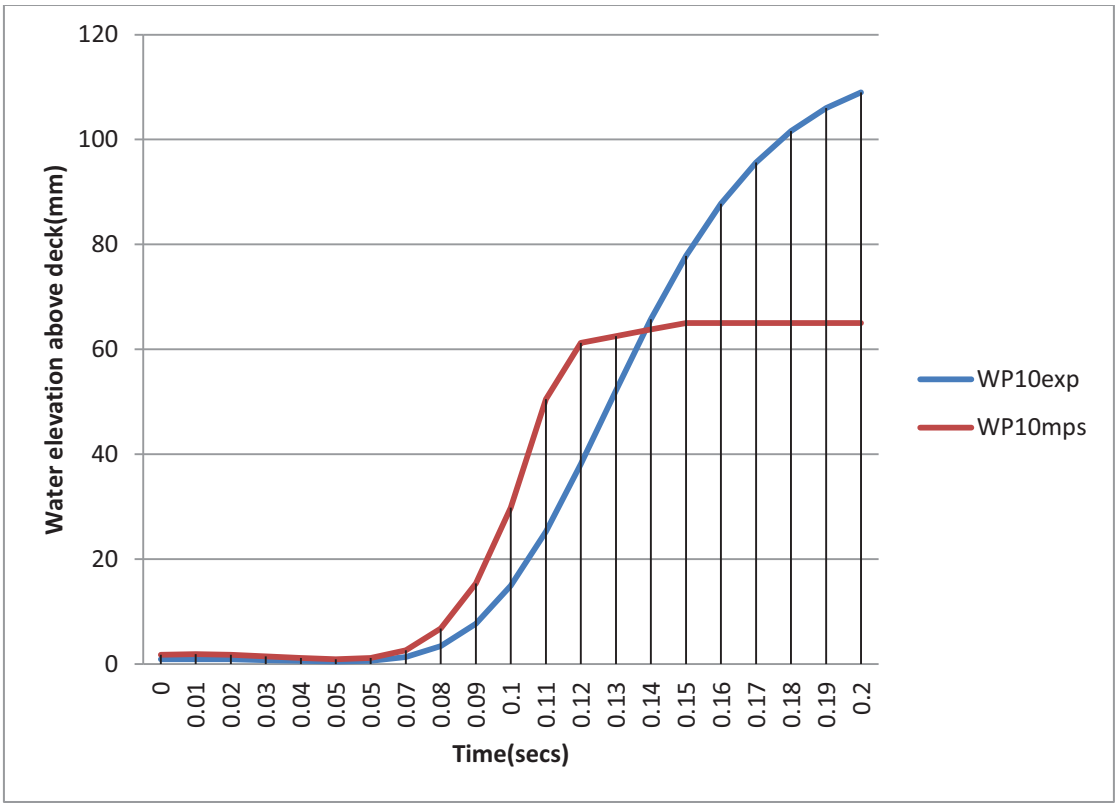

Figure 5.28 Measured and Computed water height on deck at WP10, H_0=140mm

5.7.2 Pressure due to Water on Deck

The pressure gradient due to the interaction of the water particles and the deck particles using the Poisson Pressure equation formed the basis for the pressure computation. This method enables the presentation of a pressure distribution where the water velocity component is chosen as the dominant factor in the simulation process for the green water flow simulation. Consequently, the initial horizontal velocity component of the water on deck was computed using the empirical expression, stated in equation (5.8). The pressure transducers were taken as particles at fixed points on the deck and pressure computations were recorded at the particles taking into consideration the positions relative to the experimental pressure transducers. The average pressure of the particles making up a pressure transducer or load cell is taken as the computed pressure measurement. The locations of the pressure probes were illustrated in Figure 5.21b.

There have been concerns by Shibata and Koshizuka (2007), Khayyer and Gotoh (2009) and Shibata et al (2009) with regards to the accuracy of the original MPS method to predict a quantity like the maximum impact pressure. Shibata and Koshizuka (2007) and Shibata et al (2009) attributed the problem to low spatial resolution and deck wetness. In this study, pressure fluctuations were not experienced in the simulations as a result of the set up and application of the original MPS method to the green water problem. Numerical stability and pressure prediction accuracy were maintained by the following;

- Simulation was carried out in a localized portion of the FPSO deck with constraints on inflow and outflow.
- Initial particle spacing was made small at 0.002m. In the study by Shibata and Koshizua (2007) particle spacing was 0.01m.
- The time period for the simulation of the green water problem was of short duration (0.2s).

Examination of the pressure distribution profile in Figure 5.29 shows a gradual variation for the experimental measurements compared to the rapid change of the numerical results at the pressure transducer PT1. This can be attributed to the different profiles at the beginning of the green water event. The water build up configuration for the simulation at the fore perpendicular is represented with a rectangular block of water particles. The pressure at the transducer PT1 at this stage of the numerical process indicates a sudden drop after the water particles passes over it. The time traces show similar trends for both the experiment measurements and the numerical data.

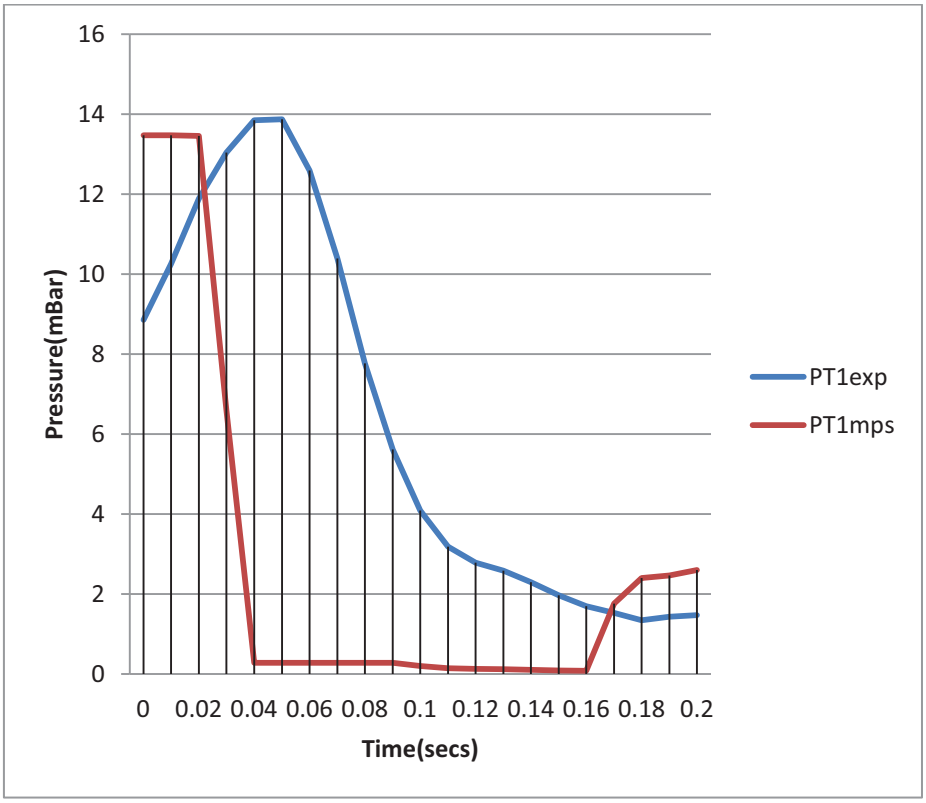

Figure 5.29 Measured and Computed pressure on deck at PT1, H_0=140mm

At the pressure transducer PT2, in Figure 5.30, there are both an initial measured recording due to the water front passing over the pressure transducer PT2 and a secondary pressure recording for both experiment and numerical computation, which is caused by water flow back on deck. Further observations reveal that at PT2, the experimental measurements increase while the numerical results decrease. This could be the effect of the deck motions which can cause rapid change in water velocity and pressure.

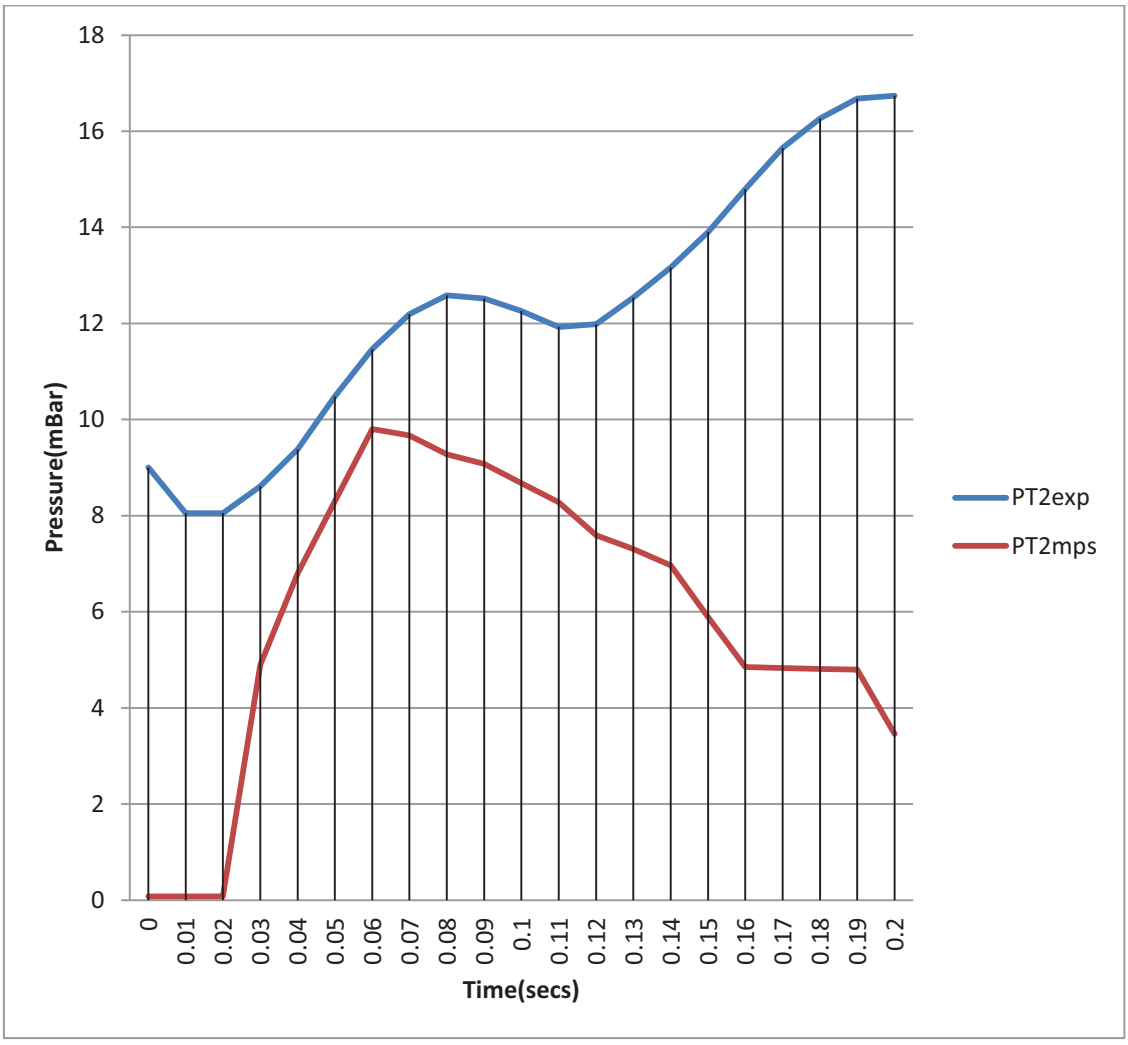

Figure 5.30 Measured and Computed pressure on deck at PT2, H_0=140mm

The time traces at the pressure transducer PT3 in Figure 5.31 show similar trends for both experiment and numerical results. There is a remarkable increase in the pressure results of the experiment, which are significantly higher than the pressure results of the numerical computation. This as in Figure 5.30 can be attributed to the FPSO motion. Also water impact has taken place at the deck structure resulting in water reflection, build up and flow back at a high pressure in the experiment. Due to the FPSO motion it is expected that the water impact at the structure will be more severe in the experiment. However, due to water flow back after impact, both numerical and experimental results show an increase of pressure at pressure transducer PT3.

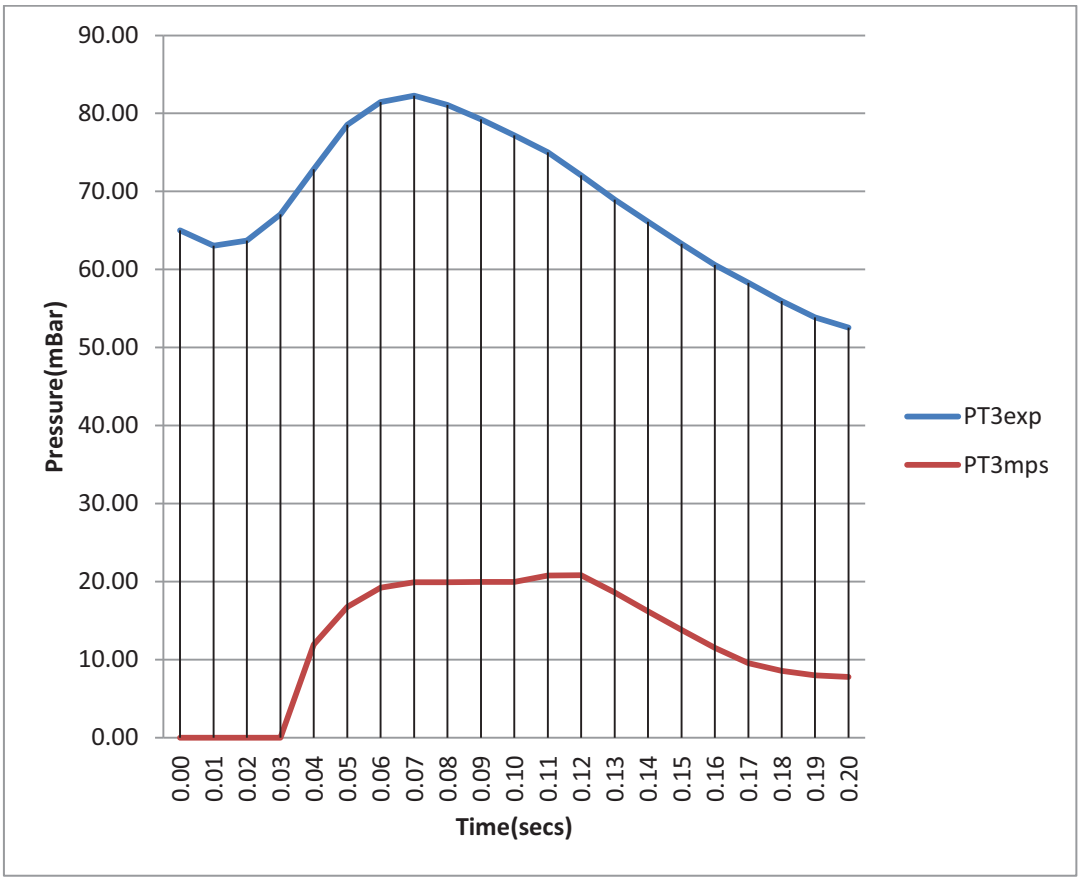

Figure 5.31 Measured and Computed pressure on deck at PT3, H_0=140mm

At PT4 in Figure 5.32 there is a drop in pressure in the experimental results when compared to the results at pressure transducer PT3. As a result of water foaming and creating bubbles after impact, the pressure transducer PT4 may record lower pressure measurements. This cannot be said for the numerical computation as foaming is not accurately modelled, although there is the possibility of the disintegration of the free surface. In the numerical simulation, the pressure profile shows a steady increase. The increase in pressure for both experiment and numerical simulation is as a result of water reflection back on deck at the pressure transducer PT4.

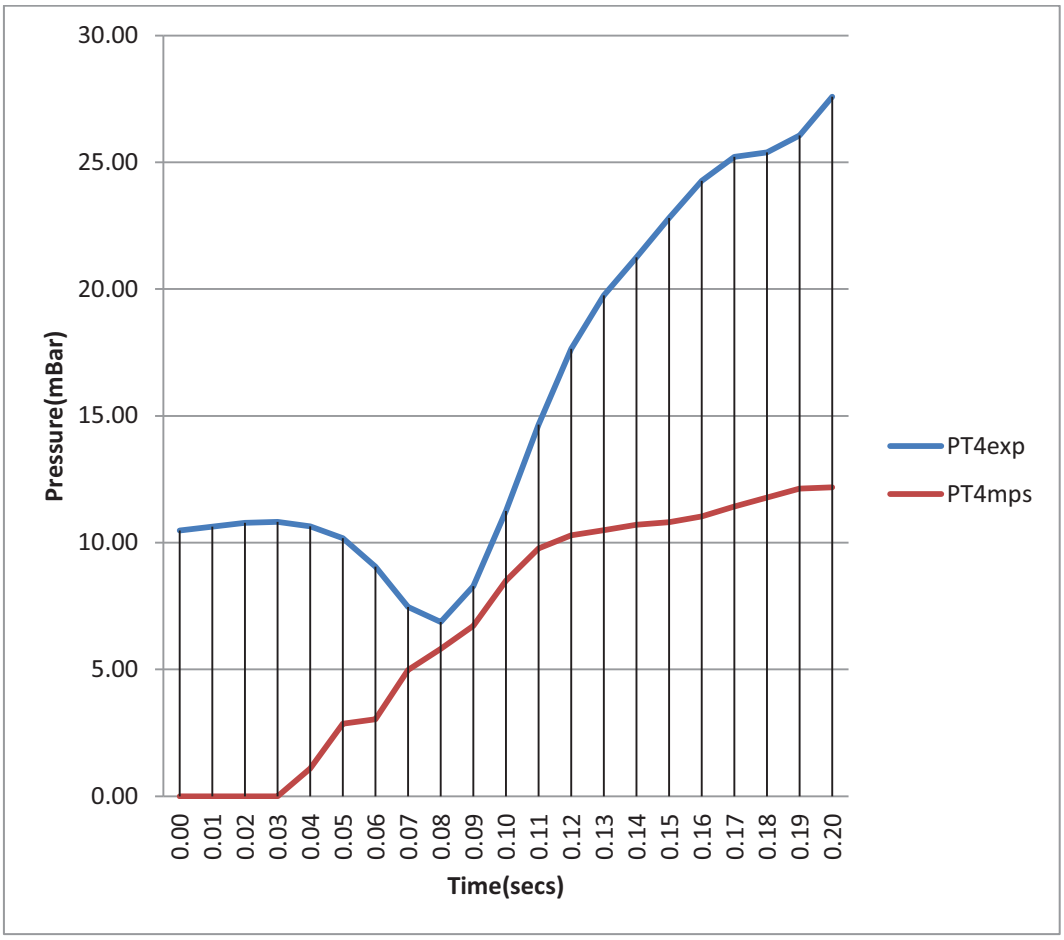

Figure 5.32 Measured and Computed pressure on deck at PT4, H_0=140mm

5.7.3 Force due to Water impact on deck structure

In Section 5.4, it was deduced that the force on the deck structure develops continuously over three stages; an impact stage, a quasi–static load stage and a plunging water stage. The flow process visualized in Figure 5.24 shows these processes as they occur in the numerical simulation using the MPS method.

In the present research, the force on the superstructure is given by;

$$\vec{F}(x,y,z) = \int p(x,y,z).\vec{n}ds \tag{5.11}$$

where,

$p(x,y,z) =$ Pressure obtained from MPS Poisson Pressure Equation.

$n =$ Exterior unit normal to deck structure

$s =$ Surface area of load cell.

Figures 5.33 and 5.34 show the water impact measurements for the experiment and numerical simulation. The graphs show similar characteristics and the impact loads are higher for the measurements in the experiment, which is due to the FPSO motion. In the numerical simulation, the force calculations at the load cells LC3 and LC4 are the same, whereas for the experiment, the FPSO motion contributed to the slight variations in values. Force calculations at the load cells LC1 and LC2 could not be made because the water run up at impact in the numerical simulation did not reach the load cells LC1 and LC2 at these positions for this Green Water event. In the experiment, the run up of water have reached the load cells at LC1 and LC2 in different time series. The graphs have already been presented in Figures 5.14 to 5.18 in this chapter.

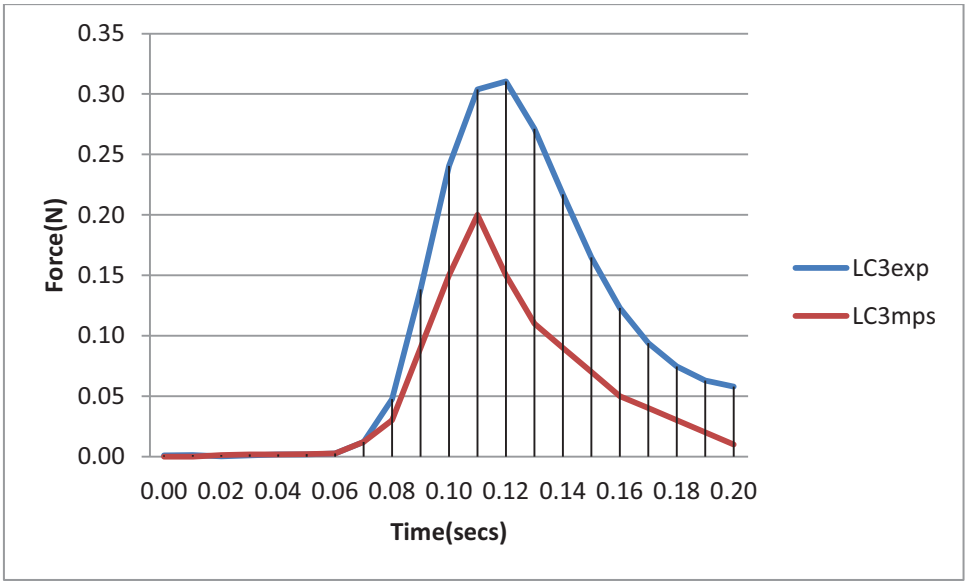

Figure 5.33 Measured and Computed impact load on structure at LC3, H_0=140mm

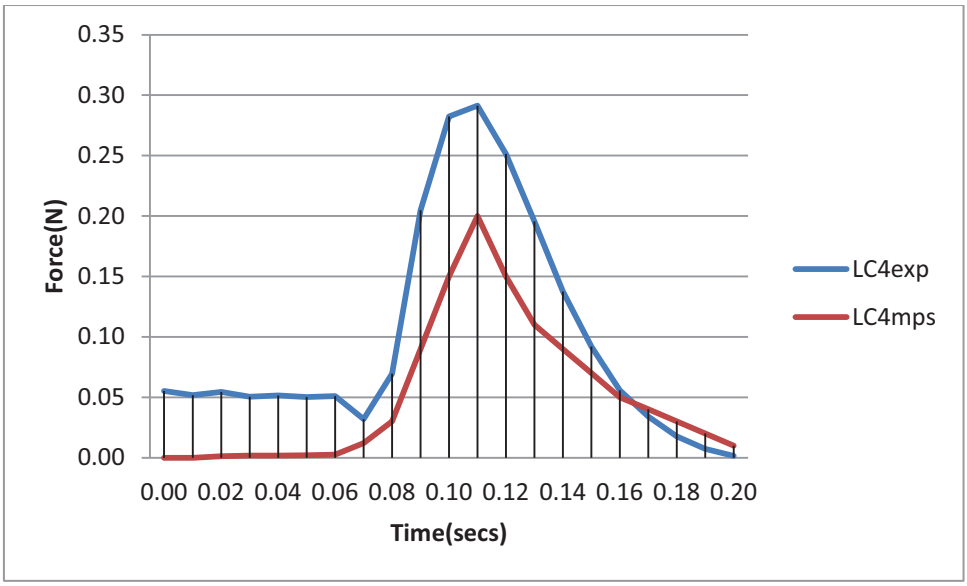

Figure 5.34 Measured and Computed impact load on structure at LC4, H_0=140mm

5.8 Conclusion

The primary aim of developing a numerical prediction method with the capability for increasing the understanding the wave impact and green water physics was achieved to a large extent. The simulation process carried out using the MPS method demonstrated that the method is capable of predicting a water flow process on deck and a short duration water impact on a structure very similar to those observed in experiments. There are a number of discrepancies between the experimental results and the numerical results, but these should be viewed in the context of the constraints imposed by the MPS method itself, and the computational resources available to the project. The latter simply imposed a limitation to the number of particles that could be employed by the model. This lead to a model that was formulated as a 3D model (to demonstrate that it was viable) but whose computational domain was restricted to a finite width strip along the centreline of the foredeck and deck structure.

The former had a number of consequences that could be summarised as follows:

- The classical MPS method is not capable of representing inflow and outflow, the number of particles remaining constant. This leads to a certain difficulty in representing green water events. The present model follows on from the 'dam breaking' approach to representing the flow. In this model the initial body of water both collapses and moves forward with a velocity initiated by behaviour observed experimentally. The model represents the leading front of the collapsing mass of water but is unable to account for the following flow that would be provided by the overtopping wave. Including this part of the flow requires a mixed Eularian/Lagrangian model which was beyond the scope of the present project.
- Restricting the flow to a strip along the middle of the deck with initial conditions determined from experimental measurements along the centre line of the deck constrains the flow. The input flow to the model is uniform in the transverse direction and so is in effect 2D. The computational mesh does not include the

curvature of the deck plan so there is nothing to introduce 3D influences into the flow, which are present in the experimental data.

- The model developed did not include the motions of the deck and in the comparing the experimental and numerical results, this effect of FPSO motion, taken together with the factors above, was seen to be quite significant.

Despite the foregoing, the results produced by the MPS model, even though there are obvious discrepancies, show some qualitative agreement with the experimental measurements. On the basis of the calculations carried out, it could be concluded that the MPS particles method can be a useful method for free surface problems in offshore engineering as has been shown with this demonstration of green water simulation. The method has the advantages of being able to handle complex boundary conditions and being easily setup initially without requiring grid generation. However, the MPS method is a time consuming numerical method and high performance computation resources are required for a fully integrated hydrodynamic problem such as green water simulation. This proviso is even more stringent in problems rigorously coupling the computation of the green water effects with vessel motion.

CHAPTER 6

CONCLUSIONS AND RECOMMENDATIONS FOR FUTURE WORK

6.1 Introduction

The aim of this study has been to further the understanding of Green Water phenomena as they relate to the environmental loading of an FPSO and to investigate methods of modelling them with a view to developing a numerical model that might also be applied to other forms of extreme environmental loading. To this end an experimental research programme was undertaken that evaluated the Green Water phenomena on a moored FPSO, and a methodology based on a numerical prediction method for the simulation and analysis of wave structure interactions was developed. The experimental research was carried out in the Marine Hydrodynamics laboratory at Newcastle University, on a 1: 127 scale model of a geosym of an FPSO hull also tested at MARINTEK Ocean Wave Basin at a scale of 1:55 (see Han 2003). In both sets of experiments the models were tested in both regular and irregular sea states (generated with JONSWAP spectra) and their motion responses were measured. In addition the profiles of the Green Water on deck and the consequent loading on the deck and deck structure were also measured. Results from these experiments, including the spectral energy density from the irregular waves and also the heave and pitch RAOs of the FPSO in head waves have been presented in Chapters 4. In Chapter 5 further investigations were performed to understand the physics of the green water phenomena.

Numerical Modelling methods currently applied to problems in the ocean environment were reviewed in earlier sections of this study. These methods are made distinct by the two approaches governing numerical methods for performing fluid flow simulation and analysis, namely the Eulerian concept and the Lagrangian concept. In this study the approaches associated with the Lagrangian concept were followed by applying a particle method called the Moving Particle Semi Implicit (MPS) method to simulate and analyse wave structure interactions.

6.2 Conclusions

A number of conclusions may be drawn from the study both with respect to the experimental work and also the numerical modelling.

6.2.1 The Experimental Programme

Although the experiments carried out in this study were on a relatively small scale , a comparison with the research work by Han(2003) on a geosym of scale 1:55 in similar environmental conditions showed that the results obtained for the heave and pitch RAO for the two cases were in good agreement. This study demonstrated that with respect to ship motions in the head wave conditions tested, useful experiments can be undertaken in small scale wave tank model testing and scale effects appear to play little part in the results.

6.2.2 Green Water Effects

The green water phenomena observed with the small scale model also showed very similar characteristics to those observed by Buchner (2002) and Han (2003). The events that occurred in the Green Water process that were studied and evaluated followed the established sequence of events namely;

- The freeboard level is exceeded by relative wave motions
- There is considerable water flow on deck with high velocity.
- The flow is in the form of an impinging jet impacting on the deck structure

The experimental study showed that the Green Water impact loading event is broken down into three stages: the impact stage, which occurs over a period of short duration and strikes the lower part of the deck structure with a high pressure distribution profile.

This is followed by the quasi–static stage, and finally a plunging stage. At the two latter stages, there is a longer duration of water build up and fall back on deck, revealing a broader pressure distribution profile up to the full height of the deck structure.

A methodology for establishing empirical data and relationships has been discussed and their use as initial conditions for the computer code developed to predict flow behaviour on deck has been presented. The experimental measurements provided initial conditions and boundary conditions for the numerical model that could not be determined theoretically within the scope of the present study. In particular, the model required input determining the relationship between the initial water velocity for the green water overtopping the bow of the FPSO and the height of the water on deck.

6.2.3 Numerical Modelling

The motivation to develop a numerical prediction method was to examine the framework in which non-linear extreme aspects of wave action are incorporated into the design of offshore structures. There is currently no generally applicable numerical modelling technique that is widely acknowledged to be entirely successful in this respect. In this study the potential of the MPS method has been explored in the context of green water effects on an FPSO for the first time with this in mind.

The MPS method has been demonstrated in previous research studies to have some advantages such as strict mass conservation, no numerical diffusion on the free surface and adaptation for computer simulation. These studies have indicated that the desirable aspects of the MPS method can be attributed to its Lagrangian description and such a mathematical formulation could be used to advantage in such applications as the green water problem.

A comprehensive MATLAB computer source code was developed to carry out the simulation and analysis of wave–structure interactions. The computer code produced some qualitative results which were presented as flow visualisation plots in Chapter 3 and Chapter 5. It should be noted that the design conditions used in the computer codes developed in this study do not limit the scope of this work as the computer codes have been written in a general sense to incorporate additional or new design conditions or parameters.

The model was applied to the classical 2D problem of Wedge Water Entry and the pressure distribution along the wedge body and pressure profile in the water calculated.

The results from this calculation were compared to experimental results and the results obtained using the SPH method, another particle method, presented by Oger et al. (2006). The results were seen to be in good agreement with the experimental results and compared favourably with the numerical results. The method was then extended into 3D to simulate and analyze the flow of water on deck of the model FPSO using empirical input for the initial conditions, although computer resources did not allow a full representation of the foredeck, and only a finite width slice of the fluid along its centreline was considered. The developing flow exhibited very similar characteristics to the sequence of events followed by the flow on deck observed in the experiments. The forces on the vertical face of the deck structure also have shown some qualitative agreements in trends displayed by experimental measurements. The forces on deck were not calculated because the vertical acceleration of the FPSO was not accounted for in the MPS model as it was considered beyond the scope of the study to couple it with the body motion.

In the opening chapter of this dissertation, the desirable attributes of a model to be used for such problems as the green water application were listed and they included such factors as robustness, and ability to accommodate complicated nonlinear free surface structures not known *a priori.* Examination of the simulation and analysis carried out for both wedge water entry and green water flow on deck has shown the ability of the MPS method to meet the requirements of this nature. It has been demonstrated that the MPS method has the capability to convincingly evaluate the pressure and water height distribution profiles in the green water problem studied and provide insights into velocity fields and pressure distribution on ocean structures in general.

Finally, despite its many advantages, it is necessary to mention that the method has some drawbacks. The most obvious is that the method is computationally intensive and requires considerable computational resources if it is to be applied to large problem domains. In green water calculations carried out for the FPSO, the computational domain was confined to a rectangular strip along the centre line of the fore deck and it involved the use of 577,500 interacting particles in a model scale. To model the wave overtopping the bulwarks and running along the whole of the foredeck would involve in the order of a million particles.

The number of computations per time step is proportional to the square of the number of particles in the flow, so that a detailed calculation of the flow phenomenon requires extensive and powerful computing resources.

The computations carried out for this study have, for this reason, been constrained by computer resources.

6.3 Suggestions for Further Work

There are a number of aspects of the work carried out in this study that have scope for further development and some possibilities of extension of the present work are as follows;

- To describe the waves overtopping the bulwarks, the MPS method must be modified to accommodate the continuous inflow of water particles into the solution domain. This requires the development of a mixed Eularian/Lagrangian methodology.
- Development of a numerical algorithm for the flow of water on deck coupled with the motions of the ship is also a logical continuation of the present research work.
- Arbitrarily shaped geometrics are characteristic of most of the equipment profiles on board offshore structures such as semi submersibles or FPSOs. Extension of the present numerical model to accommodate more realistic domains on the deck of these vessels is recommended as it can be easily incorporated into the present methodology.
- For a deeper study of the effects of the green water phenomena on the structural integrity of the vessel a mixed Eulerian–Langragian scheme can be introduced using a coupled MPS method and Ship Motion analysis tool.
- More detailed studies involving larger numbers of particles should be carried out on more powerful computers

The list of refinements to MPS models and the applications to which they can be put is open ended, but the work of this study and of other researchers has indicated that further work on the method will be well repaid by interesting results and insights into difficult flow phenomena that are unlikely to be easily achieved by other methods.

APPENDIX A

Description of Drop Tests

Description of Drop Test Equipment, Zhao et al(1997)

The rig used in the tests is shown in Figure A1. The rig is made of four major components namely the vertical guide rails, the trolley, a rotatable horizontal beam and the drop sections. A bolt is used to connect at each end the beam the rotatable to the trolley. The beam has a rotational capacity from zero to 28 degrees roll angle maximum. Use of the trolley can be achieved by engaging the vertical guide rails. The ballast weights are placed inside the rotatable beam and also the test sections are mounted on the rotatable beam. During the entire drop of the test section it is secured to the trolley. The main data of the test sections are presented in Table A1. The maximum drop height of the test rig is 2m.

The instrumentation details are shown in Figure A2, showing the location of the pressure gauges on the test sections. The pressure cells are 4mm in diameter and are of the piezoressistive type with resonance frequency of 500 kHz. The vertical acceleration of the drop rig was measured using an accelerometer. The vertical drop velocity was measured using an optical sensor. The time history of the drop velocity was calculated by using the measured drop velocity in combination with the measured vertical acceleration of the drop rig. The experiments were carried out in calm water condition and at least two drops performed for each test condition.

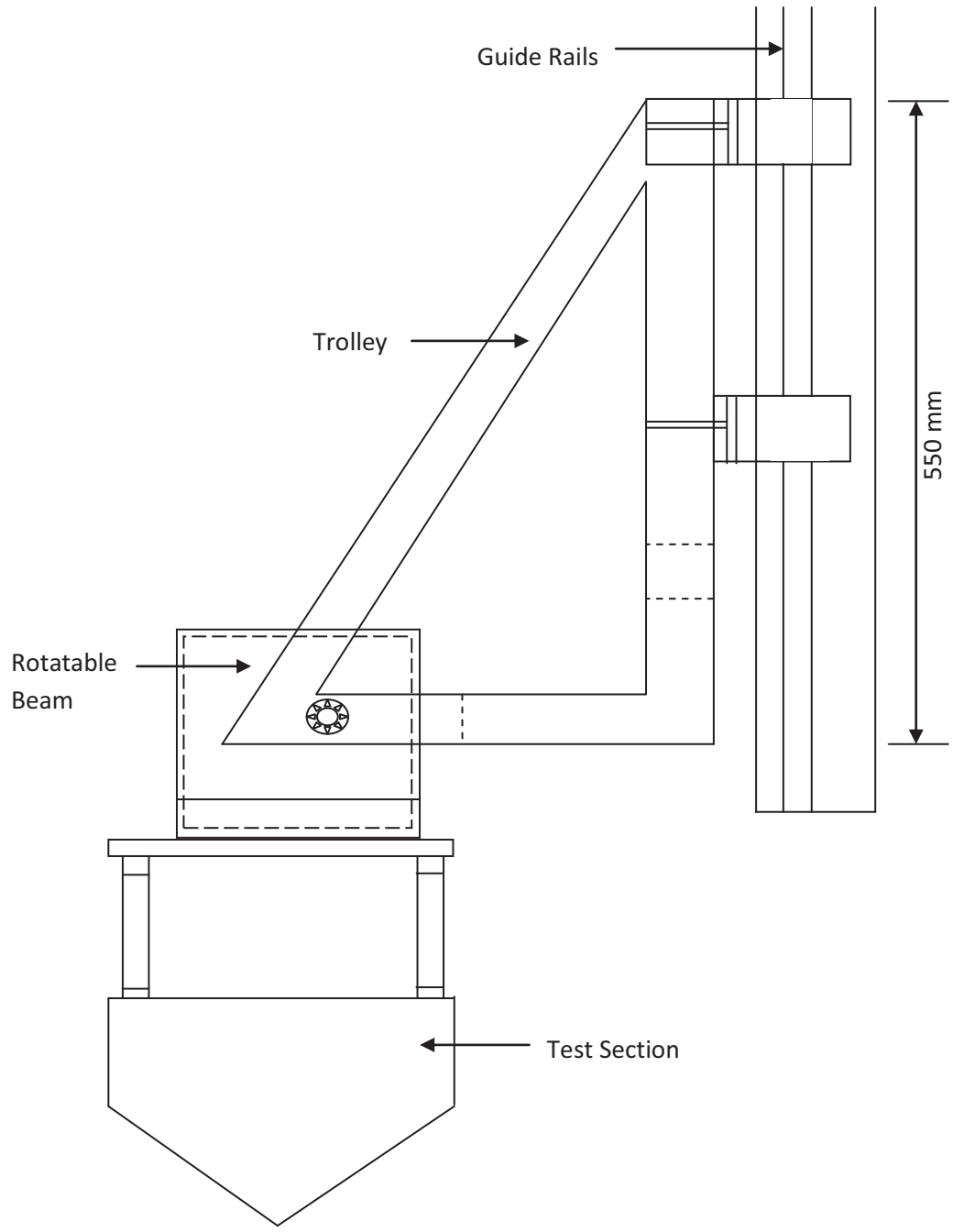

Figure A1: The free –falling rig used in the drop test

Table A1. The main data of the test sections

	V Shape	**bow flare**
Breadth of section	0.50 m	0.32 m
Vertical distance from keel to knuckles	0.29 m	0.203 m
Length of measuring sections	0.20 m	0.10 m
Length of each dummy sections	0.40 m	0.45 m
Total length	1.00 m	1.00m
Weight drop rig (without ballast)	141 kg	161 kg
Ballast weight	100 kg	100 kg
Total weight of drop rig	241 kg	261 kg
Weight of measuring section	14.5 kg	6.9 kg

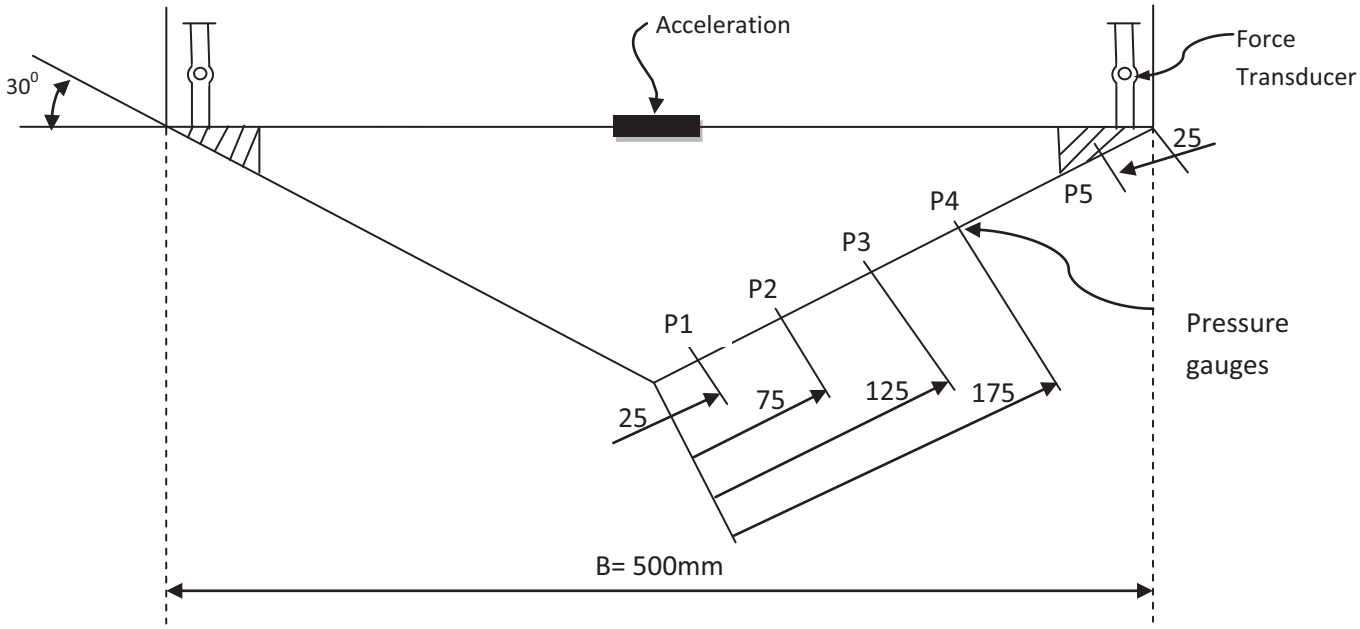

Figure A2 : Geometry of the test section and location of the pressure gauges.

APPENDIX B

Relation freeboard excedance and impact loading

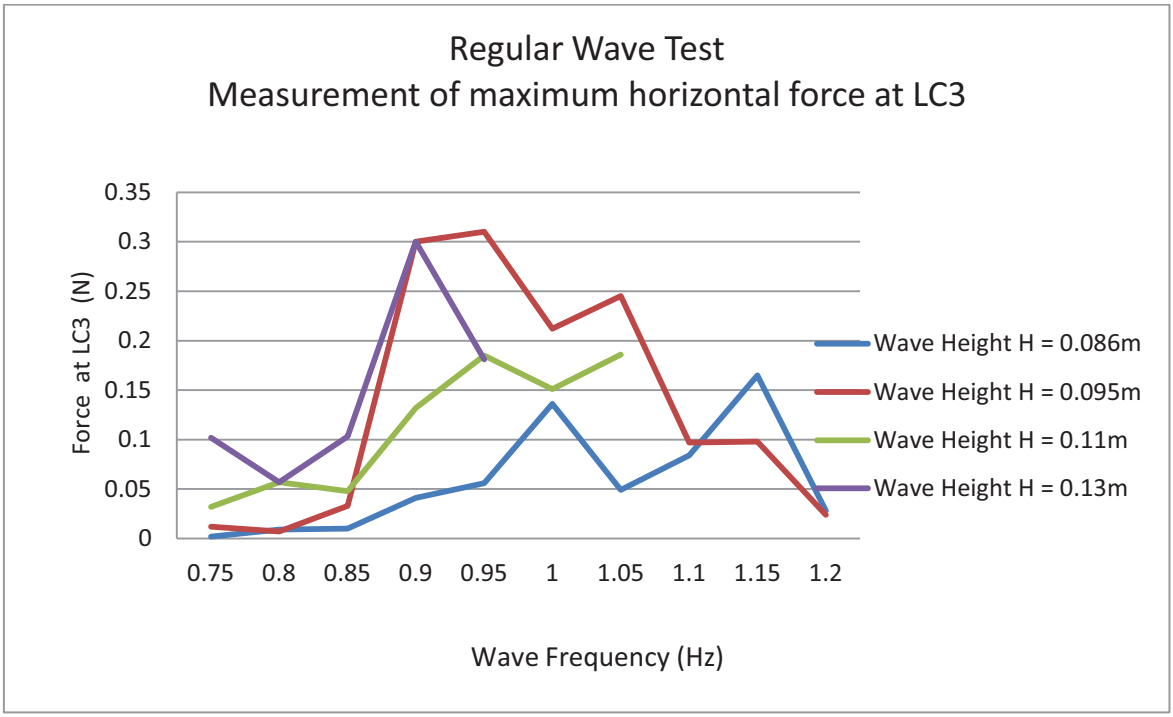

Figure B1 Force measurements at deck structure obtained from LC3 in regular waves

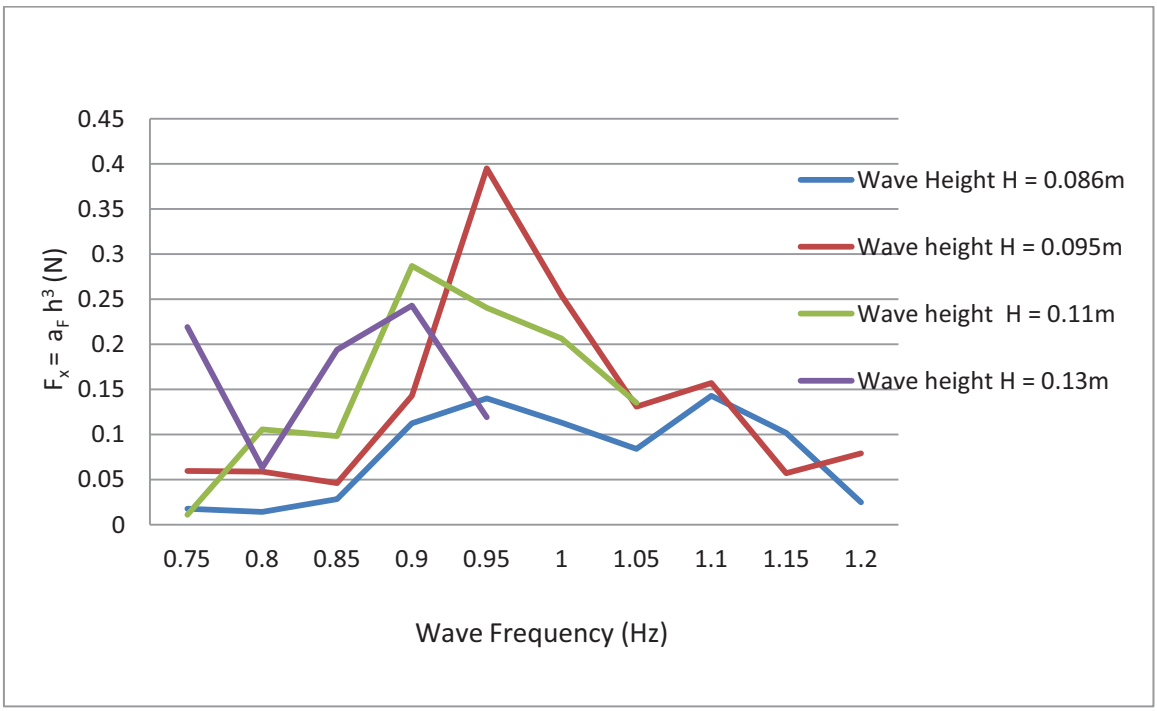

Figure. B2 Force measurements at deck structure obtained from relation $F_x = a_F h^3$ in regular waves

The expression for the horizontal F_x load was investigated for the regular wave condition carried out in the experiment. To check the assumption of a cubic relation between the freeboard exceedance and the loads on the deck structure, a direct comparison was made between the peak values in the regular wave test measured at load cell LC3 on the deck structure and the computed F_X load based on the relation equation 5.6 (the extreme freeboard exceedance was obtained at WP1 for all the regular wave tests. For a bow free angle of 10 degrees the a_F factor was taken to be 81.7 from Table 5.3

Figure B1 and Figure B2 shows some marginal variation in trend lines, with the F_X relation in Figure B2 expressing slightly larger values in some instances for the same loading condition as the measured values in Figure B1. These variations could be interpreted to mean that the impact load could be sensitive to some variation in the input conditions. In general, the relationship in equation (5.6) can be considered valid for a given bow shape and free board exceedance, however it is more likely to predict the maximum loads with a higher value for the given conditions.

APPENDIX C

Green water simulation additional results

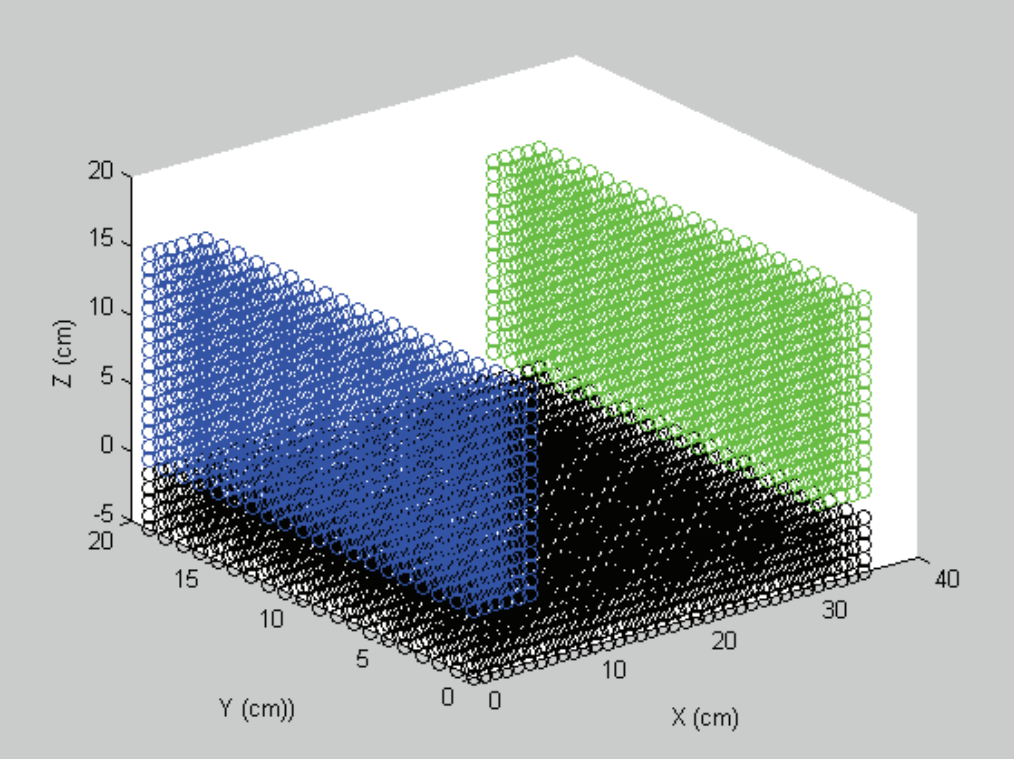

Figure C.1 Flow visualisation of green water simulation at t = 0.0s, H_0 = 16cm

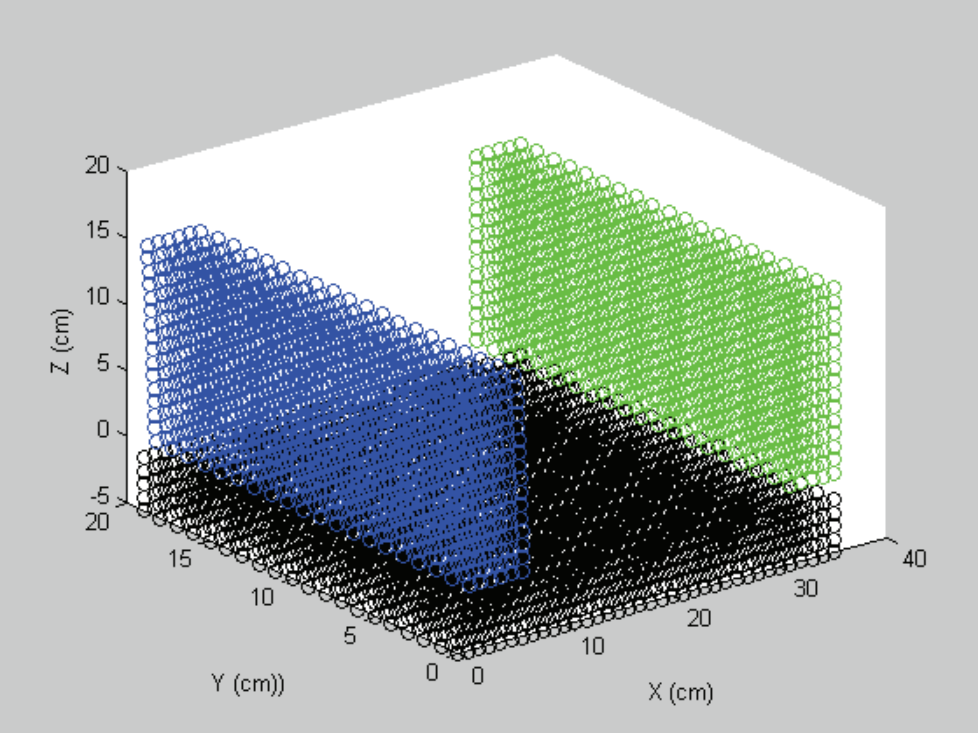

Figure C.2 Flow visualisation of green water simulation at t = 0.01s, H_0 = 16cm

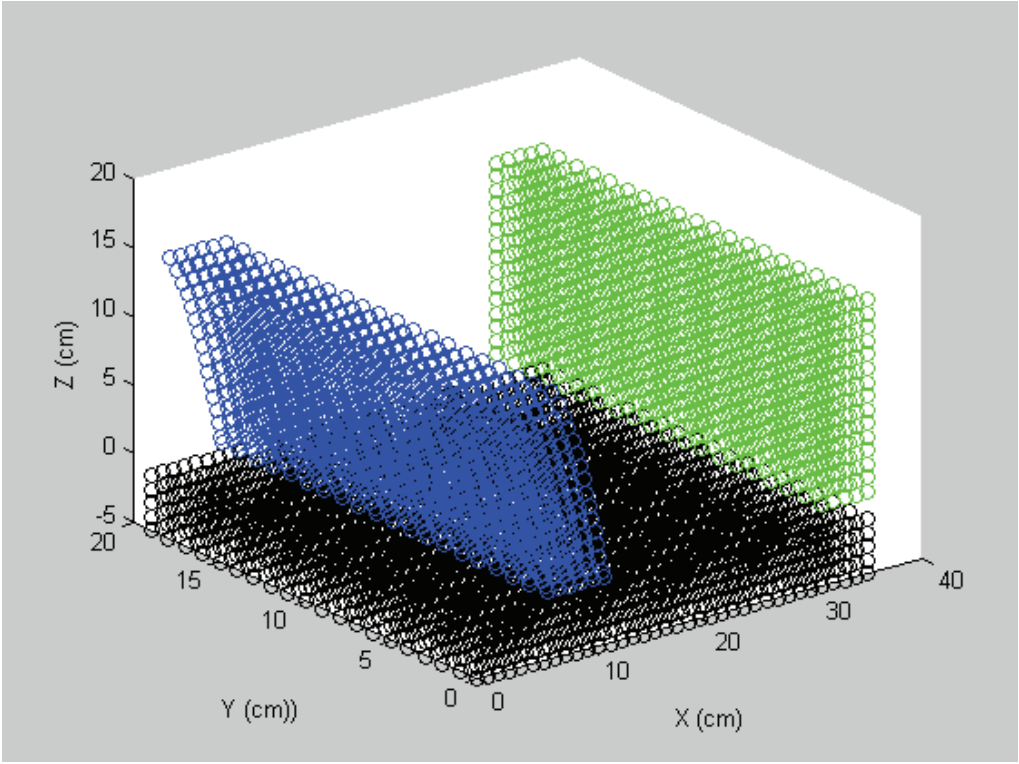

Figure C.3 Flow visualisation of green water simulation at t = 0.025s, H_0 = 16cm

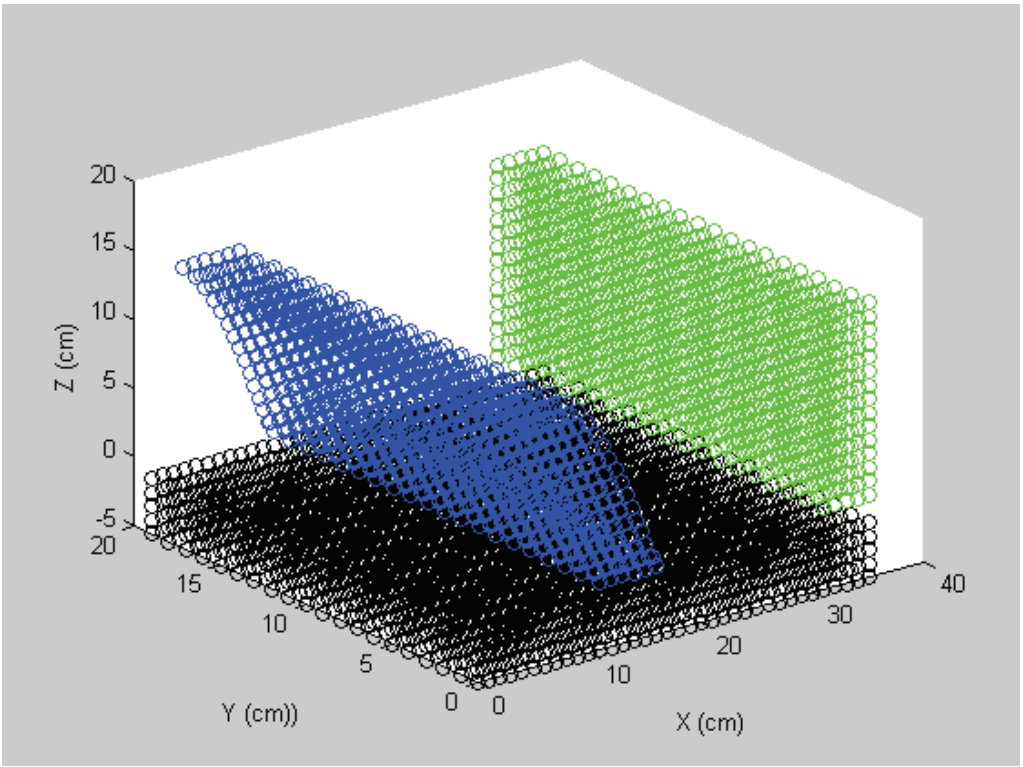

Figure C.4 Flow visualisation of green water simulation at t = 0.033s, H_0 = 16cm

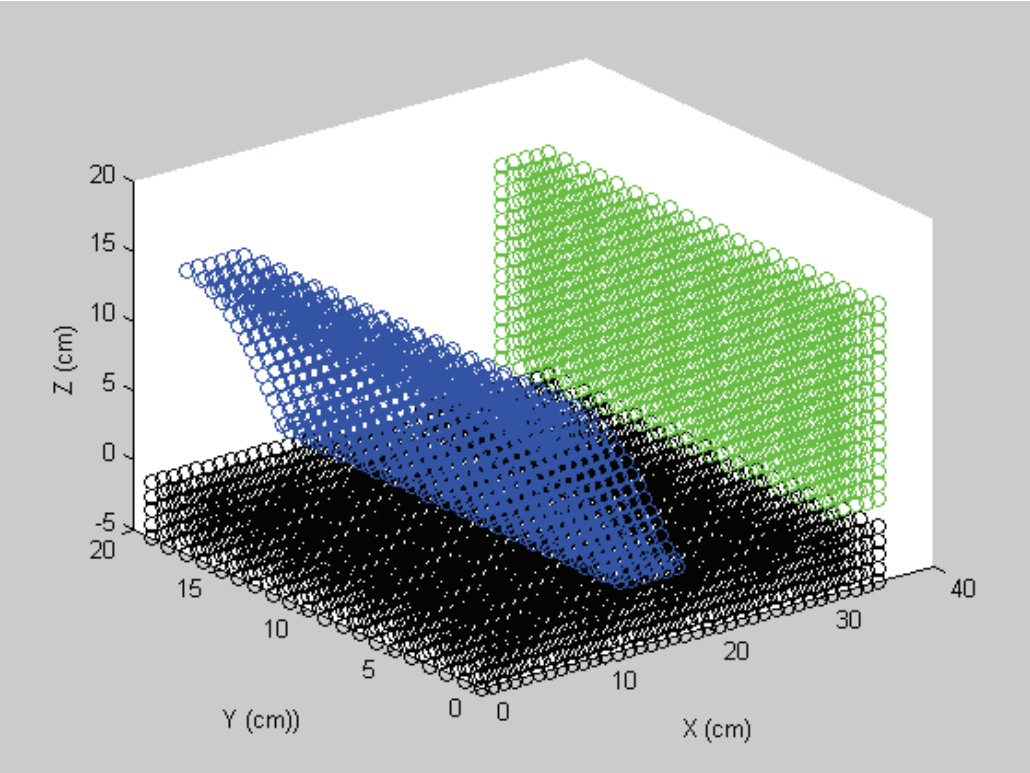

Figure C.5 Flow visualisation of green water simulation at t = 0.035s, H_0 = 16cm

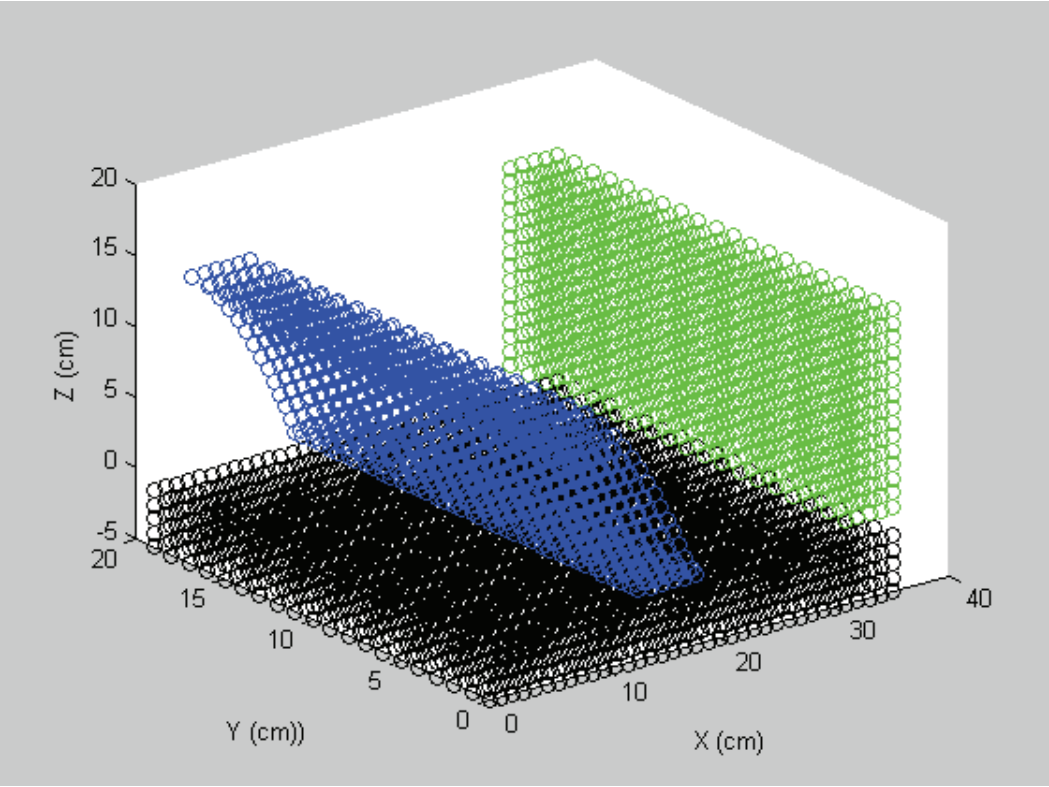

Figure C.6 Flow visualisation of green water simulation at t = 0.036s, H_0 = 16cm

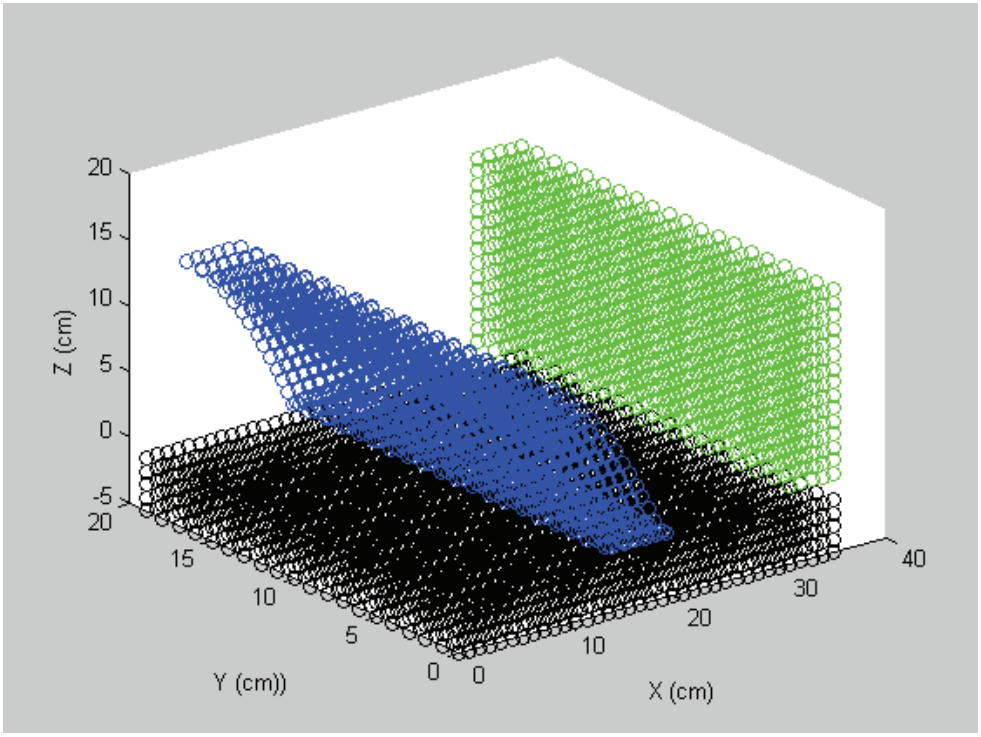

Figure C.7 Flow visualisation of green water simulation at t = 0.038s, H_0 = 16cm

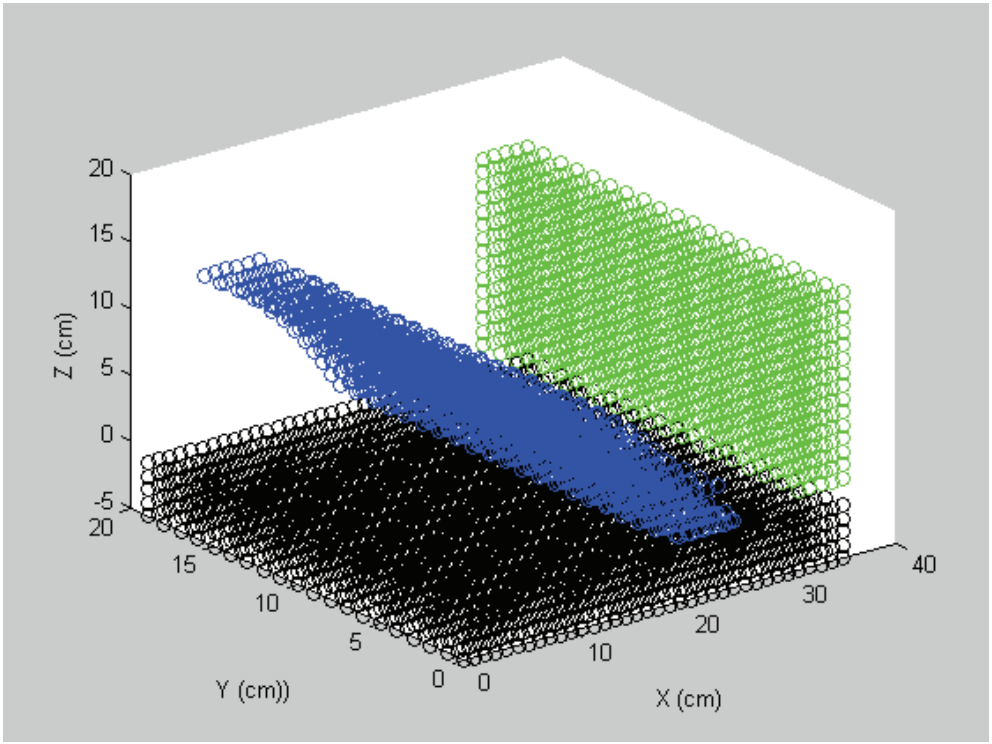

Figure C.8 Flow visualisation of green water simulation at t = 0.045s, H_0 = 16cm

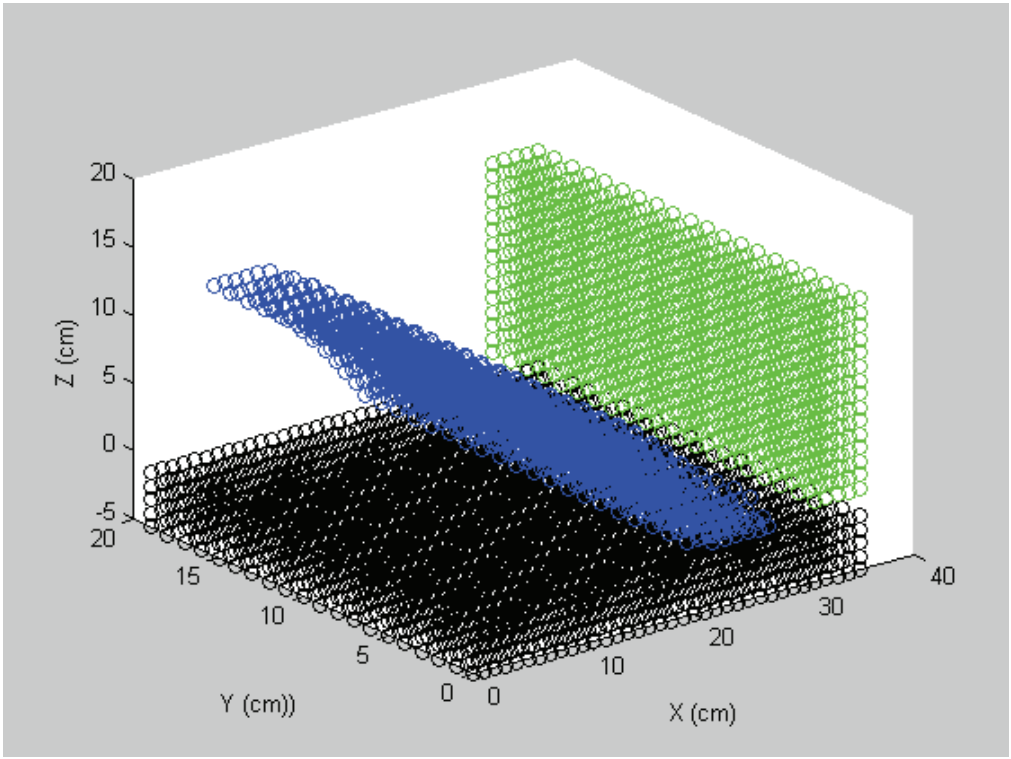

Figure C.9 Flow visualisation of green water simulation at t = 0.047s, H_0 = 16cm

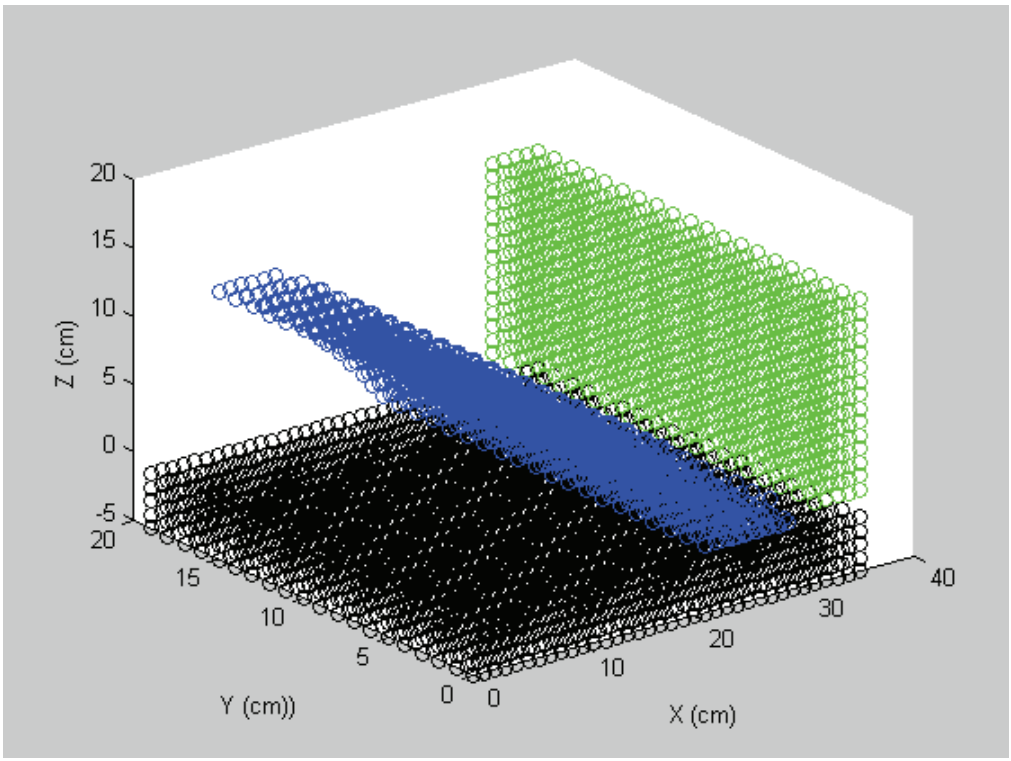

Figure C.10 Flow visualisation of green water simulation at t = 0.049s, H_0 = 16cm

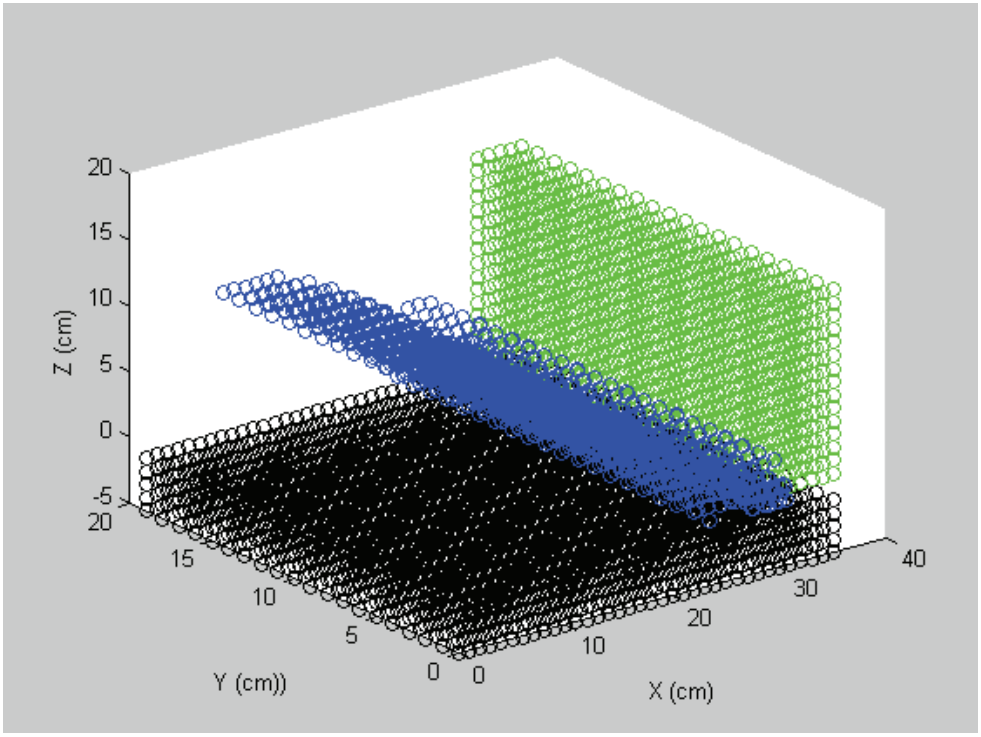

Figure C.11 Flow visualisation of green water simulation at t = 0.053s, H_0 = 16cm

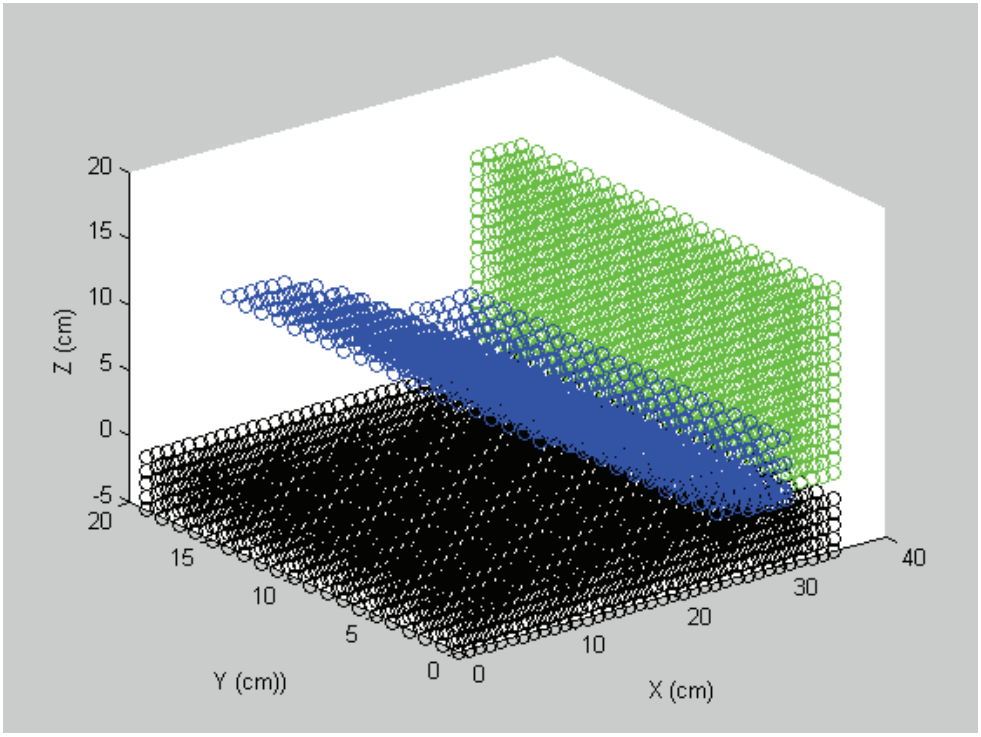

Figure C.12 Flow visualisation of green water simulation at t = 0.055s, H_0 = 16cm

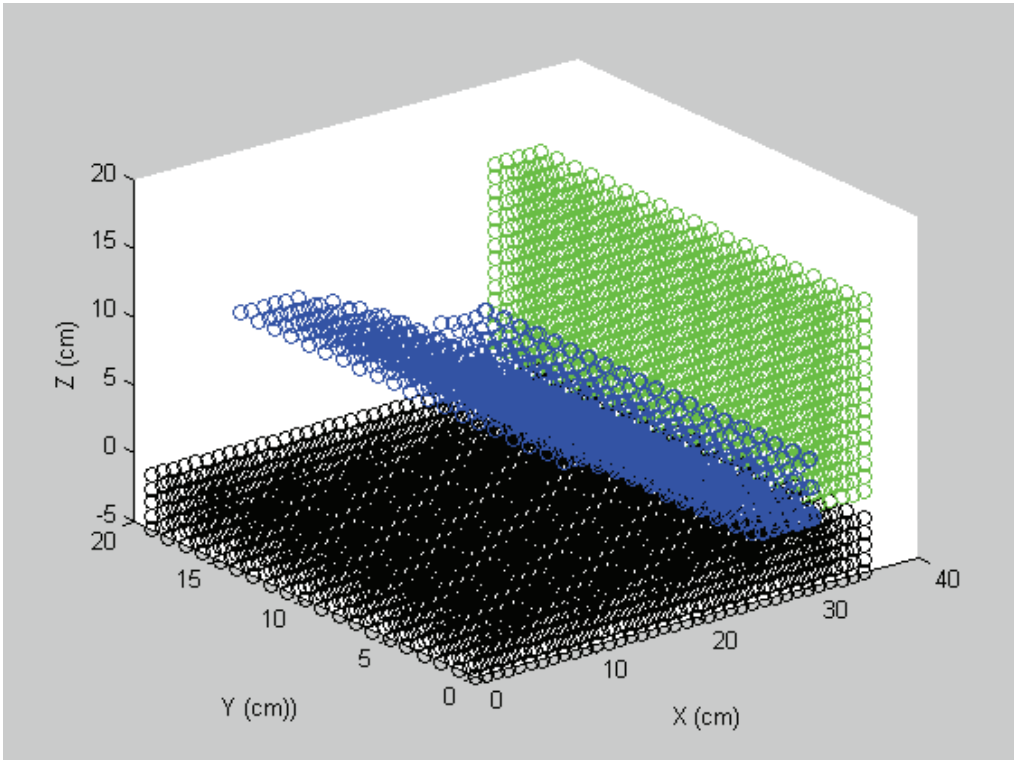

Figure C.13 Flow visualisation of green water simulation at t = 0.056s, H_0 = 16cm

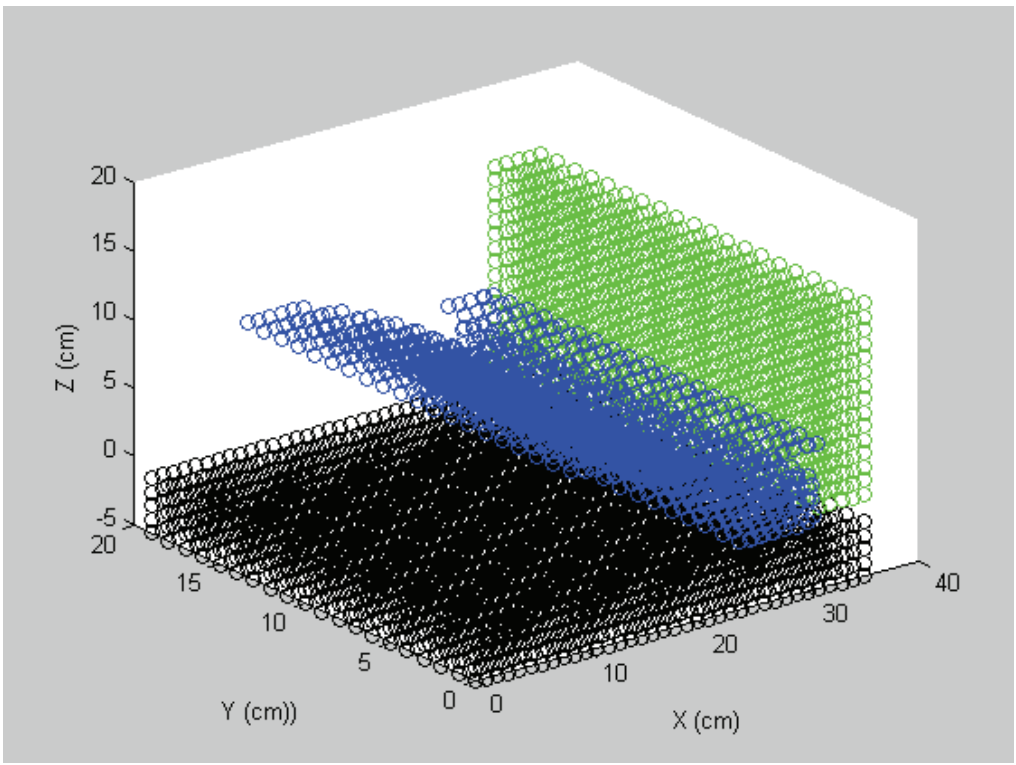

Figure C.14 Flow visualisation of green water simulation at t = 0.058s, H_0 = 16cm

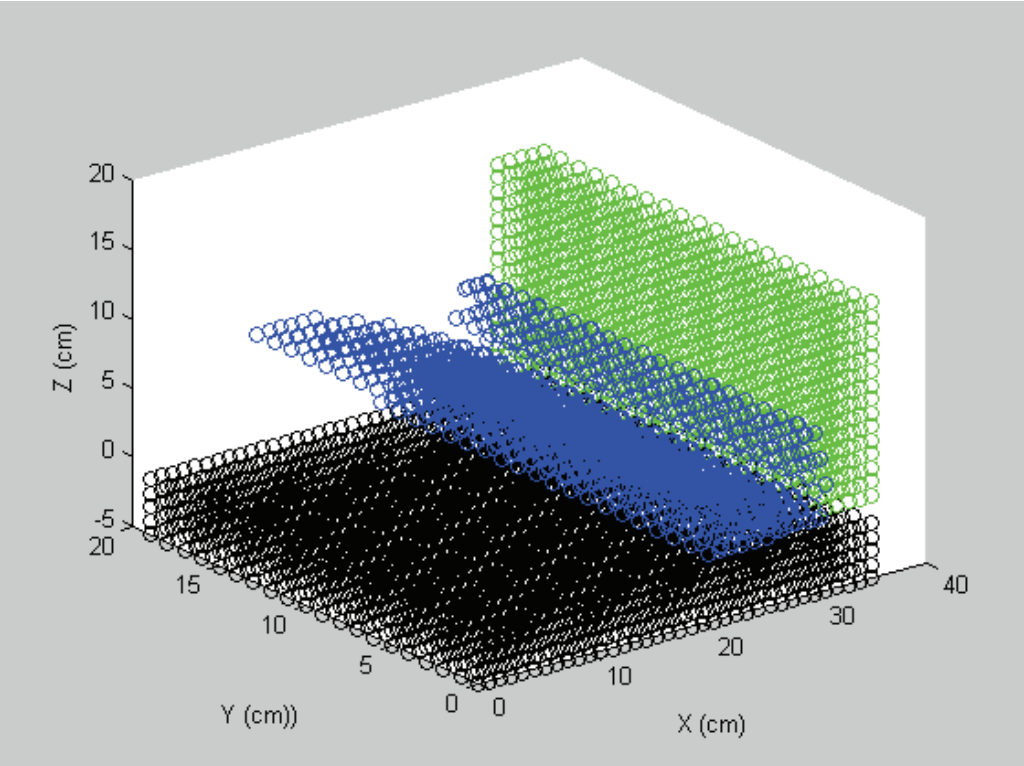

Figure C.15 Flow visualisation of green water simulation at t = 0.061s, H_0 = 16cm

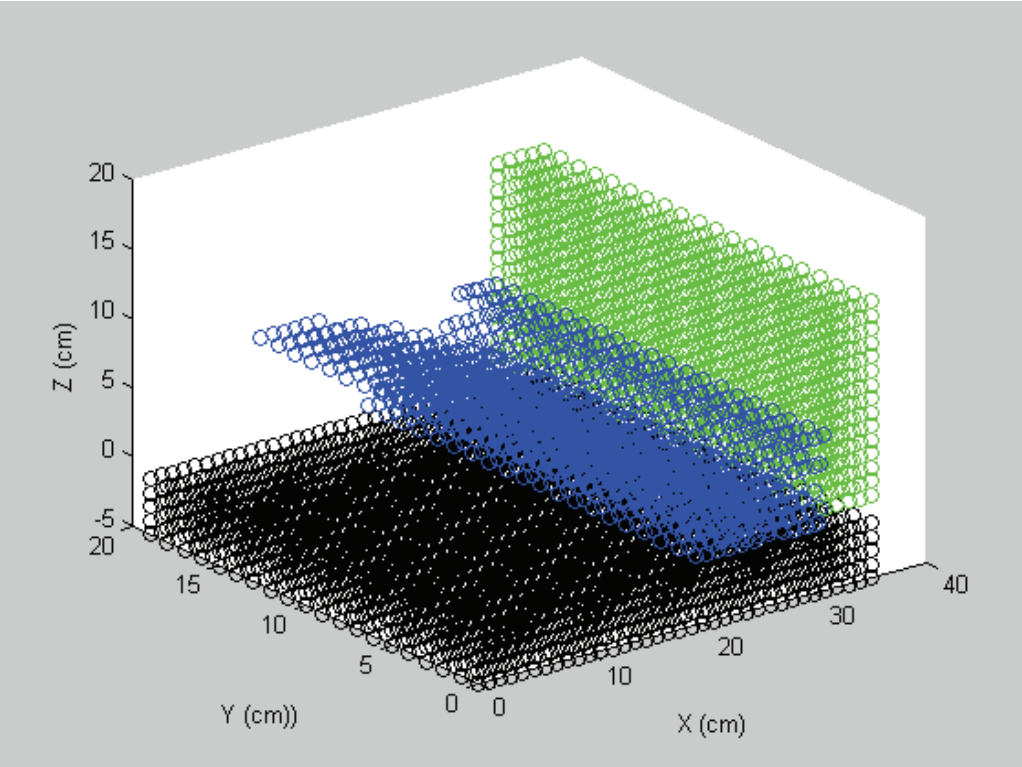

Figure C.16 Flow visualisation of green water simulation at t = 0.065s, H_0 = 16cm

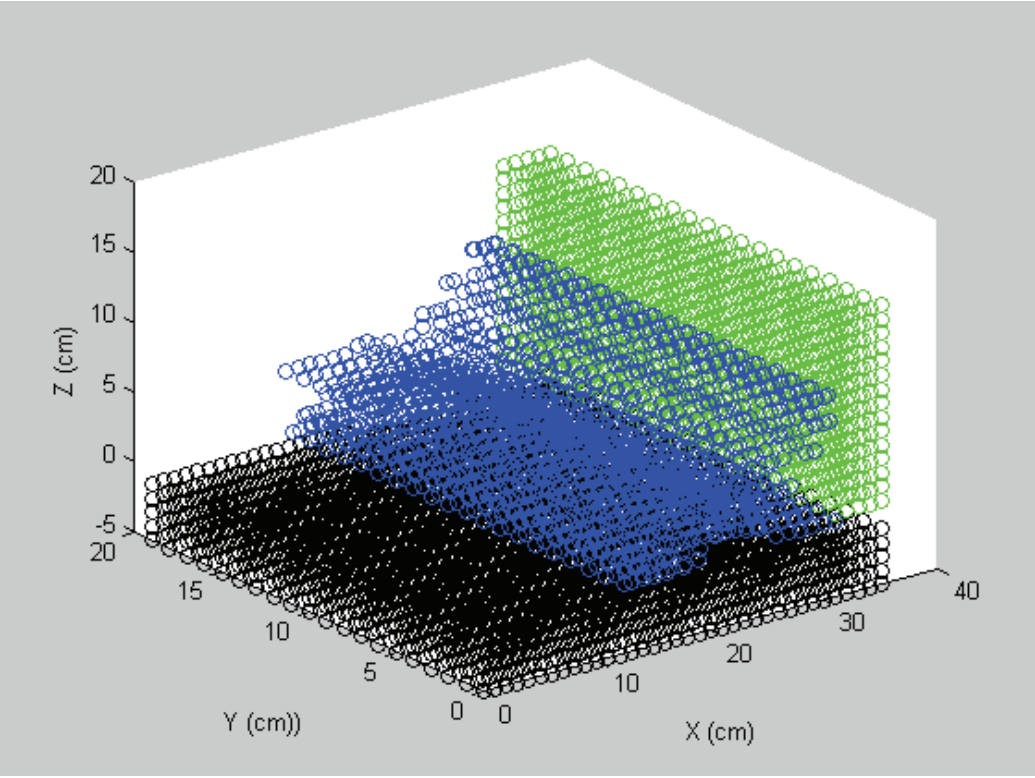

Figure C.17 Flow visualisation of green water simulation at t = 0.07s, H_0 = 16cm

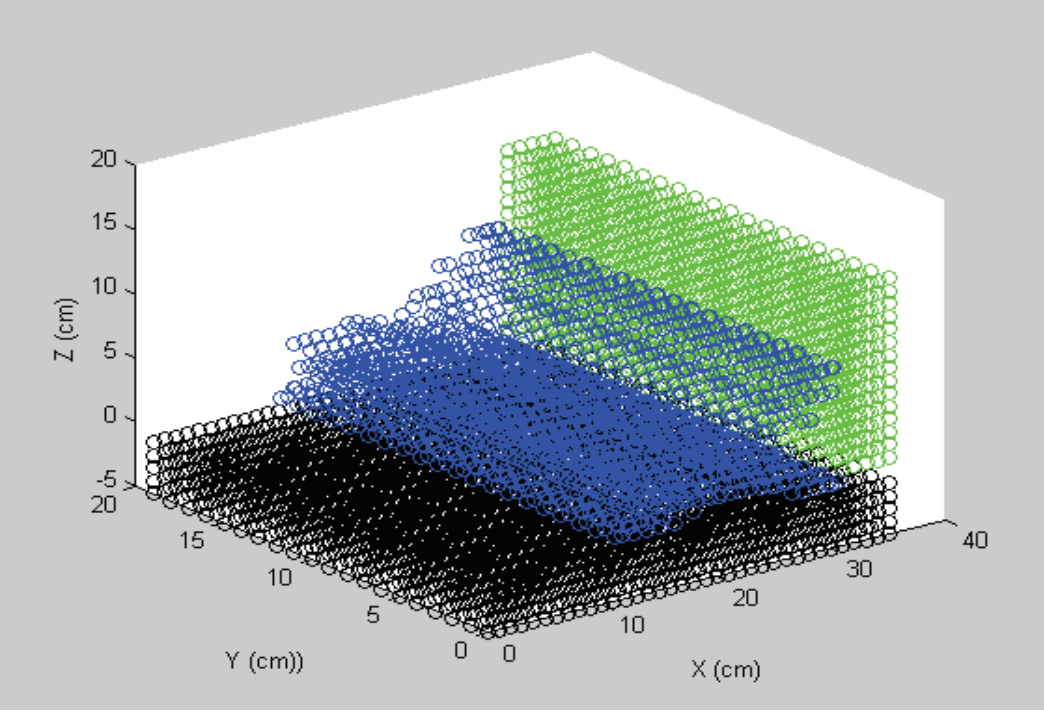

Figure C.18 Flow visualisation of green water simulation at t = 0.08s, H_0 = 16cm

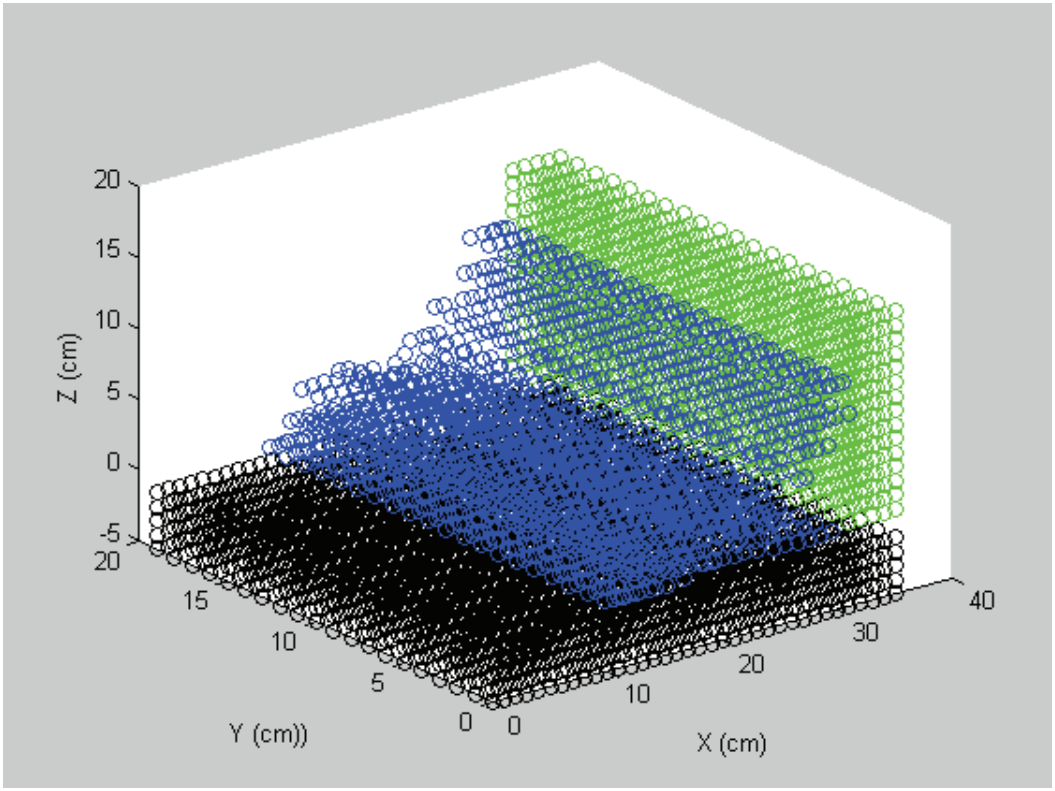

Figure C.19 Flow visualisation of green water simulation at t = 0.10s, H_0 = 16cm

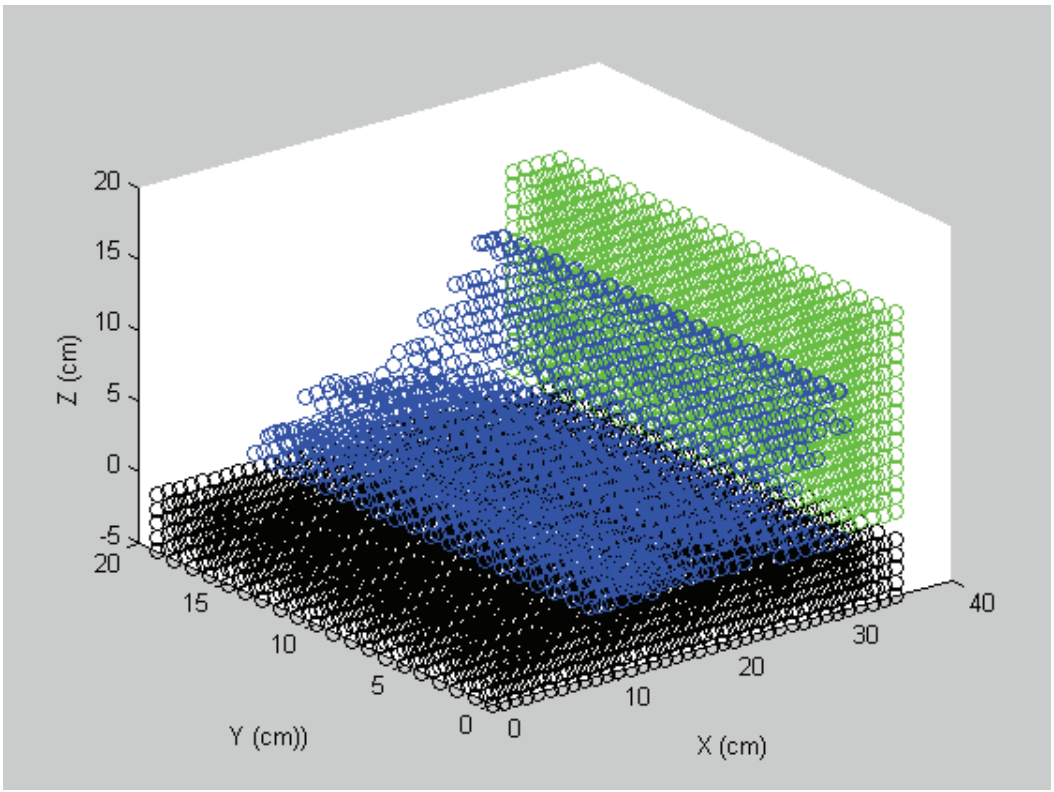

Figure C.20 Flow visualisation of green water simulation at t = 0.11s, H_0 = 16cm

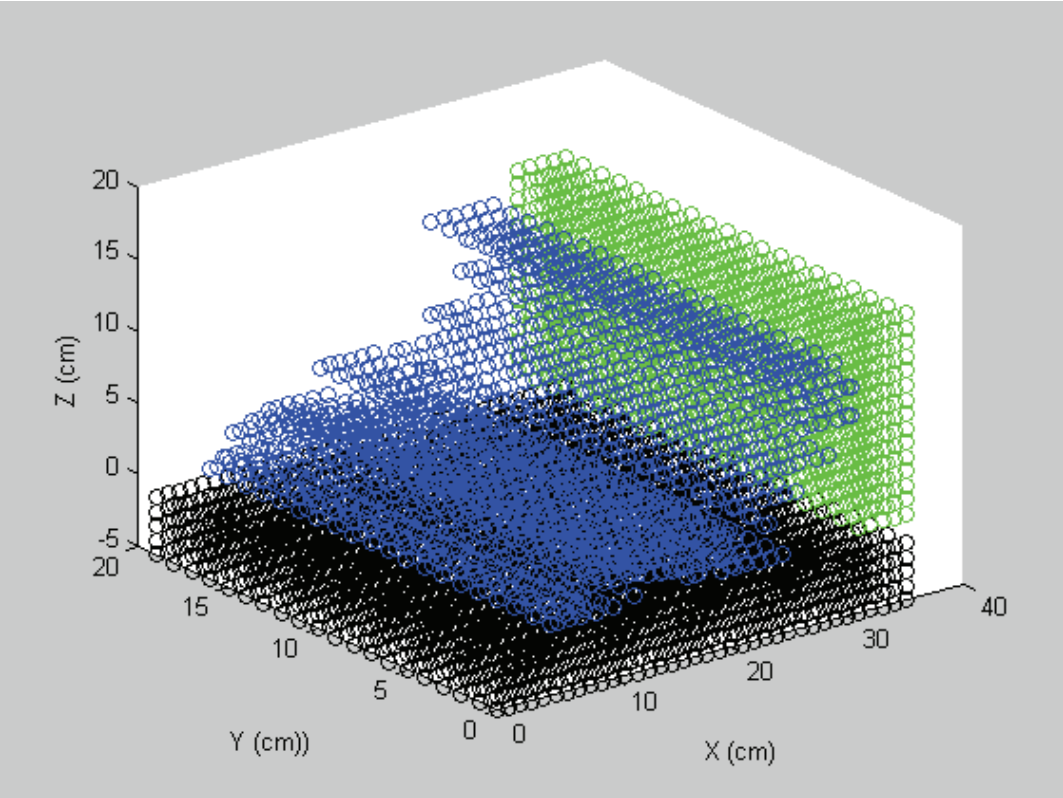

Figure C.21 Flow visualisation of green water simulation at t = 0.12s, H_0 = 16cm

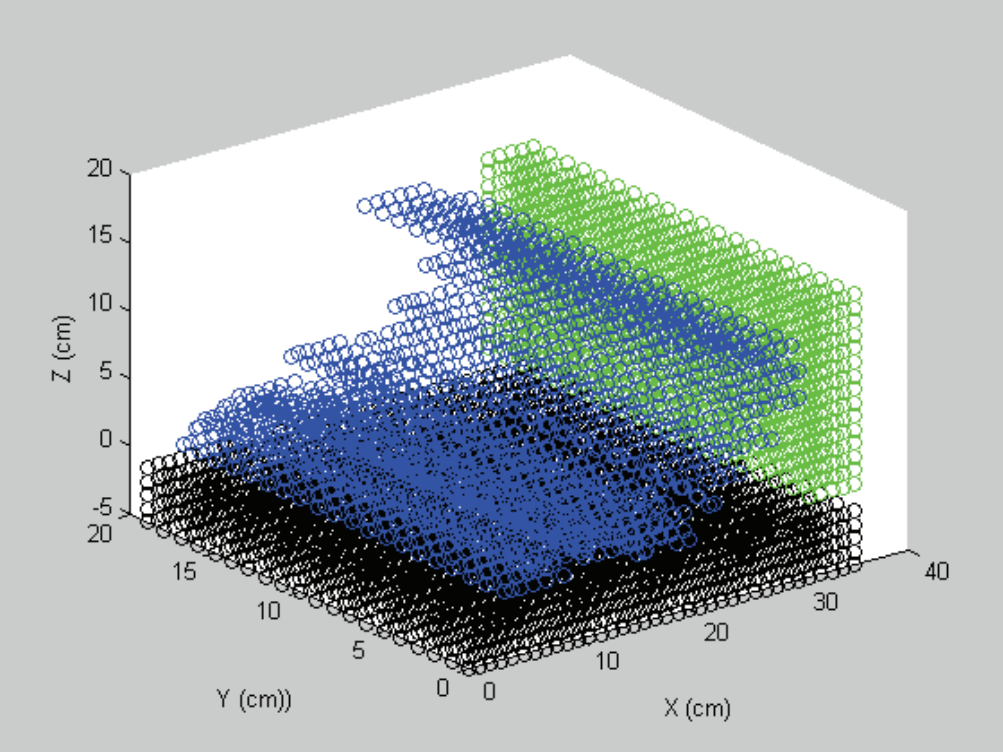

Figure C.22 Flow visualisation of green water simulation at t = 0.15s, H_0 = 16cm

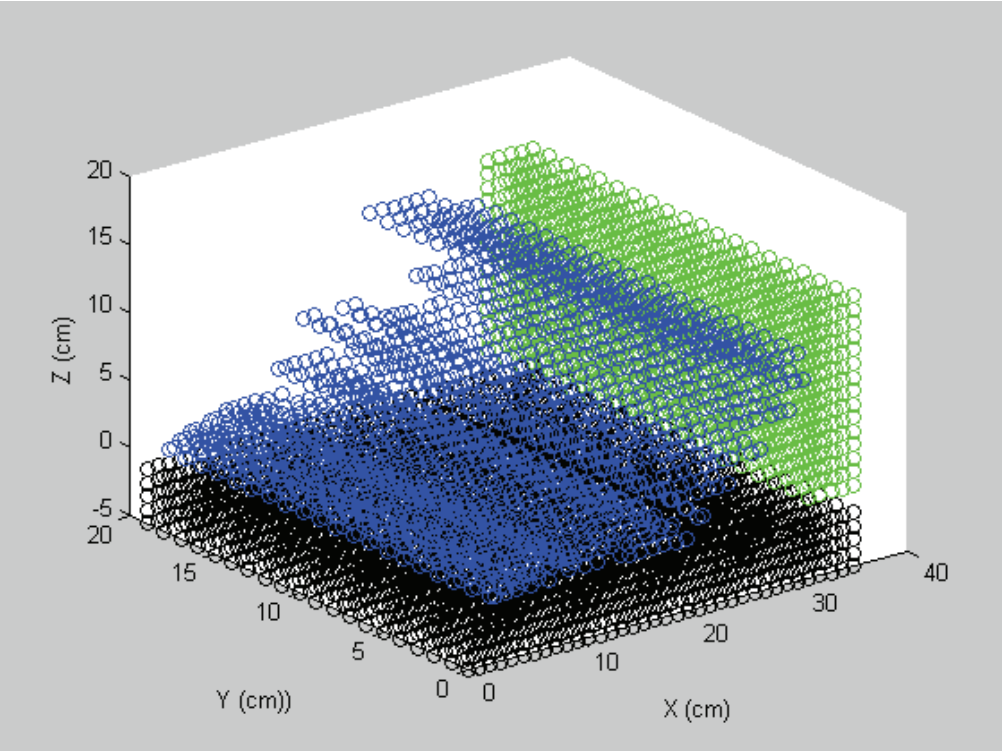

Figure C.23 Flow visualisation of green water simulation at t = 0.20s, H_0 = 16cm

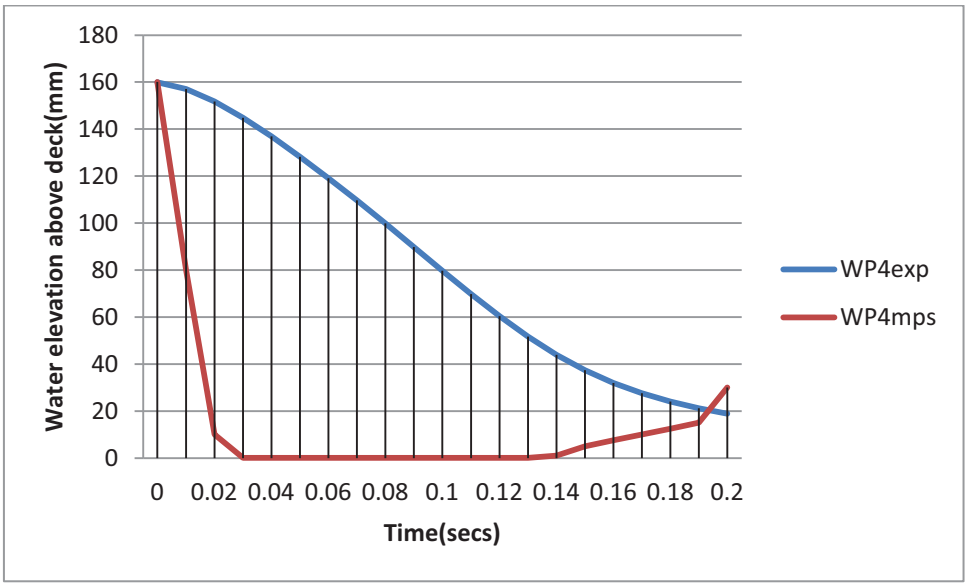

Figure C.24 Measured and Computed water height on deck at WP4, H_0=160mm

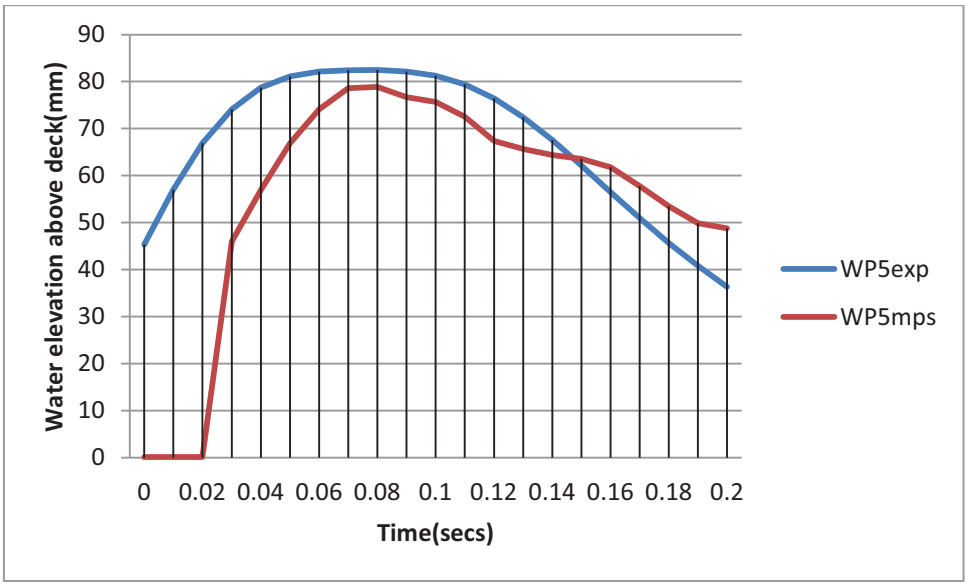

Figure C.25 Measured and Computed water height on deck at WP5, H_0=160mm

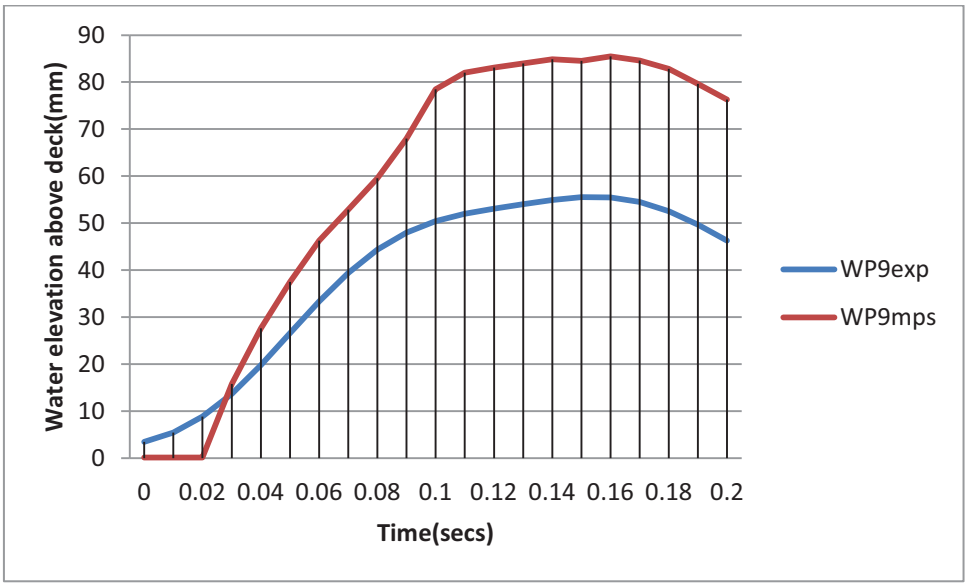

Figure C.26 Measured and Computed water height on deck at WP9, H_0=160mm

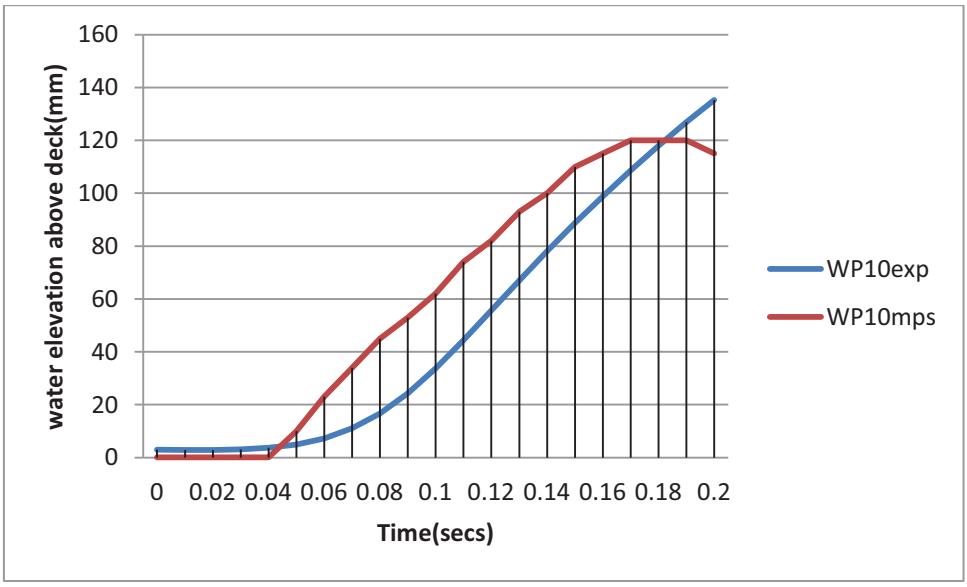

Figure C.27 Measured and Computed water height on deck at WP10, H_0=160mm

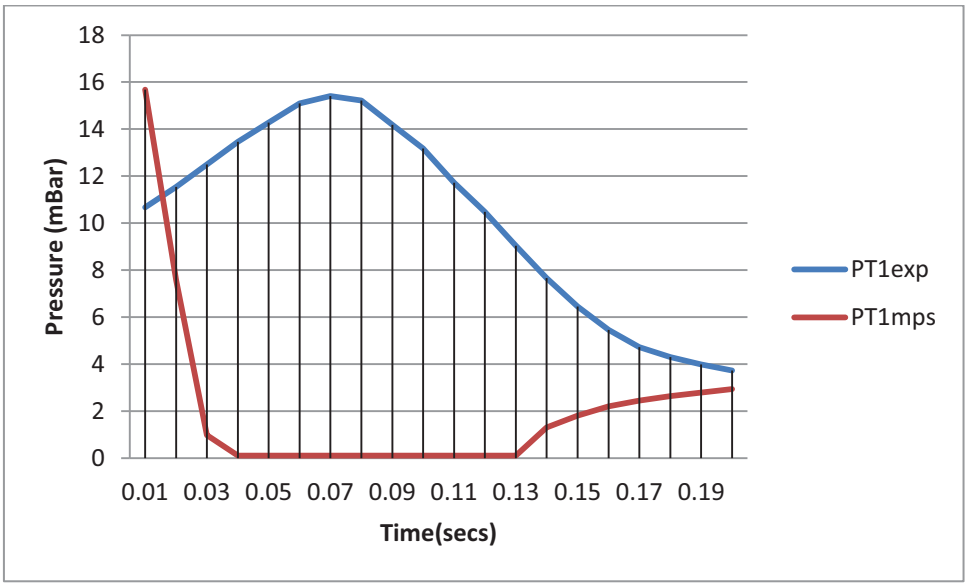

Figure C.28 Measured and Computed pressure on deck at PT1, H_0=160mm

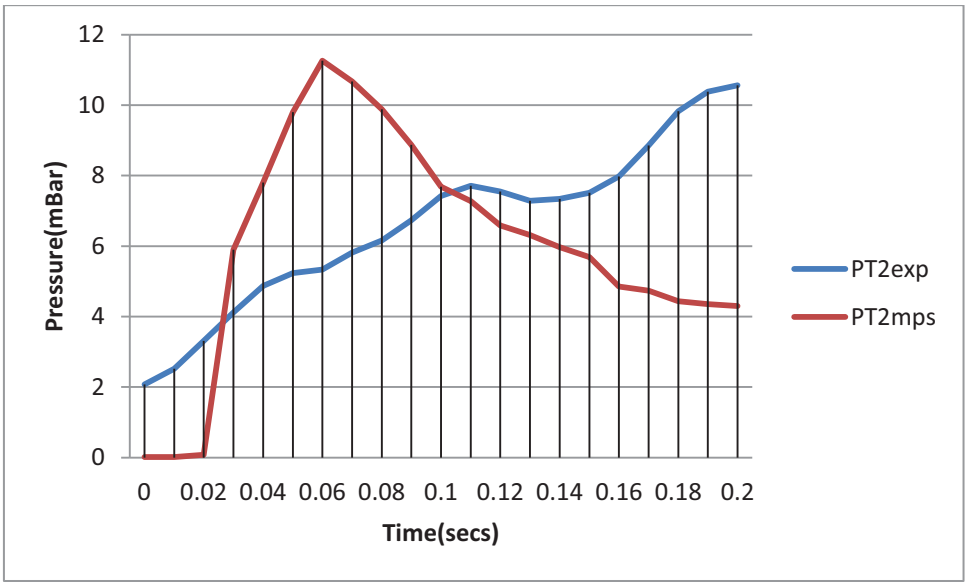

Figure C.29 Measured and Computed pressure on deck at PT2, H_0=160mm

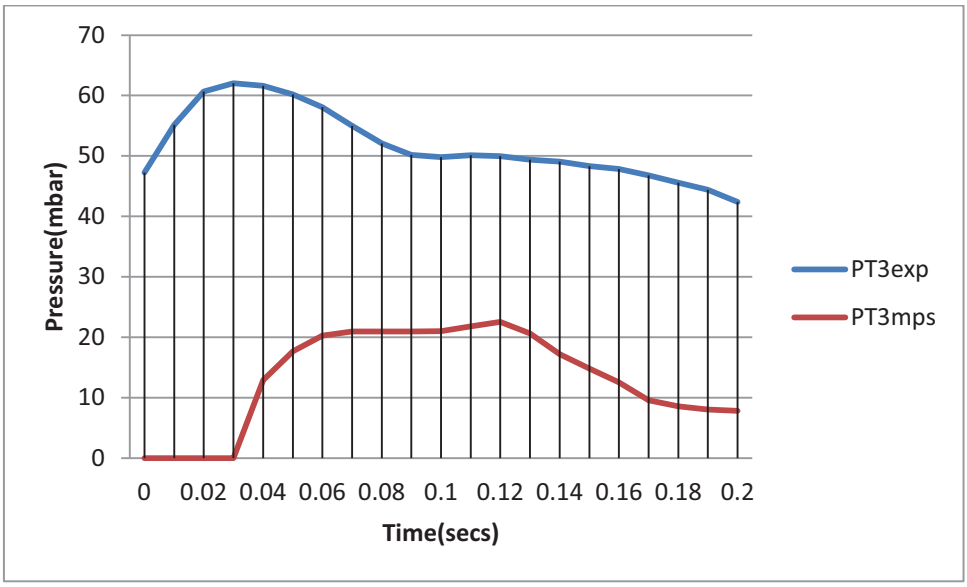

Figure C.30 Measured and Computed pressure on deck at PT3, H_0=160mm

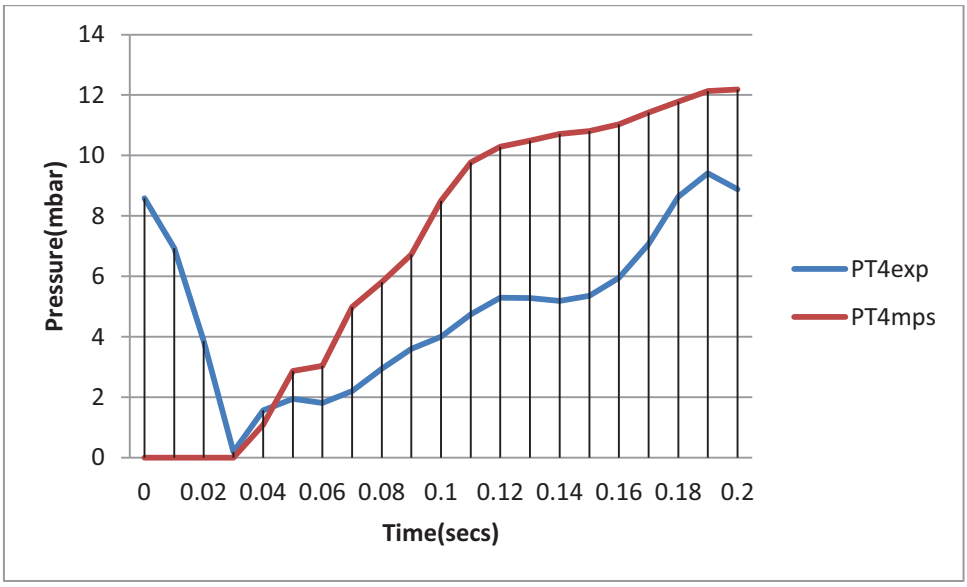

Figure C.31 Measured and Computed pressure on deck at PT4, H_0=160mm

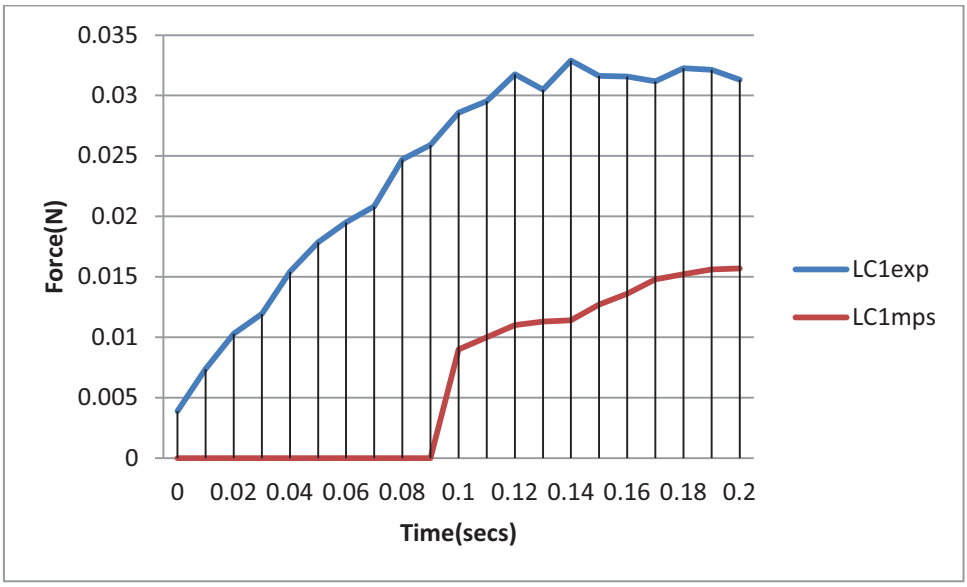

Figure C.32 Measured and Computed impact load on structure at LC1, H_0=160mm

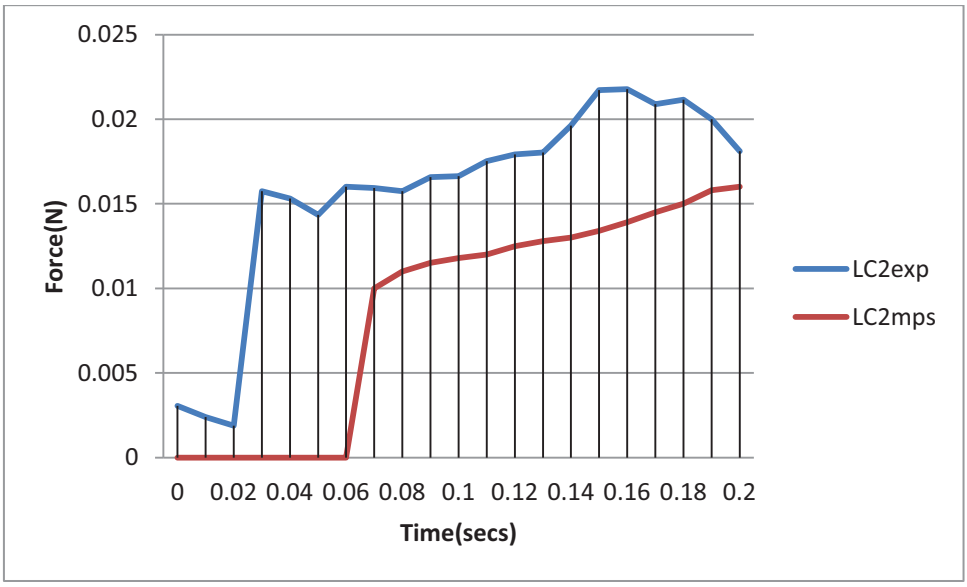

Figure C.33 Measured and Computed impact load on structure at LC2, H_0=160mm

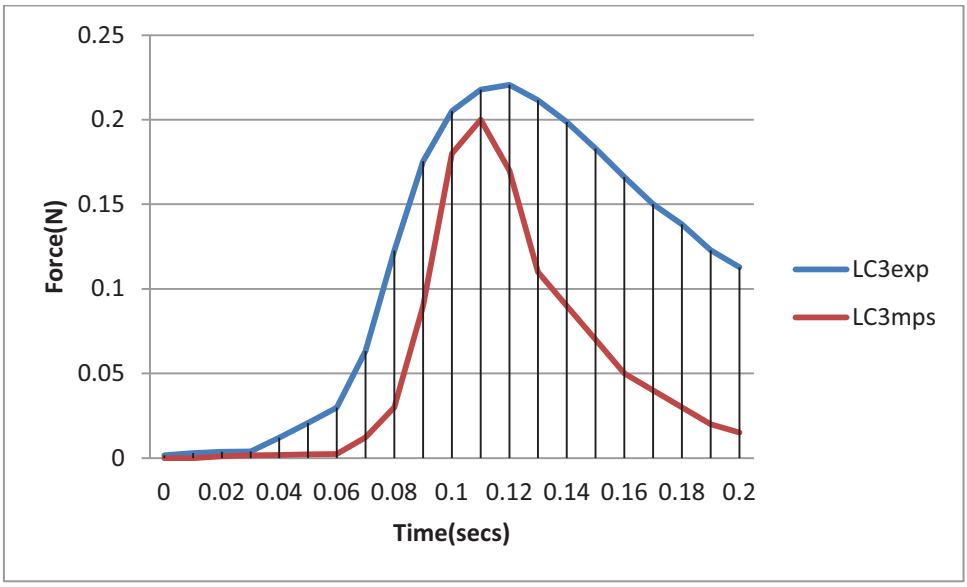

Figure C.34 Measured and Computed impact load on structure at LC3, H_0=160mm

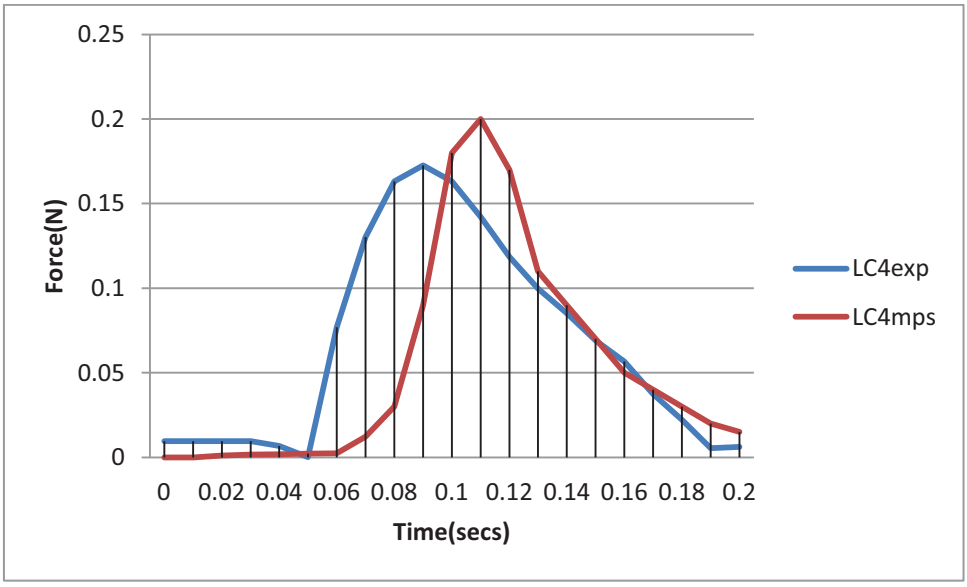

Figure C.35 Measured and Computed impact load on structure at LC4, H_0=160mm

REFERENCES

1) Ai, C. and Jin, S.: 2010, *Non Hydrostatic finite volume method for non linear waves interacting with structures,* Computers and Fluids, vol. 39, issue 10, page 2090 – 2100.

2) Andersen P. and Wuzhow H.:1985, *On the calculation of added mass and damping coefficients by simple green's function technique*, Ocean Engineering, Vol. 12 No 5 page 425 – 451. 1985

3) Ataie – Ashtiani,B. and Farhadi, Leila.: 2006, *A Stable moving particle semi – implicit method for free surface flows*, Fluid Dynamics Research, 38, page 241 -256

4) Barltrop, N.P.D. and Adams,A.J.: 1991, Dynamics of Fixed Marine Structures. Third Edition, Butterworth Heinemann Publishers. Marine Technology Directorate Ltd.

5) Benz, W.: 1990, *Smoothed Particle Hydrodynamics – A review in Num. Modelling of nonlinear stellar pulsations,* Prob. And Prosp. Kulver Academic Press, Boston.

6) Bhattacharyya, R. : 1978, Dynamics of Marine Vehicles, Ocean Engineering, A Wiley - Interscience Publication, John Wiley & Sons, Inc, ISBN 0 -471 – 07206 - 0

7) Blok,J.J. and Huisman,J.:1984, *Relative Motions and Swell – up for a Frigate Bow,* Transactions of the Royal Institution of Naval Architects, 1984,vol. 126, page 227 – 244.

8) BMT Fluid Mechanics Limited. : 2002, *Review of Model Testing Requirements for FPSOs,* prepared by BMT Fluid Mechanics Limited for Health and Safety Executive.

9) BOMEL Limited: 2001, *Analysis of green Water Susceptibility of FPSO/FSU's on the UKCS,* prepared by BOMEL Limited for the Health and Safety Executive

10) Buchner,B.: 1999, *Green Water from the side of a weathervaning FPSO.* OMAE 99, St Johns.

11) Buchner, B.: 2002, Green Water on ship Type Offshore Structures, PhD Thesis, Delft University

12) Buchner,B. and Cozijn,J.L.: 1997, *An Investigation into the Numerical Simulation of Green water,* BOSS 1997, Delft

13) Buchner, B. : 1995, *The Impact of Green Water on FPSO Design,* OTC 1995, Houston

14) Chakrabarti, S.K. :1994, *Offshore Structure Modeling,* Advanced Series on Ocean Engineering, vol. 9, World Scientific Publishing Co Pte Ltd, Singapore, 981-02-1513-4ISBN

15) Chan J. L. K. and Calisal S. M.: 1993, *A Numerical Procedure for Time Domain Non Linear Surface Wave Calculation* - Ocean Engineering vol. 20 No 1 page 19 - 32, 1993

16) Chapman, R.B.: 1979, *Large – Amplitude Transient Motion of Two Dimensional Floating Bodies.*- Journal Of Ship research, volume 23, Number 1 , March 1979, page 20 – 31. SNAME

17) Courant, R., Friedrichs, K and Lewy, H.: 1928, *On the Partial Difference Equations of Mathematical Physics,* Mathematische Annalen 100, page 32 – 74. Republished in IBM Journal, March , 1967, page 215 – 234.

18) Cox, D.T. and Ortega,J.A.: 2002, *laboratory observations of green Water Overtopping a fixed deck* Ocean Engineering, vol. 29., page 1827 – 1840.

19) Dillingham, J.: 1981, *Motion studies of a vessel with water on deck,* Marine Technology, vol. 18, no1, January 1981, page 38 – 50

20) Dobrovolskaya, Z.N.: 1969, *On some Problems of Similarity flow of Fluid with a free surface,* Journal of Fluid Mechanics, vol. 36, issue 4, page 805 – 829.

21) Elsimillawy N, and Miller, N.S: 1986, *Time Simulations of Ship Motions: a Guide to the Factors Degrading Stability.* SNAME Transactions , Volume 94, 1986, page 215 – 240

22) Ersdal,G and Kvitrud,A : 2000, *Green Water on Norwegian Production Ships,* ISOPE 2000 Seattle.

23) Faltinsen O. M. : 1998 *Sea Loads on Ships and Offshore Structures.* Cambridge Ocean Technology Service, Cambridge University Press 1998 Edition.

24) Ghoniem,A.F. and Sherman, F.S.: 1985, *Grid free simulation of Diffusion Using Random Walk Methods.* Journal of Computational Physics vol. 61, page 1 – 37.

25) Goda Y., : 2000, *" Random seas and Design of Maritime structures"* , Advanced Series in Ocean Engineering, 2nd Edition, vol.15, World Scientific Publishing Co. Ltd, ISBN -13 978-981-02-3256-6.

26) Gomez-Gesteira, M., Cerqueiro, D., Crespo, C. and Dalrymple, R.A.: 2005, *Green Water Overtopping analyzed with SPH Mode,* Ocean Engineering, vol. 32 2005, page 223 – 238

27) Gong, K., Liu, H. and Wang, B.: 2009, *Water entry of a Wedge based on SPH model with an Improved Boundary treatment,* Journal of Hydrodynamics , vol. 21 issue 6, page 750 - 757

28) Gotoh H., Sakai T.: 1999, *Lagrangian Simulation of Breaking Wave using Particle Method.* - Coastal Engineering Journal, vol. 41 Nos. 3 & 4, 1999 page 303 - 326.

29) Gotoh, H., Sakai, T. and Hayashi,M.: 2001 *Lagrangian Two Phase Flow Model for the Wave Generation Process due to large scale landslides,* Asian and Pacific Coastal Engineering - 2001, Oct 18 - 21, 2001, Dalian, China.

30) Gotoh H Shibahara,T.and.Sakai T.: 2001 *Sub Particle Turbulence Model for the MPS Method Lagrangian Flow Model for Hydraulic Engineering,* Computational Fluid Dynamics Journal. Vol. 9 No. 4 January 2001, Page 331 – 347

31) Gotoh, H., Hayashi, M. Sakai, T.: 2002 *Lagrangian Grid less Model for Structure Flow - Floats Triangular Interaction* Proceedings of the 13th IAAR - APD Congress, Singapore, 6 - 8 August 2002.

32) Gotoh H., Sakai, T.,Hayashi, M. and Andoh, S.: 2002, *Lagrangian Solid - Liquid two phase flow model for wave- seabed interaction* Proceedings of the 13 the IAHR - APD Congress, Singapore, 6-8 August, 2002

33) Gotoh, H., Hayashi, M. Sakai, T and Oda, K.: 2003 *Numerical Model of Wave Breaking by Lagrangian Particle Method with Sub-Particle –Scale Turbulence Model,* Asia and Pacific Coast Conference, 2003.

34) Greco, M.: 2001, *A Two dimensional Study of Green Water Loading*, PhD Thesis, Norwegian University of Science and Technology.

35) Greco, M. Landrini, M. and Faltinsen O. M.: 2004 *Impact Flows and Loads on Ship deck Structures,* Journal of Fluid and Structures , vol. 19, page 251 – 275

36) Greenhow, M.: 1987, *Wedge Entry into initially calm water,* Applied Ocean research, vol. 9, issue 4, page 214 – 223.

37) Gringold, R.A. and Monaghan,J.J.: 1977, "*Smoothed Particle Hydrodynamics:* Theory and Applications to Non – Spherical Stars. Mon. Not. R. astron. Soc. 181 page 375 – 389.

38) Han J.C.: 2003 *Impact of Green Water on FPSO* PhD Thesis, School of Marine Science and Technology, Newcastle University 2003

39) Han,J.C. Downie,M. J., Incecik, A. Casey,N. Kay, D. Stansberg C.T. and Moe,V.: 2004 *Extreme Loading and Responses of FPSOs in Green Seas.* Towards a Balanced Methodology in European Hydraulic Research. HYDRALAB Conference, Budapest. 2004

40) Harmoudi, B. and Varyani, K. S.: 1998, *significant Load and Green Water on Deck of offshore units/vessel,* Ocean Engineering vol. 25, no. 8 page 715 – 731.

41) Hayashi, M., Gotoh, H., Sakai, T. and Ikari, H.: 2003, *Lagrangian Gridless model of Toe Scouring of Seawall due to Tsunami return flow,* Asia and pacific Coast Conference, 2003.

42) Hellan, O., Hermundstad, O. A. and Stansberg,C. T.: 2001, *Design Tool for Green Sea , Wave Impact and Structural response on Bow and Deck Structures,* OTC 13213, OTC , April 2001, Houston.

43) Hellan, O. Hoff, J. R. and Stansberg, C. T. 2001, *A Practical Design tool for wave Impact on Bow and Deck structures,* PRADS 2001, page 611 – 619

44) Hikara, H.: 2004, *Numerical Modelling of flow in water entry of a Wedge,* 19th Proceedings, International workshop on Water Waves, National Defense Academy, Yokosuma, Japan.

45) Hirt C.W. and Nichols B. D.:1981 – *Volume of Fluid Method for the Dynamics of Free Boundaries,* Journal of Computational Physics 39, page 201 - 225.

46) HR Wallingford Limited: 2002, *FPSO Response in Long and Short Crested Seas,* prepared by HR Wallingford Limited for the Health and safety Executive

47) ITTC. 1984 : 17th International Towing Tank Conference

48) Kershaw, D.S.: 1978, *The Incomplete Cholesky Conjugate Gradient Method for the Iterative Solution of Systems of Linear Equation.* Journal of Computational Physics vol. 26 page 43 - 65

49) Khayyer, A. and Gotoh, H.: 2009, *Modified Moving Particle Semi Implicit Method for Prediction of 2D Wave Impact Pressure,* Coastal Engineering, vol. 66, issue 4, April 2009, pages 419 – 440.

50) Kim, C.H.: 2008, *Non Linear waves and Offshore Structures*, Advanced series in Ocean Engineering, vol.27 , World Scientific Publishing, ISBN 13 978 – 981 – 02 – 4884 - 0

51) Koshizuka S, Nobe A.., and Oka Y.: 1998 *Numerical Analysis of Breaking waves using the Moving Particle Semi - Implicit Method* .International Journal of Numerical Methods in Fluid Vol. 26 1998 page 751 - 769.

52) Koshizuka S and Oka Y.: 2000 *Moving Particle Semi - Implicit Method. Fully Lagrangian Analysis of Incompressible Flows* - European Congress on Computational Methods in Applied Sciences and Engineering - ECCOMAS 2000 Barcelona, 11 - 14. September, 2000.

53) Koshizuka S, and Oka Y.: 1996 *Moving Particle Semi - Implicit Method for Fragmentation of Incompressible Fluid* Nuclear Science and Engineering 1996 Vol. 123 page 121 - 434.

54) Koshizuka,S., Tamako,H. and Oka Y.: 1995 *A particle Method for Incompressible viscous flow with Fluid Fragmentation,* Journal of Computational Fluid Dynamics vol. 4 1995, page 29 – 46

55) Lee, B.H., Park,J .C., Kim, M.H., Jung,S.J., Ryu, M.C. and Kim, Y.S.:2010a, *Numerical Simulation of impact loads using a particle method.* Ocean Engineering,37, page 164 – 173.

56) Lee, B.H., Park,J .C., Kim, M.H.: 2010b, *Reply to "Discussion of" Numerical Simulation of impact loads using a particle method.* Ocean Engineering, 37, page 1480 – 1481.

57) Lee, H. and Rhee, S.H.: 2009, *Numerical Parameters Influencing two dimensional water entry simulations,* Proceedings ISOPE, 2009, Osaka.

58) Lee, C.J.K., Noguchi, H. and Koshizuka, S.: 2007, *Fluid – Shell Structure Interaction analysis by coupled particle and finite element method,* Computers and Structures, vol. 85, 2007, page 688 – 697.

59) LeTouze, D., Marsh, A., Oger,G., Guilcher,P.M., Khaddaj-Mallat, C., Alessandrini,B. and Ferrant,P.: 2010, *SPH Simulation of Green Water and Ship flooding Scenarios.* 9th International Conference on Hydrodynamics, Oct 11 – 15, 2010, Shanghai.

60) Lewis, S.G., Hudson, d.A. and Turnock, S.R.: 2010, *Simulation of a free falling wedge into water using 2D CFD with applications in the prediction of high speed craft motions,* Report, Fluid Structures Interaction Research Group, School of Engineering Science, University of Southampton, Southampton

61) Lloyd ,R.J.M., Salsich, J.O. and Zseleczky,J.J.:1985, *Effect of bow on deck wetness in Head seas.* Transactions Royal Institution of Naval Architects, vol. 128, page 9 - 25.

62) Libersky L.D., Petschek A.G., Carney ,T.C., Hipp,J.R., Allahdadi, F.A.: 1993, *High Strain Lagrangian Hydrodynamics: a three – dimensional SPH code for dynamic material response*, Journal of computational Physics vol. 109, page 67-75, 1993.

63) Lin, M.C. and Ho, T.Y.: 1994, *Water Entry of a Wedge in arbitrary water depth,* Engineering Analysis with Boundary Elements, vol. 14, page 179 – 185

64) Lin, W.M., Newman, J.N. and Yue, D.K.: 1984, *Nonlinear Forced Motions of Floating Bodies,* Proceedings of the 15th Symposium of Naval Hydrodynamics, Hamburg, Germany, page 33 - 48

65) Liu, W. K. and Li, S.: 2002, *Meshfree and Particle methods and their applications.* Appl. Mech Rev., vol. 55, no 1, January 2002.

66) Lu, H., Yang, C. and Lohner, R.: 2010, *Numerical Studies of Green Water Impact on fixed and moving bodies,* Proceedings 20th ISOPE , June 20 – 25 , 2010, Beijing.

67) Lucy, B.L., 1977, "*A Numerical approach to the testing of the fission hypothesis".* Astrophysics J., 82, page 1013.

68) Maiti, S. and Sen,D.; 2001, *Non linear heave radiation forces on two – dimensional single and twin hulls,* Ocean Engineering, vol. 28, page1031 – 1052

69) Marcer, R., Berhault, C., deJouette, C., Moirod, N. and Shen, L.: 2010, *Validation of CFD codes for Slamming,* ECCOMAS CFD, 2010, Lisbon, 14 – 17 June, 2010

70) MARINTEK - Experiments carried out at Norwegian Hydrodynamic Laboratory , Trondheim, Norway (MARINTEK) by Han et al,2004, (see ref 36).

71) Mei, X., Liu, Y. and Yue, D.P.K., 1999, O*n the water impact of general two dimensional sections,* Applied Ocean Research, vol. pages 1 – 15.

72) Meijerink, J.A. and Van der Vorst, H.A.: 1977, *An Iterative Solution Method for Linear Systems of which the Coefficient Matrix is a Symmetric M-Matrix,* Mathematics of Computation, vol. 31, number 137, pages 148 – 162.

73) Monaghan J.J. and Gingold R. A.: 1983, *Shock Simulation by the particle Method SPH-* J. comp Phys. 52, pages 374 - 389.

74) Monaghan, J.J.: 1985, *Particle Methods for Hydrodynamics,* -Comp. Phys, Report 3. Page 71 – 124

75) Monaghan, J.J.: 1992 *Smoothed Particle Hyrdodynamics* Annual Review Astron. Astrophys. 30, page 543 -574.

76) Monaghan, J.J.: 1994, *Simulating Free Flows with SPH.* J. Comp Phys. 110, page 399 – 406.

77) Monaghan, J.J.: 2000, *SPH without Tensile Instability,* Journal of Computational Physics, vol. 159, page 290 – 311.

78) Mori, N. and Cox, T.D.: 2003, *Dynamic Properties of Green Water event in the Overtopping of extreme waves on a fixed dock* , Ocean Engineering, vol. 30 2003, page 2021 – 2052

79) Naito, S. and Sueyoshi, M.: 2003, *A Numerical Analysis of Violent Free Surface Problems with Particle Method for Marine Engineering* The 8th International Conference on Numerical Hydrodynamics, Sept 22 – 25 Busan.

80) Newton, R.N.: 1960, *Wetness Related to Freeboard and Flare,* Transactions of Royal Institution of Naval Architects, 1960 vol. 102, page 49 – 68

81) Nielsen, K. B. and Mayer, S.: 2004, *Numerical Prediction of Green Water incidents,* Ocean Engineering, vol. 31, page 363 – 399.

82) Ochi, M.K.: 1964, *Extreme behavior of a Ship in Rough Seas, Slamming and Shipping of Green water,* SNAME Transactions vol. 72, page 143 – 202

83) Ogawa, Y., Taguchi, H., Watanabe, I. and Ishida, S.: 2001, *Long term Prediction Method of Shipping water Load for assessment,* Practical Design of Ships and Other Floating Structures, PRADS 2001.

84) Oger, G., Doring, M., Alessandrini, B. and Ferrant P.: 2006, *Two –Dimensional SPH Simulations of Wedge Water Entries* Journal of Computational Physics,vol. 213, page 803 – 822.

85) Pantazopoulous, M.S. : 1988, *Three – Dimensional Sloshing of water on Deck,* Marine Technology, SNAME , October, 1988, vol 25, number 4, page 253 - 261

86) Park J. C., Uno Y, Matsuo H, Sato T. and Miyaka H.: 2001, *Reproduction of fully Non-linear Multi-Directional Waves by a 3D viscous numerical wave tank* Proceedings 11th International Offshore and Polar Engineering Conference, Stavanger, Norway, June 17 - 22, 2001 Vol 11 page 140.

87) Petschek A.G and Libersky L.D.: 1993, C*ylinderical Smoothed particle Hydrodynamics,* Journal of computational Physics vol. 109, page 76 - 83, 1993.

88) Porter, W. R.:1960, *Pressure Distribution, Added mass and damping Coefficients for Cylinders in a free Surface,* University of California Institute of Engineering Research, Berkeley, Report Number AD242864, U.S. Dept of Commerce, National Technical Information service.

89) Pozrikidis C.: 1997 *Introduction to theoretical and computational fluid dynamics.* Oxford University Press Inc, New York, ISBN 0-19-509320-8

90) Randles, P.W. and Libersky, L.D. : 1996, *Smoothed Particle Hydrodynamics: Some recent improvements and applications,* Computer Methods in Applied mechanics and Engineering, vol 39, page 375 - 408

91) Rogers D. and King G.B.: 1997 *Wave Generation using Ocean and Wave, version 3.62,* Edinburgh Designs Ltd, 27, Ratciffe Terrace, Edinburg, EH9 1SX

92) Ryu, Y., Chang, K. and Mercier, R.: 2007, *Application of dam break flow to Green Water prediction,* Applied Ocean Research, vol. 29, page 128 – 136

93) Sames,P.C.: 2002, *Prediction of Green Water Loads for a RoRo Passenger Ferry* , OMAE 2002,Oslo

94) Schlatter B.: 1999, -"*A Pedagogical Tool Using SPH to model fluid flow Past a System of Cylinders"* – Research Paper , University of Oregon, June 15 1999

95) Schonberg T. and Chaplin J. R. - *Computation of Non Linear Wave Reflections and Transmissions from submerged Horizontal Cylinder*" - Proceedings 11th International Offshore and Polar Engineering Conference, Stavanger, Norway, June 17 - 22, 2001 page 280

96) Schonberg, T and Rainey, R.C.T.: 2002, *A hydrodynamic model of Green Water Incidents,* Applied Ocean Research, 24, page 299 - 307

97) Sen D.:1993, *Numerical Simulation of Motion of Two dimensional floating Bodies.* Journal Of Ship Research , December 1993 SNAME volume 37, Number4, ISSN 0022-4502

98) Shao, S.: 2009, *Incompressible SPH simulation of water entry of a free falling object,* International Journal for Numerical Methods in Fluids, vol. 59, pages 91 – 115

99) Shao, S and Lo, EYM, 2003.: *Incompressible SPH method for simulating Newtonian and non – Newtonian flows with a free surface,* Advances in Water Resources, vol 26, page 787 – 800.

100) Shirakawa, N., Horie, H., Yamamoto, Y., Okano, Y. and Yamaguchi, A.: 2001, *Analysis of Jet Flows with the Two - Fluid Particle Interaction Method,* Journal of Nuclear Science and Technology, Vol 38 No. 9, Sept 2001, pages 729 - 738.

101) Shibata, K and Koshizuka,S.: 2007,*Numerical Analysis of Shipping Water Impact on a deck using a particle method.* Ocean Engineering, vol.34 issue 3-4, page 585 – 593

102) Shibata, K., Koshizuka, S. and Tanizawa, K.: 2009, *Three – Dimensional Numerical Analysis of Shipping water onto a moving Ship using a particle method.* Journal of Marine Science and Technology, vol 14, page 214 - 227

103) Soares,C.G. and Pascoal, R.: 2002, *Experimental Study of the Probability Distributions of Green Water on the Bow of Floating production Platforms,* Proceedings 21st International conference, OMAE 2002, Oslo.

104) Spaulding M.L and Venkat K.N,.: 1990, *Numerical Simulation of Non Linear Free Surface Flows Generated by a Heaving Body of arbitrary Cross Section.* Journal of Ship Research, vol. 34 No 2, June 1990. SNAME

105) Sueyoshi, M. and Naito, S.: 2003, *A Numerical Study of Violent Free Surface Problems with Particle Method for Marine Engineering*. 8th International Conference on Numerical Ship Hydrodynamics, September 22 – 25, Busan

106) Sun, Z., Xi, G. and Chen, X.: 2009, *A numerical study of stir mixing of liquids with particle method,* Chemical Engineering science, vol. 64, issue 2, January 2009, page 341 – 350.

107) Stansberg C.T. and Nielsen, F.G.:2001, *Non linear Wave-Structure Interactions on Floating Production Systems.* Proceedings of the Eleventh International Offshore and Polar Engineering Conference, Stavanger, Norway, June 17 – 22, 2001. Vol. IV, page 363 – 372.

108) Stansberg,C.T. and Karlsen,S.I.: 2001, *Green Sea and water Impact on FPSO in Steep Random Waves.* Practical Design of Sips and other Floating Structures, PRADS 2001, page 593 - 601

109) Tagaki, K. and Niimi, A: 1990, *A Theoretical approach to Bow deck Wetness of a high- speed Ship.* Journal of Ship Research, vol. 34, no 3, page 163 - 171

110) Tanizawa, K.: 1996, *Non Linear Simulation of Floating Body Motions in waves,* Proceedings of the Sixth (1996) – International Offshore and Polar Engineering Conference, Los Angeles, USA May 26 – 31 1996.

111) Truong, T., Repalle, N., Pistani, F and Thiagarajan, K.: 2010, *An experimental study of slamming impact during forced water entry,* 17th Australiasia Fluid Mechanics Conference, Auckland.

112) Tveitnes, T., Fairlie – Clarke, A.c. and Varyani, K.: 2008, *An Experimental Investigation into Constant velocity water entry of a wedge shaped sections,* Ocean Engineering, vol. 35, page 1463 – 1478.

113) Vestbostad,T.M : 1999, *Relative wave Motions Along the side of an FPSO Hull,* OMAE 99, St Johns.

114) Wagner, H.:1932, *Uber stoss – und Gleitvergange an der Ober-flache von Flussigkeiten,* Zeitschr. F. Angew. Math. Und Mech., vol. 12 page 193 - 235

115) Wang X. M and Spaulding M. L.: 1988, *Two –Dimensional Potential Flow Model of the Wave Field Generated by a Semi submerged Body in Heave Motion.* Journal of Ship Research, vol. 32, No 2 June 1988, page 83-91, SNAME

116) Wu, M., Tulin,M.P., and Fontaine,E.: 2000, *On the Simulation of Amplified Bow Waves Induced by Motion in Head Seas.* Journal of Ship Research, vol. 44, no. 4

117) Wu, G.X., Sun, H. and He, Y.S.: 2004, *Numerical Simulation and Experimental study of water entry of a Wedge in free fall motion,* Journal of Fluid and Structures, vol. 19, page 277 – 289.

118) Wu, G.X.: 2006, *Numerical Simulation of Water Entry of twin Wedges,* Journal of Fluids and structures, vol. 22, page 99 – 108.

119) Yilmaz,O., Incecik, A., and Han, J.C.: 2003, *Simulation of Green Water flow on deck using Non Linear Dam Breaking Theory.* Ocean Engineering, 30, page 601 – 610

120) Yoon, H.Y., Koshizuka, S and Oka Y. 1999 *A particle - Grid less Hybrid Method for Incompressible Flows"* - International Journal for Numerical Methods in Fluids 30, page 407 - 424, 1999.

121) Zhang, ., Morita, K., Fukuda, K. and Shirakawa, N.: 2006, *An improved MPS method for Numerical Simulation of Convective heat Transfer,* International Journal for Numerical methods in Fluids, vol. 51, pages 31 – 47

122) Zhao, R.O. and Faltinsen,O.: 1993, W*ater Entry of Two Dimensional Bodies,* Journal of Fluid Mechanics, vol. 246, page 593 – 612.

123) Zhao R., 0. Faltisen, O. and J. Aarsnes(1997) – "*Water Entry of Arbitrary Two – Dimensional sections with and without Flow Separation"*, 21st Symposium on Naval Hydrodynamics, 1997.

124) Zhiyu Shao and Scott A., Yost – *"A Portable Numerical Method for Simulating 2D - Unsteady Free Surface Flow"*. Dept of Civil Engineering, University of Kentucky, USA.

125) Zhu, R., Lin , Z. and Miao, G.: 2006, *Numerical Simulation for Green Water Occurrence,* Conference of Global Chinese scholars on Hydrodynamics, Shanghai.